2022-2023 CALIFORNIA CURRENT ECOSYSTEM STATUS REPORT

*A report of the NOAA California Current Integrated Ecosystem Assessment Team (CCIEA)
to the Pacific Fishery Management Council, March 7, 2023*

Edited by: Chris Harvey, Andy Leising, Nick Tolimieri, and Greg Williams
Northwest and Southwest Fisheries Science Centers, NOAA

With contributions from:

Justin Ainsworth, Kelly Andrews, Dan Ayres, Tracie Barry, Jack Barth, Eric Bjorkstedt, Steven Bograd, Anna Bolm, Jerry Borchert, Caren Braby, Brian Burke, Jason Cope, David Demer, Danielle Devincenzi, Heidi Dewar, Lynn deWitt, Blake Feist, John Field, Jennifer Fisher, Zachary Forster, Toby Garfield, Thomas Good, Christina Grant, Correigh Greene, Elliott Hazen, Daniel Holland, Mary Hunsicker, Matthew Hunter, Lilah Isé, Kym Jacobson, Michael Jacox, Jaime Jahncke, Mike Johns, Tim Jones, Christy Juhasz, Stephen Kasperski, Delia Kelly, Su Kim, Dan Lawson, Connor Lewis-Smith, Kirsten Lindquist, Nate Mantua, Sharon Melin, Stephanie Moore, Cheryl Morgan, Barbara Muhling, Stuart Munsch, Catherine Nickels, Karma Norman, Rachael Orben, Julia Parrish, Scott Pearson, Stephen Pierce, Jessica Porquez, Antonella Preti, Josiah Renfree, Roxanne Robertson, Jan Roletto, Dan Rudnick, Lauren Saez, Keith Sakuma, Jameal Samhouri, Jarrod Santora, Isaac Schroeder, Kayleigh Somers, Beckye Stanton, Kevin Stierhoff, Rasmus Swalethorp, William Sydeman, Andrew Thompson, Sarah Ann Thompson, Duy Trong, Peter Warzybok, Jessica Watson, Brian Wells, Curt Whitmire, Jen Zamon, Samantha Zeman, Vanessa Zubkousky-White, Juan Zwolinski

2022-2023 CALIFORNIA CURRENT ECOSYSTEM STATUS REPORT

TABLE OF CONTENTS

Main report

Supplementary Materials

1   INTRODUCTION

The Pacific Fishery Management Council (Council) Fishery Ecosystem Plan (FEP) establishes a process wherein NOAA provides the Council with a yearly update on the status of the California Current Ecosystem (CCE), as derived from environmental, biological, economic and social indicators. NOAA's California Current Integrated Ecosystem Assessment (CCIEA) team is responsible for this report. This is our 11th ecosystem status report (ESR), with prior ESRs in 2012 and 2014-2022.

A major change this year is that we used different software to improve the efficiency of report generation (see Appendix C). One result is that the layout has changed: the main body has the same approximate word count as prior ESRs, but spans more pages because figures are larger. This report structure follows the updated guidance of the FEP (PFMC 2022a).

This ESR summarizes CCE conditions based on data and analyses that generally run through 2022 and some that extend into 2023. Highlights are summarized in Box 1.1 and described in the main report. Appendices provide additional information or clarification, as requested by the Council and its committees and advisory bodies.

Box 1.1: 2022-23 CCIEA Ecosystem Status Report Highlights

Key takeaways from 2022:

Basin-scale climate patterns started out encouragingly, but were offset in part by local dynamics and a major marine heatwave

Food web dynamics provided resilience, including ongoing production of anchovy in the south

Unfavorable Conditions and Risk Factors

- 4th-largest marine heatwave on record, with more coastal influence than recent years
- A dry spring in 2022 contributed to low snowpack and continued drought
- Extreme weather in early 2023
- Uptick in HAB activity in late 2022 led to shellfish fishery closures or delays
- Fishing portfolios continue to be less diversified, both in target species and total weeks fished
- Potential constraints of offshore wind on fishing and research are coming into focus

Mixed Ecological Signals

- Lipid-rich copepods off Oregon abundant but declined earlier than normal
- Juvenile salmon conditions were mixed
- Chinook salmon returns: encouraging signals in north, concerns for California
- Anchovies remain abundant in surveys and predator diets in central and south
- Low bird densities offshore in the north; good production in central
- A strong new year class of sablefish?

An extended graphical summary is provided in Appendix D

1.1   SAMPLING LOCATIONS

We generally refer to areas north of Cape Mendocino as the "Northern CCE," Cape Mendocino to Point Conception as the "Central CCE", and south of Point Conception as the "Southern CCE." Figure 1.1 shows sampling areas for most regional oceanographic data. Key oceanographic transects are the Newport Line off Oregon, the Trinidad Head Line off northern California, and CalCOFI lines further south, while shaded marine regions indicate sampling areas for most biological surveys. This sampling is complemented by basin-scale oceanographic observations and by outputs from various models. Figure 1.1 also shows sampling areas for most biological indicators. The shaded terrestrial areas in Figure 1.1 represent freshwater ecoregions in the CCE, and are the basis by which we summarize indicators for snowpack, flows, and stream temperatures.
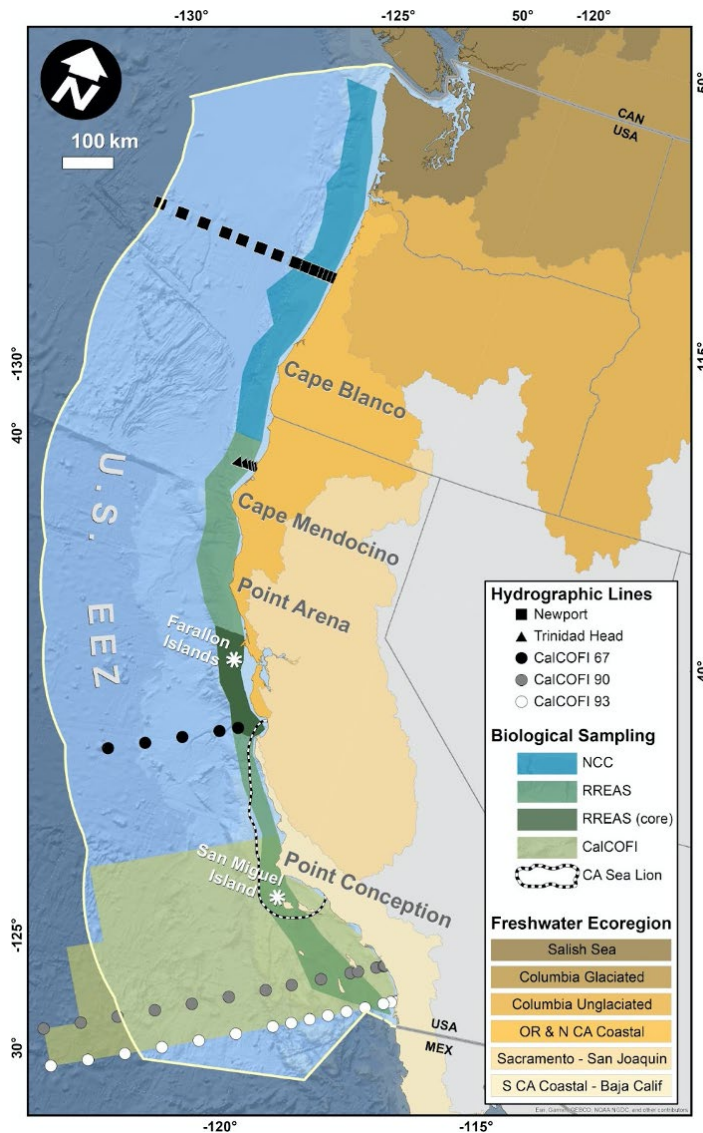

Figure 1.1: Map of the California Current Ecosystem (CCE) and U.S. west coast Exclusive Economic Zone (EEZ). Symbols indicate hydrographic line sampling stations for oceanographic data. Shaded ocean regions represent biological sampling areas for the Northern California Current (NCC), which includes the Juvenile Salmon and Ocean Ecology Survey (JSOES); the Rockfish Recruitment and Ecosystem Assessment Survey (RREAS), including its Core Area; and the CalCOFI sampling region. The NCC and RREAS shaded areas also approximate the survey footprints for NOAA's coastwide CPS acoustic/trawl survey and groundfish bottom trawl survey. Dashed line approximates foraging area for adult female California sea lions from the San Miguel colony. Shaded terrestrial areas represent the six freshwater ecoregions in the CCE.

2

2   CLIMATE AND OCEAN DRIVERS

The last seven years have been dominated by warmer than normal conditions across the Northeast Pacific (NEP) and the California Current. This is consistent with global trends in ocean warming[1], and with 2022 being the warmest year on record for the NEP[2]. Starting in 2014, there was the unprecedented marine heatwave, aka "The Blob", followed by El Niño in 2015-2016. After a brief respite during 2017-2018, there have been large heatwaves offshore each year, typically lasting from summer through fall, with occasional coastal penetrations. Environmental conditions in the CCE in 2022 followed this pattern, albeit with earlier and longer coastal intrusions of the offshore heatwave, due to an inconsistent upwelling pattern. In 2021 the heatwave was held offshore by strong and consistent coastal upwelling, which led to good productivity, whereas 2022 saw several significant periods of upwelling relaxation during the summer, causing warmer coastal conditions. 2020-2021 saw La Niña conditions, with yet another La Niña during 2022/23 winter. However, local conditions often did not line up with our typical expectations for this basin-scale index during 2022 (Appendix E).

On land, like 2021, 2022 again saw high air temperatures, continued drought, reduced snowpack in some areas, and lower streamflow that affected many regions, detailed further below.

2.1   BASIN-SCALE INDICATORS

We use three indices to characterize large-scale physical ecosystem states in the North Pacific:

- The Oceanic Niño Index (ONI) describes the equatorial El Niño Southern Oscillation (ENSO). An ONI above 0.5°C indicates El Niño conditions, associated with lower primary production, weaker upwelling, poleward transport of equatorial waters and species, and more southerly storm tracks in the CCE. An ONI below -0.5°C means La Niña conditions, which create atmospheric pressure conditions leading to upwelling-favorable winds driving productivity in the CCE.
- The Pacific Decadal Oscillation (PDO) relates to the spatial pattern of North Pacific sea surface temperature (SST) anomalies. Positive PDO is associated with warmer coastal SST and lower productivity in the CCE, while negative PDO indicates cooler coastal SST and typically higher productivity.
- The North Pacific Gyre Oscillation (NPGO), an index of sea surface height, indicates changes in circulation that affect source waters for the CCE. Positive NPGO indicates stronger equatorward flow and higher salinity, nutrients, and chlorophyll-a. Negative NPGO indicates decreased subarctic source water and lower CCE productivity.

---

[1] https://www.ncei.noaa.gov/access/global-ocean-heat-content/
[2] https://www.cpc.ncep.noaa.gov/products/GODAS/ocean_briefing_new/mnth_sst_index_1950.gif
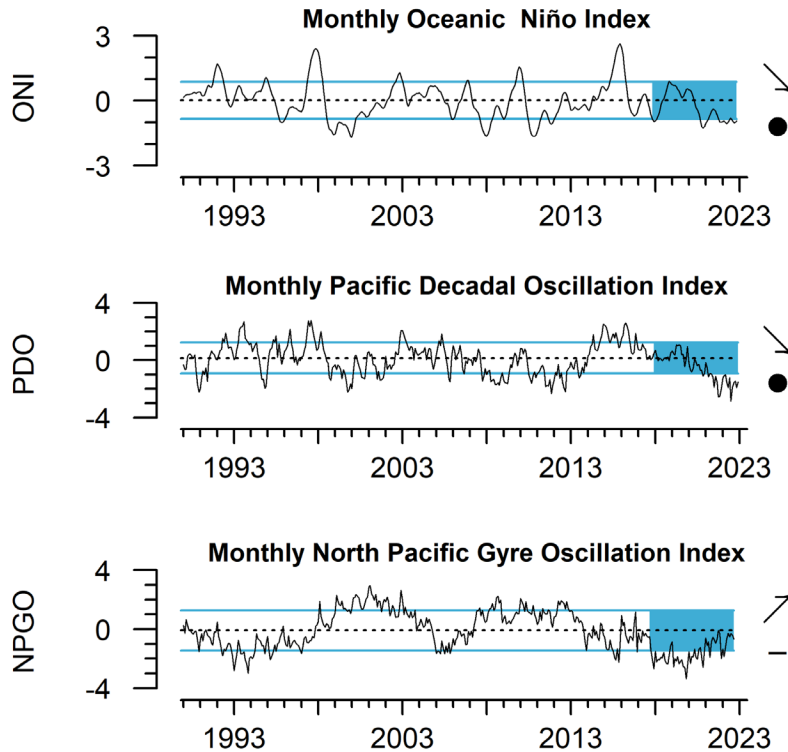
3

Figure 2.1: Monthly values of the Oceanic Niño Index (ONI), Pacific Decadal Oscillation (PDO), and North Pacific Gyre Oscillation (NPGO) from 1990-2022 relative to the mean (dashed line) ±1 s.d. (blue lines) from 1991-2020. The blue shaded area is the most recent 5 years of data. Arrows indicate if the recent 5-year trend is positive (↗), neutral (→), or negative (↘). Symbols indicate if the recent 5-year mean is above the upper blue line (+), within the blue lines (●), or below the lower blue line (−).

Basin-scale indices suggest average to above-average conditions for productivity in 2022: the ONI and PDO remained negative, while the NPGO increased towards neutral. Negative ONI suggests La Niña conditions for 2022 (Fig. 2.1, top), marking three consecutive years of La Niña conditions. As of January 2023, La Niña still persists, although NOAA forecasts a 71% chance of returning to neutral ENSO conditions by April. The PDO also remained negative for a third consecutive year, continuing a trend of decreasing values since 2016 (Fig. 2.1, middle). After reaching low values in 2019-2020, the NPGO has since risen to neutral values (Fig. 2.1, bottom). This indicates that the general circulation in the CCE may transition to average. Taken together, these indices normally would represent cool coastal conditions favorable for primary productivity, however, some of these predicted trends were interrupted by major upwelling relaxation events (discussed below). Seasonal values for all indices are in Appendix F.1.

The northeast Pacific continues to experience large marine heatwaves in surface waters. The 2022 marine heatwave formed in late January and reached its maximum size, approximately 8 million km^2, on August 30 (Fig. 2.2), and is still ongoing as of the preparation of this report. It was the 4th largest heatwave by area and the 3rd longest in duration since monitoring began in 1982. Unlike the previous year, this year's heatwave had many large intrusions into the coastal area, particularly along the central California coast (Fig. 2.2). These intrusions

were related to widespread reversals of upwelling winds, leading to upwelling relaxation events during the summer and fall (Fig. 2.4). Additional information on the 2022 marine heatwave is in Appendix F.2.
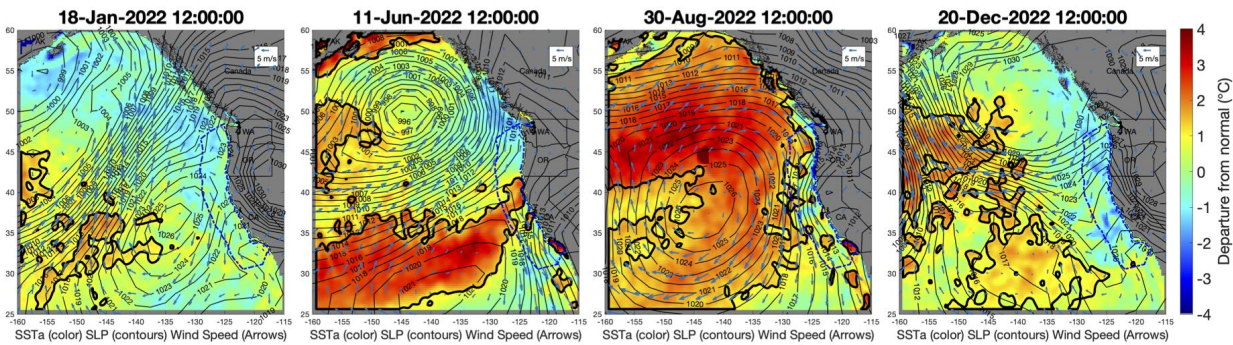

Figure 2.2: Progression of the 2022 marine heatwave in the northeast Pacific Ocean. Colors represent standardized SST anomalies. Heavy black lines denote regions that meet the criteria for a marine heatwave (see Appendix F.2). Gray contours represent sea level pressure (in hectoPascals) and arrows represent wind speed and direction.

Subsurface temperatures (>50m depth) were average in 2022 along much of the West Coast. Off Newport, Oregon, temperatures in the upper 50 m were ~2 to 3°C warmer than average on a few occasions during summer (Fig. 2.3, top), coinciding with intrusions of the marine heatwave. In the Southern California Bight (SCB), the upper 50 m was warm for much of the spring and summer, whereas subsurface waters were average (Fig. 2.3, bottom). Subsurface temperatures off Monterey Bay were average or above-average for most of 2022 (Fig. F.5).
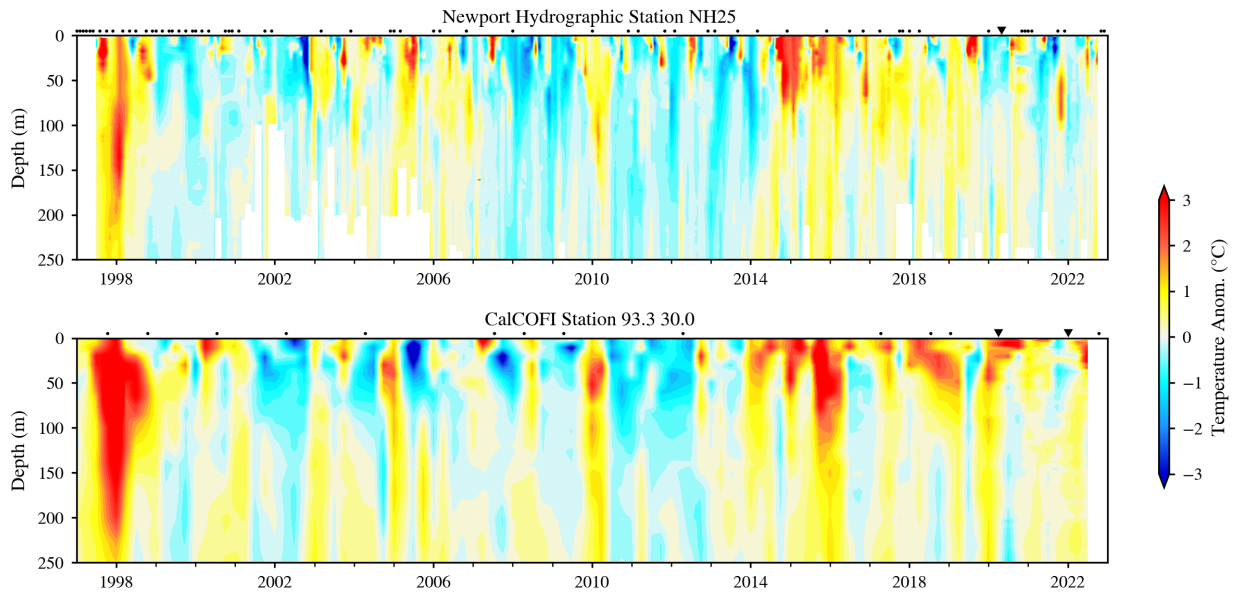

Figure 2.3: Time-depth temperature anomalies at Newport station NH25 and CalCOFI station 93.30, 1997-2022. Transect locations are in Fig. 1.1.

2.2 UPWELLING AND HABITAT COMPRESSION

Upwelling is a major driver of coastal productivity in the CCE. It occurs when equatorward coastal winds force deep, cold, nutrient-rich water to the surface. The greatest upwelling in the CCE occurs off central California and typically peaks in June. Here, we present two upwelling indices: vertical fluxes of water (Coastal Upwelling Transport Index; CUTI) and of nitrate (Biologically Effective Upwelling Transport Index; BEUTI) (Jacox et al. 2018).
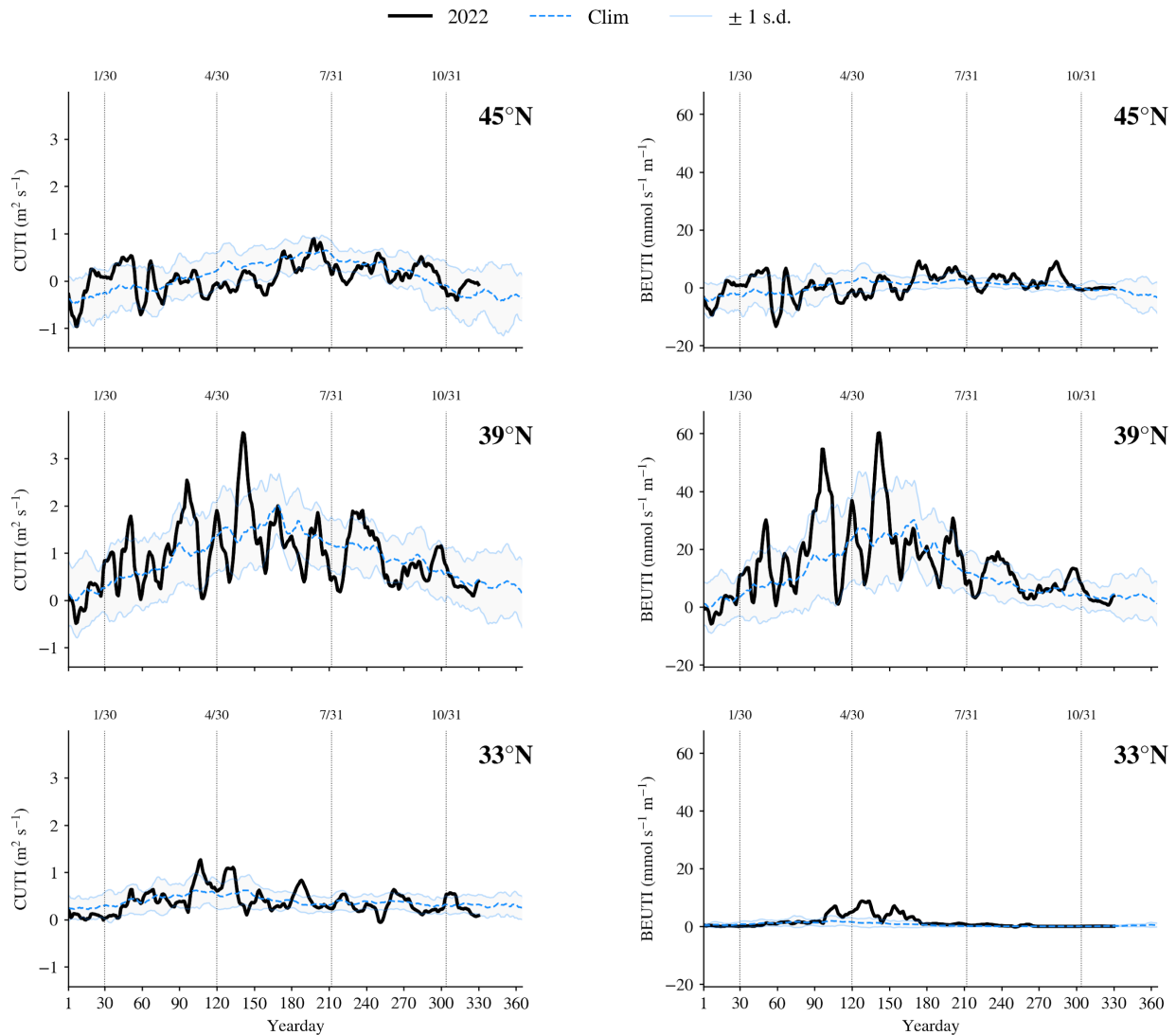

Figure 2.4: Daily estimates of vertical transport of water (CUTI, left) and nitrate (BEUTI, right) in 2022, relative to the 1988-2022 climatological average (blue dashed line) ±1 s.d. (shaded area), at 33°N (San Diego), 39°N (Pt. Arena), and 45°N (Newport).

Overall, 2022 saw average total integrated upwelling compared to previous years. However, upwelling events were more highly variable in strength and timing, consisting of periods of strong upwelling, interspersed with several periods of significant upwelling relaxation, or even downwelling (Fig. 2.4). In the north, total upwelling was lower than average. The year began with strong upwelling early in the winter, but then decreased through the spring and

6

summer, with only occasional periods of positive upwelling and nutrient transport to the surface. In the central region, upwelling was average, but with the noted high variability, having several periods of upwelling and downwelling either above or below 1 s.d. of the climatological average (Fig. 2.4). In the south, upwelling was slightly higher in the spring, but average during the remainder of the year. This is in contrast to 2021, when upwelling was moderate yet highly consistent over time. Periods of upwelling relaxation (or even downwelling) typically allow for retention of nutrients that can spur coastal production, however, during 2022 these events were longer and thus also allowed for the large offshore marine heatwave to penetrate into the nearshore coastal waters, hampering production. During 2022, the main driver of these changes in upwelling during the summer was the episodic presence of a large, low atmospheric pressure cell in the central NEP, and a displacement of the typical location and of the "North Pacific High" (a high pressure atmospheric cell that typically dominates the NEP, Fig. 2.2 June). Normally, upwelling relaxation would lead to somewhat warmer coastal waters, however, during this past year the close proximity in offshore waters of a large marine heatwave meant that these upwelling relaxation events led to much warmer coastal temperatures than expected (Fig. 2.2, Appendix Fig. F.8).

Santora et al. (2020) developed the habitat compression index (HCI) to describe how much cool, productive water is available adjacent to the coast. HCI ranges from 0 (complete coverage of warm offshore water in the region) to 1 (cool water fully extending 150 km from the coast). In general, cool coastal habitat has been expanding since 2016 (Fig. 2.5), however values were slightly lower during 2022 compared to the relative high in 2021. This lowering of the yearly HCI was again due to the variability in upwelling and subsequent frequent warming of coastal waters seen during summer and fall of 2022 (Appendix F.3).
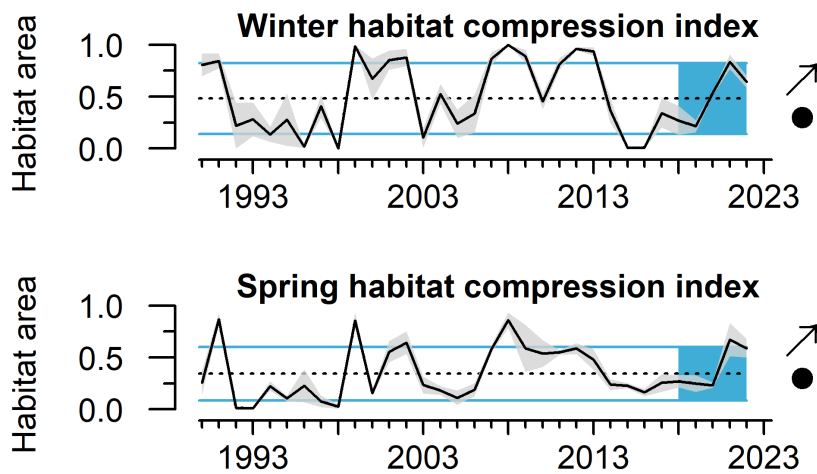

Figure 2.5: Mean habitat compression index (HCI) off central California in winter (Jan-Mar) and spring (Apr-Jun) 1990-2022. Habitat area is the fraction of coastal habitat that is cooler than the threshold (higher values indicate less compression). Gray envelope indicates ±1 s.e. Lines, colors, and symbols are as in Fig. 2.1.

2.3 HYPOXIA AND OCEAN ACIDIFICATION

Dissolved oxygen (DO) is influenced by processes such as currents, upwelling, air-sea exchange, primary production, and respiration. Low DO (aka hypoxia, concentrations <1.4 ml DO/l) can compress habitat and cause stress or die-offs in sensitive species (Chan et al. 2008). The nearshore station NH05 off Newport, Oregon experienced periods of very low DO in 2022, similar to 2021 (Fig. 2.6). Near-bottom (50m) DO values were just below or close to the hypoxia threshold during summer 2022, but were higher than the previous summer. The offshore station NH25 off Newport also experienced fairly low DO levels at deeper depths (150m). Although not hypoxic, the DO levels at depth at this station were lower through much of the year as compared to 2021. Additional DO data from the Northern CCE are in Appendix F.4. CalCOFI DO data showed similar trends, with low spring and summertime DO levels at depths of 150m, similar or lower than the previous year. Unlike Oregon, at depths of 150m to 50m DO levels were nearly always at least two times higher than the hypoxic threshold, except for a small region to the southeast of Point Conception during the spring (Appendix F.4).
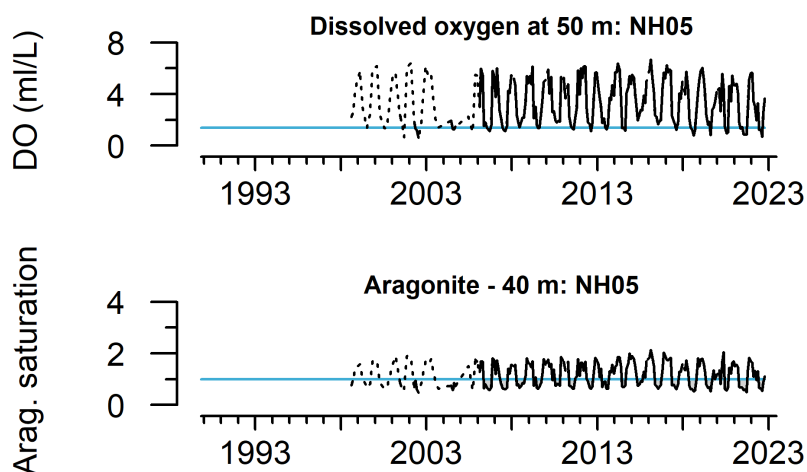

Figure 2.6: Near-bottom dissolved oxygen (top) and aragonite saturation state (bottom) off Newport, OR, 1998-2022. Blue lines indicate the hypoxia threshold (1.4 ml DO/L, top) and the biological threshold for aragonite saturation state (1.0, bottom).

Ocean acidification, caused by increased anthropogenic CO_2, reduces pH and dissolved carbonate in seawater and is stressful to many marine species (Feely et al. 2008, Busch and McElhany 2016). At station NH05 off Newport, levels of aragonite (a form of calcium carbonate) were above the reference threshold of 1.0 in winter, but decreased through spring and summer to < 1.0 (Fig. 2.6, bottom), a saturation level which is corrosive for many shell-forming organisms, but is a typical seasonal pattern at this station. Summer values were slightly higher (less corrosive, and thus more favorable for certain planktonic organisms at the base of the food chain) during 2022 than during 2021 (see details in Appendix F.4). Conversely, at depth (150m) at the offshore station NH25, saturation values were lower throughout 2022 as compared to 2021, indicating that the offshore environment may have been less favorable for certain plankton (Appendix F.4).

2.4 SNOWPACK AND HYDROLOGY

Snow-water equivalent (SWE) is the water content in snowpack, which supplies cool freshwater to streams in spring, summer and fall and is critical for salmon production (Appendix G, Appendix J). As in 2021, snowpack in 2022 exhibited some major changes between winter and spring. Early winter storms created high snowpack (125-200% of the 30-year median) in California and Oregon and more moderate conditions in Idaho and Washington. A drier spring resulted in substantial changes in SWE such that much of the Pacific Coast was well below median SWE by the April 1 benchmark, which continued a recent trend of low and declining snowpack in much of the West (Fig. 2.7). These conditions set up drought conditions in the late spring and summer for much of California, Oregon, and Idaho. though overall drought conditions were less severe than in 2021.
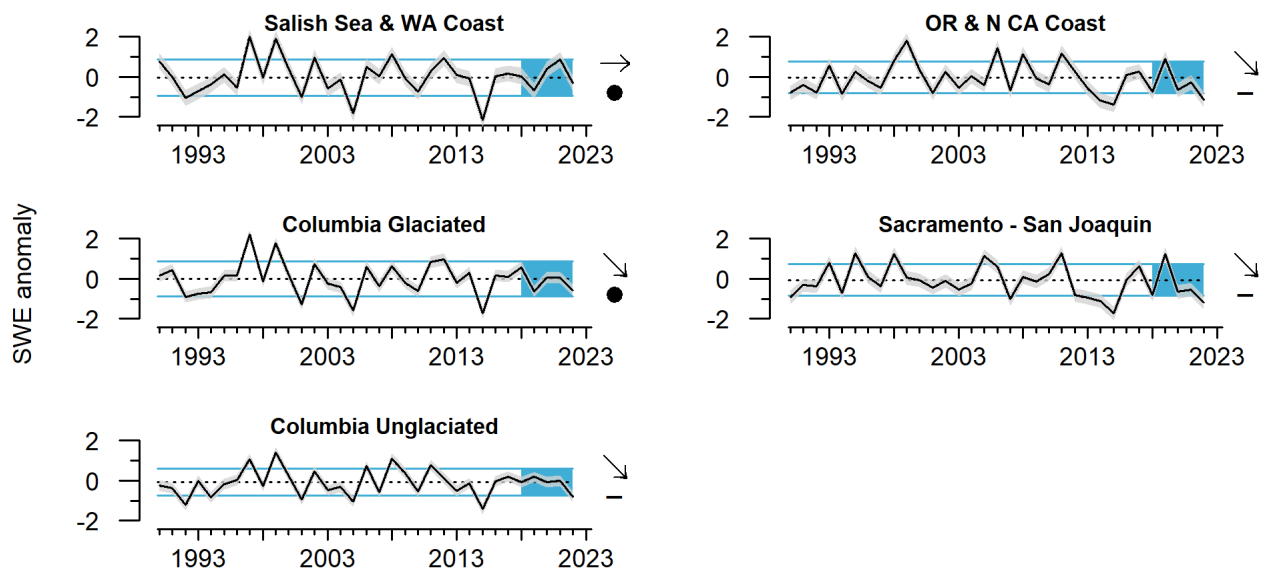

Figure 2.7: Anomalies of April 1st snow-water equivalent (SWE) in freshwater ecoregions of the CCE, 1990-2022. Error envelopes represent 95% credible intervals. Lines, colors and symbols are as in Fig. 2.1. Ecoregions are mapped in Fig. 1.1.

As of February 1, 2023, SWE in the West is mixed (Appendix G). Winter storms have created extremes in precipitation and very high SWE in California, and above average levels for much of the mountain west. However, over 70% of Washington, Oregon, Idaho, and California remain in drought conditions, and portions of central Oregon remain in the highest drought category. With recent changes in weather across the Pacific Coast, winter precipitation outlooks suggest normal precipitation.

Across ecoregions, stream flows were mixed in 2022 (Fig. 2.8, Appendix G). The Salish Sea and WA Coast have seen an increase in the recent average and recent trend in maximum streamflow, whereas the OR and North CA Coast, the Sacramento/San Joaquin, and the Southern California Bight regions all saw decreases in the recent average streamflow (Fig. 2.8). Only the Salish Sea and WA Coast saw an increase in the recent trend of minimum flow, with a slight decrease in minimum flow recent trend for the Sacramento San Joaquin region (Fig. 2.8). Maximum August stream temperatures have been relatively warm and increasing

9

in all ecoregions except the Salish Sea and WA Coast (Fig. 2.8). Overall, this suggests that the Salish Sea and WA Coast are seeing increased flows (favorable conditions) whereas the remaining regions are seeing similar and in a few cases decreasing flows (less favorable conditions).
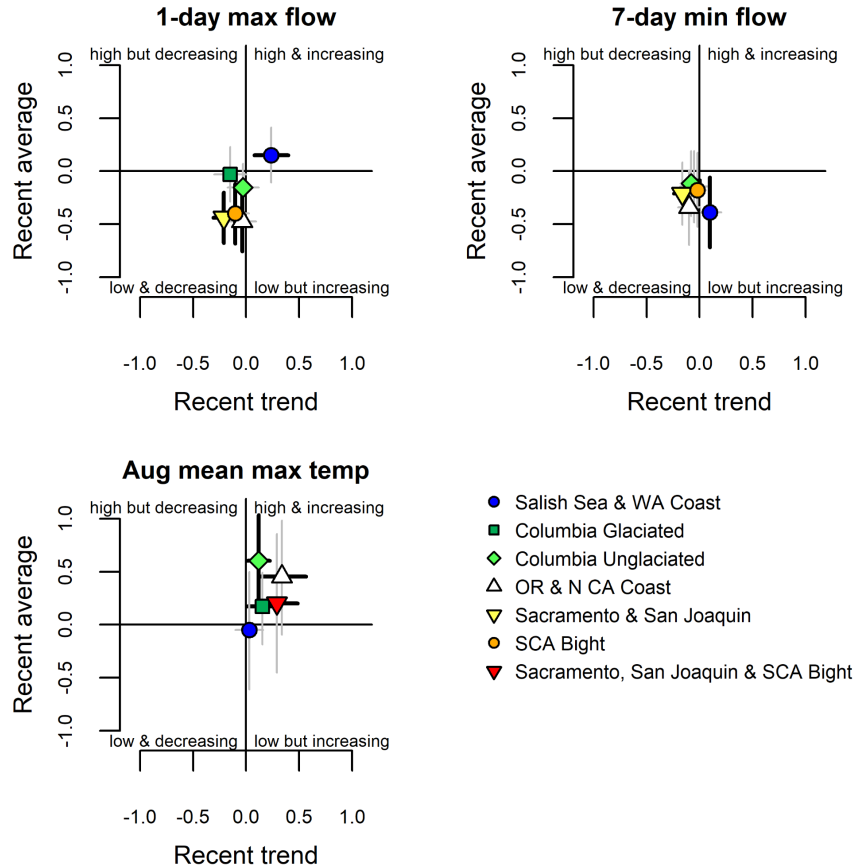

Figure 2.8: Recent (2018-2022) averages and trends in maximum and minimum streamflow and mean maximum August stream temperature in six freshwater ecoregions. Symbols for each ecoregion fall into quadrants based on recent average (high or low) and recent trend (increasing or decreasing) relative to long-term data (1980-present). Error bars represent 95% credible intervals. Heavy black error bars represent significant differences from zero. Ecoregions are mapped in Fig. 1.1.

3   FOCAL COMPONENTS OF ECOLOGICAL INTEGRITY

While La Niña and negative PDO conditions seemed to promote good conditions for marine productivity in much of the system in 2020 and 2021, ecological indicators in 2022 were more mixed, with some signals of below-average feeding conditions, particularly in the Northern CCE. Anchovy remained a highly abundant prey resource for many top predators in the Central and Southern CCE. Signals are mixed for salmon stocks returning in 2023, but more encouraging for an incoming year class of sablefish.

3.1   COPEPODS AND KRILL

Copepod biomass anomalies represent variation in northern copepods (cold-water crustacean zooplankton species rich in wax esters and fatty acids) and southern copepods (smaller species with lower fat content and nutritional quality). Northern copepods dominate the summer zooplankton community along the Newport Line (Fig. 1.1), while southern copepods dominate in winter. Northern copepods typically are favored by La Niña and negative PDO conditions (Keister et al. 2011; Fisher et al. 2015). Positive northern copepod anomalies generally correlate with stronger returns of Chinook salmon to Bonneville Dam and coho salmon to coastal Oregon (Peterson et al. 2014).

Lipid-rich northern copepods were very abundant along the Newport Line in spring and early summer of 2022, but dropped in mid-summer to average through September (Fig. 3.1, top). The spring-summer peak was among the highest of the 25-year time series, but the decline in mid-summer was earlier than normal. Local upwelling (Fig. 2.4, top) may be related to these atypical patterns: strong winter upwelling may have fueled the initial surge in northern copepods; subsequently, weak spring/summer upwelling likely contributed to the mid-summer decline. Southern copepod biomass was below-average in much of spring-summer 2022, similar to the previous two growing seasons (Fig. 3.1, bottom). These values suggest mixed feeding conditions for pelagic fishes off central Oregon in 2022, after good conditions in 2020 and 2021.
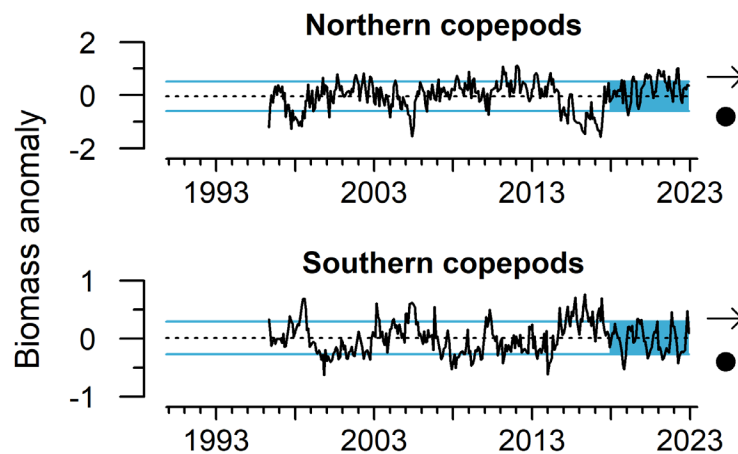

Figure 3.1: Monthly copepod biomass anomalies from station NH05 off Newport, OR, 1996-2022. Positive values indicate above-average biomass and negative values indicate below-average biomass. Lines, colors, and symbols are as in Fig. 2.1.

Krill are among the most important prey groups in the CCE. The species *Euphausia pacifica* is sampled year-round along the Trinidad Head Line off northern California (Fig. 1.1). Mean length of adult and total biomass of *E. pacifica* are indicators of productivity at the base of the food web, krill condition, and energy content for predators (Robertson and Bjorkstedt 2020). *E. pacifica* adult lengths in spring and summer of 2022 were close to average (Fig. 3.2, top), and total biomass was relatively low (Fig. 3.2, bottom). Unlike most years on record, neither mean length nor biomass exhibited a strong increase during spring and summer in 2022. Further south, in contrast to these results, springtime pelagic surveys (Figure 3.4) and

11

Cassin's auklet production (Figure 3.11) suggested average to above-average abundances of krill in the Central CCE in 2022.
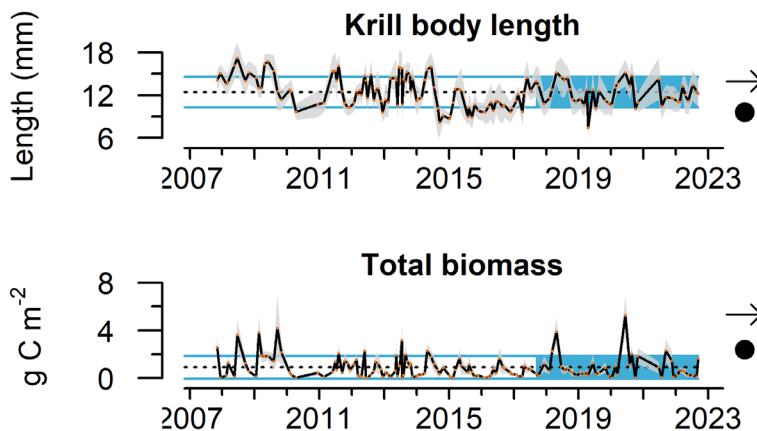

Figure 3.2: Monthly mean E. pacifica *adult length (top) and total* E. pacifica *biomass (bottom) off Trinidad Head, CA, 2007-2022. Gray envelopes indicate ±1.0 s.d. Lines, colors, and symbols are as in Fig. 2.1.*

3.2 REGIONAL FORAGE AVAILABILITY

The regional surveys that produce CCE forage data use different gears and survey designs, which makes regional comparisons difficult. We use a cluster analysis to identify regional shifts in forage composition (Thompson et al. 2019a). Those plots are shown here; see captions for how to interpret the plots. Related time series are in Appendixes H and O.

Northern CCE: The JSOES survey off Washington and Oregon (Fig. 1.1) targets juvenile salmon in surface waters, and also samples surface-oriented fishes, squid and jellies. The composition of this near-surface community has changed several times since the onset of marine heatwaves in 2014-2016, and in 2022, once again, the community experienced a temporal shift relative to the 2018-2021 assemblage (Fig. 3.3). The 2022 assemblage was characterized by increased abundances of juvenile chum, coho and sockeye salmon. Further separation from the prior assemblage was driven by increases in egg yolk jellyfish and pompano, species typically associated with warm conditions. Time series of catches from this survey are in Appendix H.1. Juvenile salmon are discussed further in Section 3.3.

Central CCE: Data in Figure 3.4 are from the "Core Area" of a nearly coastwide survey (Fig. 1.1) that targets pelagic young-of-the-year (YOY) rockfishes, and samples other pelagic species. The forage assemblage in this area, centered just off Monterey Bay, has been relatively consistent since 2018; 2022 continued that pattern (Fig. 3.4). A defining trait of this assemblage has been high abundance of adult anchovy, which remained very abundant here in 2022, while adult Pacific sardine catches remained low. Catches of YOY anchovy and sardine were both low in 2022. YOY rockfishes increased to about average, but remained below the peaks that occurred in 2013-2017. Market squid and krill catches in 2022 were slightly above average. Time series of these data are in Appendix H.2. The high occurrences of anchovy and rarity of sardine are consistent with findings from a NOAA acoustic and trawl survey for coastal pelagic species in summer 2022 (Appendix I).
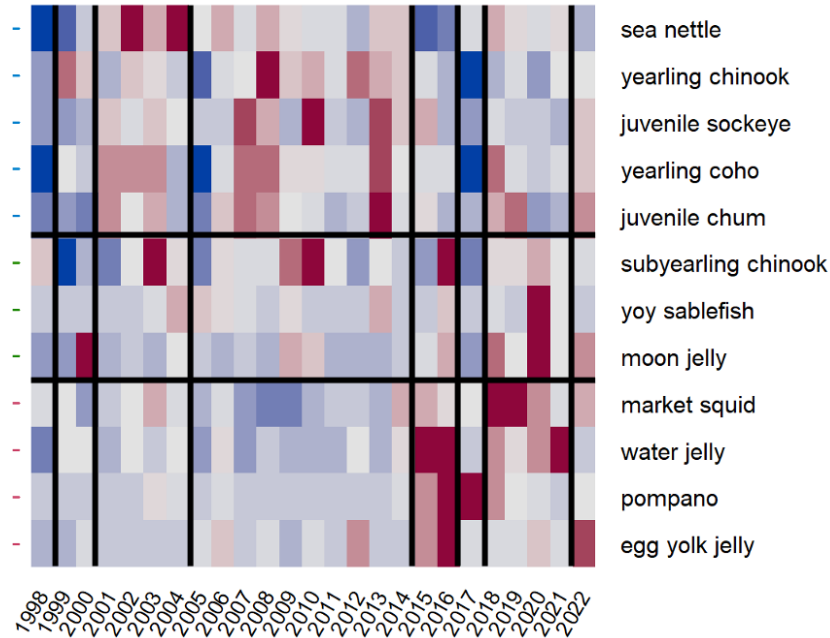
12

Figure 3.3: Cluster analysis of pelagic community indicators in the northern CCE, 1998-2022. Colors indicate relative catch per unit effort (red = abundant, blue = rare). Horizontal bars separate clusters of typically co-occurring species. Vertical bars demarcate breaks in assemblage structure between years.
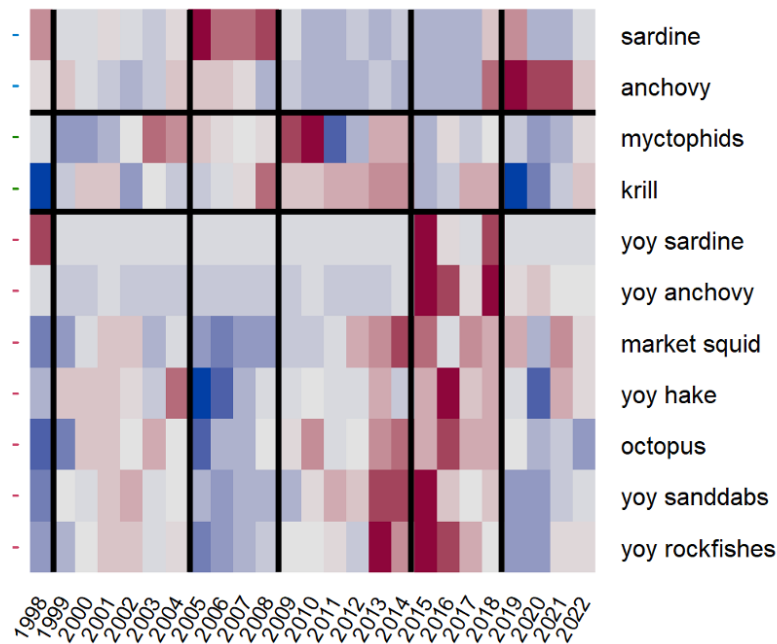

Figure 3.4: Cluster analysis of forage indicators in the Core Area of the central CCE, 1998-2022. Colors indicate relative catch per unit effort (red = abundant, blue = rare). Horizontal bars separate clusters of typically co-occurring species. Vertical bars demarcate breaks in assemblage structure between years.

13

Southern CCE: Forage data for the Southern CCE come from springtime CalCOFI larval fish surveys (Fig. 1.1). The spring 2022 assemblage clustered with the assemblages of 2017-2021 (Fig. 3.5; no data for 2020 due to COVID-19). These years are characterized by extremely abundant larvae of anchovy, southern mesopelagic fishes, and another mesopelagic fish, California smoothtongue. Rockfish larvae were close to average in 2022, while market squid paralarvae and English sole larvae were very abundant. Similar to previous years, larval sardine, Pacific mackerel, and hake were rare in 2022, but larval jack mackerel increased to the highest level in the time series (see also Appendix I). Time series of catches are available in Appendix H.3.
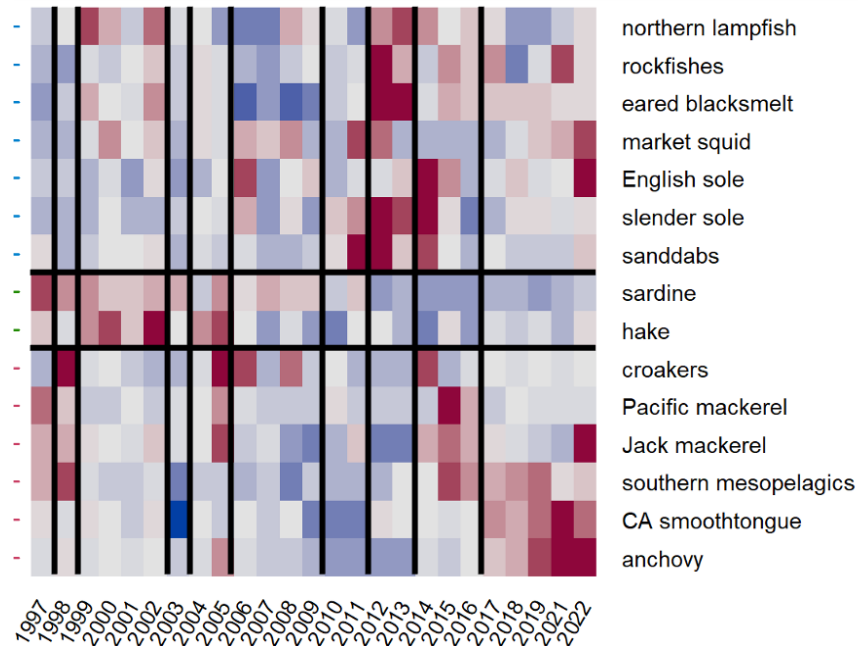

Figure 3.5: Cluster analysis of forage indicators in the Southern CCE, 1998-2022 (no data in 2020). Colors indicate relative catch per unit effort (red = abundant, blue = rare). Horizontal bars separate clusters of typically co-occurring species. Vertical bars demarcate breaks in assemblage structure between years.

Pyrosomes: Catches of pyrosomes (warm-water pelagic tunicates) in research surveys in the "Core Area" off central California (Fig. 1.1) were higher in 2022 than in any year since sampling began in 1983, even greater than observed during the large marine heatwave years of 2015-2016 (Appendix H.2). Pyrosome catches in the Southern CCE were also high in 2022 relative to previous years, but catches north of Cape Blanco were relatively low.

3.3   SALMON

Juvenile salmon abundance: Catches of juvenile coho and Chinook salmon from June surveys in the Northern CCE (Fig. 1.1) are indicators of salmon survival during their first few weeks at sea. In 2022, catch-per-unit-effort of juvenile subyearling Chinook salmon, juvenile yearling Chinook salmon, and juvenile yearling coho salmon were close to time series averages (Fig. 3.6). Catches of juvenile salmon in these surveys have been variable over the past 5 years but do not suggest significant short-term trends.
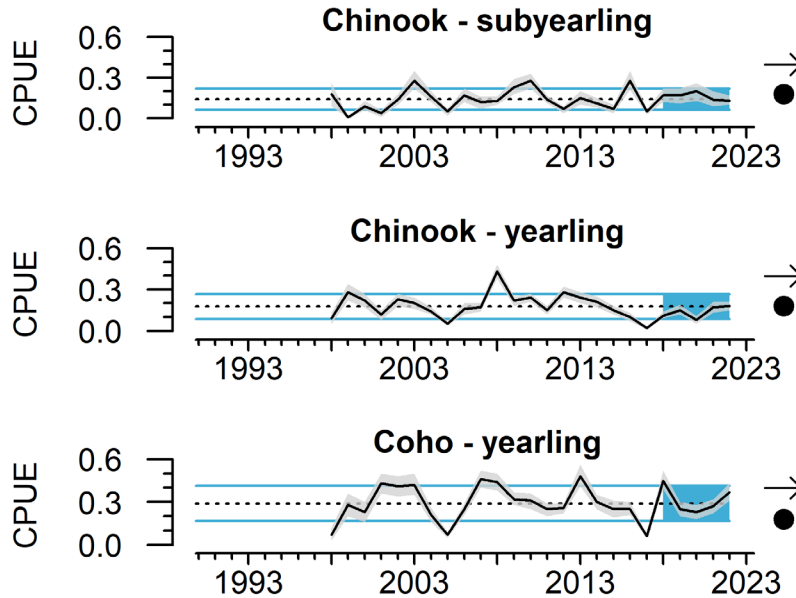
Figure 3.6: Catch per unit effort of juvenile salmon off Oregon and Washington in June, 1998-2022. Gray envelope indicates ±1 s.e. Lines, colors, and symbols are as in Fig. 2.1.

Stoplight tables: Long-term associations between oceanographic conditions, food web structure, and salmon productivity support qualitative outlooks of Chinook salmon returns to Bonneville Dam and smolt-to-adult survival of Oregon Coast coho salmon (Burke et al. 2013; Peterson et al. 2014). These relationships are depicted in the "stoplight table" in Table 3.1, which includes many indicators shown elsewhere in this report (PDO, ONI, copepods, etc.). Following discussions with the SSC, we made substantial changes to this stoplight table to make it more statistically sound and more clearly distinguish exceptional years (e.g., smolt year 2008 as a good year; 2015-2016 as bad years). Details on these improvements are in Appendix J.1.

In 2022, this suite of ecosystem indicators for the northern CCE was mixed, and may reflect "decoupling" of large-scale processes from local processes. The basin-scale climate and atmospheric indicators were consistent with cool and productive conditions that are typically highly favorable for juvenile salmon, but local physical conditions related to temperature and upwelling were relatively unfavorable and out of sync with the large-scale indices (Table 3.1). Biological indicators in 2022 were mostly intermediate. Marine conditions in 2022 were consistent with average survival for coho salmon returning to this area in 2023, relative to recent decades, but the decoupling of large-scale and local drivers suggests additional care when considering this qualitative outlook. For Chinook salmon returning to the Columbia Basin in 2023, indicators for the dominant smolt year (2021) reflect a mix of good and intermediate conditions. A related quantitative model that incorporates the indicators in Table 3.1 estimates above-average smolt-to-adult survival for most Chinook salmon returning to the Snake and Upper Columbia rivers in 2023, relative to the prior ten cohorts (Appendix J.2).

Table 3.1: Stoplight table of conditions for smolt years 1998-2022 for coho salmon originating in coastal Oregon and Chinook salmon from the Columbia Basin. Colors represent a given year's indicator relative to the reference period (1998-2020). Blue: >2 s.d. above the mean; green: >1 s.d. above the mean; yellow: ±1 s.d. of the mean; orange: >1 s.d. below the mean; red: >2 s.d. below the mean. Chinook salmon from smolt year 2021 and coho salmon from smolt year 2022 (outlined in blue) represent the dominant adult age classes in 2023.
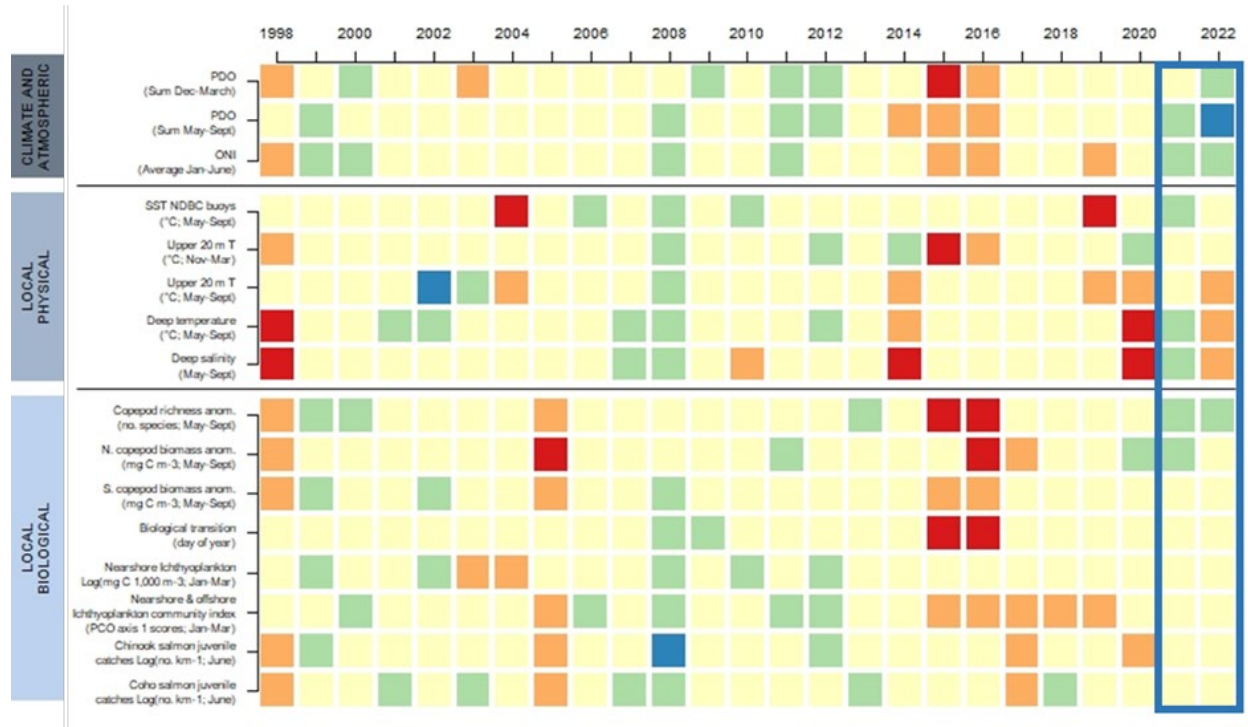
Table 3.2 is a similar indicator-based table that provides a broad ecosystem-based outlook for returns of natural-area Central Valley Fall Chinook salmon. Returns are correlated with fall egg incubation temperature and February streamflow in the Sacramento River, and the abundance and diet of common murres at Southeast Farallon Island (Friedman et al. 2019; details in Appendix J.3). For adults returning in 2023, signals are relatively unfavorable, within and across age classes. The dominant age class (age-3, from the 2020 brood year) had suboptimal egg incubation temperature and very poor winter flows for newly hatched juveniles (Table 3.2). All cohorts had unfavorably warm egg incubation temperatures (especially the 2021 cohort, which were smolts in 2022), and all but the 2018 cohort had very poor flow for juveniles. Common murre predation in recent years was near the long-term average, but that average is near zero (see Appendix M), and abundant anchovies in the Central CCE (Fig. 3.4) may be buffering salmon from murre predation. This table is best viewed as general qualitative context, as some underlying assumptions and descriptors require further data and validation (Appendix J.3); notably, the spawning escapement color designations assume an escapement goal of 122,000 natural adults, which is based on the MSY reference point in the FMP for natural + hatchery combined, but the SSC and STT have identified concerns with this value and recommended reviewing and updating it.

Table 3.2: Conditions for natural-area Central Valley fall Chinook salmon returning in 2023, from brood years 2018-2021. See text for explanation of indicators. Bold type indicates age-3 Chinook salmon, the dominant age class of returns to the Central Valley.

Spawning Escapement (t=0)	Incubation Temperature (Oct-Dec t=0)	February Median Flow (t+1)	Seabird Marine Predation Index (t+1)	Chinook Age in Fall 2023
2018: 71,689 (low)	11.7°C (poor)	21,700 cfs (high)	Near average	5
2019: 121,600 (met goal)	11.3°C (suboptimal)	6,030 cfs (very low)	Near average	4
2020: 100,100 (low)	**11.5°C (poor)**	**6,015 cfs (very low)**	**Near average**	**3**
2021: 73,230 (low)	13.0°C (very poor)	4,925 cfs (very low)	Near average	2

The Council's Habitat Committee, Salmon Technical Team, and others including CCIEA scientists have developed comprehensive stoplight tables for Central Valley spring Chinook salmon, Sacramento River fall Chinook salmon, and Klamath River Fall Chinook salmon. The tables feature indicators from throughout the stocks' life histories, spanning brood years 1983-2021. Indicators in recent years for the three stocks have been mixed (Appendix J.3). The 2021 brood years (smolts in 2023) in both systems experienced relatively poor freshwater conditions as eggs and fry.

Thiamine deficiency: Mantua et al. (2021) documented widespread thiamine deficiency as a stressor in Central Valley Chinook salmon, linked with the dominance of anchovy in the marine food web supporting these salmon (e.g., Fig. 3.4). Anchovies carry thiaminase, an enzyme that can destroy thiamine in the gut contents of its predators. Female Chinook salmon that consume large amounts of anchovy produce thiamine-deficient eggs. Effective treatments are being used at hatcheries, but there are no clear treatment options for naturally spawning populations. Thiamine deficiency may have negatively affected early survival for natural-origin Central Valley Chinook salmon from brood years 2019-2022; fortunately, eggs examined from regional hatcheries in 2020-2022 had thiamine levels that were low but generally above the level consistent with thiamine-dependent egg-to-fry mortality (data not shown). Thiamine deficiency is not represented in Table 3.2, but we may add it in the future.

3.4   GROUNDFISH

Stock abundance and fishing intensity: We regularly present the status of groundfish biomass and fishing pressure based on the most recent stock assessments. Except for Pacific whiting, there were no groundfish assessment updates in 2022, so indices for the

status of groundfish biomass and fishing pressure are essentially unchanged from last year's ESR. We will update that figure next year following the 2023 assessment cycle.

Juvenile abundance: Strong year classes can determine age structure and stock size for marine fishes, and may indicate favorable environmental conditions, increased future catches, or impending bycatch issues. In this year's ESR, we introduce estimates of juvenile abundance for West Coast groundfishes in the valuable DTS assemblage (Dover sole, thornyheads, and sablefish) as potential leading indicators of incoming year-class strength. This analysis uses catch data for post-settled juvenile size/age classes in the NOAA West Coast Groundfish Bottom Trawl Survey and a modeling approach commonly used in NOAA groundfish assessments. Details are in Appendix K.
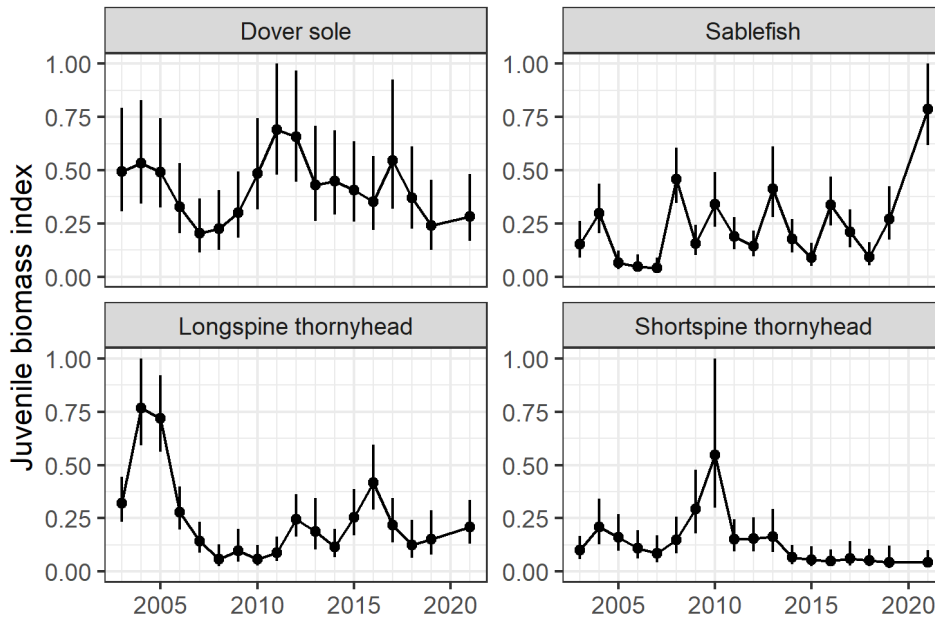

Figure 3.7: Biomass index (0-1) for selected juvenile groundfishes for 2003-2021. Error bars are 95% confidence intervals. No estimates were made for 2020 because the underlying survey was canceled due to COVID-19.

The age-0 sablefish biomass estimate increased sharply in 2021 (Fig. 3.7), suggesting a particularly strong age class and a possible leading indicator of future fishery recruitment. The 2021 peak corresponds with low springtime sea level north of Cape Mendocino, which had emerged previously as a good environmental indicator of sablefish recruitment (Appendix K). A strong 2021 year class was not predicted by the 2021 sablefish stock assessment, which included the sea level index through only 2020 (Kapur et al. 2021). Dover sole juvenile abundance was relatively low in 2021. The multiyear peaks earlier in the Dover sole time series occur in part because we had to combine age-1 and age-2 individuals to achieve acceptable model fits. Juvenile thornyhead abundance estimates have been relatively low over the most recent five years. Because thornyheads are difficult to age, we cannot connect peaks in a given year to specific cohorts.

3.5   HIGHLY MIGRATORY SPECIES (HMS)

Stock biomass and recruitment: Recent ESRs have featured stock assessment-based biomass and recruitment estimates for several HMS stocks that occur in the CCE. The only updates this year are for Pacific bluefin tuna and skipjack tuna. Biomass estimates for both stocks have increased in recent years, and bluefin tuna biomass was >1 s.d. above the time series average (Appendix L). Recruitment estimates were just below average for both stocks. Time series of biomass and recruitment estimates for all available HMS stocks through their most recent assessments are in Appendix L.

HMS diets: Last year, we introduced diet data for albacore tuna and swordfish to the ESR. Diet data from these opportunistic predators complement forage surveys, lend insight into how forage varies in space and time, and provide direct measures of forage use by HMS. An updated analysis of albacore stomachs provided by commercial and recreational fishers in Washington, Oregon and northern California through 2021 reveals that YOY anchovy, krill, saury, and YOY rockfishes were among the most important prey in recent years; the proportion of anchovy has declined since at least 2017, while saury increased (Fig. 3.8). By contrast, anchovy importance has been relatively high for swordfish off of southern California from 2017-2021, after being nearly absent from the diet before 2016 (Fig. 3.8). Pacific hake also were important to swordfish in 2021, while the importance of squid (both market squid and other squid species, which make up much of the "Other" category in Figure 3.8) has been declining. Additional information is in Appendix L.
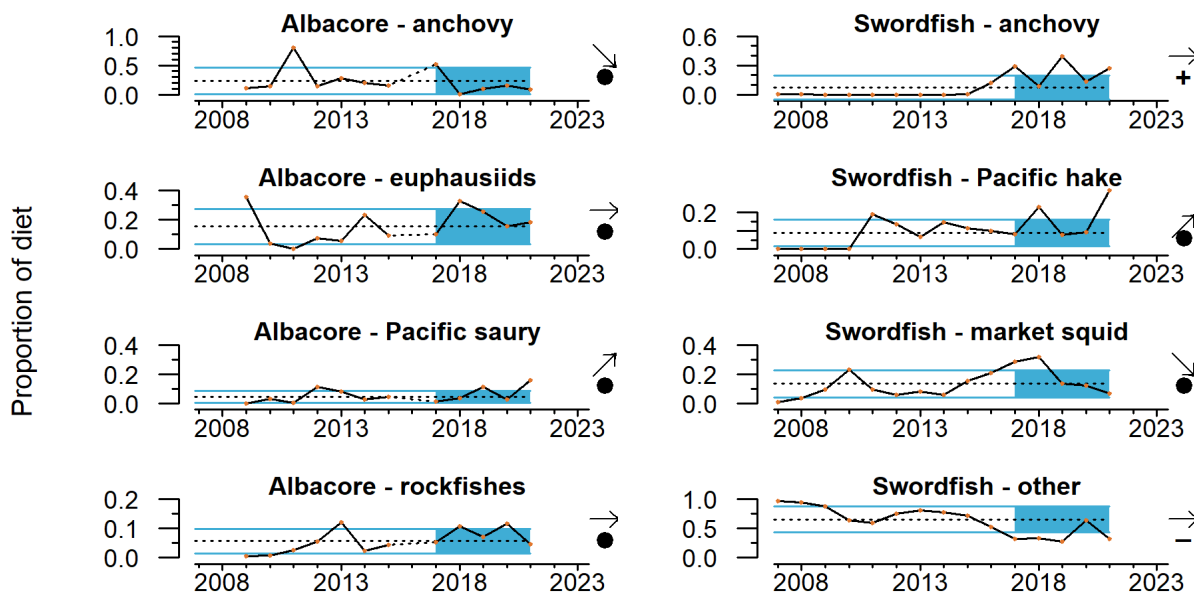

Figure 3.8: Diets of albacore (left) and swordfish (right) sampled from commercial and recreational fisheries in the CCE through 2021. Data are proportional abundances of four key prey classes for each predator. Lines, colors, and symbols are as in Fig. 2.1.

3.6   MARINE MAMMALS

Sea lion production: California sea lion pup counts and condition at San Miguel Island are responsive to changes in prey availability in the Central and Southern CCE, and are higher when energy-rich prey like sardines, anchovy or mackerel have high occurrence in adult female sea lion diets (Melin et al. 2012). Pup count relates to prey availability and nutritional status for gestating females from October to June. Pup growth from birth to age 7 months is related to prey availability to lactating females from June to February. These are robust indicators of prey quality and abundance even when the sea lion population is at or near carrying capacity (see Appendix L in Harvey et al. 2022).

NOAA conducted aerial counts of California sea lion pups in 2022, but data are not yet available. Sea lion pups were in good condition in October 2022: pup weights were nearly 1 s.d. above the long-term average, and similar to fall pup weights observed from 2016 to 2021 (Fig. 3.9). This implies good availability of high-quality prey during summer in the adult female foraging area (see Figure 1.1), which is consistent with estimates of high anchovy abundance in the Central and Southern CCE from 2016 to 2022 (Section 3.2; Appendixes H and I). Pup growth through February 2023 had not been measured as of this writing; we will provide an update when data are available.
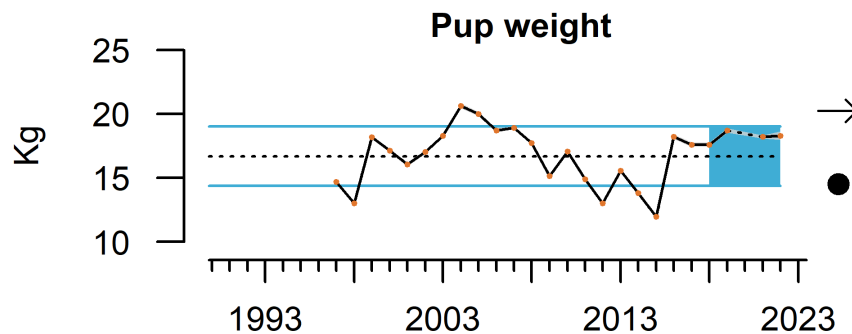

Figure 3.9: California sea lion pup weight in October on San Miguel Island for the 1997-2022 cohorts (no data in 2020). Lines, colors, and symbols are as in Fig. 2.1.

Whale entanglement: Reports of whale entanglements along the West Coast increased in 2014 and even more in the next several years, particularly for humpback whales. Based on preliminary data, West Coast entanglement reports remained higher in 2022 than pre-2014, but below the peak years of 2015-2018 (Fig. 3.10). Humpback whales continued to be the most common species reported. Most reports were in California, but reports involved gear from all three West Coast states; this includes confirmed reports from as far away as Mexico and Alaska. Reported entanglements in 2022 involved a range of sources, including commercial Dungeness crab gear from all three states, recreational hook and line gear, and unidentified gillnet fisheries. No entanglements in sablefish fixed gear or large mesh drift gillnet gear were confirmed in 2022.
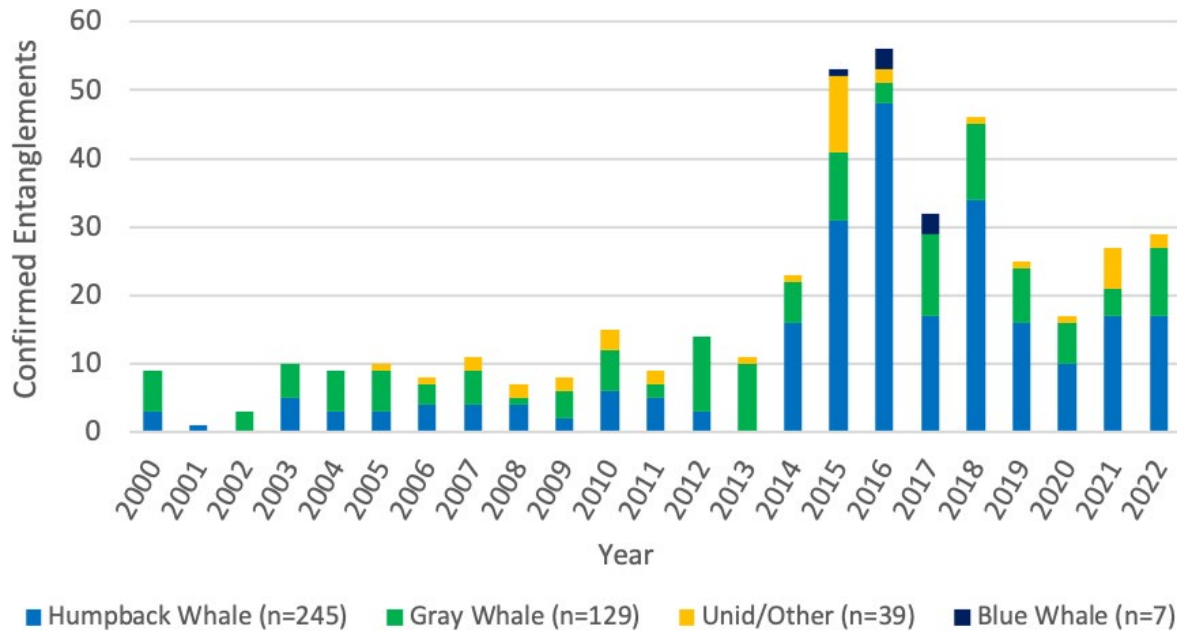
Figure 3.10: Numbers of whales reported as entangled in fishing gear along the West Coast from 2000-2022.

Many actions were taken in 2022 to reduce entanglement risk. California implemented early closures of the 2021/22 commercial and recreational Dungeness crab fisheries in response to multiple humpback whale entanglements in the spring of 2022. California also delayed its 2022/23 commercial and recreational Dungeness crab season openers due to entanglement risks. Washington and Oregon implemented late-season restrictions in the deployment of gear in the 2021/22 commercial Dungeness crab fisheries, while delays in the 2022/23 openings in these states were due to crab quality and domoic acid concerns. Other factors continue to present obstacles to risk reduction, including derelict gear, foraging by whales in nearshore waters, and growth of some whale populations.

3.7 SEABIRDS

Seabird indicators (productivity, density, diet, and mortality) reflect population health and condition of seabirds, as well as links to lower trophic levels and other conditions in the CCE. The species we report on here and in Appendix M represent a breadth of foraging strategies, life histories, and spatial ranges.

Fledgling production: Seabird colonies on Southeast Farallon Island off central California experienced average to above-average fledgling production in 2022 (Fig. 3.11). Short-term trends for these five colonies were either neutral, despite recent variability, or increasing in the case of pigeon guillemots. Just south at Año Nuevo Island, fledgling productivity among three seabird species was more mixed (Appendix M). Anchovies again dominated diets of piscivorous birds at both sites, while juvenile rockfish consumption continued to be below average (Appendix M).
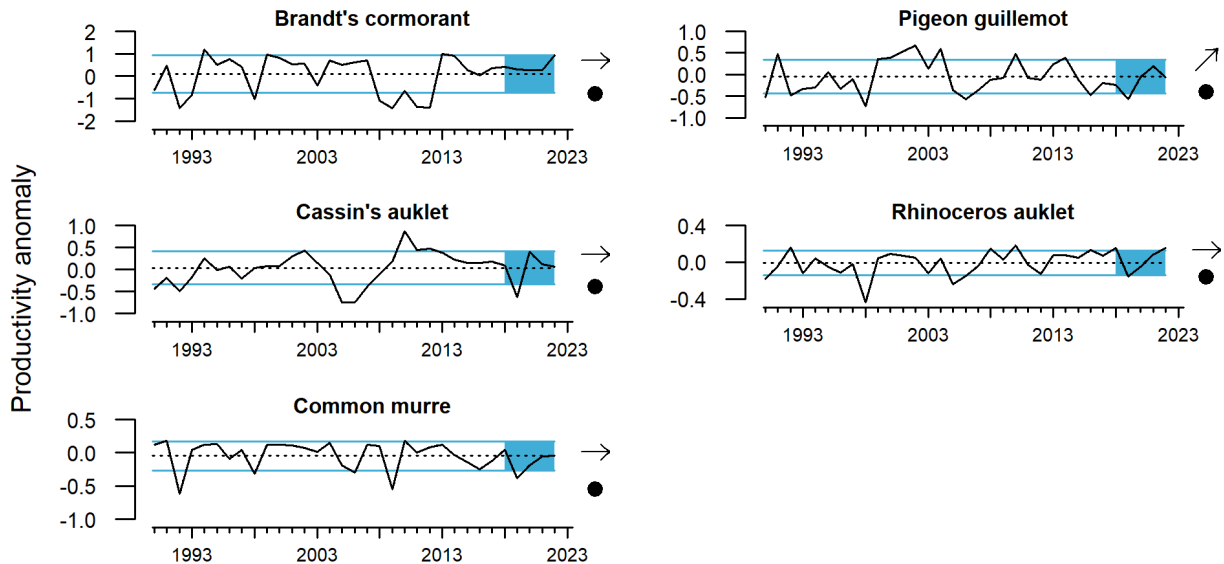
Figure 3.11: Standardized productivity anomalies (annual number of fledglings per pair of breeding adults, minus the long-term mean) for five seabird species on SE Farallon Island, 1990-2022. Lines, colors, and symbols are as in Fig. 2.1.

Further north at Yaquina Head, Oregon, fledgling production in 2022 was average for Brandt's cormorants, but common murres and pelagic cormorants experienced breeding failure due to bald eagle disturbance and predation (Appendix M).

At-sea densities: At-sea estimates of common murre and sooty shearwater densities were extremely low in the Northern CCE in spring of 2022 (Appendix M). The sooty shearwater density estimate was the lowest of the time series, which began in 2003. In contrast, at-sea densities of sooty shearwaters and common murres were above average in the Central CCE (Appendix M).

Mortality: Unusual mortality events were not evident in seabird indicator time series from the three West Coast beach monitoring programs in 2022 (Appendix M). However, a dramatic die-off of brown pelicans occurred off southern California in May-June 2022 that was attributed to starvation, even though anchovies were abundant (see Appendix M).

3.8   HARMFUL ALGAL BLOOMS (HABS)

Blooms of the diatom genus *Pseudo-nitzschia* can produce domoic acid, a toxin that can affect coastal food webs and lead to shellfish fishery closures when shellfish tissue levels exceed regulatory limits. Toxic blooms of *Pseudo-nitzschia* were active in 2022, despite negative PDO and La Niña conditions, leading to several shellfish fishery closures or delays. In late October 2022, a highly toxic bloom occurred off Oregon and Washington, which caused toxin levels in shellfish to rapidly rise above regulatory limits (Fig. 3.12), and closed razor clam fisheries along the entire Oregon and Washington coasts. Elevated domoic acid levels in razor clams in 2022 were again associated with a persistent northern California/ southern Oregon "hot spot" that began in 2015 (Trainer et al. 2020). Exceedances of domoic acid in Dungeness crab viscera were observed in southern Oregon prior to the 2022/23 commercial

fishing season, but not in Dungeness crab elsewhere (Fig. 3.12). Domoic acid levels in southern Oregon, high numbers of humpback whales on California crab fishing grounds, and low Dungeness crab meat yields in other regions resulted in delayed openings for the 2022/23 commercial Dungeness crab fishery in all three coastal states. Because crab fisheries are highly connected to many other fisheries on the West Coast, HAB impacts on crab fisheries can have indirect effects on participation in Council-managed fisheries. State-level details of HAB dynamics and fishery impacts are in Appendix N.
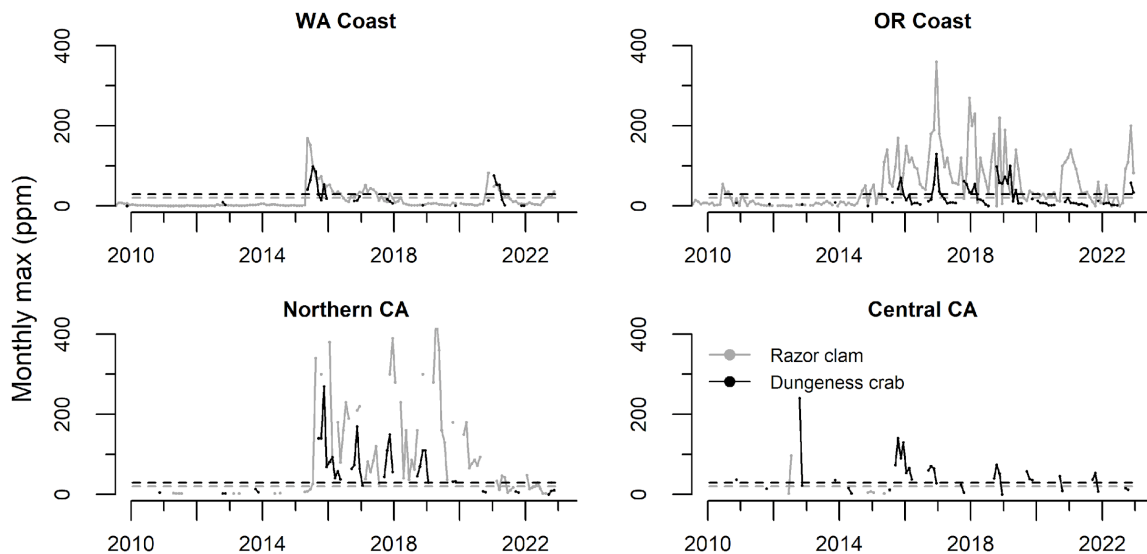

Figure 3.12: Monthly maximum domoic acid concentration in razor clams (gray solid lines) and Dungeness crab viscera (black solid lines) through 2022 for WA, OR, northern CA (Del Norte to Mendocino counties), and central CA (Sonoma to San Luis Obispo counties). Dashed lines are the management thresholds of 20 ppm (clams, gray) and 30 ppm (crabs, black).

4   FISHERIES LANDINGS, REVENUE, AND ACTIVITY

4.1   COASTWIDE LANDINGS AND REVENUE BY MAJOR FISHERIES

Total coastwide fishery landings in 2022 were close to the long-term mean for 1981-2020 (Fig. 4.1). Total landings in 2022 increased 11% from the relatively low levels in 2020 and 2021. This pattern largely tracks landings of Pacific whiting and market squid over the last five years. Landings from 7 of 9 commercial fisheries increased in 2022: HMS (111%), crab (36%), market squid (32%), other species (14%), non-whiting groundfish (11%), whiting (8%) and salmon (3%). In contrast, CPS finfish (-29%) and shrimp (-5%) landings decreased in 2022 from 2021. The most recent five-year status of Pacific whiting landings was above the long-term average, while salmon, CPS finfish, HMS and Other species landings were below long-term averages. Landings from market squid and shrimp fisheries increased over the last five years, while landings from crab fisheries decreased. State-by-state landings are presented in Appendix P.
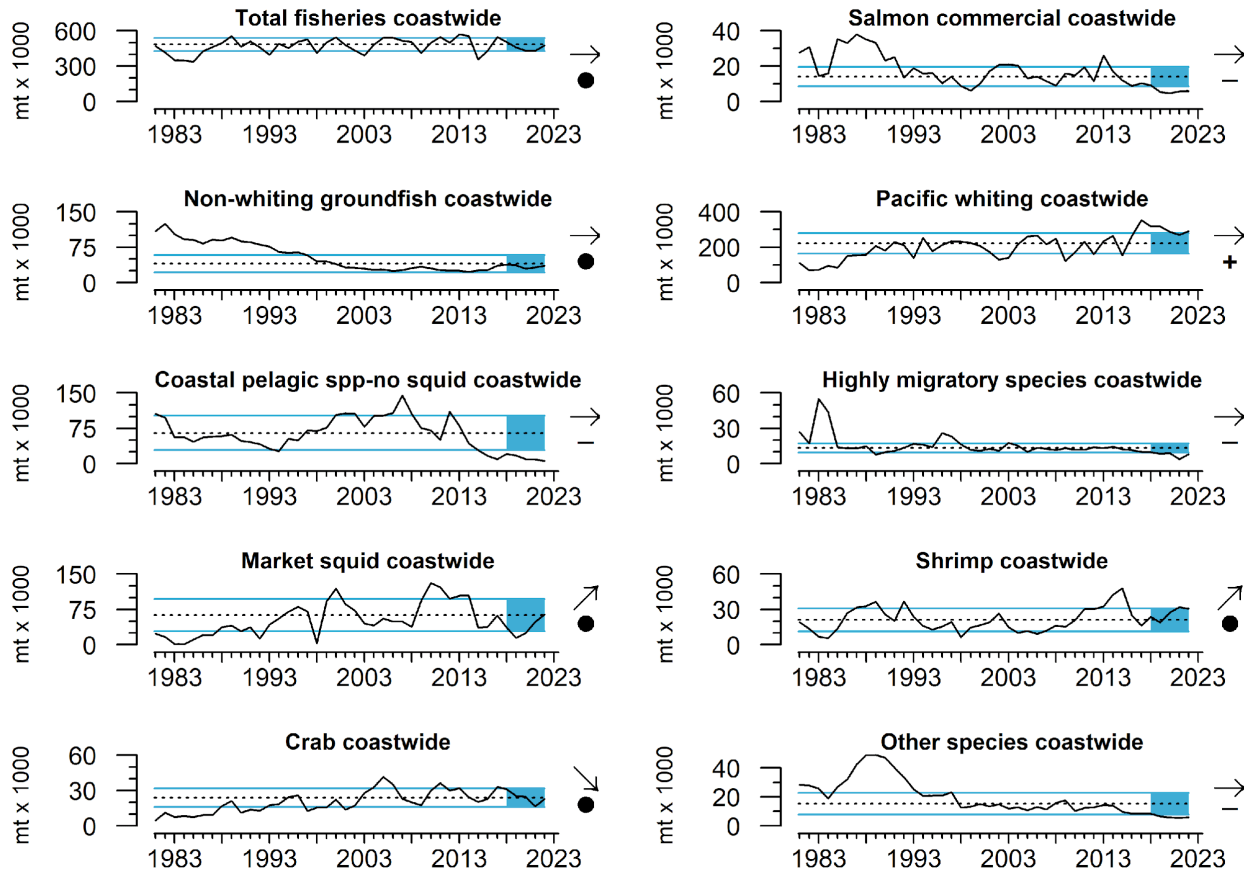
Figure 4.1: Annual landings from West Coast commercial fisheries, including total landings across all fisheries, from 1981-2022. Data were downloaded from PacFIN on January 10, 2023. Lines, colors, and symbols are as in Fig. 2.1.
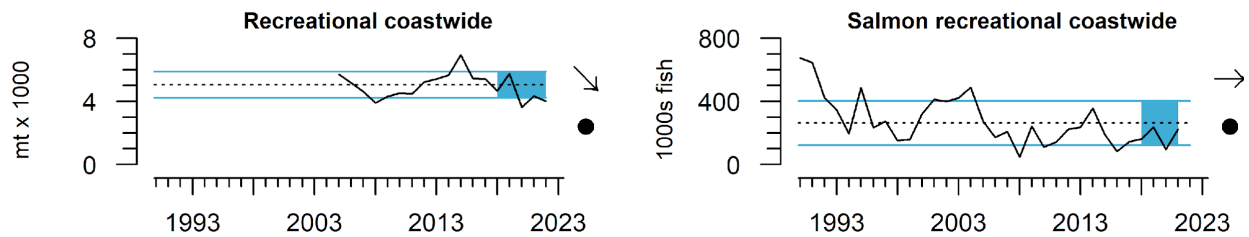
Figure 4.2: Annual landings from most West Coast recreational fisheries from 1981-2022 and from recreational salmon fisheries from 1990-2021. Data from 2022 are incomplete (see text). Lines, colors, and symbols are as in Fig. 2.1.

Recreational landings (excluding salmon, Pacific halibut and California HMS) are complete through October 2022 for California and Washington and September 2022 for Oregon. An overall decline in recreational landings has been ongoing since 2015, with one exceptional year in 2019 (Fig. 4.2, left). This can be attributed to widespread declines in landings for 8 of the 10 most-landed recreational species since 2015 (lingcod; albacore; black, vermilion and blue rockfish; yellowfin tuna; yellowtail; and chub mackerel) and unusually high albacore

landings in 2019. Coastwide recreational landings of Chinook and coho salmon, which are complete through 2021, have been highly variable but mostly within 1 s.d. of the long-term average over the most recent five years of data (Fig. 4.2, right). Estimates of recreational salmon landings in 2020 may be biased due to COVID-related restrictions on sampling in some months. State-level recreational landings are in Appendix P.

4.2   POTENTIAL INTERACTIONS BETWEEN FISHERIES AND OFFSHORE WIND ENERGY

New ocean-use sectors of the economy (e.g., renewable energy and aquaculture) are becoming a reality off the West Coast, particularly with new offshore Call Area and Wind Energy Area (WEA) designations. In this year's ESR, we focus on describing potential interactions between fisheries and NMFS scientific surveys with two offshore wind energy (OWE) Call Areas approximately 15 nm off the coast of Oregon[3]. Here, we present time series data that describe the temporal variation of commercial fishing effort and a suitability map that characterizes the combined spatial overlap of nine fisheries within the Call Areas' boundaries; in Appendix Q, we present time series data for revenue derived from landings within the Call Areas and further description of the spatial overlap of individual fisheries and NMFS surveys within the Call Areas. We used logbook and at-sea observer recorded set and retrieval coordinates, duration fished, and matched PacFIN fish ticket information from each fishery to estimate annual and cumulative fishing effort and revenue, summarized across both Call Areas and on a 2x2-km grid.
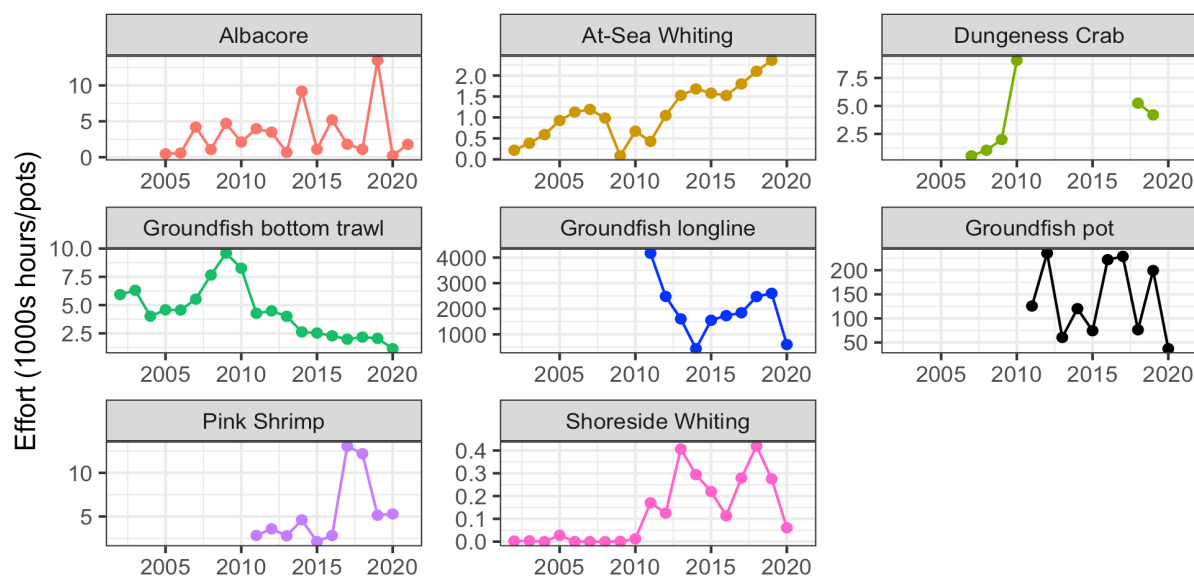
Figure 4.3: Annual commercial fishing effort within the two Oregon Call Areas, for years with available data. Effort is in: thousands of hours trawled or trolled for the groundfish bottom trawl, at-sea whiting, shoreside whiting, pink shrimp and albacore fisheries; thousands of pots set for the Dungeness crab fishery (empty years = analyses currently incomplete); and thousands of gear-hours soaked for groundfish longline and pot fisheries.

---

[3] https://www.boem.gov/renewable-energy/state-activities/Oregon

Commercial fishing effort has varied widely across the last two decades within the Oregon Call Areas for most fisheries, but particularly for albacore, groundfish pot, pink shrimp and shoreside-processed whiting (Fig. 4.3). The spatial use of these Call Areas has been steadily increasing for the at-sea whiting fleet, while steadily decreasing for the groundfish bottom trawl fleet over the last decade. Trends in revenue are detailed in Appendix Q.

We then used fishing effort and revenue data to calculate an overall suitability score for each grid cell within the two Call Areas (Fig. 4.4; see Appendix Q for methods and maps of individual fisheries). The nine fisheries included were: at-sea and shoreside whiting; groundfish bottom trawl, fixed-gear pot and fixed-gear longline; pink shrimp trawl; Dungeness crab; and commercial and charter albacore. Suitability scores near 1.00 (blue cells) are more suitable for OWE development relative to the spatial footprints of the nine fisheries, while scores near zero (orange cells) are less suitable due to greater overlap with fisheries. Large areas of the two Call Areas, particularly at depths between ~200 and ~500 m, are used heavily by fisheries, while the western half of the southern Call Area has relatively less overlap with fisheries.
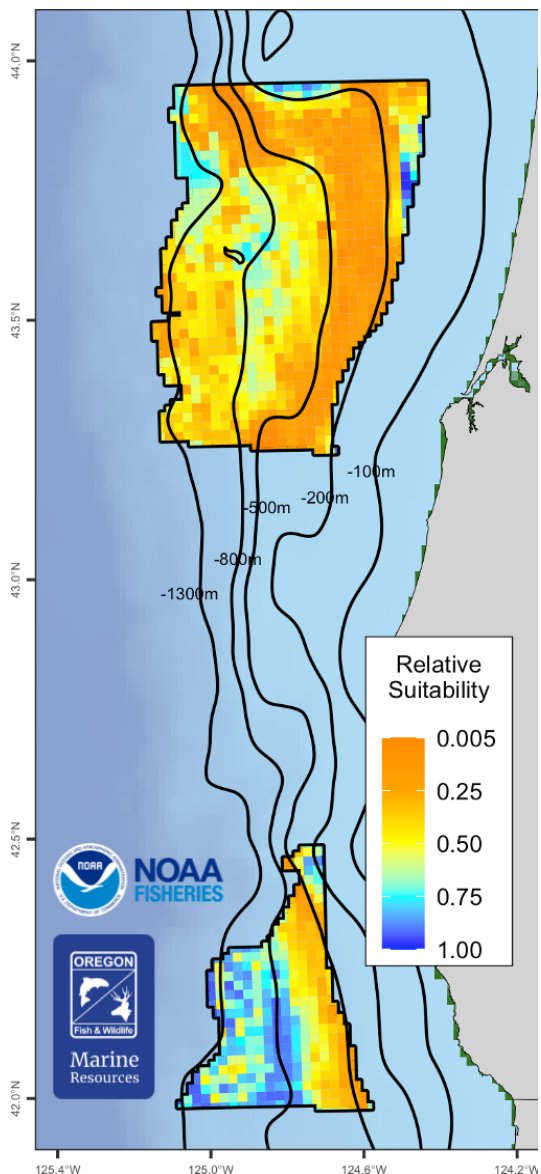
Figure 4.4: Overall relative suitability scores of 2x2-km grid cells within the Call Areas off Oregon. Scores near 1.00 (blue cells) are most suitable for offshore wind energy development relative to nine fisheries, while scores near zero (orange cells) are less suitable due to overlap with fisheries.

5   HUMAN WELLBEING

This section features indicators and analyses of human wellbeing, relating to the risk profiles and adaptive capacities of coastal communities in the face of various pressures. We are working to develop indicators that help track progress toward meeting National Standard 8 (NS-8) of the Magnuson-Stevens Act. NS-8 states that fisheries management measures should "provide for the sustained participation of [fishing] communities" and "minimize adverse economic impacts on such communities."

5.1   SOCIAL VULNERABILITY

Community vulnerability indices are generalized socioeconomic vulnerability metrics that allow for intra-community comparisons. The Community Social Vulnerability Index (CSVI) is a generalized metric that aggregates information from social vulnerability data (demographics, poverty, housing, labor force structure, etc.; Jepson and Colburn 2013). We monitor CSVI in communities that are highly reliant upon fishing. The commercial fishing reliance index reflects per capita engagement in commercial fishing (landings, revenues, permits, and processing) in each West Coast fishing community (n ≈ 250).
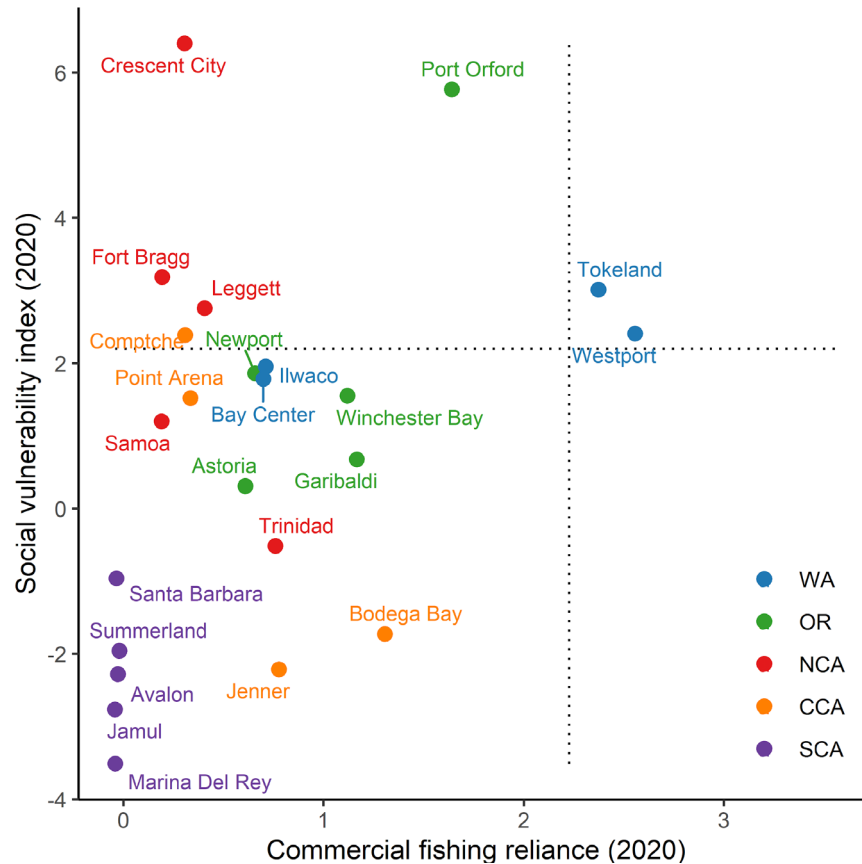
Figure 5.1: Commercial fishing reliance and social vulnerability scores in 2020 for communities in Washington, Oregon, and northern, central and southern California. The five highest-scoring communities for fishing reliance in each region are shown. Dotted lines equal 1 s.d. above the means for all communities.

Figure 5.1 plots CSVI in 2020 against commercial fishing reliance for communities that are among the most reliant on commercial fishing in different regions of the West Coast. Communities in the upper right quadrant have relatively high social vulnerability (vertical axis) and commercial fishing reliance (horizontal axis), and therefore may be especially socially vulnerable to downturns in commercial fishing. In 2020, Port Orford, OR and Tokeland, WA fell within the upper right quadrant, while Westport, WA was just outside. Details on these metrics, and on relationships between CSVI and total community-level commercial fishing engagement, are in Appendix R.

5.2 DIVERSIFICATION OF FISHERY REVENUES

Interannual revenue variability can be reduced by diversifying activities across multiple fisheries or regions, and more diversified fishers tend to have higher total revenue. Fishery diversification in the current fleet of vessels fishing along the West Coast and Alaska dropped in 2021 (the most recent year analyzed), and has declined since the early 1990s (Fig. 5.2a). Diversification declined for all categories of West Coast vessels (Fig. 5.2b-d). California, Oregon and Washington fleets each saw small decreases in average diversification in 2021 relative to 2020 (Fig. 5.2b). Additional details are in Appendix S.

Diversification can take other forms, such as spreading effort and catch throughout the year. This "temporal" form of diversification has also been trending down on the West Coast since 2015, following the onset of marine heatwaves and COVID-19 (Appendix S).
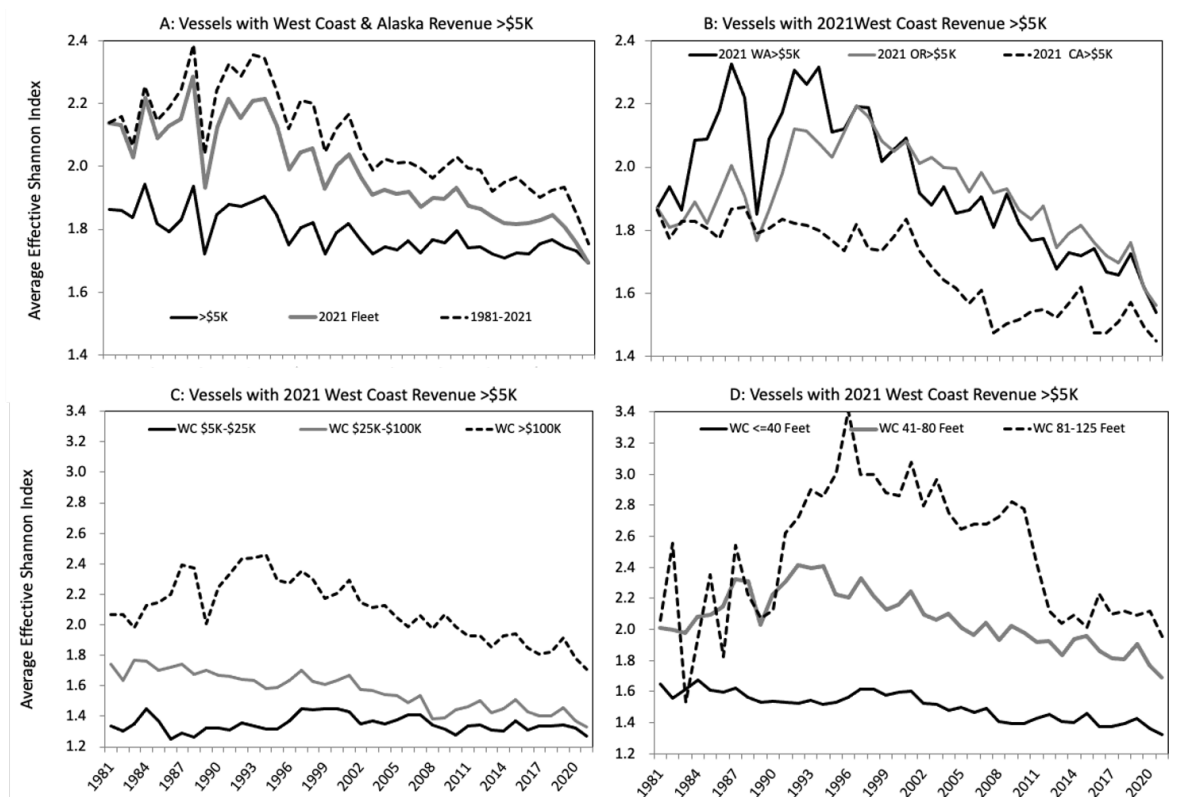
Figure 5.2: Average fishery diversification for West Coast and Alaskan fishing vessels (upper left) and for vessels in the 2021 West Coast fleet grouped by state (upper right), average gross revenue class (lower left) and length class (lower right).

5.3 PORT-LEVEL REVENUE CONCENTRATION

We use a metric called the Theil Index to assess geographic concentration of fishing revenues, at the scale of the 21 IO-PAC port groups defined by Leonard and Watson (2011). The index estimates the difference between observed revenue concentrations vs. what they would be if they were perfectly equally distributed across ports; higher values indicate greater concentration in a subset of ports.

Figure 5.3 shows annual Theil Index values for total commercial fishing revenue and six management groups. The total revenue trend is relatively flat over the 40-year time period, suggesting that total revenue has not experienced marked changes in geographic concentration. Between 2018 and 2021 (the most recent year analyzed), there was a slight increase in the total Theil Index.

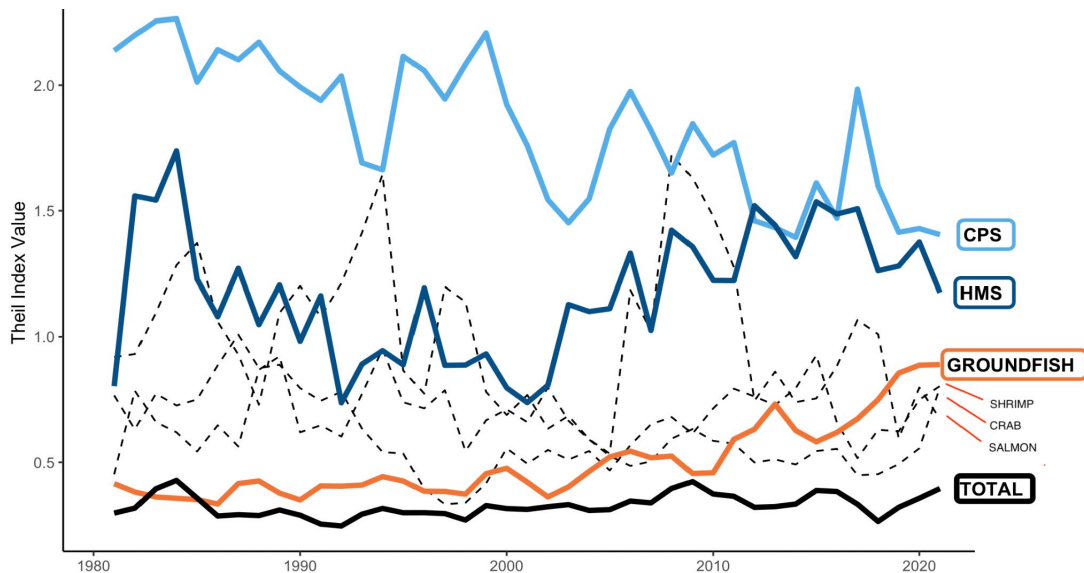*Figure 5.3: Theil Index of commercial fishery revenue concentration in West Coast IO-PAC port groups, 1981-2021. Increasing values indicate greater concentration of revenue in a smaller number of port groups. See text for descriptions of highlighted groups (total revenue, groundfish revenue, HMS revenue, and CPS revenue).*

Among individual management groups, CPS and HMS fisheries have had the highest Theil Index values for the last decade (Fig. 5.3), indicating relatively high concentrations of revenue in smaller numbers of port groups. We have updated the CPS index from last year's report to more accurately represent stocks in the CPS fishery management plan (details in Appendix T); this correction reveals a long-term decline in CPS revenue concentration (Fig. 5.3). HMS have a U-shaped trend, from high concentration of revenue in southern swordfish ports in the early 1980s, to more equal distribution in the 1990s, and back to high values in the 2000s as HMS revenues became concentrated in northern ports with substantial albacore fisheries. Theil values for groundfish have increased gradually for decades as revenue became concentrated in northern port groups. Other management groups are more variable over time. Additional information is in Appendix T.

5.4   FISHERIES PARTICIPATION NETWORKS

Fisheries participation network models (FPNs) represent how diversified harvest portfolios create connections between fisheries (Fuller et al. 2017, Fisher et al. 2021). Changes in network structure over time may reflect changes in fishing practices, ecology, management, markets, or other factors. In last year's ESR (Harvey et al. 2022), we showed how West Coast networks change in composition and connectivity over time, and how groundfish fisheries are connected to other fisheries in different IO-PAC port groups.

Here, we focus on potential vulnerability to declines in salmon fisheries. We define a port group that could be especially vulnerable to declines in the salmon fishery in the near future as one with high economic dependence on the salmon fishery, based on annual average salmon revenue over the past five years (Fig. 5.4a, vertical axis); and a low resilience index value, defined as below-average connectivity ("edge density") among all fisheries in the FPN for the port group over the past five years (Fig. 5.4a, horizontal axis). This follows published definitions of social vulnerability (e.g., Thiault et al. 2020), and invites consideration of the full cross-section of a port group that may be affected by changes in the salmon fishery (e.g., processors, deckhands, owners, captains, etc.).
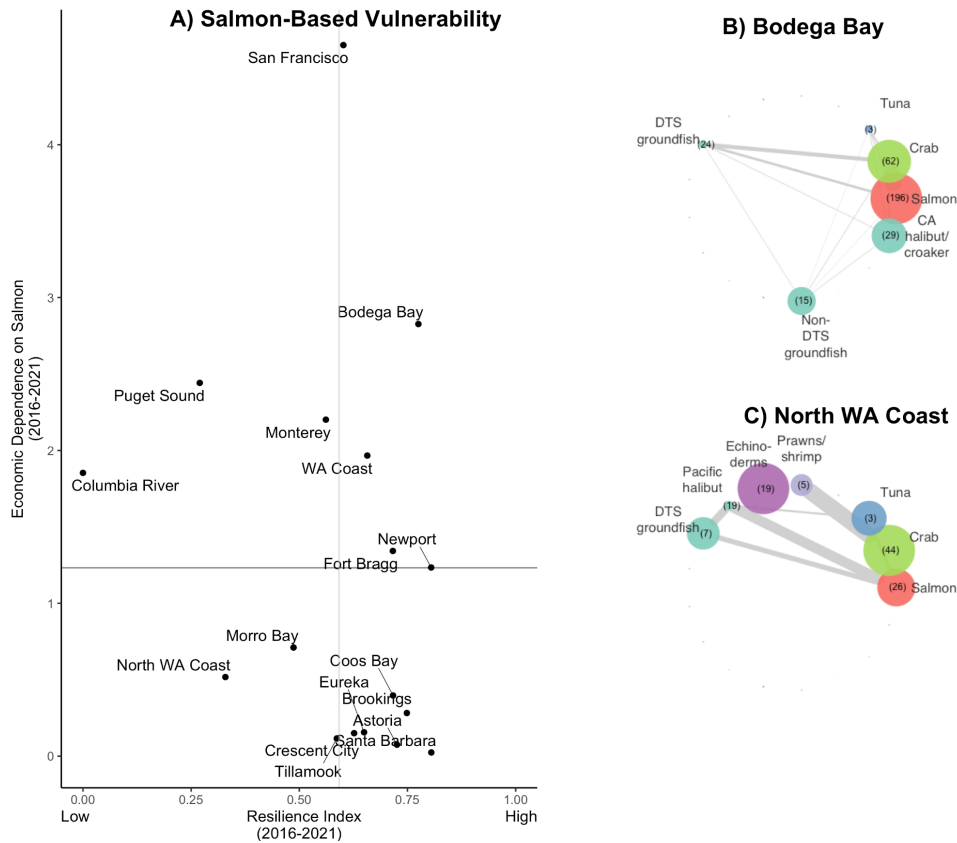
Figure 5.4: (A) Fisheries Participation Network (FPN) model metrics of overall port group fishery resilience (horizontal axis) and economic dependence on salmon (vertical axis) for IO-PAC port groups from the 2016/17 to 2021/22 fishing seasons. (B and C) FPNs for the Bodega Bay and North Washington Coast port groups, based on landings from 2020/21. Node size is proportional to the median contribution of the fishery to annual vessel-level revenue; values in parentheses are the number of vessels participating in the node; line thickness is proportional to the number of vessels participating in both fisheries, and to the evenness of revenue generated by each fishery in the pair.

Points in the upper left quadrant of Figure 5.4a (relatively high dependence and lower overall resilience) indicate port groups that would be most vulnerable to declines in the salmon fishery in the near future, while port groups in the lower right (low dependence and high resilience) would be least vulnerable. Port groups with high recent dependence on salmon and higher resilience (top right quadrant) have greater potential for adaptation, while those with lower economic dependence on salmon and lower resilience (lower left

quadrant) may have a reduced capacity to adapt to shocks in the salmon fishery if their economic dependence on salmon were to grow in the future.

Based on this framework and analysis, the Puget Sound, Columbia River, and Monterey port groups appear most vulnerable to near-future declines in the salmon fishery, while Morro Bay and the North Washington Coast (for reference, see FPN diagram in Fig. 5.4c) port groups are less exposed because of their lower recent economic dependence on salmon. The Bodega Bay (FPN diagram in Fig. 5.4b) and Washington Coast port groups are dependent upon salmon, but have greater potential to adapt to future declines in the salmon fishery given the high resilience index values in their FPNs, while the Brookings, Santa Barbara, Astoria, and several other port groups have high adaptation potential but relatively low recent salmon dependence, and are of lower concern overall for this reason. Future work to reveal the extent to which this vulnerability framework offers near-term, predictive insight into community-level impacts of shocks to the salmon fishery is possible. See Appendix T of Harvey et al. (2022) for further information on our work on FPNs.

6   SYNTHESIS

In many respects, 2022 was a mix of met and unmet expectations (Box 1.1, Appendix D). Basin-scale indices (negative PDO, La Niña) foretold a year of above-average productivity for many species groups, and indeed, the ecosystem got off to an encouraging start: strong upwelling gave rise to favorable springtime indicators for zooplankton, forage, and predators. On land, 2021/22 winter storms supplied good early snowpack. However, as the year progressed, we saw instances in which the mostly positive basin-scale conditions were modified or overridden by less favorable local conditions. In particular, frequent and lengthy upwelling relaxation events allowed intrusions of warm, less-productive conditions related to a major offshore marine heatwave. This was most evident in the north, with mid-summer declines in energy-rich copepods, below-average krill production, low densities of seabirds, warm early marine conditions for juvenile salmon, and HABs.

Thus, there was some disconnect of ecosystem responses from what we would typically expect, given our basin-scale indices of ocean conditions. Such decoupling has been documented recently throughout the Northeast Pacific (Litzow et al., 2020); it raises concerns because it may weaken resource assessments and forecasts that are grounded in old and potentially outdated ecological relationships (Szuwalski and Hollowed 2016). For example, Litzow et al. (2018) found breakdowns in statistical relationships between the PDO and other environmental signals in the Gulf of Alaska, which have complicated forecasts of Alaskan salmon survival.

Despite these disconnects, 2022 saw many instances of good productivity, notably the continuing high production of anchovy in the Central and Southern CCE. The system may retain further resilience built up in previous years, such as encouraging signals for Chinook salmon returns to the Columbia Basin, sablefish, and consistent forage structure in the Central and Southern CCE (see also Appendix O). As ever, ecological complexities and risk factors, such as poor hydrological conditions and thiamine deficiency effects on salmon, complicated outlooks and yielded mixed responses. We are also concerned by emerging

constraints for fishing communities, including declines in multiple forms of fishing diversification and potential conflicts with new sectors like offshore wind energy.

Climate change is a likely contributor to emerging disconnects between previously correlated environmental signals, and the threat of climate change must be noted again as we conclude the warmest year on record for the Northeast Pacific Ocean. This highlights the importance of improving climate prediction skills, and better understanding of how and why different species are likely to respond to novel conditions. As described in our "Climate Change Appendix" (Appendix E), ecosystem tools and information like this will be important for achieving the objectives of the new FEP Initiative, for managing species deemed vulnerable to climate change in the recently published West Coast climate vulnerability assessment (McClure et al. in press), and for supporting adaptation of West Coast fisheries and fishing communities to mitigate risks stemming from climate change and new ocean uses.

We are now moving into 2023 with new sets of expectations for the CCE. We anticipate a transition from this unusually long La Niña to ENSO-neutral conditions by April. The marine heatwave of 2022 is still present offshore, and is larger at this stage of the winter than most previous heatwaves. On land, late December and early January saw a series of "atmospheric rivers" deliver large amounts of precipitation to much of the West, with many regions receiving intense snows that may provide some drought relief. We also have lag effects and carryovers from recent years, like the enormous population of anchovy, still influencing species and fishery dynamics. We must be mindful of the potential emergence of novel interactions between large-scale and local dynamics as we develop hypotheses of how 2023 will unfold.

SUPPLEMENTAL MATERIALS to the 2022-2023 CALIFORNIA CURRENT ECOSYSTEM STATUS REPORT

Appendix A: LIST OF CONTRIBUTORS BY AFFILIATION

NWFSC, NOAA Fisheries Mr. Kelly Andrews, Dr. Brian Burke, Dr. Jason Cope, Dr. Blake Feist, Ms. Jennifer Fisher, Dr. Correigh Greene, Dr. Thomas Good, Dr. Chris Harvey (co-editor), Dr. Daniel Holland, Dr. Mary Hunsicker, Dr. Kym Jacobson, Ms. Su Kim, Dr. Stephanie Moore, Dr. Stuart Munsch, Dr. Karma Norman, Dr. Jameal Samhouri, Dr. Kayleigh Somers, Dr. Nick Tolimieri (co-editor), Mr. Curt Whitmire, Dr. Jen Zamon

AFSC, NOAA Fisheries Dr. Stephen Kasperski, Dr. Sharon Melin

SWFSC, NOAA Fisheries Dr. Eric Bjorkstedt, Dr. Steven Bograd, Dr. David Demer, Dr. Heidi Dewar, Ms. Lynn deWitt, Dr. John Field, Dr. Newell (Toby) Garfield, Dr. Elliott Hazen, Dr. Michael Jacox, Dr. Andrew Leising (co-editor), Dr. Nate Mantua, Mr. Josiah Renfree, Dr. Tanya Rogers, Mr. Keith Sakuma, Dr. Jarrod Santora, Dr. Kevin Stierhoff, Dr. Andrew Thompson, Dr. Brian Wells

California State Polytechnic University, Humboldt Ms. Roxanne Robertson

Oregon State University Dr. Jack Barth, Ms. Anna Bolm, Ms. Cheryl Morgan, Dr. Rachael Orben, Dr. Stephen Pierce, Ms. Jessica Porquez, Ms. Samantha Zeman

NOAA Fisheries West Coast Region Ms. Jennifer (Lilah) Isé, Mr. Dan Lawson, Ms. Lauren Saez

Pacific States Marine Fishery Commission Mr. Connor Lewis-Smith, Mr. Gregory Williams (co-editor)

University of California-San Diego Dr. Dan Rudnick, Dr. Rasmus Swalethorp

University of California-Santa Cruz Dr. Barbara Muhling, Dr. Catherine Nickels, Dr. Antonella Preti, Dr. Isaac Schroeder, Dr. Juan Zwolinski

California Department of Public Health Ms. Christina Grant, Mr. Duy Trong, Ms. Vanessa Zubkousky-White

California Department of Fish and Wildlife Ms. Christy Juhasz

CA Office of Env. Health Hazard Assessment Dr. Beckye Stanton

Oregon Department of Fish and Wildlife Mr. Justin Ainsworth, Dr. Caren Braby, Mr. Matthew Hunter, Ms. Delia Kelly, Ms. Jessica Watson

Washington Department of Fish and Wildlife Mr. Dan Ayres, Mr. Zachary Forster, Dr. Scott Pearson

Washington Department of Health Ms. Tracie Barry, Mr. Jerry Borchert

Beach Watch (Greater Farallones Association) Ms. Kirsten Lindquist, Ms. Jan Roletto

Coastal Observation and Seabird Survey Team Dr. Tim Jones, Dr. Julia Parrish

Farallon Institute Dr. William Sydeman, Ms. Sarah Ann Thompson

Oikonos Ecosystem Knowledge Ms. Danielle Devincenzi

Point Blue Conservation Science Dr. Jaime Jahncke, Dr. Mike Johns, Mr. Peter Warzybok

Appendix B: FIGURE AND DATA SOURCES FOR THE MAIN BODY

Figure 1.1: Map of the California Current Ecosystem (CCE) and U.S. west coast Exclusive Economic Zone (EEZ) created by B. Feist, NMFS/NWFSC. GIS layers of freshwater ecoregions derived from TNC & WWF (2008), based on Abell et al. (2008). EEZ boundary sourced from Flanders Marine Institute (2019).

Figure 2.1: Oceanic Niño Index data are from the NOAA Climate Prediction Center (https://origin.cpc.ncep.noaa.gov/products/analysis_monitoring/ensostuff/ONI_v5.php). PDO data are from N. Mantua, NMFS/SWFSC, and are served on the CCIEA ERDDAP server (https://oceanview.pfeg.noaa.gov/erddap/tabledap/cciea_OC_PDO.html). North Pacific Gyre Oscillation data are from E. Di Lorenzo, Georgia Institute of Technology (http://www.o3d.org/npgo/).

Figure 2.2: Standardized sea surface temperature anomaly plots were created by A. Leising, NMFS/SWFSC, using SST data from NOAA's optimum interpolation sea surface temperature analysis (OISST; https://www.ncdc.noaa.gov/oisst); SST anomaly calculated using climatology from NOAA's AVHRR-only OISST dataset. MHW conditions are delineated by values of the normalized SST + 1.29 SD from normal. Methods for tracking and classifying heatwaves are described in Thompson et al. (2019b) and at https://www.integratedecosystemassessment.noaa.gov/regions/california-current/cc-projects-blobtracker.

Figure 2.3: Newport Hydrographic (NH) line temperature data from J. Fisher, NMFS/NWFSC. Glider data along CalCOFI lines are from D. Rudnick, SIO/UCSD and obtained from https://spraydata.ucsd.edu/projects/CUGN/.

Figure 2.4: Daily 2022 values of BEUTI and CUTI are provided by M. Jacox, NMFS/SWFSC; detailed information about these indices can be found at https://go.usa.gov/xG6Jp.

Figure 2.5: Habitat compression index estimates developed and provided by J. Santora, NMFS/SWFSC, and I. Schroeder, NMFS/SWFSC, UCSC.

Figure 2.6: Newport Hydrographic (NH) line dissolved oxygen data are from J. Fisher, NMFS/NWFSC.

Figure 2.7: Snow-water equivalent data were derived from the California Department of Water Resources snow survey (http://cdec.water.ca.gov/) and the Natural Resources Conservation Service's SNOTEL sites in WA, OR, CA and ID

(http://www.wcc.nrcs.usda.gov/snow/). Data compilation and summary calculations by S. Munsch, NMFS/NWFSC, Ocean Associates, Inc.

Figure 2.8: Minimum and maximum streamflow data were provided by the US Geological Survey (http://waterdata.usgs.gov/nwis/sw). Data compilation and summary calculations by S. Munsch, NMFS/NWFSC, Ocean Associates, Inc.

Figure 3.1: Copepod biomass anomaly data provided by J. Fisher, NMFS/NWFSC.

Figure 3.2. Krill data were provided by E. Bjorkstedt, NMFS/SWFSC, Cal Poly, Humboldt and R. Robertson, Cooperative Institute on Marine Ecosystems and Climate (CIMEC) at Cal Poly, Humboldt.

Figure 3.3: Pelagic forage data from the Northern CCE from B. Burke, NMFS/NWFSC and C. Morgan, OSU/CIMRS. Data are derived from surface trawls taken during the NWFSC Juvenile Salmon & Ocean Ecosystem Survey (JSOES; https://www.fisheries.noaa.gov/west-coast/science-data/ocean-ecosystem-indicators-pacific-salmon-marine-survival-northern).

Figure 3.4: Pelagic forage data from the Central CCE were provided by J. Field, K. Sakuma, T. Rogers, and J. Santora, NMFS/SWFSC, from the SWFSC Rockfish Recruitment and Ecosystem Assessment Survey (https://go.usa.gov/xGMfR).

Figure 3.5: Pelagic forage larvae data from the Southern CCE were provided by A. Thompson, NMFS/SWFSC, from spring CalCOFI surveys (https://calcofi.org/); data were not collected in 2020 due to survey cancellations associated with the COVID pandemic.

Figure 3.6: Data for at sea juvenile salmon provided by B. Burke, NMFS/NWFSC and C. Morgan, OSU/CIMRS, from surface trawls taken during the NWFSC Juvenile Salmon and Ocean Ecosystem Survey (JSOES).

Figure 3.7: Estimates of juvenile abundance for West Coast groundfish were provided by N. Tolimieri, NMFS/NWFSC based on data from the NOAA West Coast bottom trawl survey (https://www.fisheries.noaa.gov/west-coast/science-data/us-west-coast-groundfish-bottom-trawl-survey).

Figure 3.8: Swordfish and juvenile albacore diet data provided by H. Dewar and C. Nickels, NMFS/SWFSC, and A. Preti, UCSC.

Figure 3.9: California sea lion data provided by S. Melin, NMFS/AFSC.

Figure 3.10: Whale entanglement data provided by D. Lawson and L. Saez, NMFS/WCR.

Figure 3.11: Seabird fledgling production data at nesting colonies on Southeast Farallon provided by J. Jahncke and P. Warzybok, Point Blue Conservation Science.

Figure 3.12: WA domoic acid data are provided by the Washington State Department of Health, OR data from the Oregon Department of Agriculture, and CA data from the California Department of Public Health.

Figure 4.1: Data for commercial landings are from PacFIN (http://pacfin.psmfc.org) and NORPAC (North Pacific Groundfish Observer Program).

Figure 4.2: Data for recreational landings are from RecFIN (http://www.recfin.org/) and the CDFW Pelagic Fisheries and Ecosystem Data Sharing index.

Figure 4.3: Data for annual commercial fishing effort within BOEM Call Areas off Oregon were compiled by NMFS/NWFSC based on logbook data from ODFW, SWFSC, and NWFSC West Coast Groundfish and At-Sea Hake Observer Programs. Boundaries of Call Areas from BOEM (https://www.boem.gov/renewable-energy/state-activities/Oregon). Figure created by K. Andrews and B. Feist, NMFS/NWFSC.

Figure 4.4: Data for annual commercial fishing revenue attributed to landings within BOEM Call Areas off Oregon were compiled by NMFS/NWFSC based on logbook data from ODFW, SWFSC, & NWFSC West Coast Groundfish and At-Sea Hake Observer Programs and matched to PacFIN fish ticket information by ODFW & NWFSC. Boundaries of Call Areas from BOEM (https://www.boem.gov/renewable-energy/state-activities/Oregon). Figure created by K. Andrews and B. Feist, NMFS/NWFSC.

Figure 5.1: Community social vulnerability index (CSVI) and commercial fishery reliance data provided by K. Norman, NMFS/NWFSC, and C. Lewis-Smith, NMFS/NWFSC, PSMFC, based on data from the US Census Bureau's American Community Survey (ACS; https://www.census.gov/programs-surveys/acs/) and PacFIN (http://pacfin.psmfc.org), respectively.

Figure 5.2: Fishery revenue diversification estimates were provided by D. Holland, NMFS/NWFSC, and S. Kasperski, NMFS/AFSC, utilizing data provided by PacFIN (http://pacfin.psmfc.org) and AKFIN (https://akfin.psmfc.org)..

Figure 5.3: Theil Index values for annual geographic concentration of commercial fishery revenues were provided by K. Norman, NMFS/NWFSC, and C. Lewis-Smith, NMFS/NWFSC, PSMFC, based on data from PacFIN (http://pacfin.psmfc.org).

Figure 5.4: Fishery Participation Network data and analyses provided by J. Samhouri, NMFS/NWFSC, based on data from PacFIN (http://pacfin.psmfc.org).

Table 3.1: Stoplight table of indicators related to salmon in the northern CCE courtesy of B. Burke, J. Fisher, and K. Jacobson, NMFS/NWFSC, and C. Morgan and S. Zeman, OSU/CIMRS (https://www.fisheries.noaa.gov/west-coast/science-data/ocean-ecosystem-indicators-pacific-salmon-marine-survival-northern).

Table 3.2: Table of indicators and qualitative outlook for 2023 Chinook salmon returns to the Central Valley courtesy of N. Mantua and B. Wells, NMFS/SWFSC.

Appendix C: CHANGES IN THIS YEAR'S REPORT

Below we summarize major changes in the 2022-2023 ESR. As in past reports, some changes are in response to requests and suggestions received from the Council and advisory bodies (including those from FEP Initiative 2, "Coordinated Ecosystem Indicator Review"), or in response to annual reviews of indicators and analyses by the SSC Ecosystem Subcommittee (SSC-ES). We also note items we have changed and information gaps that we have filled since last year's report (Harvey et al. 2022).

Request/Need/Issue	Response/Location in Document
The ESR is labor-intensive to produce, and efficiencies such as automation are needed to sustain the report and build it out to meet evolving needs of the Council and other partners. *(March 2022, Agenda Item H.2.b, Supplemental EWG Report 1)*	This ESR was produced in Bookdown, an open-source package in the R programming language, which enables more seamless incorporation of text and figures; automated updates of figures and descriptive details; and better version control and editing, compared to what we used in past reports. We also improved our internal process for submitting data and metadata. We will continue to build on these tools, which should improve ESR efficiency and reproducibility in years to come. These tools will also be compatible with developing more real-time, web-based indicator updates, as called for in the FEP (PFMC 2022). One outcome of using Bookdown is that the appearance and layout of this ESR is different from past years. However, it adheres to the specifications stated in the FEP: "The Council asked that the report...be bounded in terms of its size and page range to about 20 pages in length, *or the equivalent word and figure limit*" (PFMC 2022, emphasis added). This report's main body is 32 pages, but it has similar total content to a ~20 page report (7990 words in the main body text, compared to 7899 words in Harvey et al. (2022); 31 figures and tables in this report, compared to 32 in Harvey et al. (2022)). The figures and tables are now larger and easier to read.
COVID-19 impacts on West Coast surveys and related research	In Section 1 of our last two ESRs, we summarized COVID-19 impacts on research efforts. We removed that section for word count considerations. COVID-19 had far fewer effects on research in 2022. COVID-related effects on surveys, sample processing, and data are noted in the ESR as needed. We acknowledge that uncertainty in some indicators has been exacerbated by COVID-driven constraints on research.
General improvements to climate and ocean drivers figures and analyses	The ESR has many improvements to figures and coverage of key topics in the climate and ocean drivers sections. These include: • Added Spring and Fall SSTa map figures, Appendix F.1 • Improved subsurface temperature anomaly plots based on glider data for the Newport Line, Trinidad Line, and CalCOFI lines 66.7, 80, and 90. See Appendix F.1

	• Added Habitat Compression Index plots for summer and fall 2022 in Appendix F. • Added summary maps of sea surface temperature anomalies for spring and fall (previously only had summer and winter) in Appendix F
Benthic dissolved oxygen maps are missing this year	Due to lack of preparation time, maps of minimum dissolved oxygen concentrations over the Oregon and Washington shelf were not available this year for inclusion in Appendix F.
Expanded CPS information	In last year's ESR, we included for the first time information from NMFS SWFSC's acoustic and trawl surveys of CPS. We enhanced that content this year in Appendix I, with new figures on estimated total biomass of key CPS in the survey area and maps of stock distributions over time. The section also includes a description of survey methods modifications in 2022.
Refinements to salmon stoplight tables and suite of indicators *(long standing point of discussion with CCIEA team, SSC, and other advisory bodies, and with feedback from SSC-ES review in September 2022)*	The CCIEA team and SSC agreed in March 2022 that the salmon indicator suite should be reviewed by the SSC-ES in September 2022. Based on the review, we made several changes: • Stoplight tables of indicators of salmon growth and survival conditions have been refined to be more statistically robust. Details of changes are in Appendix J.1. • We added a stoplight table for natural-origin Sacramento River Spring Chinook salmon. See Appendix J.3. • We removed escapement time series from the ESR, except as used in stoplight tables. We also streamlined hydrology indicators: in recent ESRs we analyzed streamflow by ecoregion, and at the finer scale by Chinook salmon ESU. Given the ESR's intended broad scope, we will no longer include hydrology time series at the ESU scale, except as used in stoplight tables. Details are in Appendix J.1.
The report needs indicators of groundfish recruitment *(requested by GMT and SSC during FEP Initiative 2 process)*	In this ESR, we introduce annual indexes of the abundance of post-settled juvenile groundfish in the DTS complex, based on data from the NMFS West Coast Groundfish Bottom Trawl Survey and modeling tools that have been reviewed by the SSC and used in West Coast stock assessments. These estimates may prove to be good leading indicators of recruitment into the fishery. The analyses are in Section 3.4 and Appendix K.
The report needs HMS information, including links between HMS and CCE prey *(requested by EWG during FEP Initiative 2 process)*	In our last ESR, we introduced data from fishery-dependent sampling of albacore stomachs from 2009-2021. This year we update that dataset and also present data from fishery dependent sampling swordfish stomachs from 2007-2021 (see Section 3.5 and Appendix L). In future ESRs, we may add additional species, though sample processing has been severely delayed by COVID-19, and is foreseeably likely to lag for at least one year due to staffing limitations.

Delays in marine mammal sample processing	Due to delays in aerial survey image processing, sea lion pup counts were not available yet for this year's ESR, thus Figure 3.9 includes only pup weights.
Offshore wind energy is likely to emerge as a major human activity in the CCE	In last year's ESR, we introduced analyses that mapped the potential overlap between groundfish bottom trawling activity and wind energy areas off California and prospective wind energy development zones in Oregon. We updated the analysis to feature time series of effort and revenue from multiple fisheries that would be affected by the Oregon Call Areas (Section 4.2, Appendix Q.1). We also developed maps of overlap between the Oregon Call Areas and multiple NOAA biological and oceanographic surveys (Appendix Q.2). These analyses have been provided to the Marine Planning Committee.
Changes in fishery participation networks analysis	Last year's ESR featured analysis of fishery participation network variation over time and the connections between groundfish fisheries and other fisheries in different port groups. In this ESR, we conducted fishery participation network analysis to explore the potential resilience of port groups to future shocks to salmon fishing (Section 5.4). We also did not believe a fishery participation network appendix was needed in this year's report.
Advance progress within the "Climate Change Appendix" (*response to feedback from the Council and advisory bodies, and with feedback from SSC-ES review in September 2022*)	In March 2022 the CCIEA team added an appendix to the ESR on "developing indicators of climate change". In September 2022 the CCIEA team gave an additional presentation to the SSC-ES on furthering the material within this appendix. Based on feedback from those two meetings, the current "climate change appendix" (Appendix E) has been updated, mostly with the goal of continuing the "conversation" between the council and the IEA-ESR team in terms of how to advance towards providing indices of climate change that would be useful to management through the ESR. This year's installment includes three sections: 1) a review of key terms, and lists of indices that could be used for providing climate-related information; 2) a discussion of how indices could be operationalized for use in the ESR; and 3) a discussion of next steps and possible ways in which climate-related indices would be incorporated into future installments of this appendix.
Council interest in condensing multiple indices into a single more descriptive index of ecosystem state	In response to interest from the Council and several advisory bodies, the CCIEA team has engaged in research to take information from a large number of indicators and reduce them down to a smaller number of indexes that can summarize overall changes in ecosystem state and potentially provide early warnings of pending changes in ecosystem structure and function. This information has been added as Appendix O.

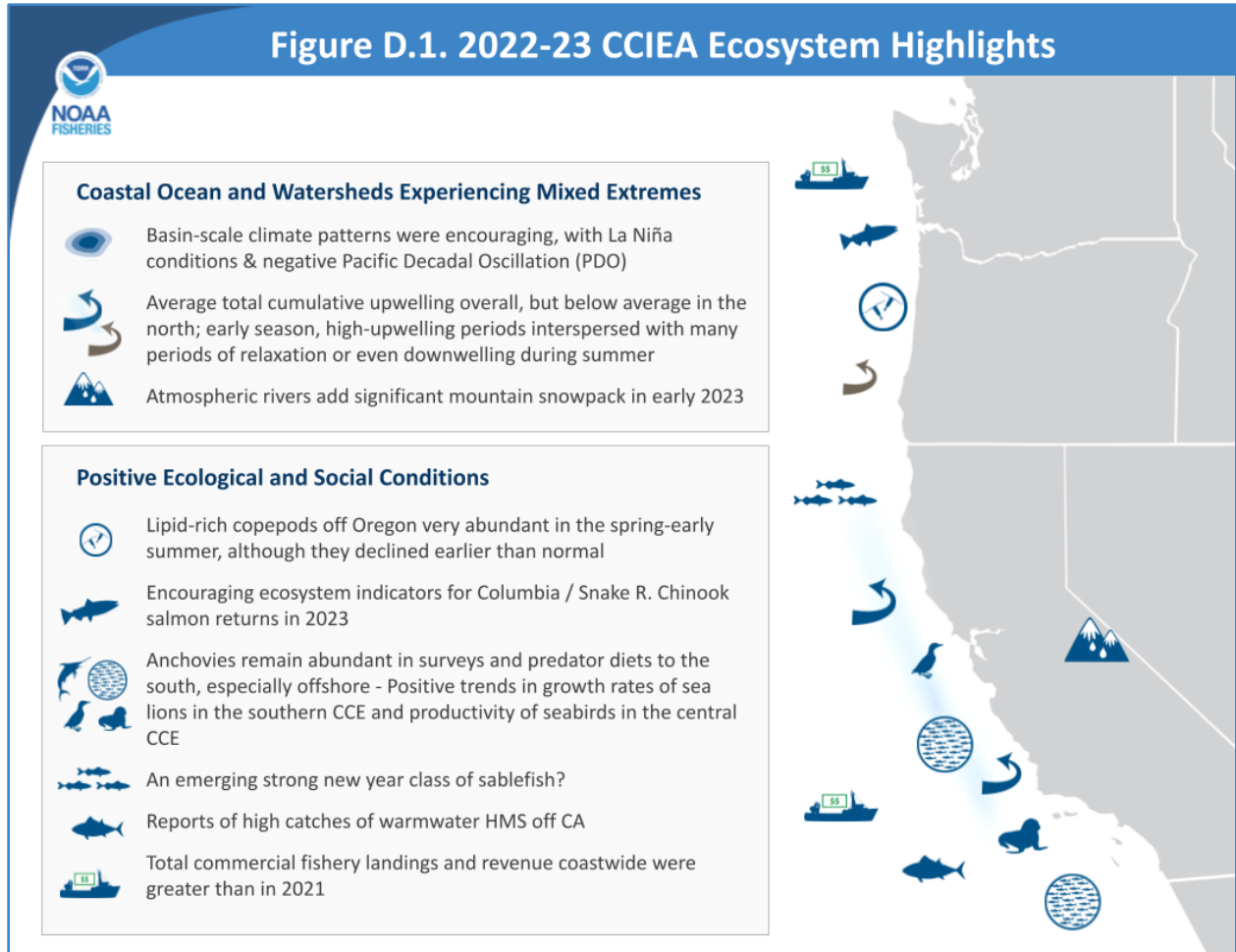# Appendix D: SUMMARY INFOGRAPHICS FOR THE 2022-2023 ECOSYSTEM STATUS REPORT

Figure D.1. 2022-23 CCIEA Ecosystem Highlights

Coastal Ocean and Watersheds Experiencing Mixed Extremes

Basin-scale climate patterns were encouraging, with La Niña conditions & negative Pacific Decadal Oscillation (PDO)

Average total cumulative upwelling overall, but below average in the north; early season, high-upwelling periods interspersed with many periods of relaxation or even downwelling during summer

Atmospheric rivers add significant mountain snowpack in early 2023

Positive Ecological and Social Conditions

Lipid-rich copepods off Oregon very abundant in the spring-early summer, although they declined earlier than normal

Encouraging ecosystem indicators for Columbia / Snake R. Chinook salmon returns in 2023

Anchovies remain abundant in surveys and predator diets to the south, especially offshore - Positive trends in growth rates of sea lions in the southern CCE and productivity of seabirds in the central CCE

An emerging strong new year class of sablefish?

Reports of high catches of warmwater HMS off CA

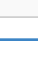Total commercial fishery landings and revenue coastwide were greater than in 2021

Figure D.2. 2022-23 CCIEA Ecosystem Highlights

Unfavorable Conditions/Risk Factors

Ocean Temperature & Marine Heatwave: 4th largest marine heatwave on record since 1982, with episodic intrusions into US EEZ in 2022, consistent with trend of overall ocean warming in the NEP

Terrestrial Disturbances: A dry spring in 2022 contributed to low snowpack and continued drought. Extreme weather in early 2023

California Chinook Salmon: Very poor freshwater conditions for 2023 smolt classes, and thiamine deficiency impacts in Central Valley natural-area fish.

Pyrosomes: record high observations off Central California

At-sea bird densities: very low concentrations of sooty shearwaters and murres off Oregon and Washington

Hypoxia: Near-bottom hypoxia during summer off OR; dissolved oxygen levels off soCA lower than previous year

Whale Entanglement: Still above-average in 2022

Mixed Ocean Uses: Potential constraints of offshore wind on fishing and research are coming into focus

Fishery Landings & Revenue: Fishing portfolios continue to be less diversified, both in target species and total weeks fished

HABs: Uptick in HAB activity in late 2022 led to shellfish fishery closures or delays

Appendix E: DEVELOPING INDICATORS OF CLIMATE CHANGE

This installment of the "climate change appendix" continues the ongoing "conversation" between the CCIEA team and the Council as to how information in the regular annual ESR to the Council could include considerations of current and future climate change impacts. This effort stems from a recommendation by the EAS that the CCIEA team could incorporate climate change information into the ESR for Council management considerations (Supplemental EAS Report 1, March 2021, Agenda item I.2.b). Any such future climate change information that we could provide will necessarily hinge on the CCIEA's stock in trade: indices of various ecosystem parameters, interpretive analyses and narratives, and (where possible) information on the ability to make skilled forecasts or future projections. We are eager to incorporate this type of information further into our reports, as Council needs, CCIEA team workload, and page limits allow.

This second iteration of the climate change appendix is divided into three parts: first, we review our efforts so far, including a review of some of the materials presented to the Council's SSC-Ecosystem Subcommittee during the September 2022 Council meeting. Second, we offer further examples of how various indices could be moved towards operational status for use in the ESR. Third, we discuss the direction of where our next efforts may lie.

E.1 Review of efforts to date

In our last installment, and at the September SSC-ES review, we introduced several key concepts which we reiterate here, noting that it is critical to understand different time scales of predictability, what predictions are based on, and the sources of uncertainty (Fig. E.1). This helps to clarify the types of information that forecasting tools are capable (or incapable) of providing to support fisheries activities and management.
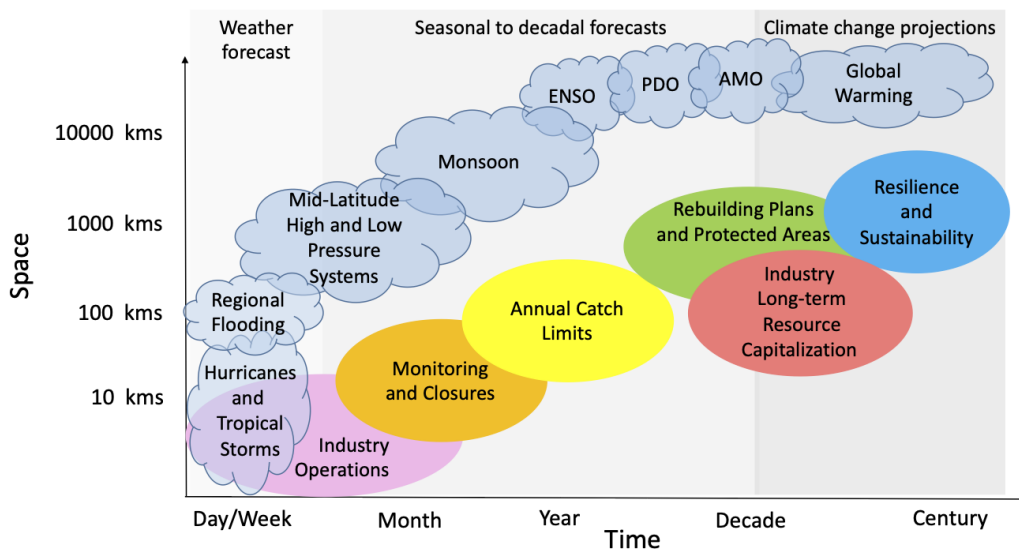

Figure E.1: Time and space scales of climate and weather variability, and fisheries-related activities and decisions. From Tommasi et al. (2017).

Following Tommasi et al., 2017 (Fig. E.1), we further describe the time scales of climate/ocean forecasts and projections into a series of categories:

• **Nowcasts/Hindcasts.** Nowcasts/hindcasts typically try to describe the exact state of a variable or index at a specific time and space, up to the current date. (Hypothetical example: "on January 10th, it was 12°C at the surface, 100 km west of Newport.") Nowcasts/hindcasts are based on observations, but are usually supplemented by models and statistical tools. We can generally provide more up-to-date and confident nowcasts for physical indices than for biological or biogeochemical indicators, which tend to have delays in sample processing or lower spatial or temporal resolution.

• **Seasonal Forecasts.** Seasonal forecasts typically try to describe an index in terms of a limited range of values over the next few months to a year. (Hypothetical example: "two months from now, it will be 10°C ±2°C at the surface in Monterey Bay.") They are typically based on either persistence (forward projection of the most recent observations), statistical modeling techniques, or coupled climate and biogeochemical models. Confidence is based on factors such as how well past forecasts have performed, and our understanding of current conditions (nowcasts).

• **Decadal Forecasts.** Decadal forecasts typically try to describe an index in terms of its statistical probability over relatively broad spatial scales at some future point from a year to ten years in the future. (Hypothetical example: "we are currently in year 8 of a positive phase of the PDO, which has a roughly decadal cycle; thus, in 5 years, there is a 75% chance we will be in a negative PDO phase.") Decadal forecasts are based on knowledge of past cycles, statistical models, and coupled climate and biogeochemical models. Like seasonal forecasts, confidence is based on factors like past forecast performance and knowledge of the state of the climate at the time forecasts are made.

• **Climate Projections.** Climate projections typically try to predict the overall statistical state of an index at scales of decades to centuries in the future. (Hypothetical example: "under the B1 and A1B greenhouse gas emission scenarios, a given region of the ocean will warm by X to Y°C by 2100.") Climate projections are based on output from global climate models, which can be scaled down to regional levels with additional modeling tools. Climate projections are meant to capture the influence of long-term changes in forcing (such as atmospheric CO_2 levels). Therefore, confidence reflects how well we can anticipate the general direction and magnitude of future change, not our ability to predict conditions at a specific place and time.

Critically, our degree of confidence in the various forecasting scales stems from the nature of the different forecasts, what kind of information they are actually forecasting, and the methods wrapped into such forecasts. Proceeding from our discussions with the SSC-ES, we propose to adopt the IPCC recommended method for classifying uncertainty, as illustrated in Figure E.2.
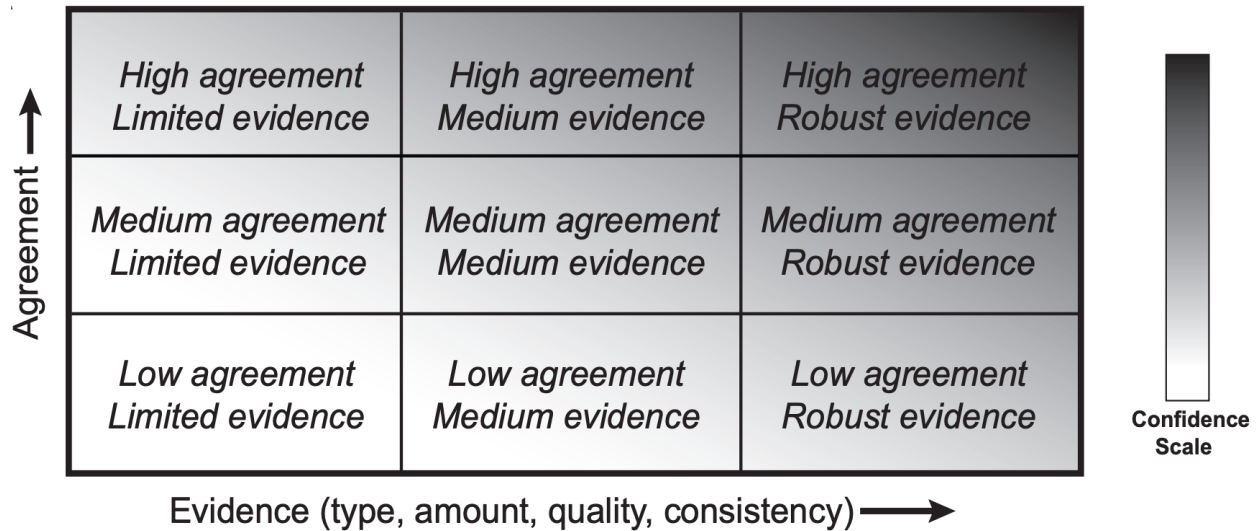
High agreement Limited evidence	High agreement Medium evidence	High agreement Robust evidence
Medium agreement Limited evidence	Medium agreement Medium evidence	Medium agreement Robust evidence
Low agreement Limited evidence	Low agreement Medium evidence	Low agreement Robust evidence

Agreement →

Evidence (type, amount, quality, consistency) →

Confidence Scale

Figure E.2: A depiction of evidence and agreement statements and their relationship to confidence. Confidence increases towards the top-right corner as suggested by the increasing strength of shading. Generally, evidence is most robust when there are multiple, consistent independent lines of high-quality evidence. From Mastrandrea et al. (2010).

At the September 2022 Council meeting, the CCIEA team also presented the SSC-ES with several examples of indices that could be used towards fisheries management in a climate change context. Based on a survey of indices in use, or likely to see future usage in the ESR, it was suggested that such indices could be grouped into three categories: "operational", "hot topic", and "cutting edge" (Table E.1).

- "Operational" indices consist of those indices that are already in use, have high confidence, already have a forecasting component or could be readily adapted to include a forecasting component, and deliver mostly "nowcast/hindcast" and/or "seasonal forecasts". An example of such an index would be the Habitat Compression Index.
- "Hot topic" indices would address an emerging need, might require additional work to be used for forecasting, and deliver mainly "climate projections". An example of this type of index would be the current work on groundfish SDM (species distribution model) forecasting (Karp et al., 2023, also see Brodie et al., 2022 for an extensive review and example of other SDMs).
- "Cutting edge" indices would be those indicators that are still under development for possible future use, are at the stage where they may be ready for examination by the SSC, and may deliver either "forecasts" or "projections".

Examples of these categories of indices, the types of forecasts they could support, and requirements to make them more fully operational are in Table E.1:

Table E.1. Categories and examples of indices that could be used for assessing climate change impacts on managed fisheries

Index	Type of Forecast	Requirements
"Operational" Indices		
Habitat Compression Index	Not currently done, but could be if coupled with forecast models (e.g., JSCOPE)	Effort to link to forward models
Heatwave index	Nowcast, Seasonal Forecast: days to months, based on trends, 1-12 month forecasts publicly available with web tool	Web maintenance
WCOFS	Nowcast: physical data, possibly some biological, days to weeks	Operational
JSCOPE	Seasonal Forecast: phys and bio data, days to months	Operational
"Hot topic" Indices		
Groundfish SDMs	Climate Projection: to 2100 with various model forcing	Needs input on focal species and metrics to track
CPS SDMs	Climate Projection: to 2100 with various model forcing	Needs input on focal species and metrics to track
HMS SDMs	Climate Projection: to 2100. No plan on regular updates.	Evaluation of model results
port responses to climate	Hindcast: Backwards-looking, shock/event specific, no plan on regular updates	Linkage to forward models
"Cutting Edge" Indices		
Environmental Niche Affinity	Seasonal forecast: could generate short term (1-2 year) forecasts via time series models with high confidence	Linking with models
Sardine subpopulation habitat	Climate Projection: no plan on regular updates. Model development and evaluation on historical period relied on obs and ROMS reanalysis/ROMS-NEMURO hindcast, up to 2100	Model evaluation
Pacific NW contribution to sardines		
albacore habitat		
Climate envelope, novel habitat	Climate Projection: no plan on regular updates. Input from UCSC ROMS/NEMURO downscaling	Evaluation of model results

Beyond these categories of indices, an additional short review was given at the September 2022 meeting of the current indices from the main body of the ESR (minus the fisheries and human dimensions indicators) The possibility of these indices being adapted to a forecasting or climate projection mode are summarized in Table E.2.

Table E.2. Current indices in the main ESR and their prospectus for use in climate forecasts.

Index	Source	Currently Forecasted?	Forecastable?
ONI	NOAA climate center/ERDDAP	yes, ENSO probability	Yes, based on NOAA climate prediction center expert analysis of multiple models
PDO	N. Mantua, SWFSC, https://www.ncei.noaa.gov/	yes	Yes, using large scale model ensembles
NPGO	DiLorenzo	no	Yes, same as above
CUTI	Jacox/ERDDAP	no	Yes, using physical model such as ROMS
BEUTI	Jacox/ERDDAP	no	Yes, using physical model such as ROMS
HCI	Santora/ERDDAP	no	Yes, using physical model such as ROMS, or larger scale model ensembles
DO at NHL	Siedlecki	yes	JSCOPE
Aragonite NHL	Siedlecki	yes - pH	JSCOPE
Snow water Eq	NOAA-CPC	yes - limited fashion	NOAA CPC, several month forecast
NW Stream Flow	NOCC-CPC	yes - limited fashion	NOAA CPC, several month forecast
Copepods and Krill	NWFSC	no	unlikely, but could possibly be predicted in limited fashion by detailed coupled bio-phys model forecast
Forage Dynamics	NWFSC/SWFSC trawls	no	SDMs
Juvenile Salmon	NWFSC	yes	Adult return outlooks based on stoplight tables
HMS diets	SWFSC/NWFSC	no	SDMs of prey
Sea lion pups	SWFSC/NWFSC	no	SMDs or prey projections
Whale entanglement	NMFS WCRO	no	HCI or other forecastable index
Seabird abundances		no	unknown, many non-oceanographic complicating factors (disease, predators, etc.)
HABS	SWFSC/NWFSC	no - but model nowcast	with ROMS or other physical-biological model
Fishery landings	PacFIN, RecFIN	no	partially with SDM projections

E.2   Operationalizing indices

Here, we discuss some of the above examples of climate change indicators in more detail as to how they might be adapted for use in future editions of the ESR and the climate change appendix.

E.2.1 Physical-based indices

As described further below (Appendix F), Santora et al. (2020) developed the Habitat Compression Index (HCI) to quantify how offshore warming may restrict the cool upwelling habitat along the coast. When the habitat is compressed, this may lead to altered prey

community composition and distribution, spatial aggregation patterns of top predators, and contribute to increased rates of whale entanglements in fixed fishing gear.

The HCI is an example of a physical-based index and is also an excellent candidate for adapting to a forecasting mode based on the following criteria: it has already been in use and vetted by the PFMC, it expresses a simple quantity (0-1) which has a broad and readily interpretable meaning for many aspects of the ecosystem, and it is calculated directly from the CCE configuration of the Regional Ocean Modeling System (ROMS) model with data assimilation (Neveu et al. 2016), and as such, forecasts could be readily calculated by forecast runs of ROMS. The HCI can also be calculated over different regions and at different time periods, adding additional interpretable insights into ecosystem forecasts. The last step towards making this index able to provide an operational forecast would be coupling the calculations to an appropriate forecast run of the proper ROMS configuration.

This final step of linking the index to model output, however, is not trivial. Jacox et al. ([2020](#)) reviewed the prospectus for using ROMS or similar models for monthly to yearly forecasts. For example, an HCI forecast could use what is known as a "dynamically downscaled" regional forecast. What this means is that some implementation of a relatively fine-scale physical model, such as ROMS, would be run in a forecast mode constrained by boundary data from much more coarse (albeit more skillful) global scale models (or an ensemble of models) in order to produce actual forecast data at the resolution necessary to calculate the HCI. The current problem in taking this step is that while the larger global-scale forecast models are run fairly regularly (thus providing the boundary conditions for the fine-scale physical model), the actual running of the forced fine-scale models is not regularly conducted. Alternatively the HCI, and other similar physical-based indices, could be driven by the larger-scale global forecast models (or even an ensemble of models, discussed further below).

For the west coast, the only two current examples of forecasting with high resolution physical models are the JSCOPE (https://www.nanoos.org/products/j-scope/) and WCOFS (https://tidesandcurrents.noaa.gov/ofs/dev/wcofs/wcofs.html) efforts. Although both of these projects provide physical (and some biological) forecast data at the proper resolution, in this specific case, neither is exactly the same configuration as the original HCI implementation, and thus would require further adaptation for HCI calculation. Both of these modeling efforts have the ROMS as their base physical model, and thus share many similarities. An advantage of WCOFS is that it is fully operational, with posted daily updates, and coverage for the entire US west coast. The downside of WCOFS is that the forecasts are currently only 72 hrs, limiting its usefulness for our intended application of seasonal to yearly predictions. JSCOPE, while semi-operational, is limited in that its forecasts are only updated twice per year, and its operational region does not cover the entire US west coast EEZ. On the positive side, JSCOPE does provide forecasts that span an entire year.

Besides these two modeling efforts, it is of note that under the new Climate, Ecosystems, and Fisheries Initiative (CEFI)[4], and under the auspices of the West Coast Regional Action Plan (WRAP)[5], NOAA has committed to promoting the Modular Ocean Modeling system (MOM6) for use in climate-atmospheric-ocean forecasting and. The MOM6 is a cutting edge physical ocean model, similar to ROMS, albeit with a different coordinate system and other subtle technical differences, and has already seen initial use for ocean forecasting in the NE U.S. through a project led by NOAA's Geophysical Fluid Dynamics Laboratory[6], and thus we expect similar efforts to come online for the pacific in the near future, which would be amenable to our proposed use.

Similar to the example given here for the HCI, many of our other physical-derived indices, such as the PDO, NPGO, etc. (see list in Table E.2), could be adapted to provide seasonal forecasts, but would also face the same challenges of being dependent on downscaled model output. However, if such model forecast data were available to calculate these additional indices, we anticipate that it would provide a significant advancement in our ability to deliver forecast advice in future ESRs. Alternatively, it should be noted that global climate models. even with relatively coarse resolution, can often provide accurate forecasts (Brodie et al., in prep.). The larger ensembles available for global (dozens of members) compared to downscaled models (generally only a few) can provide skillful forecasts, particularly for variables well represented in the models (e.g. SST). Hence indices like the HCI could be driven by these models and likely produce somewhat skillful results, if not on as fine a scale as they are currently used.

E.2.2 Species Distribution Models (SDM)

Another example of indices that are near the "operational" state are outputs from species distribution models (SDM) driven by climate projections. One specific example comes from Smith et al. (2021), which made a projection of sardine distributions in the CCE out to the year 2100 (Fig. E.3 shows an example out to 2055).

In this example, the sardine SDM projection was driven by a coupled physical-bioegochemical model (ROMS + NEMUCSC, see Smith et al., 2021), which is run forward in time and then constrained by coarser, basin-scale data from different whole-earth coupled atmospheric-ocean simulation models (Fig. E.3 shows the results of three different Earth System Models (ESM): GFDL, HadGem2, and IPSL, which represent different possible future warming scenarios). Similar SDM projections have been carried out for several other species in the CCE (groundfish, certain HMS, and other CPS, see also review in Brodie et al., 2022).

---

[4] https://media.fisheries.noaa.gov/2021-08/NOAA%20Climate%20and%20Fisheries%20Initiative%20Fact%20Sheet.pdf

[5] https://media.fisheries.noaa.gov/2022-04/Western-RAP-Draft-for-Public-Comment.pdf

[6] https://www.gfdl.noaa.gov/improving-ocean-habitat-forecasts-for-the-northeast-u-s/
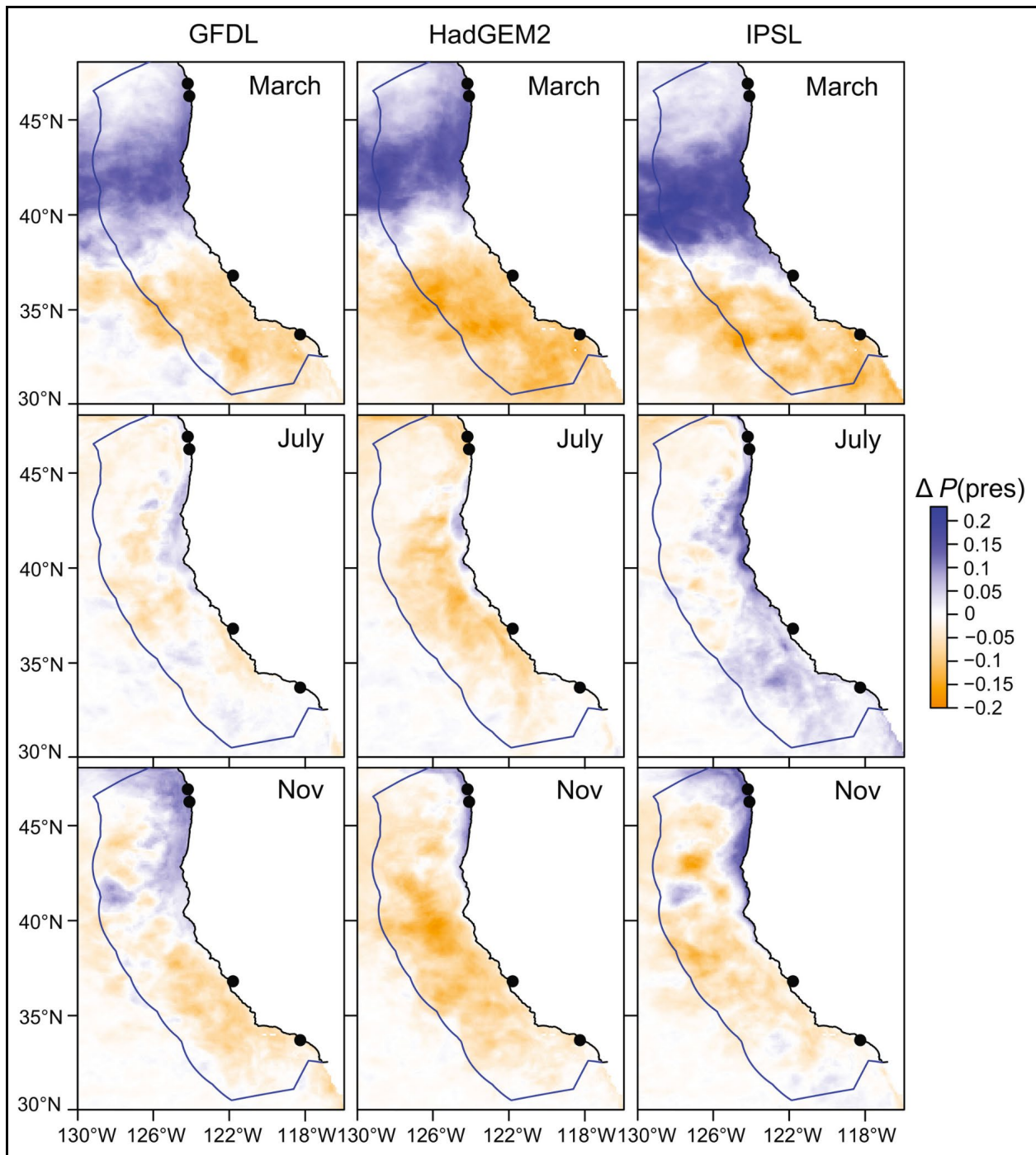
Figure E.3. Mean change in projected sardine habitat suitability (2040–55 period minus 2000–2015 period), in the three ESMs in three representative months. Blue indicates an increase in habitat suitability, and orange a decrease, over this ~40-year period. Black dots indicate major CPS ports. Units of change represent probability of sardine presence. (Figure taken from Smith et al., 2021).

What remains to make such work "operational" is generally publication of the manuscripts involving such work, review by the SSC and Council, and continued support to update the projections and analyses from these models periodically. This last step is important to

account for any changes in the base SDMs, or if there are new climate projections available, and lastly, to account for possible non-stationarity in climate-SDM relationships. Such updates would likely only occur every several years, and not on an annual basis.

E.3   Next steps

Feedback from our first installment of the "climate change appendix" along with feedback and discussions from the September 2022 SSC-ES review, has led to the following conclusions regarding possible next steps: 1) the most desirable forecasts are likely to be those that can provide information about the upcoming months, out to 1-2 yrs (e.g. *seasonal forecasts*, as defined above); 2) longer-term projections (*decadal forecasts* and *climate projections*, as defined above) are useful for strategic planning on the management of climate-vulnerable stocks; 3) both of these components will require further scoping and discussion between the CCIEA team and various Council bodies to specifically identify the target species/indices of highest priority/highest confidence; and 4) those discussions should include further identification of how any described work would be supported and/or retasking/prioritization of personnel to achieve these objectives.

Regarding 1) and 2), the CCIEA team consensus is that when (if) *seasonal forecasts* do become a regular feature of the ESR (item 1), we propose that such forecasts would be mostly incorporated into the main ESR body (and where appropriate with supporting information in the appropriate appendix), whereas *climate projections* (item 2, and as per SSC-ES recommendation) would reside in the "climate change appendix". One constraint with item 1 would be the added length to the main body of the report, although this would be minimal. With regard to item 2, we foresee that such an effort would likely only occur every few years (2-5), or as new simulations/forcing scenarios arise, and/or as particular species/FMPs require attention.

One final caveat to address is the status of our *current* ability to make forecasts. As described in the main report body, 2022 represented a year where some of the observations did not match our general "expectations" based on the basin-scale predictors of ecosystem state; namely the PDO, ONI (ENSO), and NPGO indices. The CCIEA team relies on these basin-scale indicators to provide an overall context of expectations for an upcoming year, and hence these indices provide a rough "nowcast/forecast" of ecosystem state. Unfortunately, it has been noted that there has been an increasing "decoupling" of such indicators from ecological expectations over different time periods within the CCE (Litzow et al., 2020). Additionally confounding is that the PDO and NPGO have become increasingly correlated (Joh and DiLorenzo, 2017), decreasing their utility for independent forecasting of ecosystem status. The decoupling of these basin-scale indicators from ecological observations is likely a result of what is termed "nonstationarity", which roughly means that the underlying statistics (mean, standard deviation etc.) of a variable or set of variables is changing over time, and hence we do not always expect past correlative relationships to hold as we attempt to forecast the future. Indeed, nonstationarity is to be expected under a changing climate. However, these indices are useful in that they still can improve our ability to judge the likelihood of a particular outcome for a coming year; e.g., in 2022, although we did not observe all of the ecological responses typical of La Niña conditions, we still observed some favorable outcomes, and certainly did not observe the opposite, El Niño-like conditions.

When assessing our current "forecasting" abilities, it is also important to clearly differentiate between the types of information about future climate impacts that can be provided, and highlight gaps in the current state of the science. As outlined in Appendix E.1, indicators of the impacts of future climate change fall into two general categories, *forecasts* and *projections*. "Forecasts" usually refer specifically to attempts to predict fairly exact values at some specific location and time in the future, and thus often require fairly detailed mechanistic modeling approaches. On the other hand, "projections" typically offer statistical probabilities of a variable of interest at some far point in time (e.g., 50-100 years), and are usually based on comparisons of ensembles of large whole earth system models. Whereas forecasts are typically good at short intervals (days to weeks) they typically decrease in accuracy at longer intervals. Conversely, by using ensembles to drive climate projections, we have some confidence in their results over longer time periods, and yet lower confidence at shorter intervals. Thus there currently remains a gap at the interannual time scale in our ability to make "forecasts" about climate impacts. We remain hopeful that the next generation of forecast models (such as the CEFI support of MOM6 efforts) will help to fill this void in the near future.

In summary, the CCIEA team plans to: 1) continue incorporation into the main ESR of the limited forecasting based on basin-scale indicators (albeit with recognition of the caveats discussed above), 2) continue to seek out ways to incorporate seasonal forecast data (when available) into our currently used indices, 3) proceed with discussions to identify target species/systems of highest priority for future work, and 4) encourage research and incorporation into this appendix of work related to long-term climate projections of identified target species/indices. Lastly, we again emphasize that whereas the NWFSC and SWFSC have many of the personnel capable of conducting the research and efforts outlined above, much of this work would require additional funding and/or personnel, and/or retasking/reprioritization of current work flows. We also acknowledge that one of the key ingredients–operationalization of coupled biophysical model (ROMS, MOM6, etc.) seasonal forecast runs, e.g. the production of detailed physical/biological data from these near-future simulations that would be used to generate our seasonal forecasts–would require significant resources and collaborations beyond NWFSC/SWFSC.

Appendix F: CLIMATE AND OCEAN INDICATORS

F.1   BASIN-SCALE CLIMATE/OCEAN INDICATORS AT SEASONAL TIME SCALES

These plots (Figure F.1) show seasonal averages and trends of the three basin-scale climate forcing indicators shown in the main report in Figure 2.1.
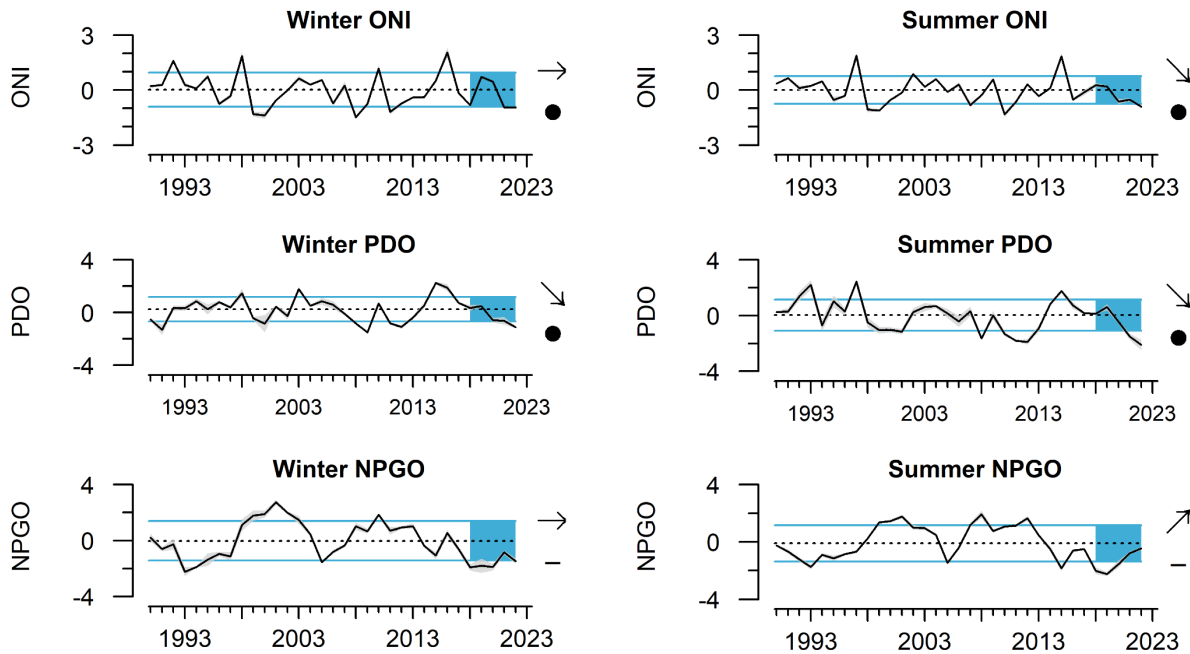

Figure F.1: Winter (Jan-Mar) and Summer (July-Sep) values for the basin-scale climate indicators: Ocean Niño Index (ONI), Pacific Decadal Oscillation (PDO), and North Pacific Gyre Oscillation (NPGO) through 2022. Mean and s.d. for 1991-2020. Lines, colors, and symbols are as in Fig. 2.1.

Satellite data, which has been collected in a similar fashion since 1982, allows for a basin-scale view of sea surface temperature (SST) at up to daily and sub-degree (spatial) resolution. Here we show seasonal averages of SST anomalies (SSTa, the difference from climatology) across the Northeast Pacific (NEP) in 2022 (Fig. F.2). Winter saw anomalously high SST in the SW, which was an expression of the large marine heatwave that began in winter that year. This trend in warming in the SW continued during spring, with the warm waters expanding throughout the region, coming closer to the US west coast. During spring, the Southern California Bight also began to warm. Coastal temperatures remained cool due to moderate early upwelling. During summer 2022, average temperatures throughout the NEP were warmer than normal. Fall saw the largest warm anomaly in basin-scale SST, with temperatures often >3°C warmer than normal for much of the region. This coincides with the maximum areal extension of the marine heatwave of 2022, which penetrated to the coastline during August into September for much of the coastal region.
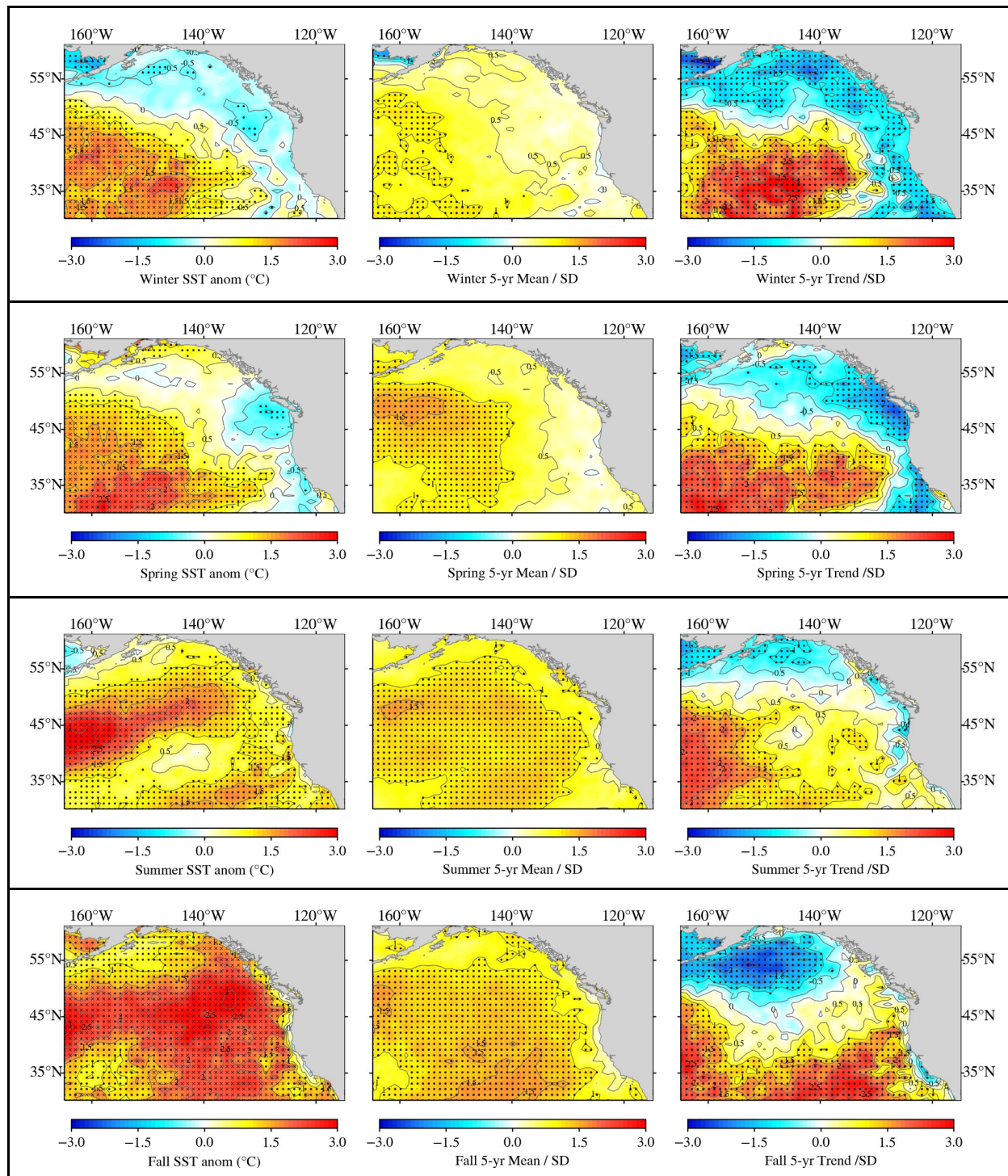
Figure F.2: Left: Sea surface temperature (SST) anomalies in 2022, based on 1982-present satellite time series in (top to bottom) winter (Jan-Mar), spring (Apr-Jun), summer (July-Sept), and fall (Oct-Dec). Center: Mean SST anomalies for 2018-2022. Right: trends in SST anomalies from 2018-2022. Black dots mark cells where the anomaly was >1 s.d. above the long-term mean (left, middle) or where the trend was significant (right). Black x's mark cells where the anomaly was the highest in the time series.

Glider data have become an increasingly useful tool for analyzing trends in subsurface water temperatures over time. The following series of plots represents data from subsurface gliders, which generally sample in onshore-offshore transects on a weekly to monthly basis, and have been in service long enough for the development of climatologies, which are then used to compute temperature anomalies. Examination of these subsurface anomalies over time suggests that during 2022 subsurface temperatures off Oregon were generally cooler than previous years (Fig. F.3). Off Northern California, subsurface temperatures were also generally cool, although during the summer, the intrusion of the marine heatwave can be seen in the upper 50m for several periods (Fig. F.4). Off Monterey, 2022 saw warmer-than-normal surface and subsurface temperatures (Fig. F.5). From Pt. Conception south (Fig. F.6, F.7), there has been an increase in stratification, due to a return of deeper waters (>50m) to a more "normal" temperature (i.e., anomalies close to zero), while surface waters remained anomalously warm, as in previous years. It is important to note that these time series are relatively short, and thus the anomalies are relative only to the time span shown, which therefore likely overestimate the "coldness" of the cool anomalies compared to longer climatologies, for example (Fig. 2.3 in main text).
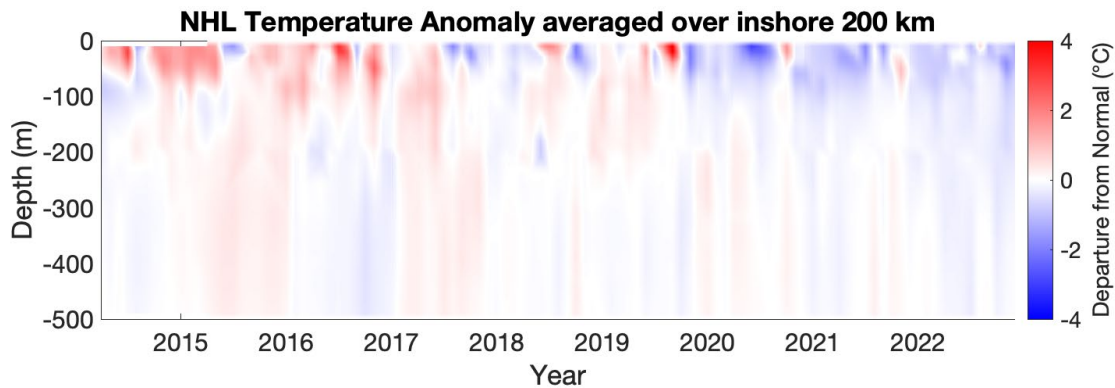
Figure F.3: Time-depth plot of average subsurface temperature anomalies from the shore to 200 km offshore along the Newport Hydrographic Line (see Fig. 1.1), based on OSU-OOI coastal endurance array gliders (https://ceoas.oregonstate.edu/ocean-observatories-initiative-ooi). Climatology based on monthly averages created over 2014-2022.
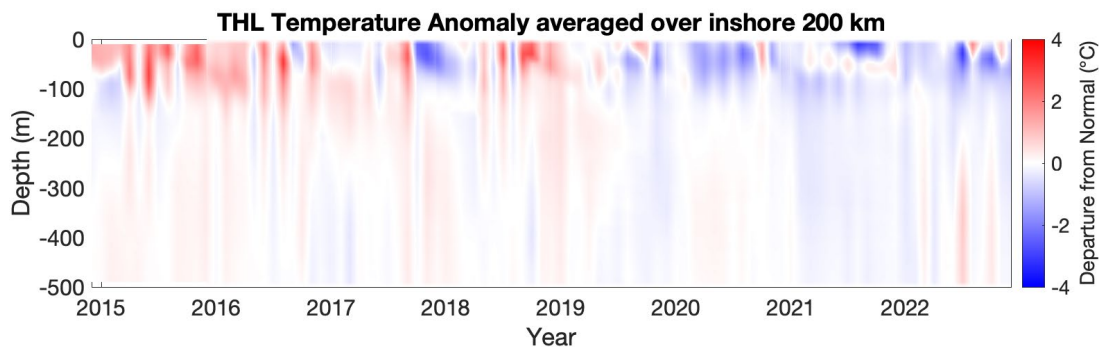
Figure F.4: Time-depth plot of average subsurface temperature anomalies from the shore to 200 km offshore along the Trinidad Head Line (see Fig. 1.1). Data courtesy of CeNCOOS and NANOOS.
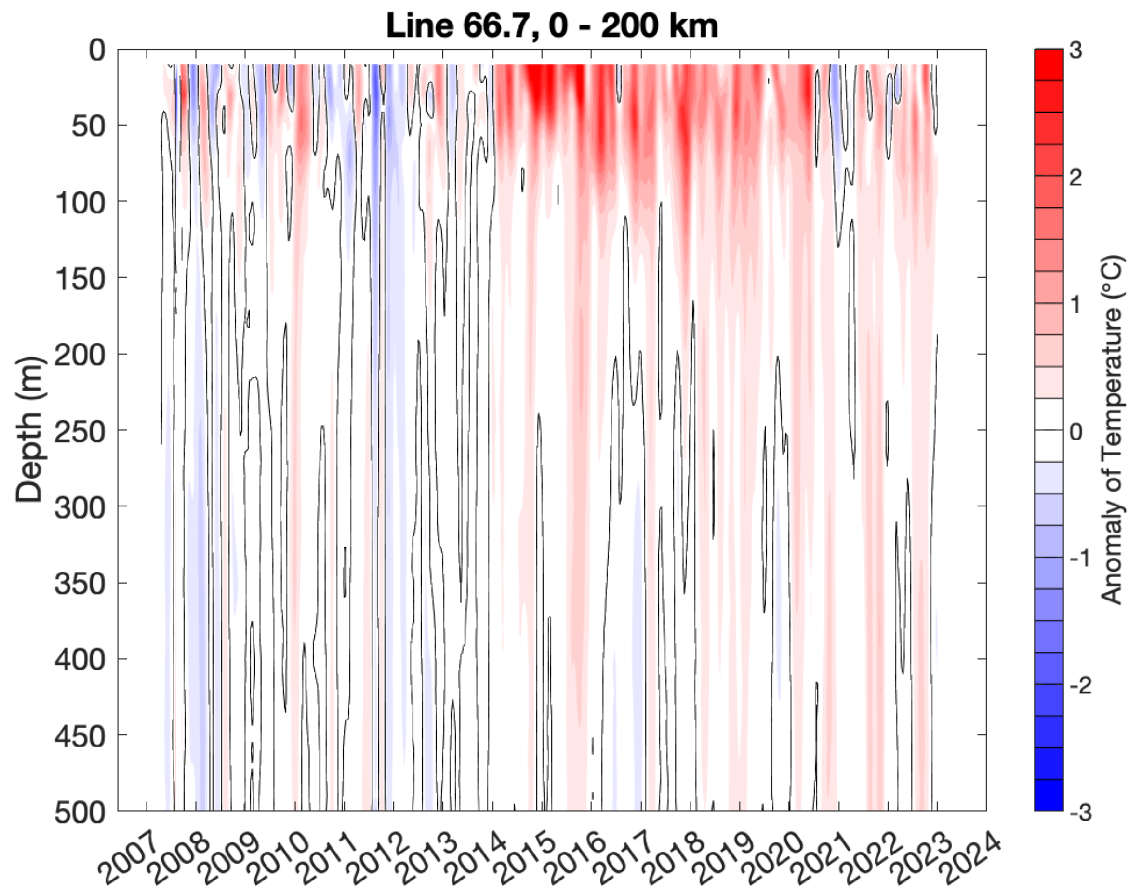
Figure F.5: Time-depth plot of average subsurface temperature anomalies from the shore to 200 km offshore along CalCOFI line 66.7 (see Fig. 1.1), based on SPRAY gilder data and climatology. Data from the California Underwater Glider Network are provided by Dr. Dan Rudnick, Scripps Institute of Oceanography Instrument Development Group (doi: 10.21238/S8SPRAY1618).
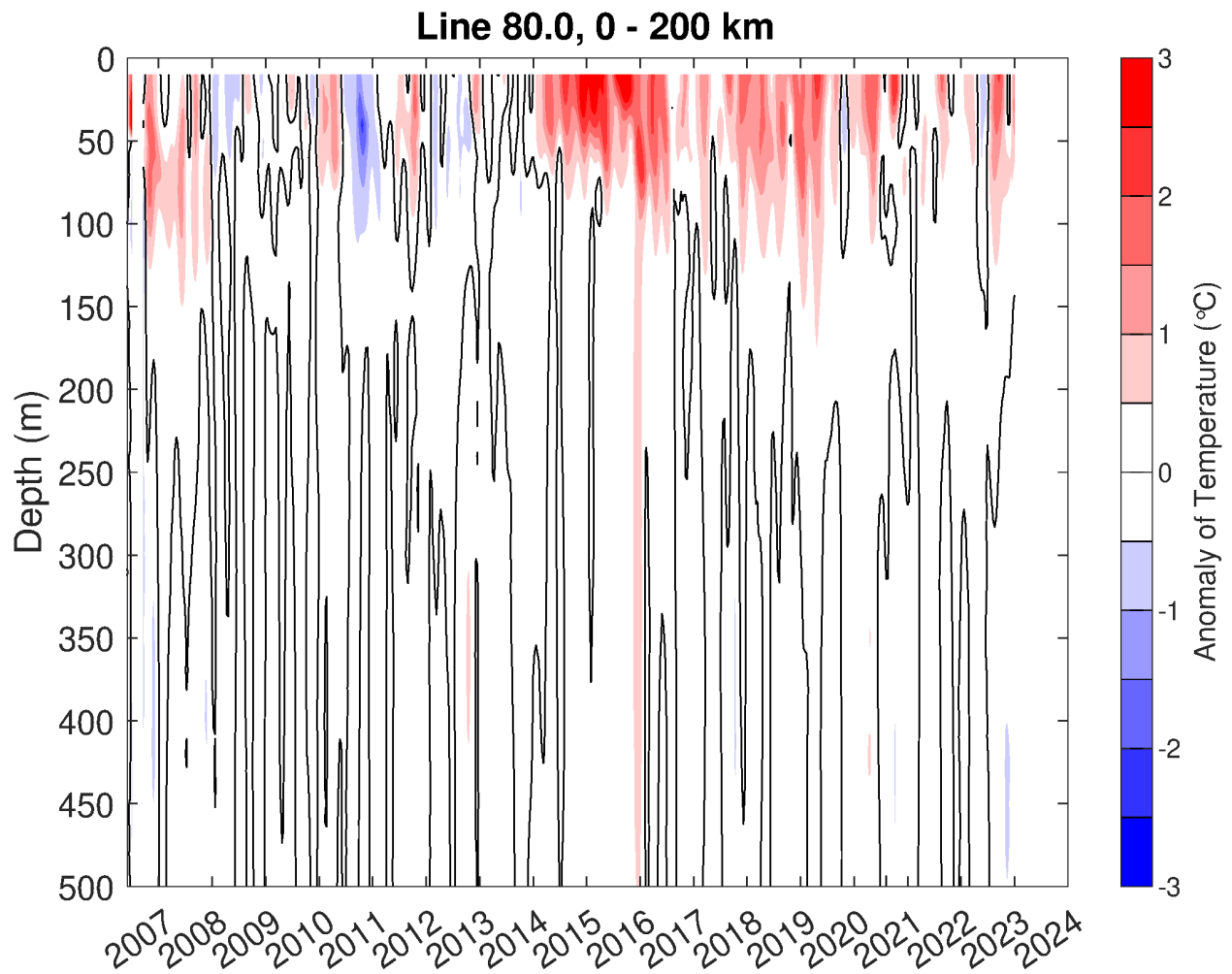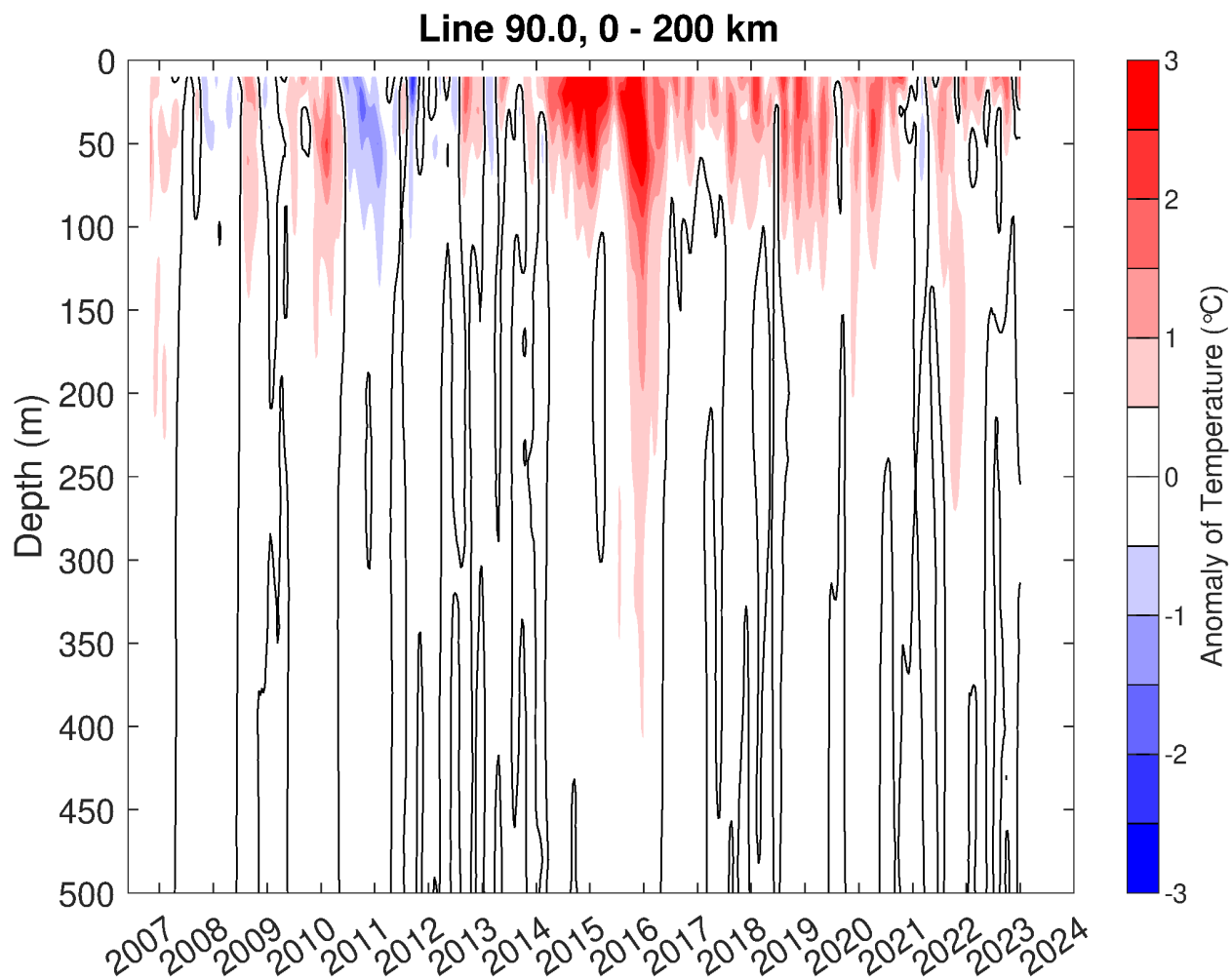
Figure F.6: Time-depth plot of average subsurface temperature anomalies from the shore to 200 km offshore along CalCOFI line 80 (see Fig. 1.1), based on SPRAY gilder data and climatology. Data from the California Underwater Glider Network are provided by Dr. Dan Rudnick, Scripps Institute of Oceanography Instrument Development Group (doi: 10.21238/S8SPRAY1618).

Figure F.7: Time-depth plot of average subsurface temperature anomalies from the shore to 200 km offshore along CalCOFI line 90 (see Fig. 1.1), based on SPRAY gilder data and climatology. Data from the California Underwater Glider Network are provided by Dr. Dan Rudnick, Scripps Institute of Oceanography Instrument Development Group (doi: 10.21238/S8SPRAY1618).

F.2   ASSESSING MARINE HEATWAVES IN 2022

There is growing recognition that marine heatwaves can have strongly disruptive impacts on the CCE (e.g., Morgan et al. 2019). Based on an analysis of sea surface temperature anomalies (SSTa) obtained from satellite measurements[7], we define marine heatwaves as: 1) times when normalized SSTa >1.29 s.d. (90th percentile) of the long-term SSTa time series at a location, and 2) lasts for >5 days; these are analogous to the thresholds suggested in Hobday et al. (2016). Here, we further report on statistics concerning large heatwaves (LHW), which were tracked through space and time, with LHW defined as those heatwaves with an area >400,000 km² (these denote the top 20% of all heatwaves by area as measured since 1982 when satellite data became available for tracking; Leising in revision). During 2022 we observed extensive coverage of the US west Coast EEZ by marine heatwaves from

---

[7] https://psl.noaa.gov/data/gridded/data.noaa.oisst.v2.highres.html

August through November (Fig. F.8). The 2022 heatwave was the 4th largest by area, and 3rd longest (Fig. F.9) recorded since monitoring began in 1982.
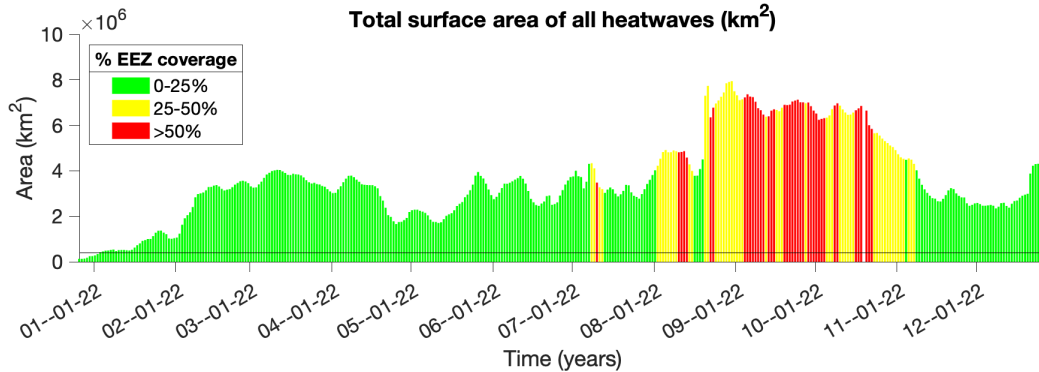

Figure F.8: Areas of North Pacific marine heatwaves during 2022. The horizontal line represents 400,000 km², the area threshold that we use for tracking individual events over time (top 15% of heatwaves by area; Leising [in revision]). Color indicates the percentage of the US West Coast EEZ that was in heatwave state.
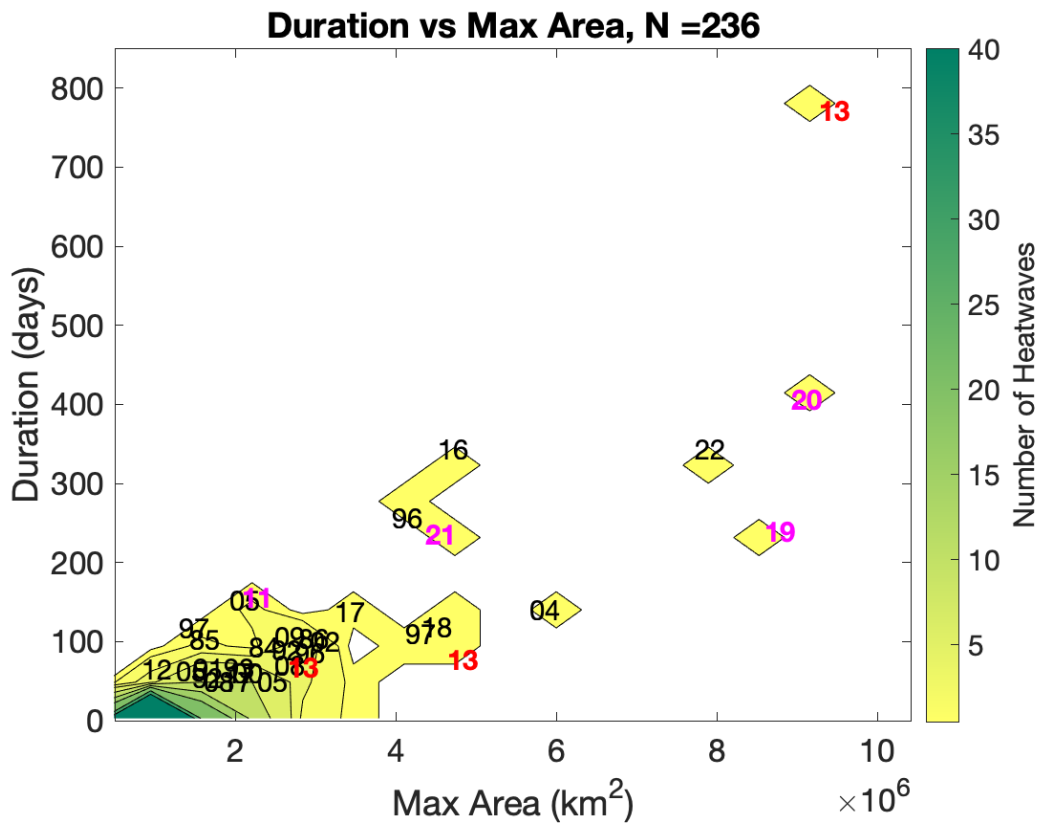

Figure F.9: Duration and maximum areas of NE Pacific large marine heatwaves, 1982-2022. Shading indicates the number of heatwaves (out of 236). Outliers are marked with numbers indicating the year the heatwave formed.

F.3   HABITAT COMPRESSION INDEX

Spatial variability in patterns of upwelling, including the distribution of upwelled water and associated development of hydrographic fronts, is important for ecosystem monitoring and assessment of marine heatwaves and ecosystem shifts that can impact coastal fishing communities. Coastal upwelling creates a band of relatively cool coastal water, which is suitable habitat for a diverse and productive portion of the CCE food web. Monitoring the area and variability of upwelling habitat provides regional measures of habitat compression—an indicator to monitor the incursion of offshore warming (e.g., from heatwaves or reduced upwelling conditions) over shelf waters, which relates to shifts in the pelagic forage species community in space and time. Santora et al. (2020) applied principles of ecosystem oceanography and integration of fisheries surveys to develop the Habitat Compression Index (HCI) to quantify how offshore warming during the 2013–2016 marine heatwave and previous warming events restricted the cool upwelling habitat to a narrower-than-normal band along the coast. This compression of habitat consequently altered prey community composition and distribution, spatial aggregation patterns of top predators, and contributed to increased rates of whale entanglements in fixed fishing gear.

HCI is derived from the CCE configuration of the Regional Ocean Modeling System (ROMS) model with data assimilation (Neveu et al. 2016), and is estimated in four biogeographic provinces within the CCE: 30°-35.5°N, 35.5°-40°N, 40°-43.5°N, and 43.5°-48°N. HCI is defined as the area of monthly averaged ROMS model temperatures at a depth of 2 m that fall below a temperature threshold. Each region/month has a unique temperature threshold, based on its distinct historic climatology. Winter and spring means for central California are shown in the main body of the report (Fig. 2.5). Winter and spring means (Fig. F.10) and summer and fall means (Fig. F.11) for all four regions are shown here. For all regions, HCI was favorable during winter and spring (e.g. more cool water habitat), but then declined during summer, in accordance with the timing of upwelling relaxation and coastal heatwave intrusion.
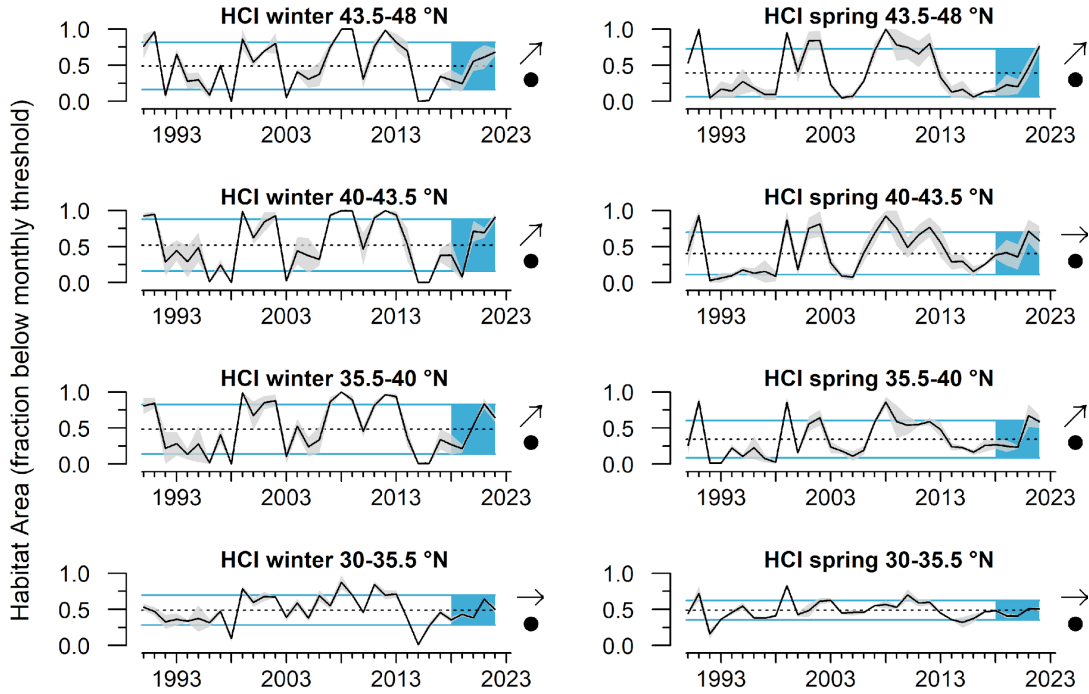
Figure F.10: Mean winter (Jan-Mar) and spring (Apr-Jun) habitat compression index by region, 1990-2022. Gray envelope indicates ±1s.e. Data provided by J. Santora, NMFS/SWFSC, and I. Schroeder, NMFS/SWFSC, UCSC. Lines, colors, and symbols are as in Fig. 2.1.
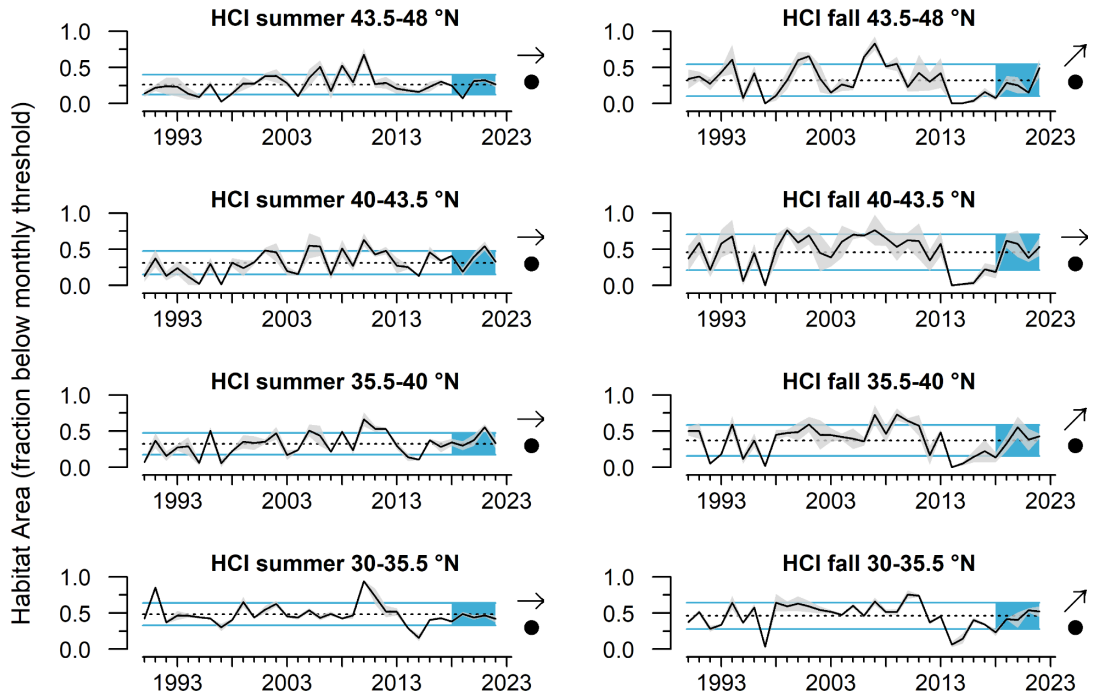

Figure F.11: Mean summer (July-Sep) and fall (Oct-Dec) habitat compression index by region, 1990-2022. Gray envelope indicates ±1s.e. Data provided by J. Santora, NMFS/SWFSC, and I. Schroeder, NMFS/SWFSC, UCSC. Lines, colors, and symbols are as in Fig. 2.1.

F.4   SEASONAL DISSOLVED OXYGEN AND OCEAN ACIDIFICATION INDICATORS

Nearshore dissolved oxygen (DO) depends on many processes, including currents, upwelling, air–sea exchange, and community-level production and respiration in the water column and benthos. DO is required for organismal respiration; low DO can compress habitat and cause stress or die-offs for sensitive species. Waters with DO levels <1.4 mL/L ($\approx$ 2 mg/L) are considered to be hypoxic; such conditions may occur on the shelf following the onset of spring upwelling, and continue into the summer and early fall months until the fall transition vertically mixes shelf waters (Fig. F.12). Upwelling-driven hypoxia occurs because upwelled water from deeper ocean sources tends to be low in DO, and microbial decomposition of organic matter in the summer and fall increases overall system respiration and oxygen consumption, particularly closer to the seafloor (Chan et al. 2008).
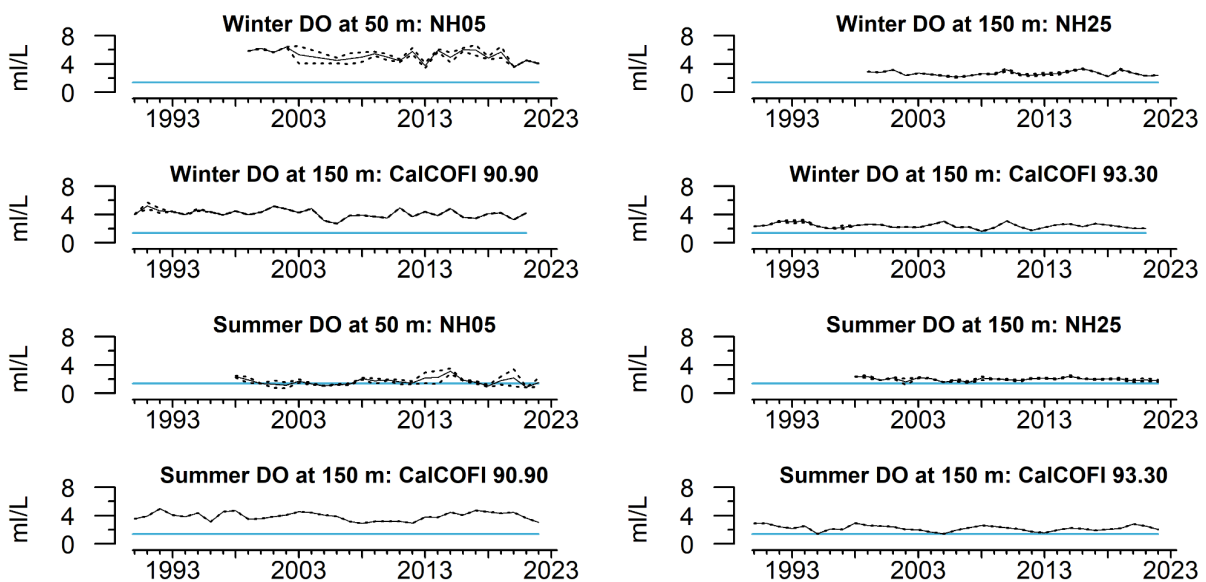
Figure F.12: Winter (Jan-Mar) and summer (Jul-Sep) dissolved oxygen (DO) at depth off Oregon (NH05, NH25), and southern California (CalCOFI 93.30, 90.90). Stations NH05 and NH25 are 5 and 25 nautical miles offshore, respectively. CalCOFI stations 93.30 and 90.90 are <50-km and >300-km offshore, respectively. Blue line indicates hypoxic threshold of 1.4 ml DO/L. NH05 and NH25 data courtesy of J. Fisher, NMFS/NWFSC. CalCOFI data courtesy of R. Swalethorp, UCSD/SIO.

Ocean acidification (OA), which occurs when atmospheric CO2 dissolves into seawater, reduces seawater pH and carbonate ion levels. Upwelling transports hypoxic, acidified waters from deeper offshore onto the continental shelf, where increased community-level metabolic activity can further exacerbate OA (Feely et al. 2008). A key indicator of OA is aragonite saturation state, a measure of the availability of aragonite (a form of calcium carbonate). Aragonite saturation <1.0 indicates relatively acidified, corrosive conditions that are stressful for many CCE species, particularly shell-forming invertebrates. OA impacts on these species can propagate through marine food webs and potentially affect fisheries (Marshall et al. 2017). Aragonite saturation states tend to be lowest during spring and summer upwelling, and highest in winter. Figure F.13 shows time series of winter and summer aragonite saturation from near-bottom at stations NH05 and NH25.
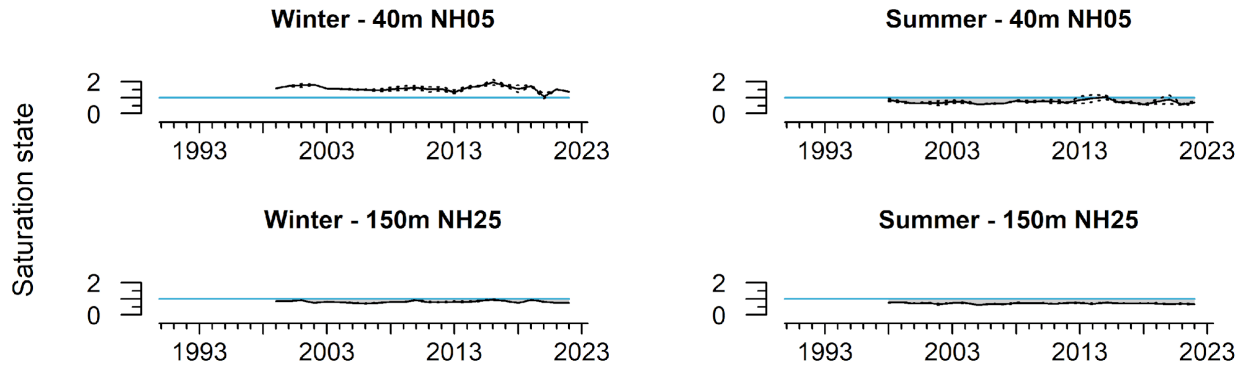
Figure F.13: Winter (Jan-Mar) and summer (Jul-Sep) mean aragonite saturation states at stations NH05 and NH25 off Newport, OR, 1998-2022. The blue line indicates aragonite saturation state = 1.0, below which is corrosive conditions for many shell-forming species. Dotted lines indicate ±1.0 s.e. Data provided by J. Fisher, NMFS/NWFSC.

The corrosive water on the shelf at NH05 is largely driven by seasonal upwelling, and upwards of 80% of the water column becomes corrosive each summer (Fig. F.14). In 2022, at the most nearshore station, NH05, water column conditions were less corrosive than the past year, as evidenced by the deeper summertime saturation depth, consistent with the decreased upwelling observed during summer. Offshore saturation levels were similar for 2022 as for 2021, as evidenced by the profile at the offshore station, NH25 (Fig. F.14).
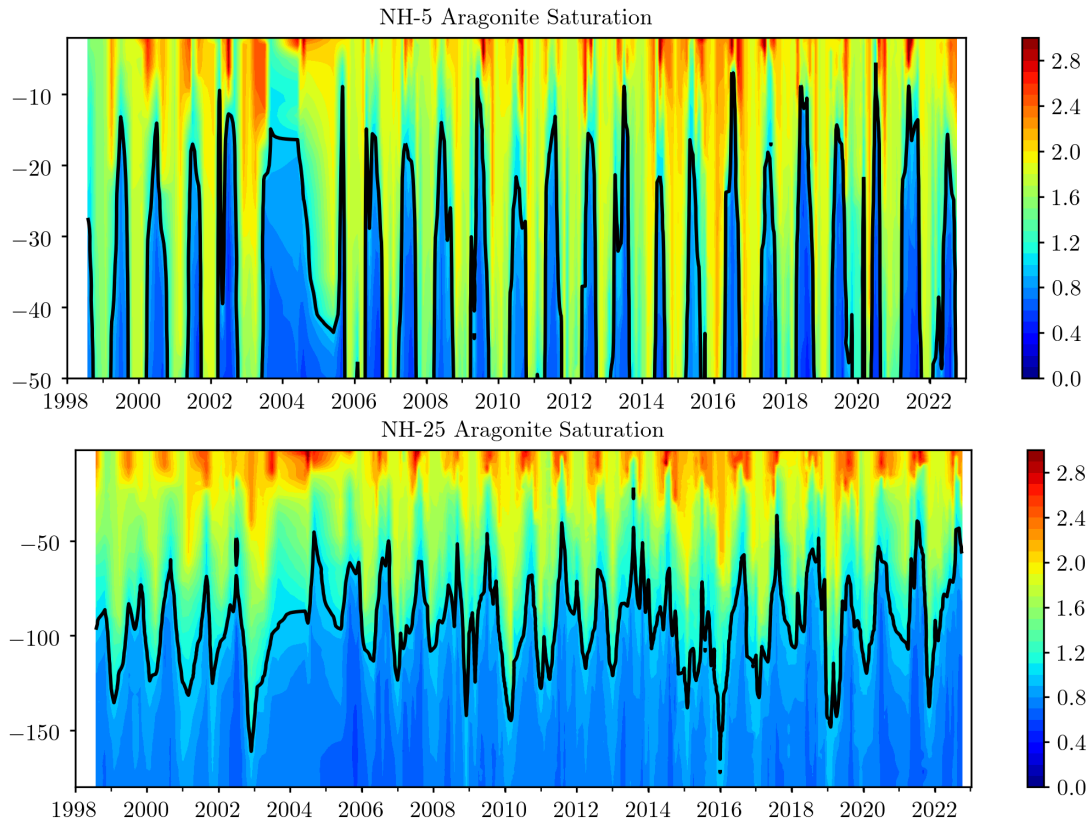

Figure F.14: Aragonite saturation state profiles for stations NH05 and NH25 off Newport, OR. Depths (y-axis) are in m. Black line indicates the depth at which aragonite saturation state = 1.0. Data provided by J. Fisher, NMFS/NWFSC, plots created by I. Schroeder, UCSC.

Appendix G: SNOWPACK, STREAMFLOW, AND STREAM TEMPERATURE

Freshwater habitat indicators are reported at the spatial scale of freshwater ecoregions (Fig. 1.1). Freshwater ecoregions are based on the biogeographic delineations in Abell et al. (2008), see also www.feow.org, who define six ecoregions for watersheds entering the California Current, three of which comprise the two largest watersheds directly entering the California Current (the Columbia and the Sacramento-San Joaquin Rivers). Status and trends for all freshwater indicators are estimated using space-time models that account for spatial and temporal autocorrelation (Lindgren and Rue 2015).

Snow-water equivalent: Snow-water equivalent (SWE) is measured using data from the California Department of Water Resources snow survey program (California Data Exchange Center, cdec.water.ca.gov) and The Natural Resources Conservation Service's SNOTEL sites across Washington, Oregon, California and Idaho. Snow data are converted into SWEs based on the weight of samples collected at regular intervals using a standardized protocol. Measurements on April 1 are considered the best indicator of maximum extent of SWE; thereafter snow tends to melt rather than accumulate.

As of February 1, 2023, SWE was very high throughout the Sierra Nevada, often exceeding 200%, whereas mountain ranges in western Oregon and Washington were somewhat less, but ranged from 50-100% (Fig. G.1). Southern Idaho also showed higher than normal SWE (up to 150%), whereas central and northern Idaho saw values typically lower than in the south, but still relatively high (75-100%) for this point of the winter. In general, southern regions had higher SWE than northern regions, but in most cases, the outlook at this same time period is better than the previous year, when SWE was generally lower and much more variable within regions. Thus 2023 begins with a very favorable SWE overall.

Figure G.1: Snow water equivalent as of February 1, 2023, relative to the 1991-2020 median. Data are from the California Data Exchange Center and the Natural Resource Conservation Service SNOTEL database. Open circles indicate stations that either lack current data or long-term median data.
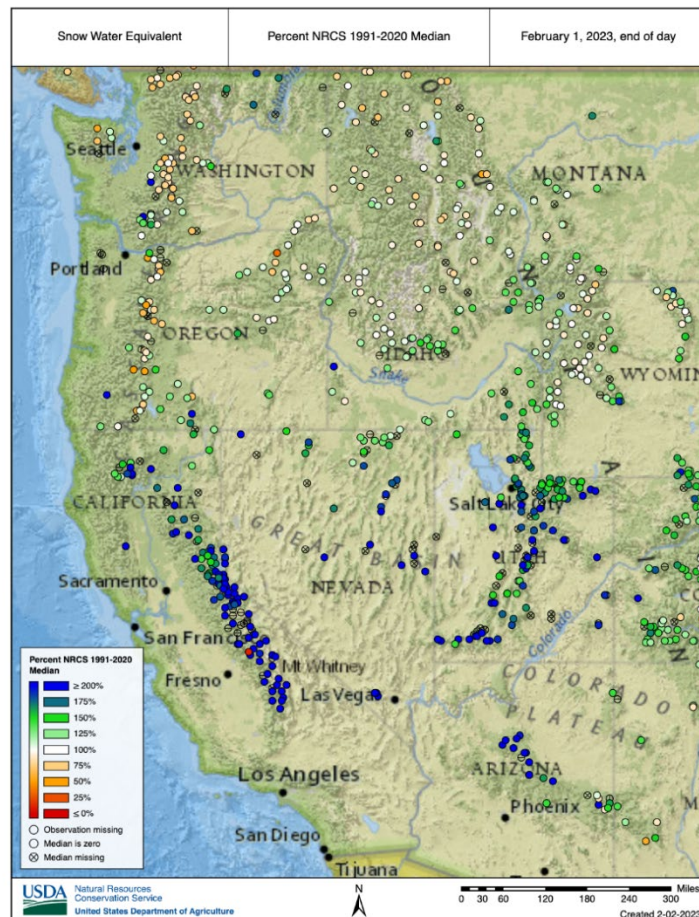
Stream temperature: Mean maximum stream temperatures in August (Fig. G.2) were determined from 446 USGS gages with temperature monitoring capability. While these gages did not necessarily operate simultaneously throughout the period of record, at least two gages provided data each year in all ecoregions. Stream temperature records are limited in California, so two ecoregions (Sacramento/San Joaquin and Southern California Bight-Baja) were combined. Maximum temperatures exhibit strong ecoregional differences in absolute temperature (for example, Salish Sea and Washington Coast streams are much cooler on average than California streams). Stream temperatures at the ecoregion scale have an increasing trend over the past five years in all regions except the Salish Sea and Washington Coast (Fig. G.2).
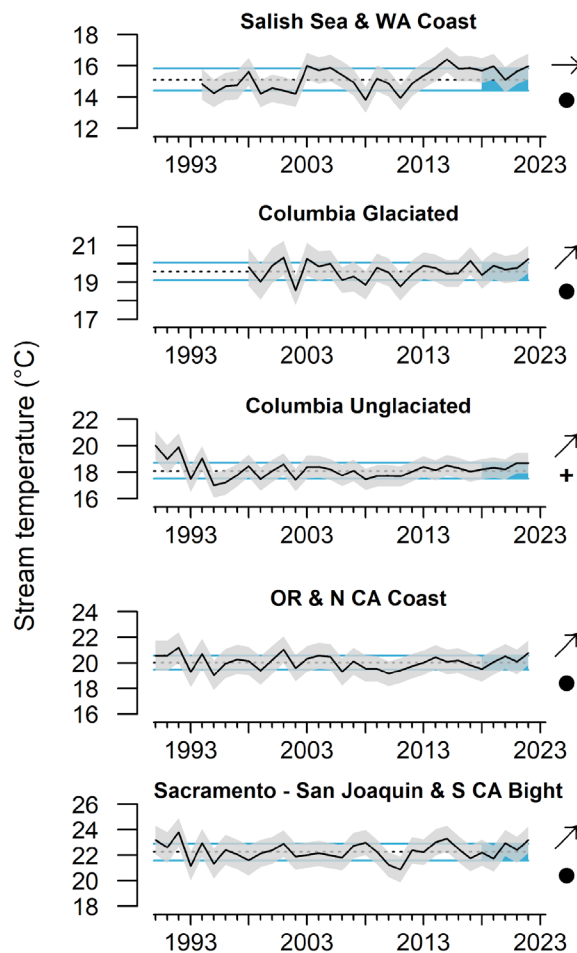

Figure G.2: Mean maximum stream temperatures in August measured at 466 USGS gages from 1990-2022. Gages include both regulated (subject to hydropower operations) and unregulated systems, although trends are similar when these systems are examined separately. Error envelopes represent 95% credible intervals (CI). Lines, colors and symbols are as in Fig. 2.1.

Minimum and maximum streamflow: Flow is derived from active USGS gages with records that are of at least 30 years' duration (waterdata.usgs.gov/nwis/sw). Daily means from 213 gages were used to calculate annual 1-day maximum and 7-day minimum flows. These indicators correspond to flow parameters to which salmon populations are most sensitive.

We use standardized anomalies of streamflow time series from individual gages. Seven-day minimum flows in 2022 were average to below-average, and five-year trends are level except for a decreasing trend in the Sacramento-San Joaquin ecoregion (Fig. G.3).
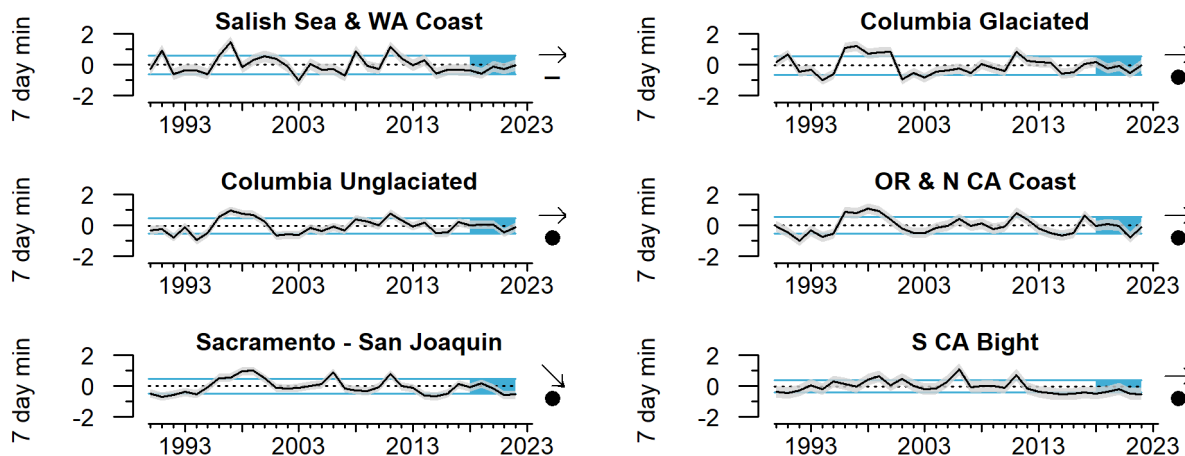

Figure G.3: Anomalies of 7-day minimum streamflow measured at 213 gages in six ecoregions from 1990-2022. Gages include regulated (subject to hydropower operations) and unregulated systems, though trends are similar when these systems are examined separately. Gray envelopes represent 95% credible intervals. Lines, colors and symbols are as in Fig. 2.1.

One-day maximum flows in 2022 were above average in the Salish Sea and Washington Coast ecoregion, but average to below-average in other ecoregions (Fig. G.4). Five-year trends are mixed, from increasing in the Salish Sea and Washington Coast ecoregion to decreasing in the Sacramento-San Joaquin ecoregion.
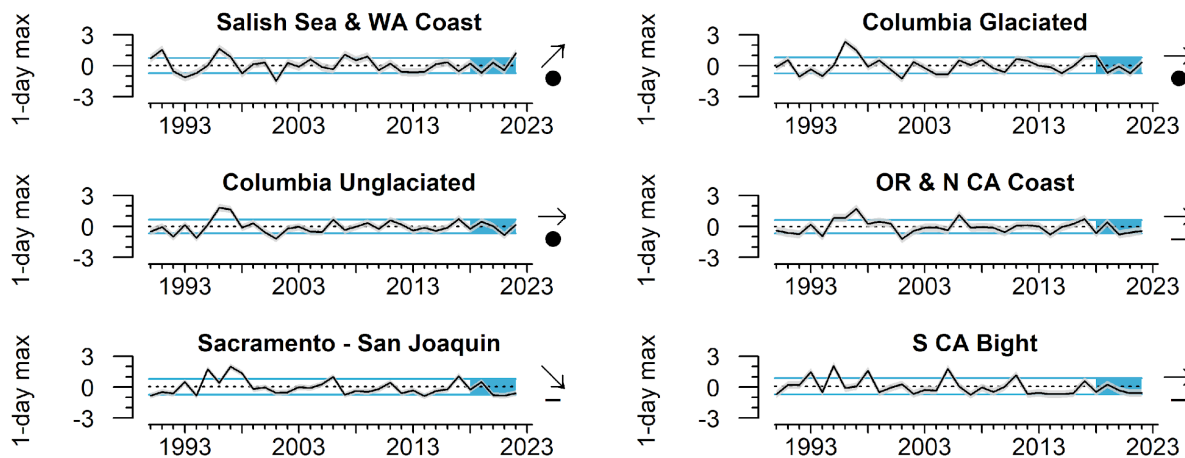

Figure G.4: Anomalies of 1-day maximum streamflow measured at 213 gages in six ecoregions from 1990-2022. Gages include both regulated (subject to hydropower operations) and unregulated systems, although trends are similar when these systems are examined separately. Gray envelopes represent 95% credible intervals. Lines, colors and symbols are as in Fig. 2.1.

Appendix H: REGIONAL FORAGE AVAILABILITY

H.1 NORTHERN CALIFORNIA CURRENT FORAGE

The Northern CCE survey (known as the Juvenile Salmon Ocean Ecology Survey, JSOES) occurs in June and targets juvenile salmon in surface waters off Oregon and Washington (Fig. 1.1). It also collects adult and juvenile (age 1+) pelagic forage fishes, market squid, and gelatinous zooplankton with regularity. A Nordic 264 rope trawl is towed at the surface (upper 20 m) for 15-30 min at approximately 6.5 km/hr. The gear is fished during daylight hours in near-surface waters, which is appropriate for targeting juvenile salmon.

In 2022, catches of juvenile chum salmon were nearly 1 s.d. above the long-term survey mean, while juvenile sockeye catches were closer to the long-term mean; both had non-significant 5-year trends (Fig. H.1, top). As shown in the main body of the report (Fig. 3.6), catches of juvenile subyearling and yearling Chinook salmon and juvenile coho salmon were close to average in 2022 (data not shown here).
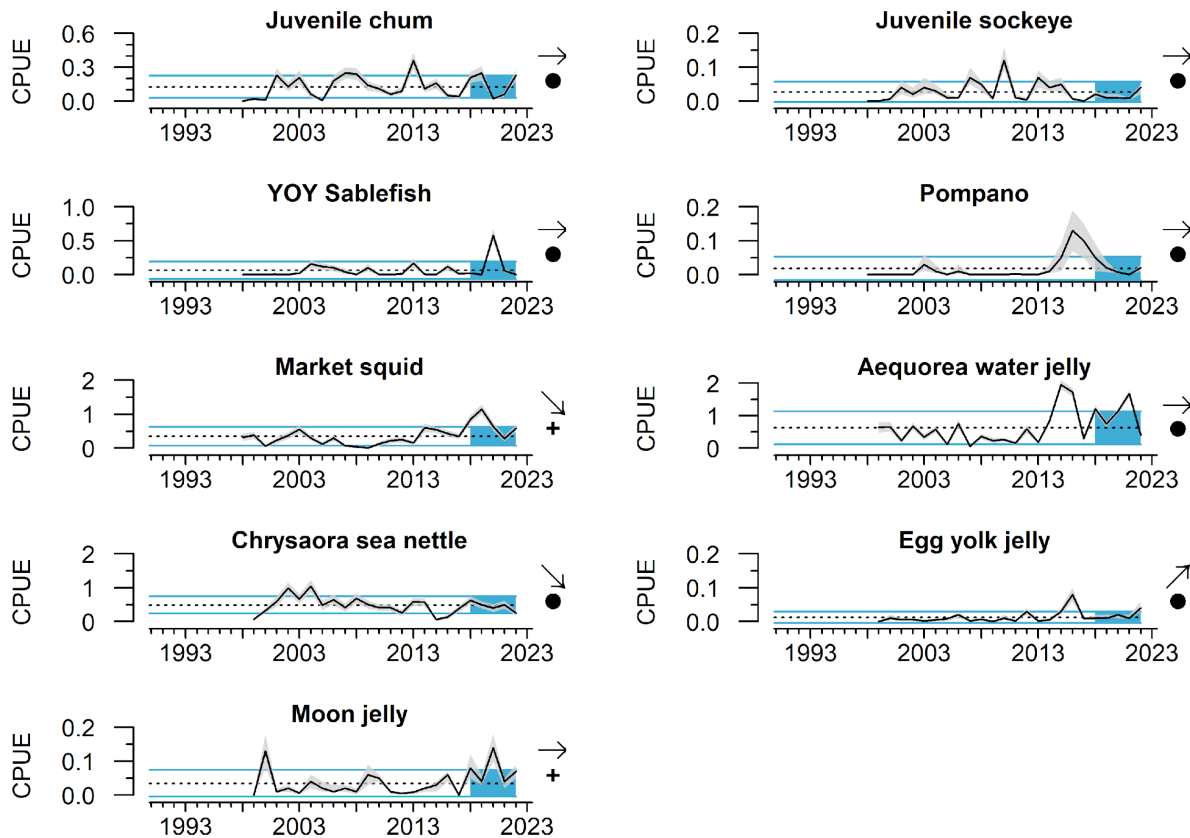

Figure H.1: CPUE (log₁₀(number/km+1)) for pelagic species in the Northern CCE, 1998-2022. Lines, colors, and symbols are as in Fig. 2.1.

Among non-salmonids, catches of many species have been dynamic since the values associated with the 2013-2016 marine heatwave (Fig. H.1). Catches of age-0 sablefish were close to average again in 2022, and well below the sharp peak in 2020. Pacific pompano (butterfish), a warmer-water fish whose catches peaked in 2016, were close to the time

series average in 2022. Catches of market squid in 2022 increased compared to 2021 and were about 1 s.d. above the time series average, and market squid catches over the most recent five years have been above average overall in this survey. Among the gelatinous zooplankton off Washington and Oregon, beginning in 2015 community composition transitioned from dominance of the large, cool-water sea nettle jellyfish (*Chrysaora fuscescens*) to the more offshore-oriented water jellyfish (*Aequorea* spp.). By 2019, both had returned to roughly average densities. In 2022, catches of both sea nettles and water jellies were low relative to the time series averages (Fig. H.1). Catches of egg yolk jellies were above average, resulting in a short-term positive trend, and moon jelly catches were above average, as they have tended to be in over the most recent five years. These two jellyfish species tend to be associated with warmer or offshore water masses.

Preliminary results (data not shown) from a related survey, which samples waters north of Cape Mendocino using the same methodology as the survey for the Central CCE (midwater trawls deployed at night; see next section), suggest that abundances of effectively sampled fish (YOY rockfish, YOY Pacific hake, YOY sanddabs, adult anchovy, and myctophids) and pelagic invertebrates (market squid, octopus, and krill) were below time series averages. We note, however, that the time series for this survey of the Northern CCE is short compared with other West Coast surveys, extending only from 2011-2022. We hope to include more results from this survey in future reports.

H.2   CENTRAL CALIFORNIA CURRENT FORAGE

The Central CCE forage survey (known as the Rockfish Recruitment and Ecosystem Assessment Survey, RREAS) samples much of the West Coast each May to mid-June, using midwater trawls sampling between 30 and 45 m depths during nighttime hours. The survey targets young-of-the-year (YOY) rockfish species and a variety of other YOY and adult forage species, market squid, adult krill, and gelatinous zooplankton. Juvenile rockfish, anchovy, krill, and market squid are among the most important prey for CCE predators (Szoboszlai et al. 2015). Time series presented here are from the "Core Area" of that survey, centered off Monterey Bay (Fig. 1.1). Catch data were standardized by using a delta-lognormal GLM to estimate year effects while accounting for spatial covariates to yield relative abundance indices, shown with their approximate 95% credible intervals (Santora et al. 2021). This modeling approach was adopted in recent reports to reduce bias in 2020, when sampling effort and spatial coverage was severely constrained by the COVID-19 pandemic (see Appendix G of Harvey et al. 2021). The 2022 survey effort in the "Core Area" was comparable to previous years apart from 2020. The relative CPUE reported is the standardized mean ln(index + 1).

Indices of key forage taxa in 2022 suggest continued high abundance adult northern anchovies, despite a decline from recent record high levels, while YOY anchovy declined to the time series average (Fig. H.2). Very few Pacific sardine were encountered in the central region in 2022, and catches in recent years of sardine are insufficient to say anything meaningful about abundance other than that it is very low. The anchovy and sardine results in this region are consistent with findings from a coastwide acoustic-trawl CPS survey in 2022 (see Appendix I).
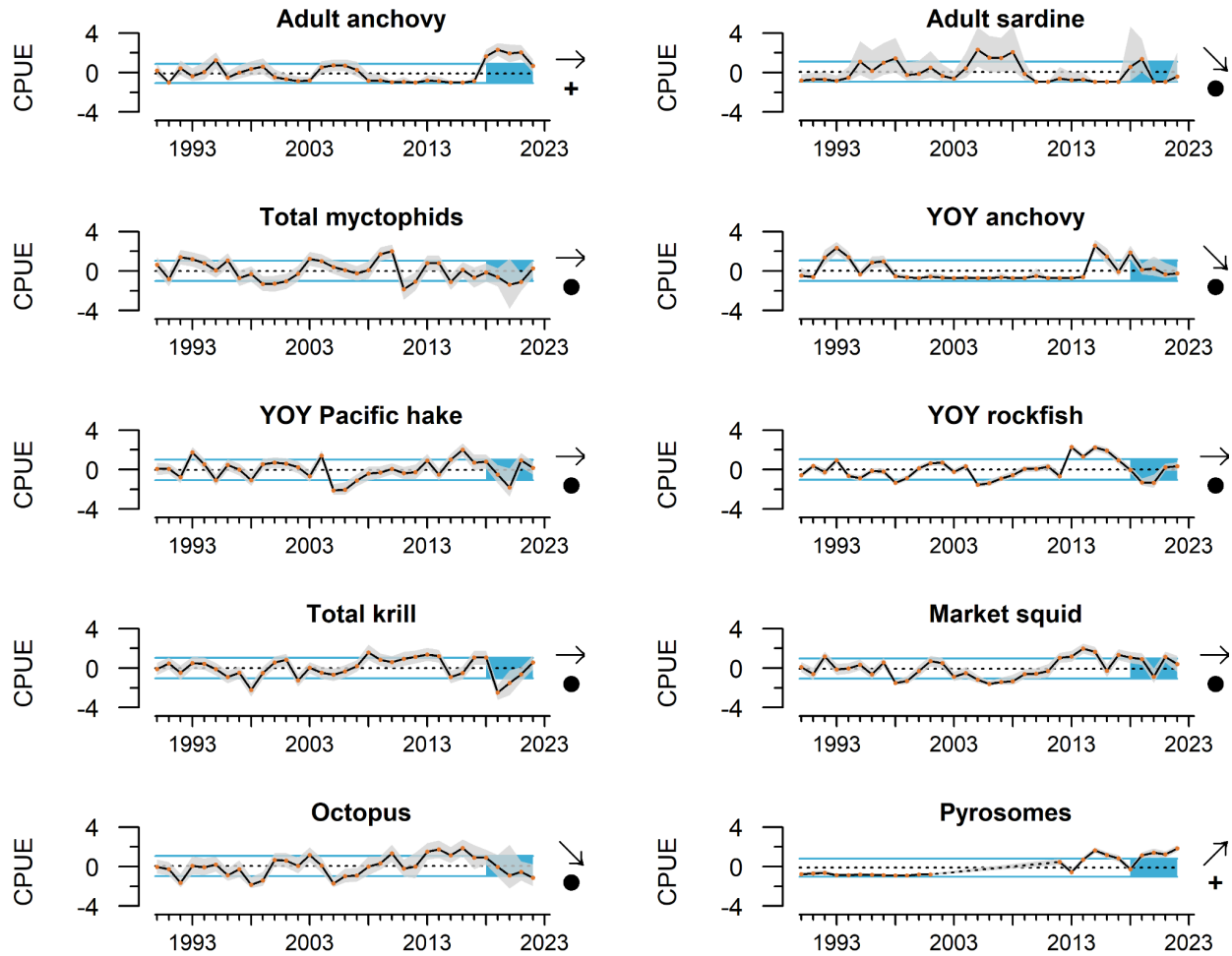
Figure H.2: CPUE (mean ln(delta-GLM index +1) and 95% CI) anomalies of a subset of key forage groups in the Core Area of the Central CCE, 1990-2022. Lines, colors, and symbols are as in Fig. 2.1.

We observed close to long-term average abundance levels of YOY groundfish (rockfish, sanddabs, and Pacific hake) in 2022 (Fig. H.2). Krill abundance continued a steady increase from the low levels observed in 2019, and myctophids (lanternfishes) were more abundant than the previous few years, but close to long-term average levels. Market squid and octopus were slightly less abundant in 2022 relative to recent years. Overall these trends indicate a fairly productive ecosystem, with anchovy continuing to dominate the forage community but with a greater abundance of alternative forage, and with very few taxa being at low abundance levels. The consistency of community structure is further reflected in the "ecosystem state index" in Appendix O.

Indices of abundance for key gelatinous zooplankton off of central California indicate that catches of pyrosomes in 2022 were at the highest observed levels of the time series, even greater than observed during the large marine heatwave of 2015-16 (Fig. H.2). However, catches of salps (*Thetys vagina* and other unidentified salp species) were close to long-term average levels (data not shown). Catches of large scyphozoan jellyfish (sea nettles and moon jellies) were at fairly high levels in 2022, generally in more nearshore waters (data not shown).

H.3   SOUTHERN CALIFORNIA CURRENT FORAGE

Abundance indicators for forage in the Southern CCE come from fish and squid larvae collected in the spring (May-June) across all core stations of the CalCOFI survey (Fig. 1.1). Larval data are indicators of the relative regional abundances of adult forage fish, such as sardine and anchovy, and other species, including certain groundfishes, market squid, and mesopelagic fishes. The survey samples a variety of fish and invertebrate larvae (typically <5 d old) from several taxonomic and functional groups, collected via oblique vertical tows of fine mesh Bongo nets to 212 m depth. In 2020, the spring larval survey was canceled due to COVID-19, but spring survey operations resumed in 2021.
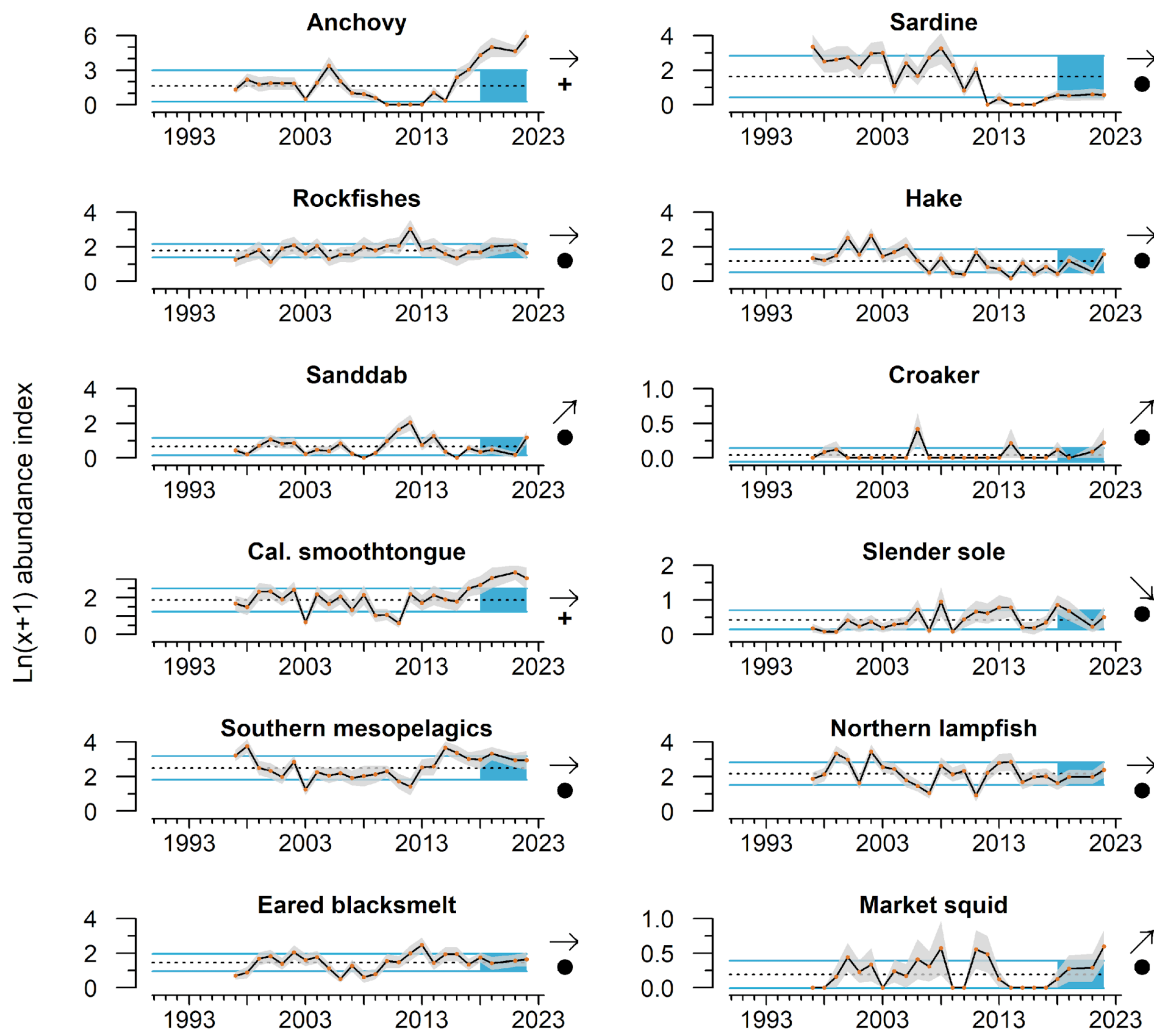

Figure H.3: Mean abundance (ln(x+1)) index of the larvae of key forage species in the Southern CCE, from spring CalCOFI surveys during 1997-2022 (no data from 2020). Lines, colors, and symbols are as in Fig. 2.1.

Catches of larval anchovy in spring 2022 were the highest in the time series for this region, surpassing the previous record high in 2021, and larval anchovy numbers continued their strongly significant increase in recent years (Fig. H.3). This included unusually large catches of larval anchovy well beyond the shelf break (A. Thompson, SWFSC, pers. obs.). Catches of

sardine larvae have been low since 2012 and remained low in 2022. Larval rockfish catches were down from 2021 and just below the time series average, while larval Pacific hake catches increased from 2021 and were close to 1 s.d. above the average. Larval sanddabs and croaker catches were above average in 2022 and contributed to short-term increasing trends. Larval slender sole were close to average in 2022 after several years of declining from a peak in 2018. Among mesopelagic taxa, larval California smoothtongue continued a strongly increasing trend and had the second highest catch in 2022, and an assemblage of southern mesopelagics remained relatively abundant. Northern lampfish and eared blacksmelt were close to average. Market squid paralarvae, which were absent from 2013-2017 have increased steadily and significantly since 2017 and had the second highest abundance in 2022. Data on this community structure are critical components of the "ecosystem state index" in Appendix O.

Preliminary results (data not shown) from a related survey, which samples waters south of Point Conception using the same methodology as the survey for the Central CCE (midwater trawls deployed at night, targeting YOY and adult forage taxa; see previous section), suggest that YOY northern anchovy in the Southern CCE were abundant relative to the long-term trend, while adult anchovy were close to the regional average and less abundant than in central California (however, that related survey, which is the southernmost extent of the RREAS, was restricted to the shelf, whereas the CalCOFI larval survey found copious anchovy west of the shelf). YOY rockfish and krill in Southern CCE waters were slightly below long-term mean levels, while YOY hake and pelagic octopus were slightly above long-term mean levels. We hope to include more results from this survey in future reports.

Appendix I: COASTAL PELAGIC SPECIES FROM SUMMER 2022

Acoustic-trawl method (ATM) surveys have been used by the NOAA Southwest Fisheries Science Center in most years since 2006 to map the distributions and estimate the abundances of coastal pelagic fish species (CPS) in the coastal region from Vancouver Island, Canada, to San Diego, California (e.g., Demer et al. 2012; Zwolinski et al. 2014; Stierhoff et al. 2020) but in 2021 and 2022, expanded to include portions of Baja California, Mexico (Stierhoff et al. 2023, Stierhoff et al., in prep.). Surveys cover waters to at least the 1,000-fathom (1829-m) isobath, or 65 km from shore. The five most abundant CPS in this domain are northern anchovy, Pacific herring, Pacific sardine, jack mackerel, and Pacific mackerel (Fig. I.1). The ATM combines data from echosounders, which record CPS echoes, and trawls, which produce information about the composition, sizes, and ages of the fishes that produce them. This survey also samples the density of CPS eggs in near-surface water using a continuous underway fish egg sampler (CUFES) mounted on the ship's hull at 3-m depth (Stierhoff et al. 2020).

In summer 2022, the plan was to survey from Cape Flattery, WA to Punta Eugenia, Baja California. However, due to insufficient crew, the first of four cruise legs on the NOAA Ship *Lasker* was canceled. To mitigate, the chartered F/V *Lisa Marie* and two uncrewed surface vessels (Saildrones) were reassigned to sample the area north of Cape Mendocino in tandem. From July 21 to August 2, the *Lisa Marie* sampled 33 acoustic transects from Cape Flattery to

Bodega Bay, and made 41 purse-seine sets. From July 23 to August 31, the Saildrones acoustically sampled 24 transects from Neskowin, OR to Beaver Point, CA. Meanwhile, the *Lasker* sampled 62 transects and conducted 88 trawls from Cape Mendocino, CA to Punta Baja, Baja California. A separate chartered vessel, F/V *Long Beach Carnage*, sampled 129 nearshore transects and conducted 53 purse-seine sets from Bodega Bay to San Diego and around Santa Cruz and Santa Catalina Islands (Fig. I.1).

Acoustic backscatter from CPS was mapped throughout the survey area (Fig. I.1a). Egg samples showed that jack mackerel spawned north of Bodega Bay, CA and offshore between Long Beach, CA and San Diego, CA, and northern anchovy spawned principally from Bodega Bay to San Diego, but extending to El Rosario, Baja CA (Fig. I.1b). Northern anchovy were caught in trawls primarily from Bodega Bay south to San Diego (Fig. I.1c). The northern stock of Pacific sardine were caught from the Columbia River to Fort Bragg, CA; and Pacific herring were caught off Washington (Fig. I.1d). Larger jack mackerel, some schooling with relatively few Pacific sardine, escaped capture in the daytime purse-seine sets, while smaller jack mackerel were caught nearshore.
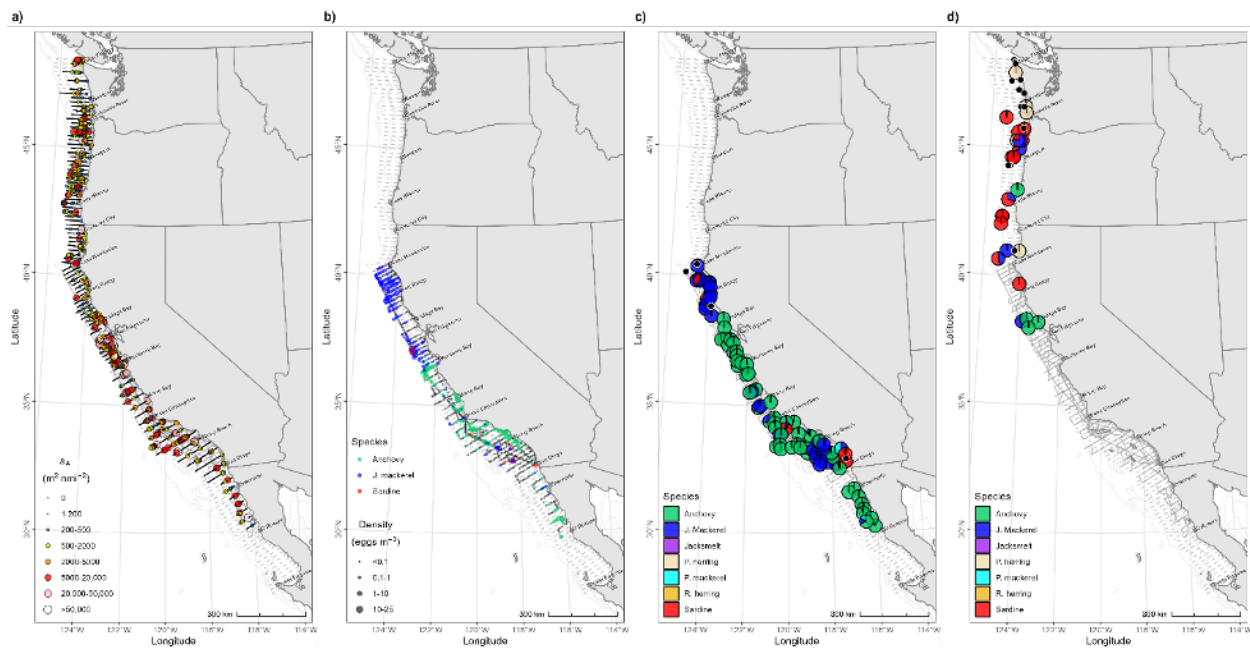

Figure I.1: Data from the summer CPS 2022 survey: a) integrated 38-kHz volume backscatter coefficients attributed to CPS; b) CPS eggs collected with a Continuous Underway Fish Egg Sampler; c) proportions of CPS in R/V Lasker*'s nighttime trawl catches; and d) proportions of CPS in F/V* Lisa Marie*'s daytime purse-seine catches. (Note: jack mackerel escaped many purse-seine sets, so are underrepresented in catch proportions north of Cape Mendocino.)*

The survey time series of estimated CPS biomasses from summer 2008 to 2022 (Fig. I.2) shows that the forage fish assemblage in the CCE was dominated by the northern stock of Pacific sardine until 2013, a low biomass of jack mackerel in 2014 and 2015, and then the central stock of northern anchovy since 2015. In 2022, as it was a half century ago (Mais et al., 1974, 1977), the CPS assemblage is now mostly comprised of northern anchovy and to a lesser extent jack mackerel (preliminary data, subject to change; Stierhoff et al., in prep.).

The central stock of northern anchovy began to resurge in 2015 and grew exponentially to ~2.75 million t by 2021 (Fig. I.2; Stierhoff et al. 2023). In 2022, the stock biomass declined by roughly 18% (preliminary data, subject to change; Stierhoff et al., in prep.), suggesting that the stock may have reached its carrying capacity. While the jack mackerel biomass has increased within the survey area since its low in 2013 (Fig. I.2), the biomass of Pacific mackerel has remained low throughout the survey area. The northern stock of sardine has remained relatively low since 2013. The southern stock of sardine has also been present in U.S. waters in recent years (Fig. I.2. and I.3); while Figure I.2 represents the estimated biomass throughout the survey area, including Mexico in 2021 and 2022, the estimated portion of the southern stock in U.S. waters has ranged from 33,093 t in 2018 (Stierhoff et al., 2019), 14,890 t in 2019 (Stierhoff et al., 2020), to 76,823 t in 2021 (Stierhoff et al., 2023), and roughly 70,000 t in summer 2022 (preliminary and subject to change; Stierhoff et al., in prep.).
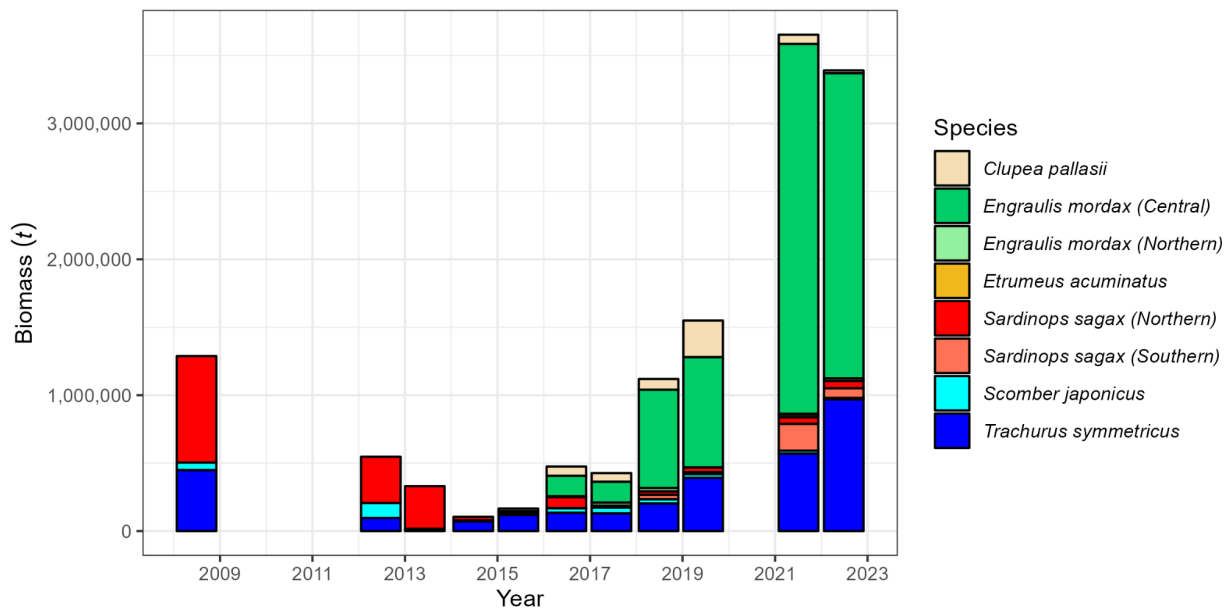

*Figure I.2: Cumulative estimated biomass for Pacific herring (*Clupea pallasii*), northern anchovy (*Engraulis mordax*), round herring (*Etrumeus acuminatus*), Pacific sardine (*Sardinops sagax*), Pacific mackerel (*Scomber japonicus*), and jack mackerel (*Trachurus symmetricus*) within the summer CPS survey areas, 2008-2022. Surveys typically span the area between Cape Flattery and San Diego, but in some years also include Vancouver Island, Canada (2015-2019) and portions of Baja CA (2021-2022). (Note: 2022 data are preliminary and subject to change.)*

Since the resurgence of the central stock of northern anchovy, beginning in 2015, there has been consistency in the regional distributions of the three dominant species: northern anchovy, jack mackerel and Pacific herring (Fig. I.3). Pacific herring are caught mostly north of central Washington. Lower biomasses of northern stock Pacific sardine and northern stock northern anchovy are resident off Oregon and Northern California (Stierhoff et al., 2023, in prep). Jack mackerel are caught between central Washington and Cape Mendocino, often along with fewer northern stock Pacific sardine in recent years. Central stock northern anchovy are caught south of Cape Mendocino and, with the exception of summer 2021, mostly south of Bodega Bay. The smaller northern stock is resident from central Washington

to northern California. The summer 2022 distribution of northern anchovy appears to have shifted south, better aligning with its distributions during 2015-2019. In contrast to earlier surveys in the time-series, the southern stock of Pacific sardine has been persistently present in U.S. waters, mostly in the Southern California Bight (Fig. I.3).
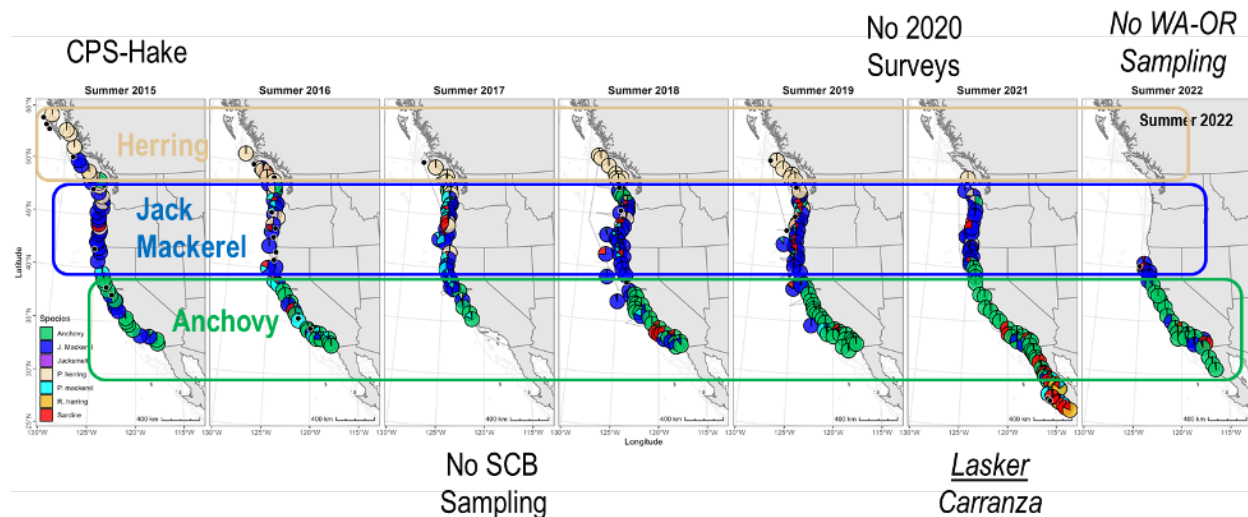

Figure I.3: Distributions of species proportions in the R/V Lasker*'s nighttime trawl catches, summer 2015 through 2022. In 2015, the integrated CPS-hake survey sampled northward of Vancouver Island. In 2017, there was no sampling in the Southern California Bight (SCB). In 2020, there was no survey due to the COVID-19 pandemic. In 2021, through a collaboration with Mexico, the CPS survey extended farther south into Baja California. In 2022, there was no nighttime trawl sampling north of Cape Mendocino, California.*

Appendix J: SALMON

J.1 GENERAL CHANGES TO THE SALMON INDICATOR PORTFOLIO

The CCIEA team and SSC-ES met in September 2022 for our annual discussion and technical review of topics selected in March, as was outlined under FEP Initiative 2. One of the topics in September 2022 was to review and possibly revise the suite of indicators and analyses related to salmon. Three of the main outcomes of that review are described here.

Hydrology Indicators: In recent reports, we have reported maximum and minimum streamflow indicators at two spatial scales: whole ecoregions (as mapped in Fig. 1.1) and also at a finer scale of 16 Chinook salmon evolutionarily significant units (ESUs) spanning from the Salish Sea to central California and inland. With the support of the SSC-ES, we have opted to only present plots of the large-scale streamflow indicators going forward (see Appendix G). We made this decision mainly because ecoregion-level indicators are more appropriate for the broad, contextual focus of this report, and also to save space and promote efficiency of report production. The ESU-level indicators will remain available on the CCIEA's indicator webpage, and some fine-scale hydrological indicators remain in use in stock-specific stoplight tables Section 3.3 and below in Appendix J.3.

Escapement indicators: In past reports, we have included time series of Chinook and coho salmon escapements at the scale of ESUs. These time series have potential value as ecosystem indicators, particularly on the numbers of juveniles likely to be produced in natural spawning areas, and potentially some indication of overall ecosystem productivity for salmon stocks from different regions. However, following discussions with the SSC-ES in September 2022, we have concluded that we should no longer present escapements in our report, with the exception of the spawning escapement indicator in the Central Valley Fall Chinook salmon stoplight table (main body, Table 3.2). We made this change, due to a range of concerns. Chiefly, the averages and trends within the scale of the time series available to us may not be representative of historic escapement levels and variability, or of the magnitude of change that may be needed to reach target reference points for particular stocks. Thus, short-term increases or "above average" escapements within our time series may appear overly optimistic. In addition, our time series have consistently been out of date by one or more years, and some ESUs have relatively few and possibly decreasing numbers of index populations to provide status data. Finally, the Council is getting more comprehensive and up-to-date information on salmon escapements and run size reconstructions from the Salmon Technical Team in concurrent reports (e.g., PFMC 2022b).

Stoplight table format: For both the stoplight tables presented in Table 3.1 and below in Appendix J.3, we use color to represent anomalous years. Prior to revision, the tables separated years into three ranked bins of equal size (one third of values, those with the lowest rankings of the respective time series, were colored red and represented "poor" values for salmon; the next third were yellow and represented "average" values; and the highest-ranking third were green and represented "good" values). This approach was easy to digest, but was criticized over the years by the SSC and others for many reasons, including that with each new year of data, some past values could readily shift from one category to another (e.g., from yellow to red) simply on the basis of their updated ranking, with illogical disregard for the underlying biology or ecology. Also, as the time series grew longer, large numbers of years were being lumped together into just three categories, which could leave the impression that, for example, slightly above-average years were qualitatively similar to exceptionally above-average years.

We have addressed these concerns by developing a more statistically based stoplight table format that produces five bins that are determined relative to a fixed baseline reference period. In the new version of the tables, we assumed a normal distribution for each of the indicators, estimating a mean and standard deviation for the base period. For each cell within a given indicator, we determined how many standard deviations the values were from their respective base period mean and used a five-color set to indicate whether a value was >2 s.d. below the mean, within 1 and 2 s.d. below the mean, within 1 s.d. of the mean in either direction, 1 to 2 s.d. above the mean, or >2 s.d. above the mean. We did this for the years within the base period, and then used the same base period mean and s.d. for the more recent years. This approach overcomes many of the issues that have been previously identified (e.g., better highlighting values that represent truly exceptional years; past values are now static and do not suddenly change colors; etc.).

J.2   ECOSYSTEM INDICATOR-BASED OUTLOOKS FOR CHINOOK SALMON ESCAPEMENT IN THE COLUMBIA BASIN

In the main report, Table 3.1 provides a qualitative, ecosystem-based "stoplight" outlook of returns of Columbia Basin Chinook salmon in 2023, based on indicators of conditions affecting early marine growth and survival. A related quantitative analysis, which is still being refined in response to feedback from the SSC-ES and other partners, uses an expanded set of >40 ocean indicators and mark-recapture data to estimate smolt-to-adult survival of Chinook salmon from the Upper Columbia and Snake River basins.

In this analysis, models are fit to the smolt-to-adult return data, and these models use the most recent ecosystem indicator data to predict what smolt-to-adult survival will be for cohorts that have gone to sea but not yet returned. Separate models have been developed for spring and fall Chinook salmon from the Upper Columbia Basin and Snake River basins. The specific approach uses a Dynamic Linear Model, founded on linear regressions of single ecosystem indicators vs. survival rates of PIT-tagged fish that left Bonneville Dam as smolts and returned as adults (Fig. J.1, black lines). Through a combination of ranking models based on predictive ability and eliminating potential variables using Variance Inflation Factors, the number of ecosystem indicators is reduced iteratively (arbitrarily to ~10) while minimizing the covariance among the remaining indicators. Rather than relying on any single model, we present results from multiple models (Fig. J.1, colored points) that use: 1) the first Principal Component (PC1, derived from a Principal Components Analysis) of the NOAA stoplight chart and 2) the PC1 calculated from a new set of ocean indicator variables specific to each stock.

For Snake River smolts that went to sea in 2021 (which should dominate adult returns in 2023), the survival estimates are well above the averages for the past ten years. For Snake River spring/summer Chinook (Fig. J.1, upper left) and Snake River fall Chinook salmon (Fig. J.1, lower left), the 2021 smolt year is estimated to have survival up to almost double the ten-year average, though there are large differences between the various estimates and moderate uncertainty within the estimates. Similarly, for Upper Columbia spring and fall Chinook smolts that went to sea in 2021 (Fig. J.1, right column), estimated survival is substantially higher than the average of the past ten years, and greater than what was modeled or observed for the 2020 cohort. Uncertainty in the estimates (95% Prediction Intervals, gray vertical lines in Fig. J.1) is relatively high compared to the time series confidence intervals, particularly for the fall-run stocks.

For all four ESUs, survivals of the 2022 smolt cohorts, which will dominate returns in 2024, are estimated to be similar to or lower than survival for the 2021 cohort. Decreases in estimated survival reflect the very favorable ocean indicators observed in waters off of Washington and Oregon in late 2020 and the first half of 2021 and the decline in conditions during 2022 (main body of the report, Table 3.1).
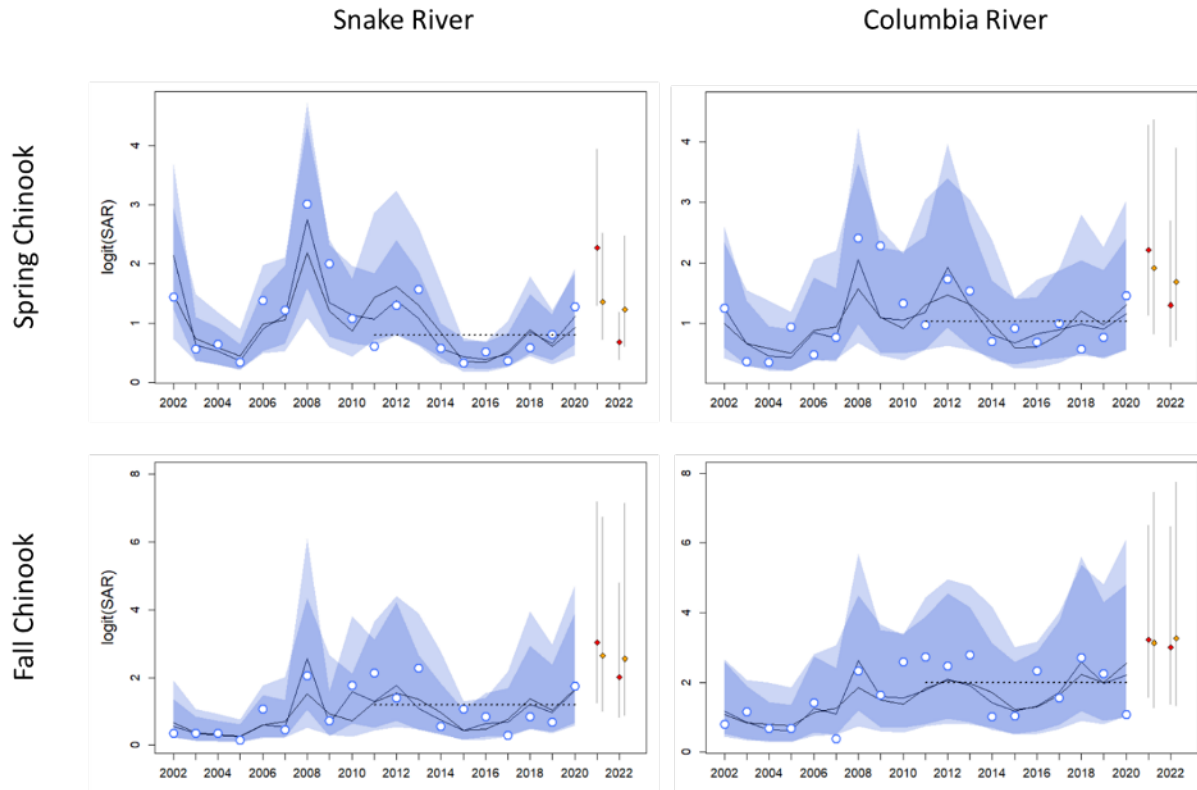
Figure J.1: Observed and modeled smolt-to-adult returns (SAR) of Chinook salmon from the Snake River and Upper Columbia River ESUs (summer-run fish are included with spring-run fish in the Snake River and with fall-run fish in the Upper Columbia River). Years on the x-axes are smolt migration years. Dark lines are different model fits; blue shaded areas are 95% confidence intervals; open circles are estimated SAR values based on PIT tag data; dashed lines are recent 10-year averages; and colored points are model outlooks with 95% prediction intervals for smolt years 2021 and 2022 (dominant return classes in 2023 and 2024, respectively). Red points are from models that use the original stoplight chart Table 3.1 and orange points are from unpublished stock-specific stoplight charts.

Although Table 3.1 represents a general description of ocean conditions related to multiple populations, we acknowledge that the importance of any particular indicator will vary among salmon species and runs. These new analyses represent progress toward greater distinction among different ESUs than some results shared in previous ecosystem status reports. NOAA scientists and partners continue to work toward stock-specific salmon outlooks by using both correlative and mechanistic methods that can optimally weight the indicators for each response variable in which we are interested. We will continue to work with the Council and advisory bodies to identify data sets for Council-relevant stocks for which analyses like these could be possible.

J.3   ECOSYSTEM CONDITIONS FOR FALL CHINOOK SALMON IN CALIFORNIA

Central Valley Fall Chinook salmon stoplight table: In our 2019-2020 ecosystem status report, we introduced a relatively simple "stoplight" table of ecosystem indicators that were shown by Friedman et al. (2019) to be correlated with returns of naturally produced Central Valley Fall Chinook salmon. An updated stoplight chart for adult Fall Chinook salmon

returning to the Central Valley in 2023 is in Table 3.2. Reflecting discussions with the SSC-ES in September 2020 and September 2022, we emphasize that Table 3.2 is strictly qualitative and contextual decision-support information, although the qualitative descriptors (color-coded terms like "very poor" in Table 3.2) are rooted in quantitative biological or ecological relationships in the fall Chinook salmon life cycle, or in management targets. The description below provides additional information relative to past ESRs, and follows from the September 2022 meeting with the SSC-ES.

The biological and ecological relationships in Table 3.2 are summarized in Figure 5 in Friedman et al. (2019). According to that analysis, the most influential processes related to Sacramento River fall Chinook salmon escapement to natural areas included river temperature during the incubation period, (winter) freshwater flow during rearing and outmigration, and environmentally mediated predation during the 1st spring at sea, along with spawning escapement and ocean harvest rates. The focal ecosystem indicators are: spawning escapement of parent generations; egg incubation temperature between October and December at Red Bluff Diversion Dam (Sacramento River); median flow in the Sacramento River in the February after fry emergence; and a marine predation index based on the abundance of common murres at Southeast Farallon Island and the proportion of juvenile salmon in their diets. The relationship between river temperature and egg mortality is derived from an in-river temperature-dependent egg mortality model by Martin et al. (2017) that is supported by lab and field data. February median flow is related to rearing area quantity and quality, and also is correlated with outmigration success (Munsch et al. 2020); it is also positively correlated with March-May net river delta outflow, and is therefore likely an indicator of hatchery smolt outmigration success (Michel 2019). The ocean predation index as an indicator of early marine survival was described by Wells et al. (2017) and may also be connected to the influence of "habitat compression" on food web dynamics (Santora et al. 2020); we note, however, that we have not been able to access the underlying data for several years due to data-sharing constraints, and have populated this column of the table based on visual inspection of Figure M.3 in the Seabird Appendix of this ESR.

It is likely that the tremendous biomass of northern anchovy off of central California in recent years has provided juvenile salmon with some buffering from avian predation, and has also promoted marine growth and size-at-age of Central Valley Chinook salmon. IN contrast, predation by female salmon on anchovy can lead to thiamine deficiency in eggs, which presents a potential survival constraint. We do not yet have enough information to determine the net effect of anchovy on Central Valley fall Chinook salmon, and how to best represent it in Table 3.2.

The escapement descriptor is a qualitative evaluation of how natural-area escapement of a parent generation relates to the natural area + hatchery escapement goal of 122,000–180,000 fish, with 122,000 spawners as the S_{MSY} target (PFMC 2022d). Natural area escapement is relevant to Table 3.2 as an indicator of total natural area egg production (e.g., Munsch et al. 2020). However, the qualification of this indicator requires future research. Obviously, our using a natural+hatchery target as the qualifier for natural-only escapement is problematic. Perhaps more importantly, the SSC and STT have both recommended

research and reconsideration of the Sacramento River fall Chinook S$_{MSY}$ objective (PFMC 2022e,f), and Satterthwaite (2022) has concluded that an escapement of 122,000 adults is insufficient to maximize natural production.

Finally, the qualitative nature of this stoplight table is in part due to the fact that some of the parameters used by Friedman et al. (2019) were estimated using information from both natural-origin and hatchery-origin fish, and while it is reasonable to assume that true parameter values would be similar, given correlations between natural and hatchery escapements, additional data specific to natural-origin fish are likely necessary in order to improve model fits, evaluate other potential covariates, and support adequate testing of model predictive skill.

The CCIEA team will continue to explore improvements to Table 3.2 in future ESRs, in concert with the SSC and other interested advisory bodies.

Stoplight tables for Sacramento River and Klamath River Fall Chinook salmon: Rebuilding plans in 2019 for Sacramento River and Klamath River fall Chinook salmon runs prompted annual updates of habitat indicators for these stocks (Harvey et al. 2020). After review by multiple scientists and members of various advisory bodies, members of the Habitat Committee developed a suite of 22 indicators for Sacramento River Fall Chinook salmon (SRFC) and 18 indicators for Klamath River Fall Chinook salmon (KRFC), spanning the full life history of natural-area fish and also including indicators related to hatchery-origin fish (Table J.1). These indicators illustrated a combination of poor freshwater and marine conditions associated with the poor productivity of three critical brood years that triggered the rebuilding plan. Recognizing that these leading indicators could inform risk assessment for poorly assessed stocks, PFMC recently requested additional indicators be developed for Central Valley Spring-run Chinook salmon (CVSC).

Many of the indicators combined in these habitat stoplight tables are already included in other portions of this Ecosystem Status Report. The indicators in Table J.1 have been shown in previous studies or were proposed in rebuilding plans to be strongly related with life-stage specific Chinook salmon productivity, and these studies helped determine expected directionality of indicators with stock productivity (see Harvey et al. 2020 for additional justification). Four of the five broad categories of indicators in the stoplight charts align with the simpler stoplight chart for Central Valley fall Chinook salmon presented in the main body of this report (Table 3.2): Adult Spawners, Incubation conditions, Freshwater/Estuarine Residence conditions, and Marine Residence conditions (for the first year of marine residence). The fifth category of indicators, Hatchery Releases, expands the scope of these tables relative to the 4-indicator chart (Table 3.2) that focuses only on natural-area fish. The habitat indicator charts also share qualities with the stoplight chart developed for Columbia Basin Chinook salmon and Oregon coast coho salmon (Table 3.1) by including regional and basin-scale oceanographic indicators as part of early marine residence conditions. Data on krill biomass off northern California (Figure 3.2) are also presented within the table for KRFC.

Table J.1. Klamath River Fall (KF), Sacramento Fall (SF), and Central Valley Spring-run (CS) Chinook salmon habitat indicators, definitions, and key References. Months indicate the time period for which indicators were summarized, Effect is the predicted directionality of the indicator's effect on productivity, and Stock indicates the runs for which indicators were produced. With the addition of Central Valley Spring indicators, abbreviations of indicator names have changed slightly from previous Ecosystem Status Reports.

Life stage-specific indicator	Abbreviation	Months	Effect	Reference	Stock
Adult spawners					
Spawner counts	Spawners		+	Friedman et al. 2019	KF, SF, CS
Fall closures of Delta Cross Channel	CChannel.F	Sep-Oct	+	Rebuilding plan	SF
Low flows during upstream migration	Flows.U	Sep-Oct*	+	Strange 2012	KF, SF, CS
Temperatures during upstream mainstem	Temp.U	Sep-Oct*	--	Fitzgerald et al. 2021	KF, SF
Holding period flows in Butte Creek	Flows.H	Jun-Sep	+	USFWS, 1995	CS
Holding temperature in Butte Creek	Temp.H	Jun-Sep	-	USFWS, 1995	CS
Prespawn mortality rate	PrespawnM		-	USFWS, 1995	CS
Incubation and emergence					
Fall-winter low flows in tributaries (7Q10)	Flows.I	Oct-Dec*	+	Jager et al. 1997	KF, SF, CS
Egg-fry temperatures (avg of max daily)	Temp.I	Oct-Dec*	–	Friedman et al. 2019	KF, SF, CS
Egg-fry productivity	FW.surv		+	Hall et al. 2018	KF, SF, CS
Freshwater/delta residence					
Winter-spring tributary flows	Flows.T	Feb-May	+		CS
Winter-spring mainstem outmigration flows	Flows.O	Dec-May	+	Friedman et al. 2019	KF, SF, CS
Delta outflow index	Delta	Apr-Jul	+	Reis et al. 2019	SF, CS
7-day flow variation (SD)	SDFlow.O	Dec-May	–	Munsch et al. 2020	KF, SF, CS
Maximum flushing flows	Max.flow	Nov-Mar	+	Jordan et al. 2012	KF
Total annual precipitation	Precip	Annual	+	Munsch et al. 2019	KF, SF, CS
Spring outmigration temperatures	Temp.O	May-Jun	–	Munsch et al. 2019	KF, SF, CS
Spring closures of Delta Cross Channel	CChannel.S	Feb-Jul	+	Perry et al. 2013	SF, CS
Days floodplain bypasses were accessible	Floodpln	Annual	+	Limm & Marchetti 2009	SF, CS
Marine residence					
Coastal sea surface temperature	CSTarc	Mar-May	–	Wells et al. 2008	KF, SF, CS
North Pacific Index	NPI	Mar-May	+	Wells et al. 2008	KF, SF, CS
North Pacific Gyre Oscillation	NPGO	Mar-May	+	Wells et al. 2008	KF, SF, CS
Marine predation index	Predation		–	Friedman et al. 2019	SF, CS
Krill biomass	Prey	Mar-Aug	+	Robertson & Bjorkstedt 2020	KF
Hatchery releases					
Release number	Releases		+	Sturrock et al. 2019	KF, SF, CS
Prop net pen releases	Net.pen		+	Sturrock et al. 2019	SF, CS
Release timing relative to spring transition	FW.Timing	Jan-Aug	+	Satterthwaite et al. 2014	KF, SF, CS
Release timing relative to peak spring flow	M.Timing	Jan-Aug	+	Sykes et al. 2009	KF, SF, CS

*For CS, adult upstream migration time period and incubation period is Feb-May and Sep-Dec, respectively.

The indicators in Table J.1 and in the stoplight tables below have undergone several important adjustments from previous reports:

- Updates to SRFC and KRFC include changes in some indicators to ensure more reliable and timely data capture. Due to delays in posting of online datasets, broken links, and reduced monitoring budgets, over 10 indicators could not be automatically updated, which necessitated the assistance of many individuals at different agencies to update indicators. Even so, brood year updates for egg-fry indicators can no longer be included in the current ESR, and the seabird predation indicator will no longer be updated. These challenges underscore the importance of including multiple indicators, highlight the potential fragility of these annual summaries, and point to the importance of many individuals for maintaining the databases required for summarizing habitat indicators.
- This is the first year that habitat indicators for CVSC have been developed. This run differs from SRFC not only in migration timing but also in their behavior and spatial distribution. These differences necessitated modifications to the suite of habitat indicators to characterize early upstream migration starting in February, holding in pools through the summer, and spawning in a small number of creeks in the late summer and fall. Adult numbers focused on spawner counts in Butte, Mill, and Deer Creeks. Butte Creek spawners migrate from the Sacramento River through Sutter Bypass to Butte Creek, and outmigrants may rear within Sutter Bypass during outmigration. Hence, flow and temperature metrics relied on gages from these systems in addition to the Sacramento mainstem, and Sutter Bypass inundation instead of Yolo Bypass. Finally, the sole hatchery for CVSC is from Feather River, so releases and timing metrics focused on data from just this hatchery.
- The stoplight tables are categorized from favorable to poor conditions using the same new approach as described for the Northern California Current salmon indicator stoplight table (see main body, Table 3.1). Specifically, after indicator datasets were collected, all indicators were "directionalized" to account for potential inverse relationships of some indicators with stock productivity (based on the "Effect" column in Table J.1) and converted into standardized values. These values are reported in the stoplight tables below, with colors delineating statistically meaningful departures (>2 s.d.) toward poorer (warm shades) or more productive (cool shades) conditions compared to near-average years (within ±1 s.d., yellow). The main difference for the tables shown here relative to Table 3.1 is that we have not yet determined a fixed historic reference period for the SRFC, KRFC and CVSC tables, due in part to missing data from one or more indicators in large portions of the time series.

Below we present stoplight table updates for habitat indicators for all three stocks. Previous examination of the KRFC and SRFC stoplights indicated that these indicators tended to cycle every 5 to 10 years; that the cycles were out of phase for freshwater and marine conditions; and that freshwater conditions for the Klamath stock exhibited a long-term decline since the 1990s. Updates for the most recent brood year and previous trends show that these patterns continue to hold. In addition, indicators trended negative for all three stocks in 2021 (fall spawning) and 2022 (outmigration). These results suggest that a combination of poor freshwater and marine habitat conditions continued for KRFC, and may have returned for Sacramento stocks.

Klamath River Fall Chinook salmon: For brood year 2021, 14 of 18 habitat indicators were within 1 s.d. of the long-term average (Table J.2A). However, 10 of those 14 were below average, in addition to the four indicators that were >1 or >2 s.d. below normal; this resulted in 2021 being the second-worst brood year for the cumulative freshwater score, which continued a 25-year declining trend (Table J.2B). It was also the fourth-worst year for marine conditions. The coincidence of relatively poor freshwater and marine conditions resulted in the poorest overall year for this indicator suite in the 39-year record. All three indicators for adult migration were <1 s.d. below average. Two of three incubation indicators were below average, and incubation temperature was the third-worst on record.

Table J.2: (A) Habitat indicators for five life stages of Klamath River Fall Chinook salmon. Each row is an indicator (grouped by life stage at left) and each column is a brood year. Colors represent a given year's indicator relative to the full time series. Blue: >2 s.d. above the mean (= highly favorable); green: >1 s.d. above the mean; yellow: ±1 s.d. of the mean; orange: >1 s.d. below the mean; red: >2 s.d. below the mean (= highly unfavorable). (B) Trend by brood year in the average of freshwater habitat indicators (black line; includes adult migration and spawning, incubation, freshwater and delta residence, and all hatchery indicators except marine timing) and marine habitat indicators (blue line; includes marine timing and early marine residence suite). Brood years on x-axis match years of the indicator suite in A.
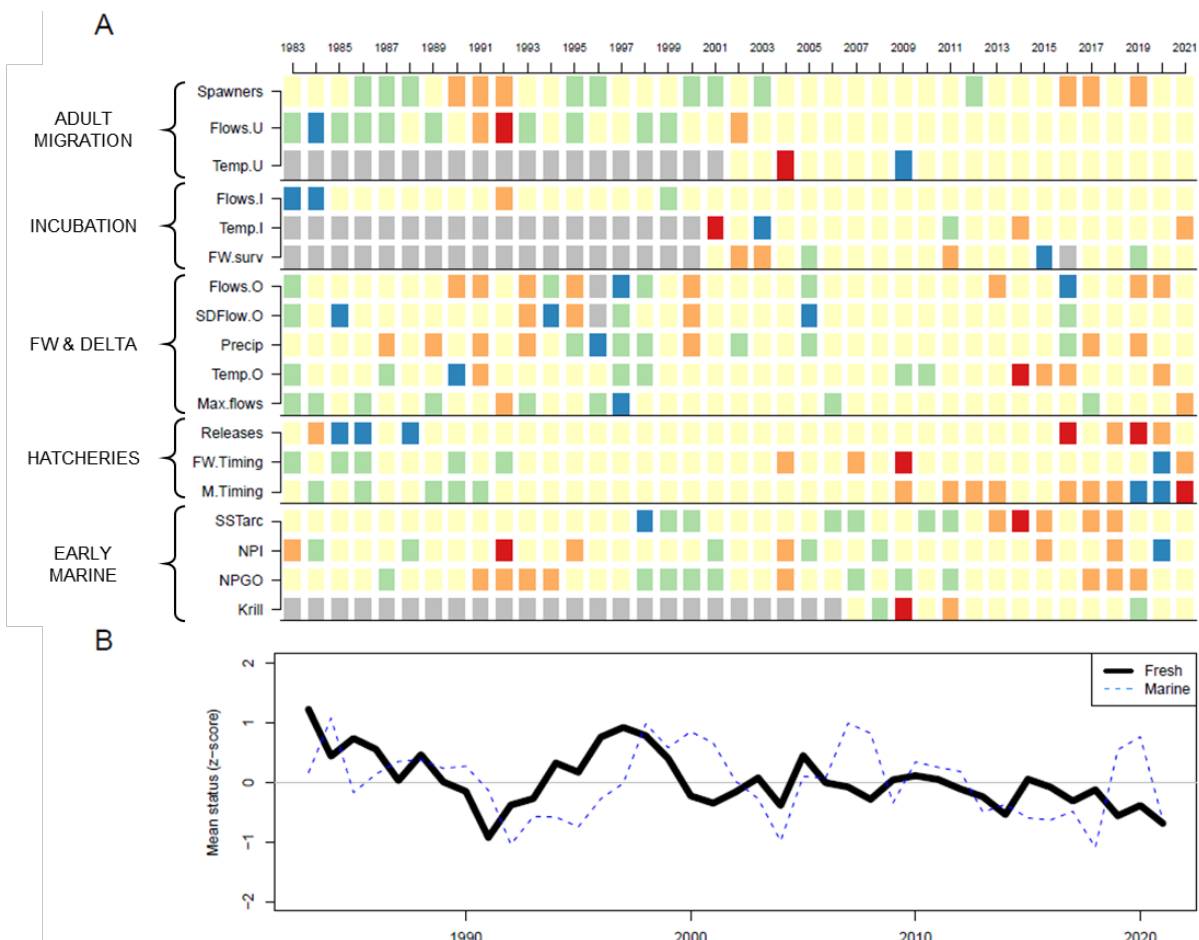
Likewise, freshwater residence indicators tended to score poorly: four of five indicators were below average and maximum flushing flow was the worst year in the 39-year record. In addition, all indicators of hatchery releases trended negative. Timing of releases was >2 s.d. below average and marine timing was the worst on record. FW timing was the second-worst on record. In addition, three of five marine indicators were below average.

Sacramento River Fall Chinook salmon: Habitat indicators for SRFC did not trend much better. As with the KRFC table, most of the indicators for the 2021 brood year fell within 1 s.d. of average (Table J.3A). However, 13 of 20 indicators for which there are data were below-average or worse (Table J.3A). Three of four habitat indicators for spawners were below-average, and incubation temperature and flow indicators were the third- and fourth-worst on record, respectively. Six of seven freshwater and delta residence indicators were below-average, and Sacramento mainstem flows were the second-worst in this 39-year

Table J.3: (A) Habitat indicators for five life stages of Sacramento River Fall Chinook salmon. Each row is an indicator (grouped by life stage at left) and each column is a brood year. Colors are as in Table J.2A. (B) Trend over brood years in the average of habitat indicators for freshwater life stages (black line, as in Table J.2B) and marine habitat indicators (blue line, as in Table J.2B). Brood years on x-axis match years of the indicator suite in A.
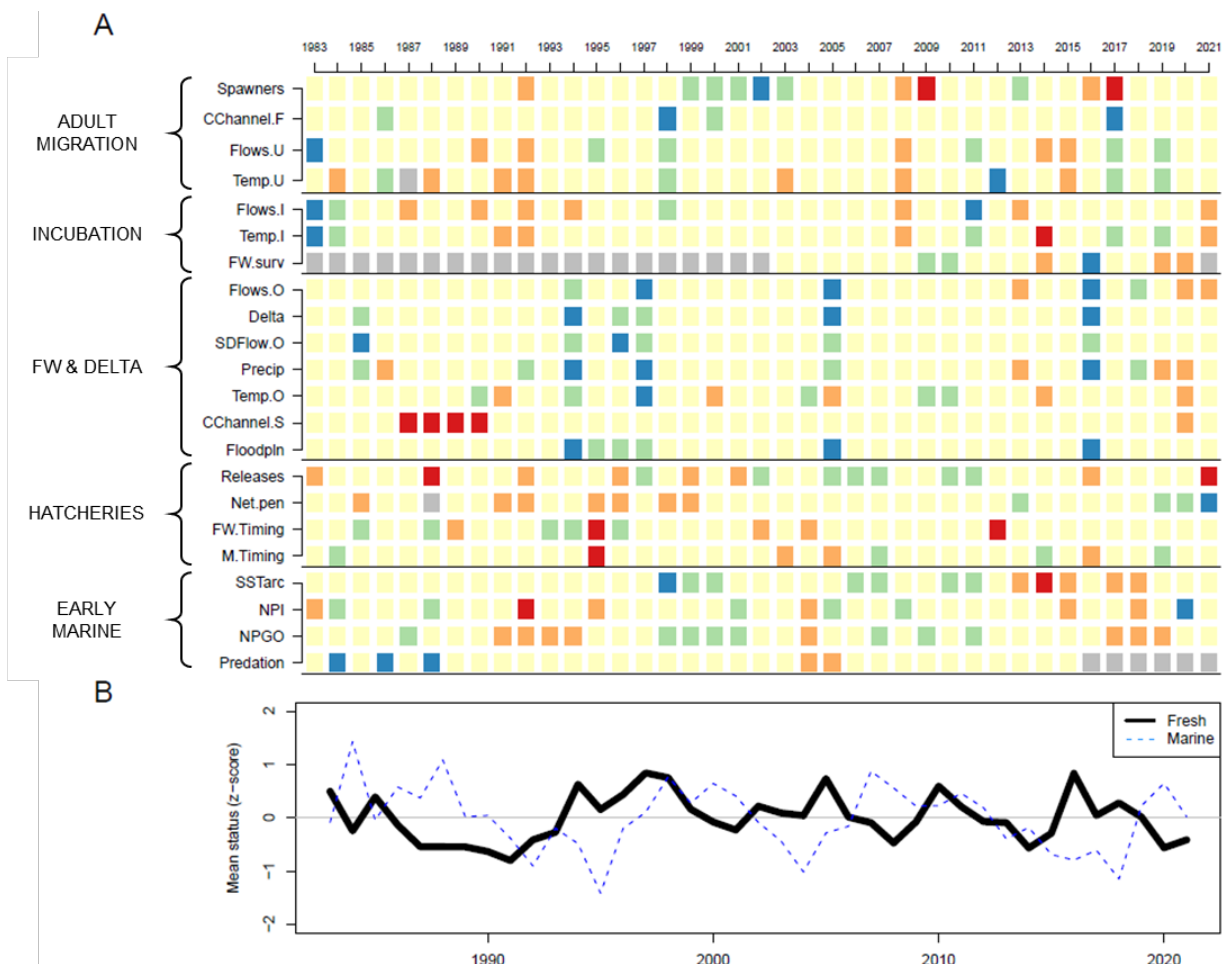
record. Hatchery release indicators were mixed. Release year 2022 was the second-worst year for release number, and all releases were made out of system, resulting in the best Net.pen score but indicative of the very poor conditions for in-stream releases. Early marine conditions were mixed, as one of four marine indicators were below average. The cumulative effects of multiple poor indicators resulted in the fourth-worst freshwater score since the early 1990s (Table J.3B). Cumulative marine conditions were just above average; hence, across all indicators, conditions for the 2021 brood year have been below-average.

Central Valley Spring Chinook salmon: CVSC shares 11 indicators with SRFC, so it should come as no surprise that habitat conditions for CVSC were also relatively poor for brood year 2021. Again, a majority of the indicators for brood year 2021 were within 1 s.d. of their time series averages (Table J.4A). However, 19 of 23 indicators were below average, and some and some indicators trended worse than those of their Fall-run counterparts. Indicators for

Table J.4: (A) Habitat indicators for five life stages of Central Valley Spring Chinook salmon. Each row is an indicator (grouped by life stage at left) and each column is a brood year. Colors are as in Table J.2A. (B) Trend over brood years in the average of habitat indicators for freshwater life stages (black line, as in Table J.2B) and marine habitat indicators (blue line, as in Table J.2B). Brood years on x-axis match years of the indicator suite in A.
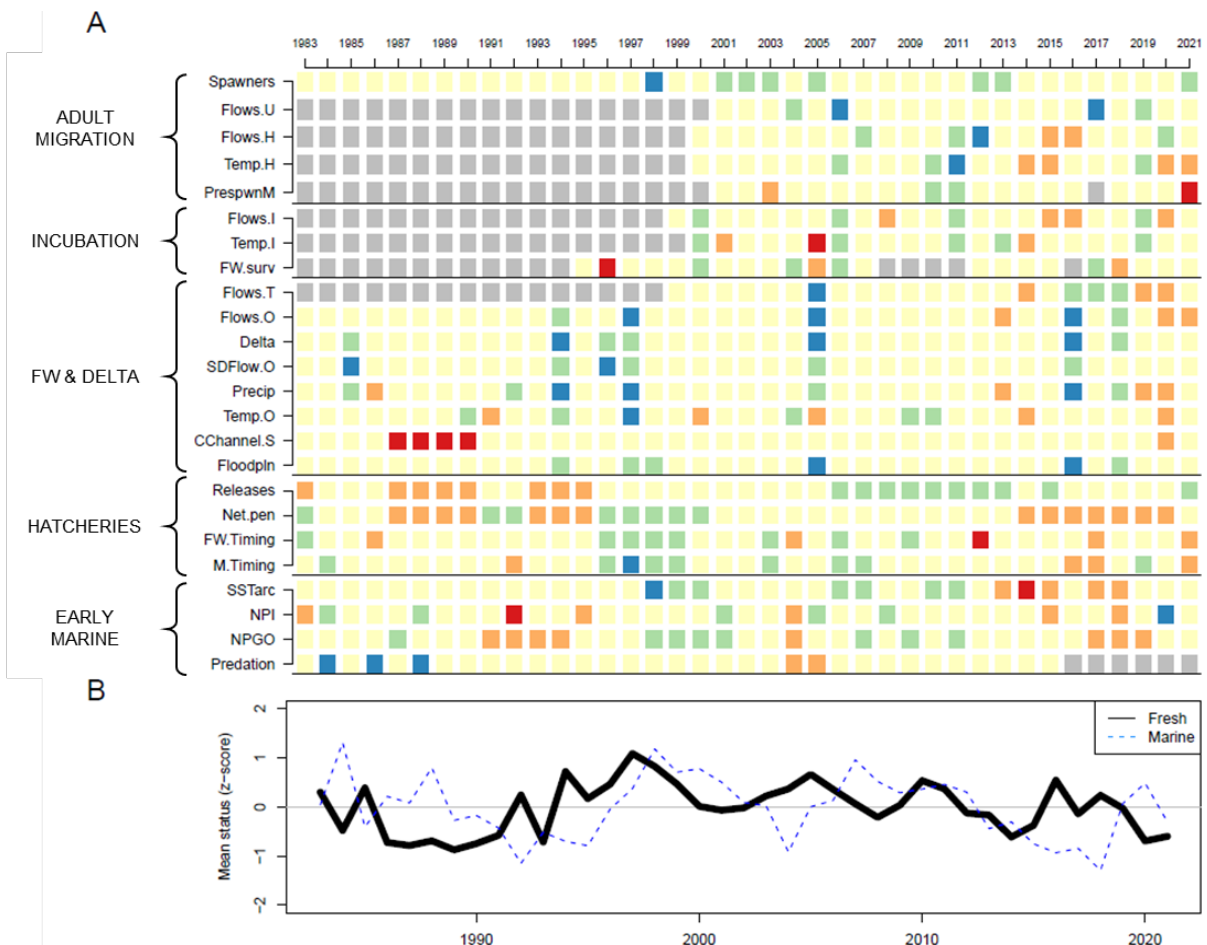
upstream migration and spawning were mixed, as four of five indicators were below average. Despite the second-strongest adult return of the time series, the Butte Creek spawning run suffered the worst holding temperatures in its 22-year record as well as record pre-spawn mortality (nearly 92%), severely impacting juvenile production. Furthermore, all three incubation indicators and all eight freshwater/ delta indicators were below-average. Hatchery release indicators were mixed. Despite the largest hatchery release of the time series, the other three indicators were below-average, and timing indicators were both >1 s.d. below average (i.e., relatively poor conditions for natural-area fish). Three of four early marine residence indicators were below-average.

Brood year 2021 contributed to a recent trend of declining freshwater indicators for CVSC, cycling between good and poor conditions about every five years (Table J.4B). Like other populations, marine habitat indicators vary in an opposite phase compared to freshwater indicators, and there have been a few years when both freshwater and marine conditions are below average. Like SRFC, this occurred most recently for CVSC during the 2014-2015 marine heat wave. Based on the combined score across both freshwater and marine indicators, brood year 2021 was the third-worst in the 39-year record. In summary, these indicators suggest a year of poor productivity for CVSC, and likely below average adult returns in 2024-25.

Management implications: The Council has a long history of engaging with other agencies to advocate for improved habitat conditions for the Sacramento and Klamath Chinook salmon. While many possible management "dials" exist for improving habitat, few can easily be tracked annually. In both systems, river flow is highly managed through reservoir operations, diversions and export pumping, and flows at particular stages can influence water temperature. Flow and water temperature indicators have shown evidence of long-term change as well as recent variability during brood years highlighted by the rebuilding plan (2012-2014) and years thereafter. In particular, temperature conditions for the Sacramento River (during spawning and spring rearing) and flow conditions for the Klamath River continue to remain at relatively low status, suggesting that improved flow management can support improvements for populations (Munsch et al 2020). In the Klamath River, freshwater conditions have trended very poorly, so efforts to initiate dam removal this year come at a fortuitous time to restore the natural flow regime; we will continue to track these conditions as dam removal proceeds to determine if restoration leads to improvements in these indicators over time. In the Sacramento River, above-average flows favor adult survival and rearing conditions in freshwater, in the floodplain, and in the delta; thus, improved management of flows during freshwater residence periods would likely ameliorate the poor conditions of 2021-2022 for both Fall and Spring runs. From an ecosystem indicator perspective, the outlook for both Klamath and Sacramento stocks suggest below-average adult ocean abundance in 2024-2025.

Appendix K: GROUNDFISH

Yearly indices of the abundances of juvenile sablefish, Dover sole, shortspine thornyhead and longspine thornyhead along the West Coast were calculated using species distribution

models. The analysis follows the general approach used by Tolimieri et al. (2020), which was reviewed by the SSC-ES in September 2021, but this update uses the sdmTMB modeling package (Anderson et al. 2022) instead of the VAST package (Thorson 2019). The sdmTMB approach is being used by many West Coast groundfish stock assessment biologists to assimilate survey data, and was reviewed favorably by the SSC-Groundfish Subcommittee in summer of 2022 (PFMC 2022c).

Data for indicators come from the West Coast Groundfish Bottom Trawl Survey (WCGBTS) (Keller et al. 2017) for 2003-2021. There are no data for 2020 because the WCGBTS was canceled due to the COVID-19 pandemic. The survey data includes estimates of age, length, and biomass for subsamples of each haul, and occasionally for the entire haul when catch is low. Length is measured (cm total length) for all individuals in the subsample, but many individual fishes lack weight or age data due to time constraints in the field and ageing lab. To expand the subsample, individuals with length data only were given estimated weights based on species-specific length-weight relationships. Individual fish were allocated to age classes following Tolimieri et al. (2020) by using length-age relationships from the WCGBTS data to determine age-class maximum lengths (Table K.1). The proportional biomass of juveniles in each subsample was calculated and then used to extrapolate total estimated juvenile fish biomass in the full trawl. See Tolimieri et al. (2020) for more detail.

Table K.1: Length, age, and depth range information for juvenile size/age classes of groundfish in this analysis. The trawl data do not contain ages for the thornyheads.

Species	Max length (cm)	Age class (yr)	Depth range (m)
Dover sole	17	1 & 2	50 - 465
Sablefish	29	0	50 - 250
Longspine thornyhead	7	unknown	385 - 1245
Shortspine thornyhead	8	unknown	160 - 625

For reference, raw estimates of juvenile CPUE and total CPUE for each species are shown in Figures K.1 and K.2. These raw estimates were simple means of all trawls within the depth range in a given year.
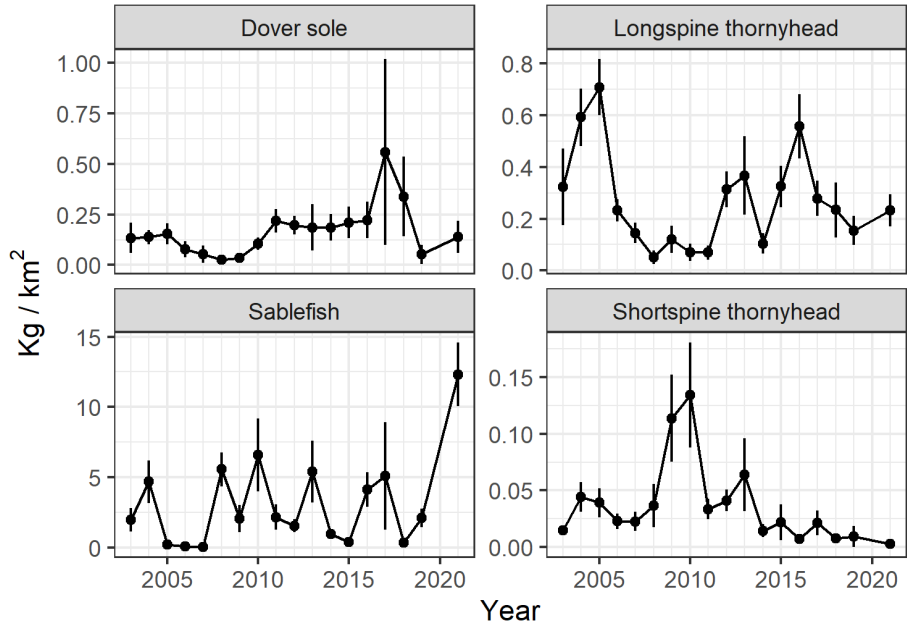
Figure K.1: Simple catch per unit effort (CPUE) of juvenile fishes of four focal groundfish species, calculated as the mean kg/km² for all trawls in a year. Data come from the West Coast Groundfish Bottom Trawl Survey and are available from the FRAM data warehouse: https://www.webapps.nwfsc.noaa.gov/data/map.
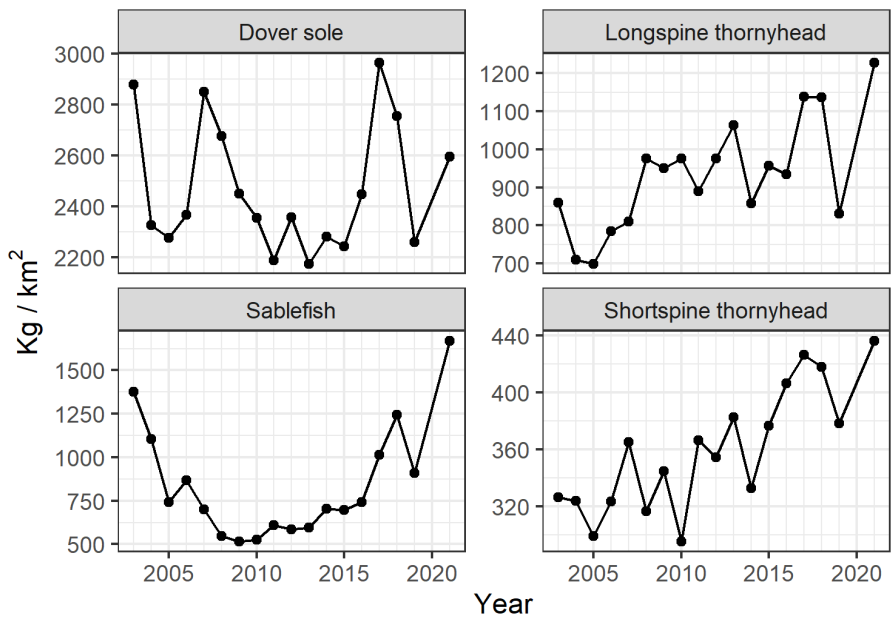

Figure K.2: Simple catch per unit effort (CPUE) of total biomass of four focal groundfish species, calculated as the mean kg/km² for all trawls in a year. Data come from the West Coast Groundfish Bottom Trawl Survey and are available from the FRAM data warehouse: https://www.webapps.nwfsc.noaa.gov/data/map.

Coastwide juvenile groundfish abundances were estimated using a spatially explicit, species distribution model evaluated with the sdmTMB package in R. The response variable was

CPUE quantified as kg of juveniles per km². The models included one common intercept across years, and spatial and spatiotemporal random fields, with anisotropy to account for different rates of autocorrelation with latitude versus longitude ($\sim$ depth). The common intercept prevents the model from forcing biomass to increase or decrease coastwide in a given year (thereby potentially overestimating recruitment in some areas) as would be the case for yearly intercept. Depth was scaled and included to account for differences in density across depths. To avoid projecting to areas with zero biomass, the depth range of the data used for each species in the analysis was restricted based on the distribution of positive biomass observations (Table K.1). Again, the values used here follow Tolimieri et al. (2020) with the exception that the lower depth limit for sablefish was set to 250 m, which encompasses more than 99% of their observed juvenile biomass. Pass was included as a fixed factor (as a proxy for time of year; the WCGBTS conducts two coastwide passes each year, in May-July and August-October). Models were fit with a delta-gamma distribution to account for the prevalence of zeros in the data, and the mesh was set to 10 km, resulting in 650-800 knots depending upon species. Model fits were then extrapolated to a 2x2 km grid of the West Coast to estimate total abundance in kg for juveniles in a given year. For some species, it was necessary to combine age or size classes to obtain enough data for models to converge (Table K.1). The resulting biomass estimate was converted to an index scaled between 0-1 by dividing all values by the greatest upper 95% confidence limit in the time series. Finally, we also evaluated different error distributions, including Tweedie and delta-Poisson-link-gamma (used in Tolimieri et al 2020). Based on examination of the residuals, the delta-gamma distribution was chosen as the most appropriate error distribution.

(To address previous suggestions by the SSC-ES, we also evaluated models with year included as a fixed factor or allowed year to have a random intercept. When included as a fixed factor, models failed to converge likely due to identifiability problems due to also including the spatiotemporal random field. For sablefish and Dover sole, inclusion of year with a random intercept also created fit problems leading to very large standard errors for some estimated parameters. Therefore, we excluded the term from the final models.)

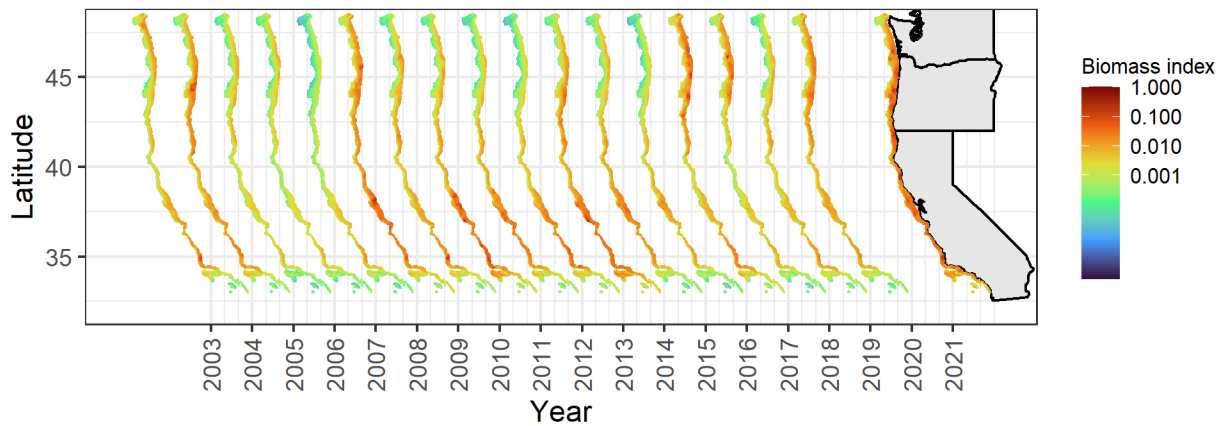The large 2021 sablefish year class was evident coastwide (Fig. K.3).

Figure K.3. Distribution of age-0 sablefish along the West Coast from 2003-2021, according to sdmTMB analysis. Results are projected to a 2x2 km grid that excludes the Cowcod RCA. Biomass is scaled to 0-1 by dividing by the

Sablefish recruitment is negatively correlated with sea surface height (SSH) north of Cape Mendocino (Haltuch et al. 2019, Tolimieri, in press). The strong age class of sablefish in 2021 (main report, Fig. 3.7) corresponds to the low SSH index in the same year (Fig. K.4). The SSH index for 2022 is consistent with moderate to low recruitment.
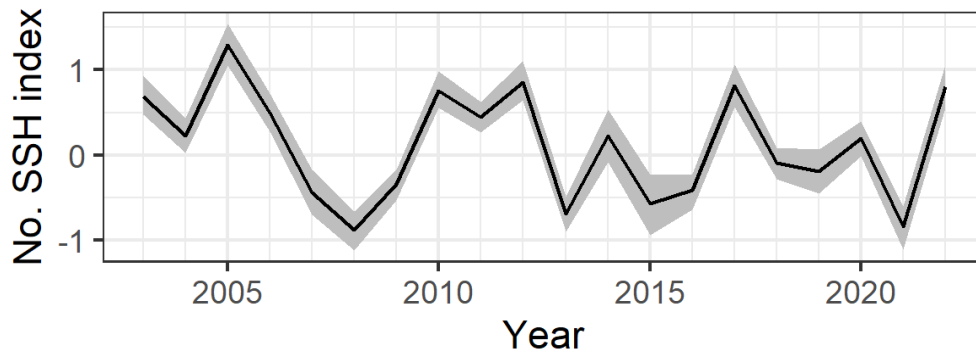

Figure K.4: Northern sea surface height (SSH) index derived from a dynamic factor analysis of 16 tide gauge locations along the West Coast. See Tolimieri et al 2020 for data availability and index calculation.

Appendix L: HIGHLY MIGRATORY SPECIES (HMS)

L.1 HMS STOCK ASSESSMENT INFORMATION

Biomass and recruitment estimates for many HMS stocks that occupy the California Current are available from stock assessments conducted by collaborators under the International Scientific Committee for Tuna and Tuna-like Species in the North Pacific Ocean (ISC) or the Inter-American Tropical Tuna Commission (IATTC). The only assessment updates since last year's ecosystem status report are for Pacific bluefin tuna (ISC 2022) and skipjack tuna (Maunder et al. 2022). The skipjack assessment underwent major changes from previous assessments, and therefore the time series for biomass and recruitment are different than in previous ecosystem status reports.

We should emphasize that the status and trends symbols shown below in Figures L.1 and L.2 reflect short-term patterns relative to time series averages (with a period of reference of 1991-2020), and do not necessarily reflect reference points based on, e.g., unfished stock biomass. Thus for example, bluefin tuna is considered to be overfished relative to potential biomass-based reference points adopted for other tuna species (ISC 2022) even though it falls >1 s.d. above the biomass time series average in our Figure L.1.

According to the most up-to-date assessments, the most recent spawning stock biomass estimates range from above the assessment time series average (bluefin tuna, swordfish) to

~1 s.d. below average (yellowfin tuna, bigeye tuna), with generally wide error estimates (Fig. L.1). Estimated SSBs of bluefin tuna and skipjack tuna have positive five-year trends.

HMS recruitment trends from the most recent assessments are generally trending either neutrally or positively, typically with high uncertainty (Fig. L.2). The recruitment trends from the updated bluefin tuna and skipjack assessments are both neutral.
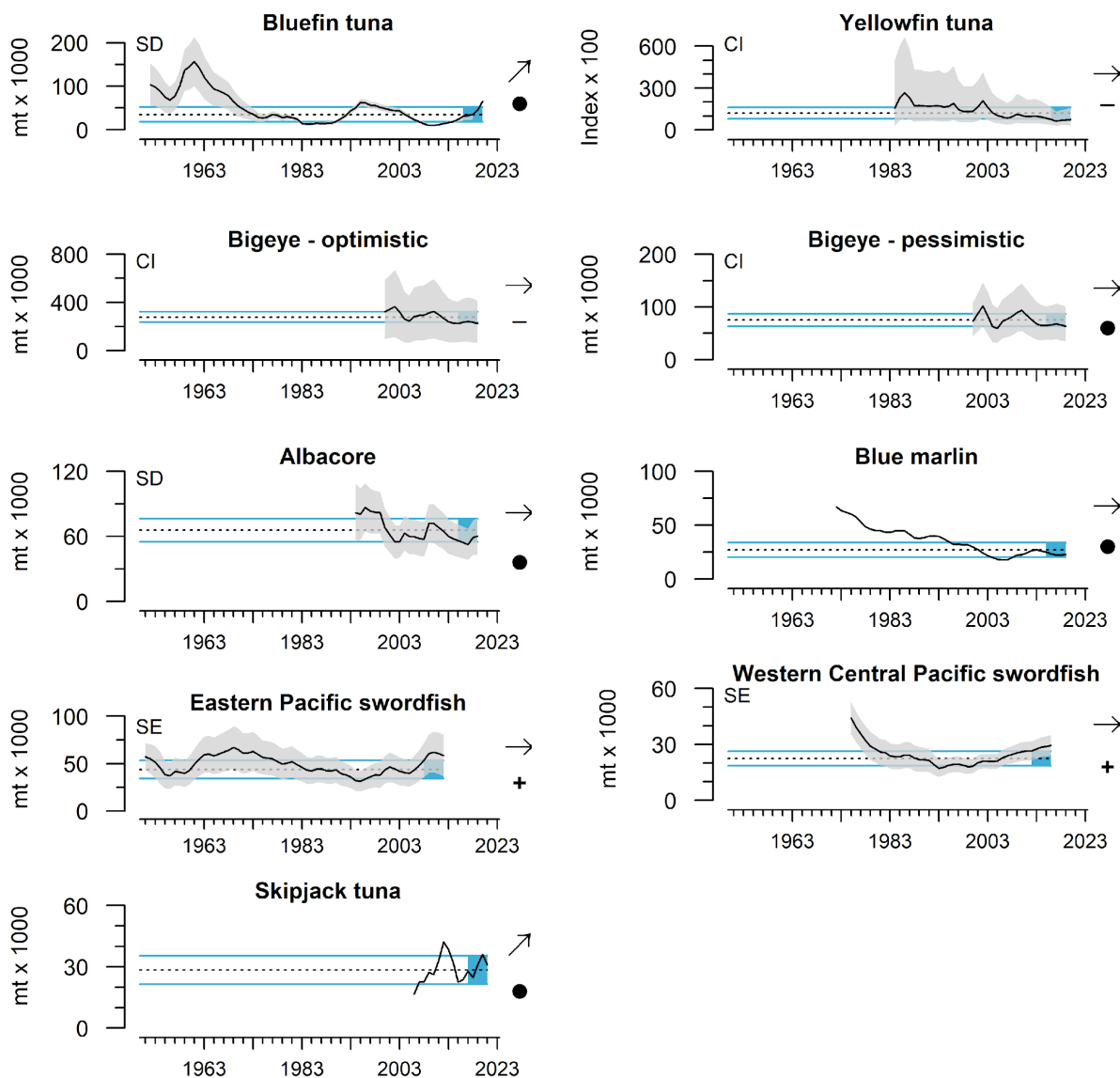

Figure L.1: Biomass for highly migratory species in the north Pacific. The type of error envelope is indicated in the upper left of each panel: SD = ±1 s.d.; SE = ±1 s.e.; CL = ±95% C.L. Assessment dates were: Albacore (2019), Bigeye tuna (2019), Blue marlin (2021), Bluefin tuna (2022), Eastern Pacific swordfish (2012), Skipjack tuna (2022), Western Central Pacific swordfish (2016), and Yellowfin tuna (2020). Lines, colors, and symbols are as in Fig. 2.1. Compiled by B. Muhling, UCSC, NMFS/SWFSC from the most recent stock assessments provided by ISC or IATTC.
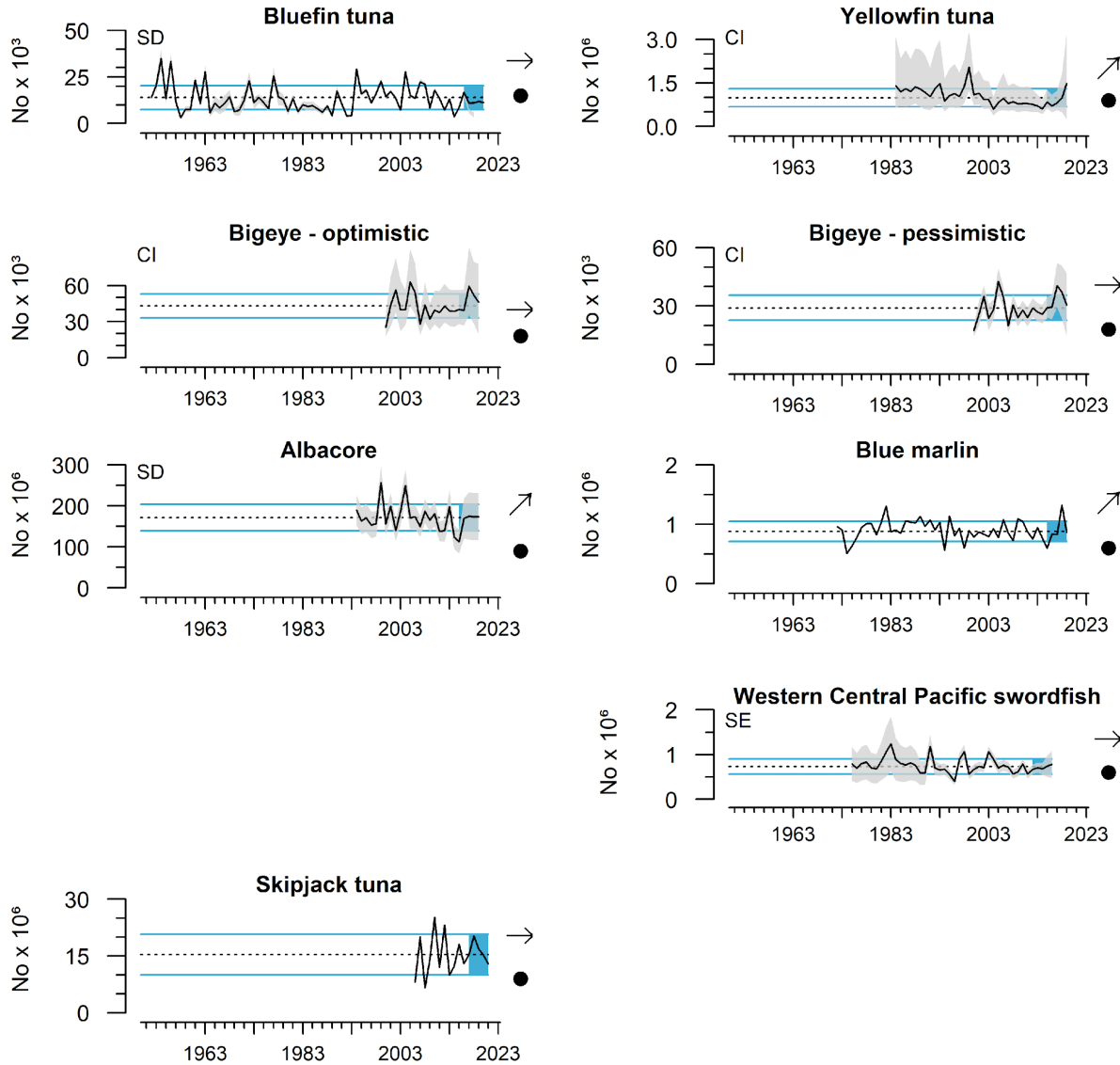
Figure L.2: Recruitment for highly migratory species in the North Pacific. The type of error envelope is indicated in the upper left of each panel: SD = ±1 s.d.; SE = ±1 s.e.; CL = ±95% C.L. Assessment dates were: Albacore (2019), Bigeye tuna (2019), Blue marlin (2021), Bluefin tuna (2022), Eastern Pacific swordfish (2012), Skipjack tuna (2022), Western Central Pacific swordfish (2016), and Yellowfin tuna (2020). Lines, colors, and symbols are as in Fig. 2.1. Compiled by B. Muhling, UCSC, NMFS/SWFSC from the most recent stock assessments provided by ISC or IATTC.

L.2   HMS DIET INFORMATION

Quantifying the diets of highly migratory fishes in the CCE can complement existing trawl-based assessments of the available forage, provide insight into how forage varies over time and space, as well as provide a direct metric of forage utilization. Juvenile albacore tuna and broadbill swordfish are both opportunistic predators that consume a wide variety of prey taxa across a range of depths and habitats. Albacore and swordfish stomachs were provided by commercial and recreational fishers. Prey were identified from whole or hard part

remains and are reported as a mean proportional abundance. A subset of diets are presented in the main report (Fig. 3.8) and in greater detail here, with a focus on prey that are either themselves under a management plan, or considered ecosystem component species.

Albacore diets have been collected off Northern California, Oregon, and Washington in the summer and fall fishing season since 2009 and are complete on samples provided through 2021. The dominant prey in 2021 were anchovy, krill, and Pacific saury (Fig. L.3). Anchovy accounted for 9% of albacore prey items in 2021, below the long term mean and well below the most recent peak in 2017. Pelagic juvenile rockfish consumption was close to the time series average, and declined in 2021 relative to 2018-2020. Sardine consumption in 2021 was above the long term mean, though <10% of total prey items. Jack mackerel and saury have increased in occurrence over the last five years. The most important contributors among prey items not targeted by fisheries were the squid *Onychoteuthis borealijaponica*, amphipods, and slender barracudina.
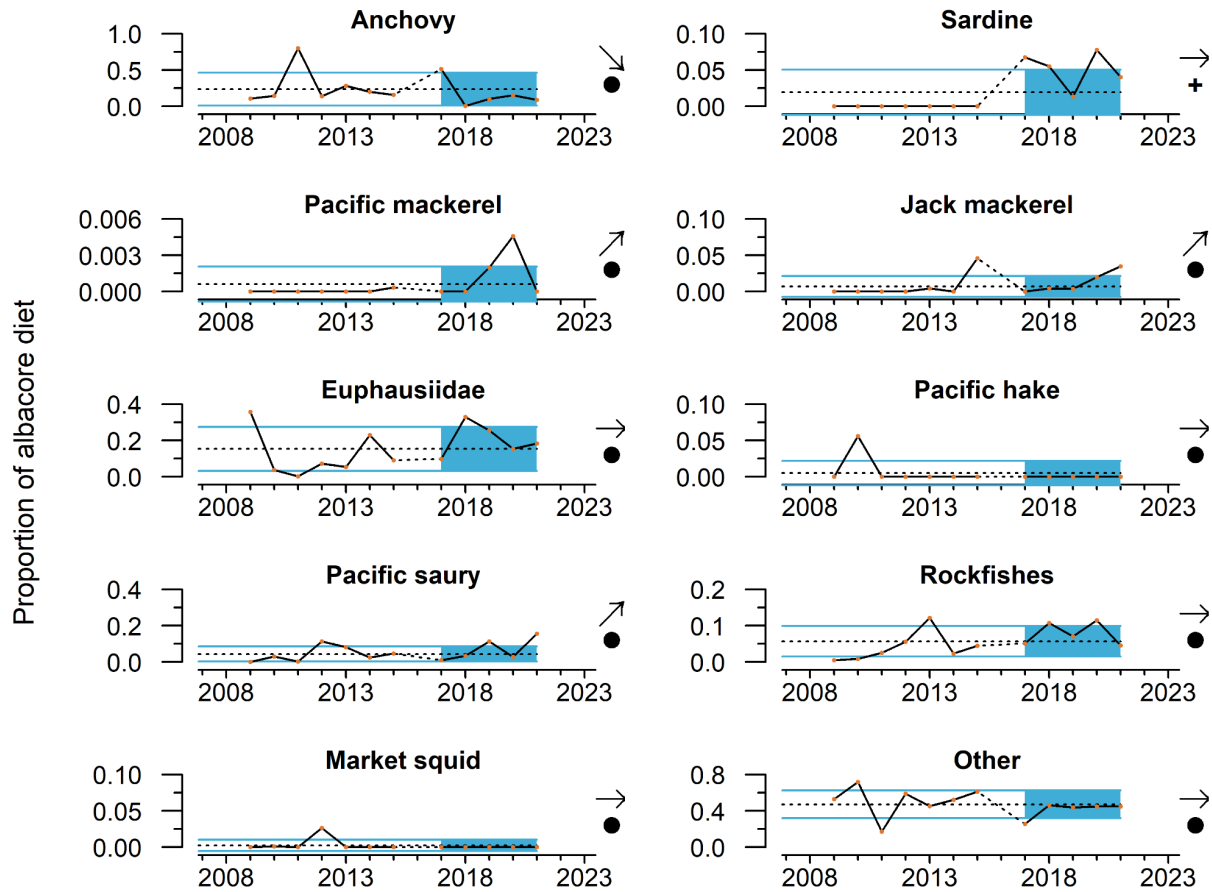
Figure L.3 Diets of albacore tuna sampled from commercial and recreational fisheries in the northern and central CCE, 2009-2021. Data are proportional contributions by number, relative to total number of prey items consumed. Lines, colors, and symbols are as in Fig. 2.1. Albacore diet data provided by H. Dewar and C. Nickels, NMFS/SWFSC.

Swordfish diets were collected off southern and central California during the commercial drift gillnet season (August 15th through January 31st) and are classified by the year the fishing season began (stomachs from January are assigned to the previous year's fishing

season). Starting in 2018 additional samples were collected during the deep-set buoy gear season (May to December). Swordfish analyses are complete through 2014 and partially complete from 2015-2021. Swordfish stomachs analyzed to date mainly reflect a diet of fish and cephalopods (Fig. L.4). Anchovy proportions have been >1 s.d. above the mean over the most recent five years, including samples processed so far from 2021. Market squid appear to have declined in importance over that period, while Pacific hake have shown peaks >1 s.d. above the mean in 2018 and 2021. Other CPS, juvenile rockfish, krill, and saury were minor parts of swordfish diets (0-10%) across years. Across the time series, the most important "Other" prey were various squids. Humboldt squid were the most important prey in the early portion of the time series, although their importance declined in 2010 during a peak in market squid consumption, and in 2011 and 2014 as hake became more important. Fished species were less important in swordfish diets overall compared with albacore.
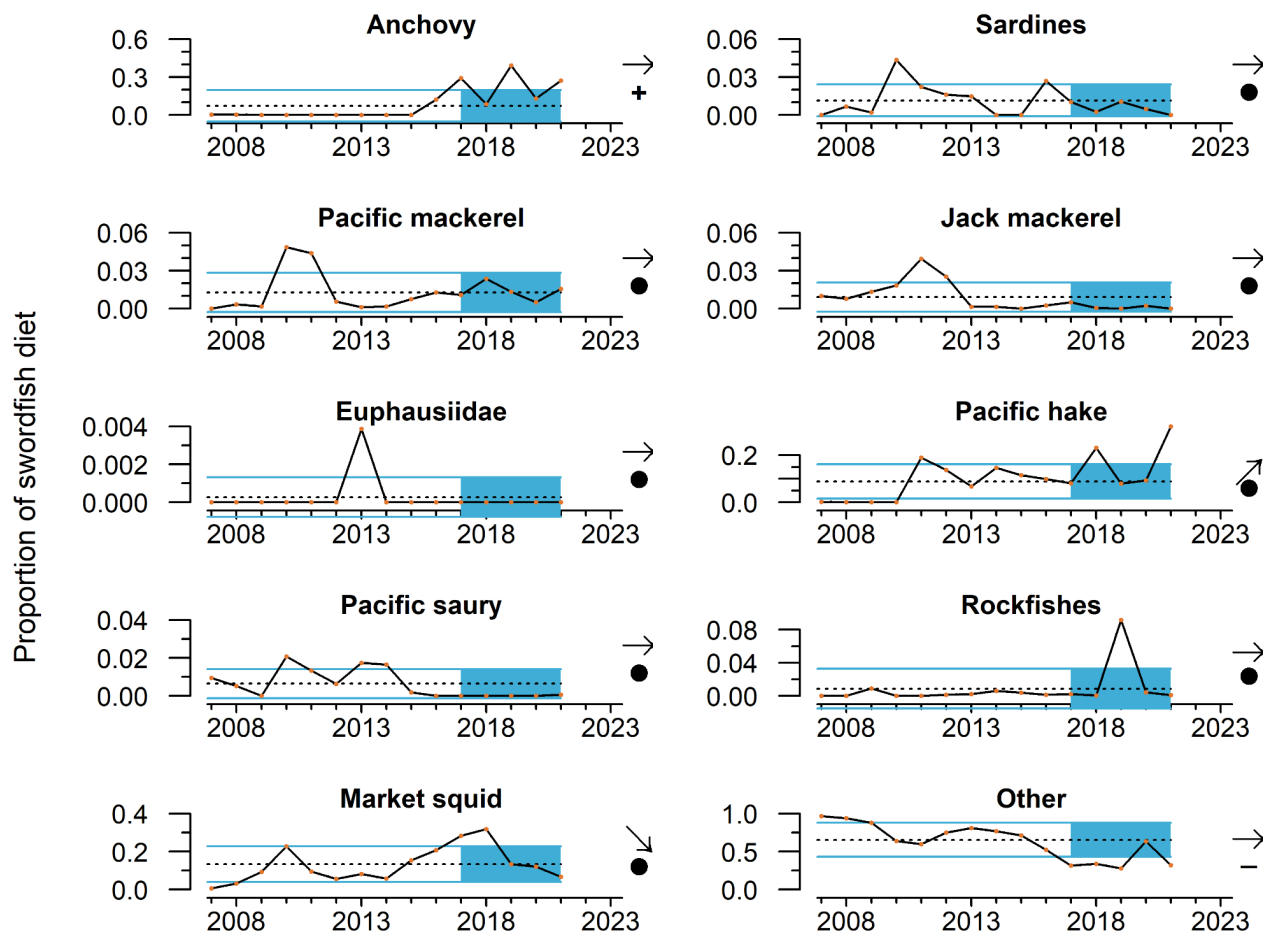
Figure L.4 Diets of swordfish sampled from commercial and recreational fisheries in the central and southern CCE, 2007-2021. Data are proportional contributions by number, relative to total number of prey items consumed. Lines, colors, and symbols are as in Fig. 2.1. Swordfish diet data provided by H. Dewar, NMFS/SWFSC, and A. Preti, UCSC.

Appendix M: SEABIRD PRODUCTIVITY, DIET, AT-SEA DENSITY, AND MORTALITY

M.1 SEABIRD PRODUCTIVITY

Seabird population productivity, as measured through indicators of reproductive success, tracks marine environmental conditions and often reflects forage production near breeding colonies. We monitor and report on standardized anomalies of fledgling production per pair of breeding adults for three species at Yaquina Head, Oregon in the Northern CCE and five species on Southeast Farallon Island in the Central CCE. Collectively, these six focal species span a range of feeding habits and ways of provisioning their chicks, and thus a broad picture of the status of foraging conditions.

Table M.1. Preferred forage type and location by colonial seabird species in the CCE.

Species	Forage Items/timing	Foraging location
Brandt's cormorants	pelagic and benthic fishes, daytime	shelf, within 20 km of colonies
Cassin's auklet	zooplankton, day and night	shelf break, within 30 km of colonies
Common murres	pelagic fishes, daytime	deeper shelf and shelf break waters, within 80 km of colonies
Pelagic cormorants	pelagic and benthic fishes, daytime	shelf, within 20 km from colonies
Pigeon guillemots	small benthic and pelagic fishes, daytime	shelf, within 10 km of colonies
Rhinoceros auklets	pelagic fishes, day into early evening	shallow shelf, within 50 km of colonies

Data and interpretation for fledgling production of the five species at Southeast Farallon Island are in the main body of the report in Section 3.7. Production was generally positive in 2022, with above-average chick production for Brandt's cormorants and rhinoceros auklets and average chick production for Cassin's auklets, common murres, and pigeon guillemots. At Año Nuevo Island, just south of Southeast Farallon Island, mixed chick production was observed in 2022 (data not shown). Rhinoceros auklets experienced above-average productivity, while other species experienced average (Pelagic cormorant) or below-average productivity (Brandt's cormorant, Cassin's auklet). See Devincenzi et al. (2021) for details.

At Yaquina Head, fledgling production in 2022 varied widely among the three monitored seabird species (Fig. M.1). Brandt's cormorant production was close to the long-term average in 2022, while Brandt's cormorant fledgling production over the past five years has been above the long-term mean. However, both common murres and pelagic cormorants suffered complete breeding failure in 2022, resulting in declining short-term trends. Bald eagles can

be major drivers of seabird reproductive failures at Yaquina Head; their disturbances and egg predation contributed substantially to common murre reproductive failure in 2022, while pelagic cormorants were not observed to attempt nesting at all at Yaquina Head in 2022.
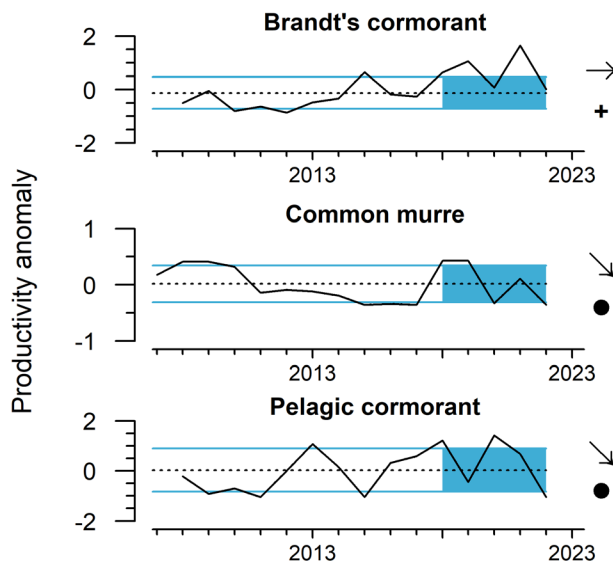

Figure M.1: Standardized productivity anomalies (annual number of fledglings per pair of breeding adults, minus the long-term mean) for three seabird species breeding at Yaquina Head, OR through 2022. Data courtesy of R. Orben, Yaquina Head Seabird Colony Monitoring Project, OSU (rachael.orben@oregonstate.edu). Lines, colors, and symbols are as in Fig. 2.1.

M.2   SEABIRD DIETS

Seabird diet composition during the breeding season tracks marine environmental conditions and often reflects production and availability of forage within regions. Here, we present seabird diet data from the northern and central regions of the CCE that may shed light on foraging conditions in 2022.

In the Northern CCE, rhinoceros auklet chick diet data were collected in 2022 at Destruction Island, WA. Northern anchovy were nearly absent from diet samples, continuing a trend observed since 2018. This is consistent with forage and CPS surveys that show the bulk of the current anchovy population to be in the Central and Southern CCE (Section 3.2, and Appendices H and I). Pacific herring formed almost half of the observed chick diet in 2022, while smelts formed almost one-third of the observed chick diet. The Pacific sandlance diet proportion in 2022 was close to the long-term average, but its dominance in the diet in 2021 and above-average proportion in 2019 suggest its importance has increased in recent years. Rockfish juveniles formed a small proportion of the observed rhinoceros auklet chick diet at Destruction Island in 2022.
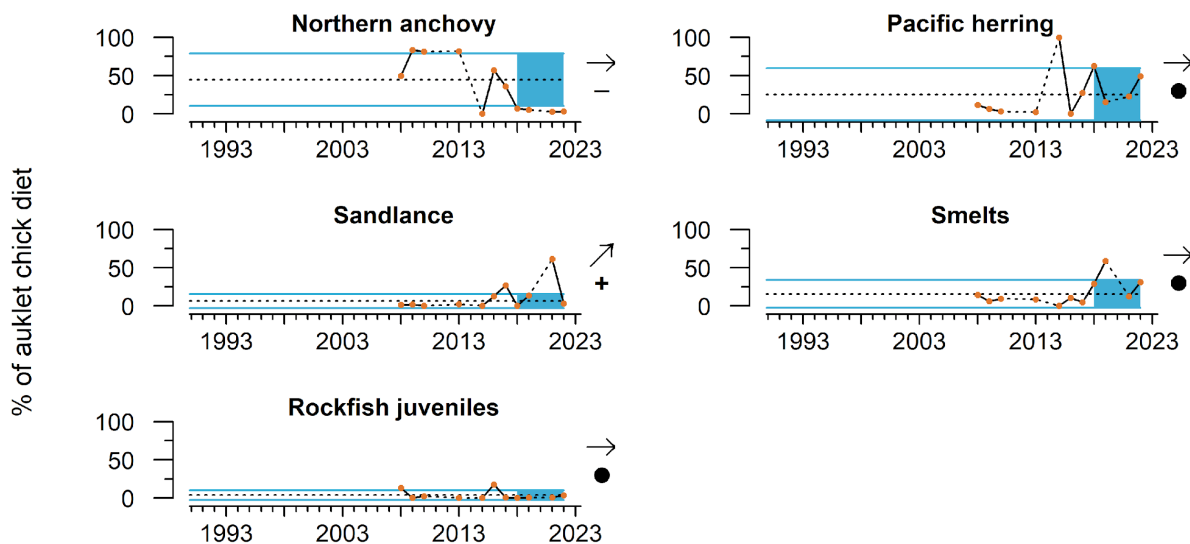
Figure M.2: Rhinoceros auklet chick diets at Destruction Island, WA through 2022. Data courtesy of S. Pearson, WDFW. Lines, colors, and symbols are as in Fig. 2.1.

Breeding failure of common murres precluded observing diet at Yaquina Head, but common murre diets just north at Depoe Head, OR showed similar patterns to Yaquina Head murres from previous years, dominated by smelts, anchovy, herring and sardines, along with some juvenile salmon (R. Orben, pers. comm.).

In central California, long-term diet data are collected for seabirds at breeding colonies on Southeast Farallon Island. These colonies are near the most intense upwelling region in the CCE and are thus a valuable source of information about system productivity and prey availability to higher trophic levels. Piscivorous birds at this colony continue to rely on northern anchovy rather than juvenile rockfish (Fig. M.3). Proportions of northern anchovy in the observed diets of Brandt's cormorants and rhinoceros auklets were well above average in 2022. These proportions were the highest ever recorded for Brandt's cormorant and among the highest recorded for rhinoceros auklets at Southeast Farallon Island, and contributed to five-year averages that were significantly greater than long-term means. Similarly, the proportion of northern anchovy/sardine in the observed diets of common murres was nearly 1 s.d. above average in 2022. Proportions of juvenile rockfish in all four piscivore diets were again below average in 2022, consistent with relatively low catches of YOY rockfish in forage sampling off central California over the same time period (see Section 3.2 and Appendix H).

The proportion of Pacific salmon in the observed diet of common murres was again very low in 2022 (Fig. M.3; see also the Central California salmon stoplight Table 3.2 and Appendix J). For Cassin's auklets, which feed primarily on zooplankton, the proportions of the two focal krill species *Euphausia pacifica* and *Thysanoessa spinifera* were below average in 2022 (Fig. M.3), and the bulk of their remaining diet was made up of other krill species. Not all Cassin's auklet diet samples from 2022 have been processed, so these values may change. High prevalence of *T. spinifera* in the Cassin's auklet chick diet, as was observed in 2020 and 2021, is linked to increased late-winter upwelling and decreased habitat compression, which enhances productivity in the species' nearshore coastal habitats.
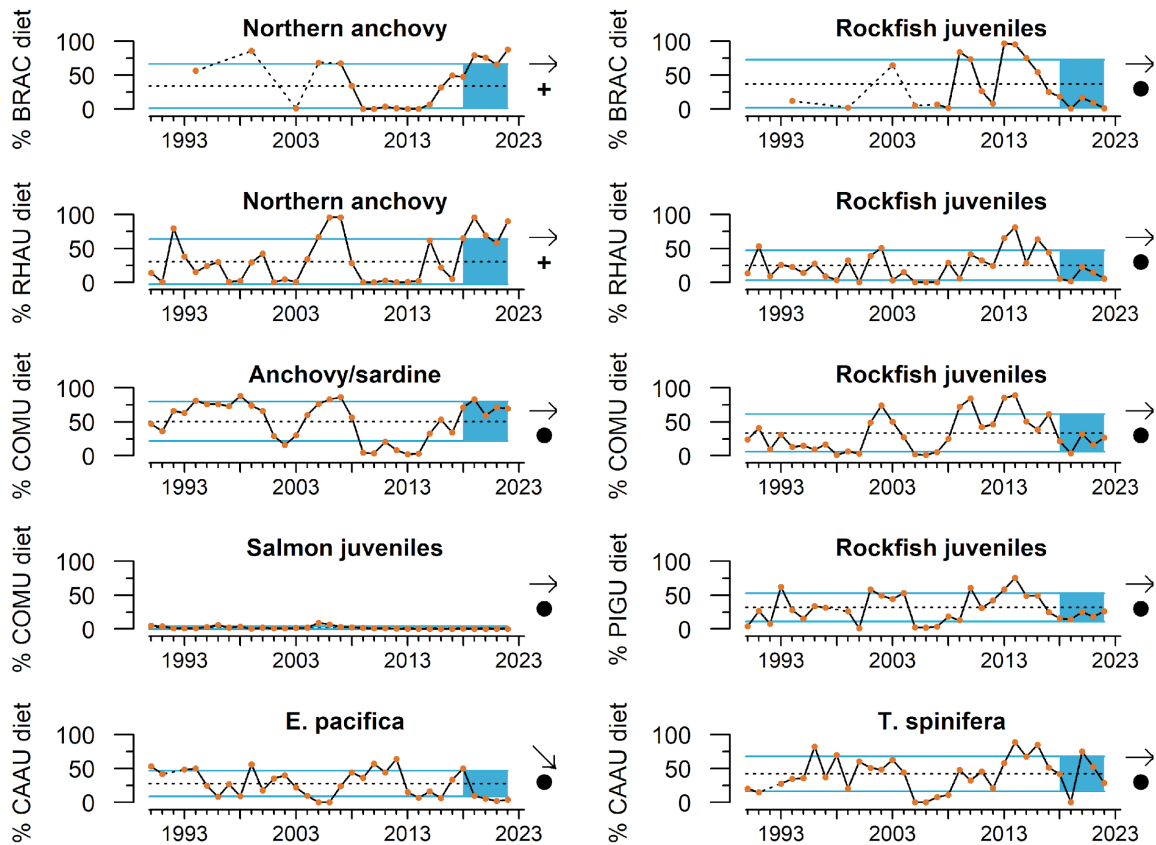
Figure M.3: Percentages of key prey items delivered to seabird chicks at Southeast Farallon Island, CA through 2022. BRAC = Brandt's cormorant; RHAU = rhinoceros auklet; COMU = common murre; PIGU = pigeon guillemot; CAAU = Cassin's auklet. Data provided by J. Jahncke, Point Blue Conservation Science (jjahncke@pointblue.org). Lines, colors, and symbols are as in Fig. 2.1.

Long-term diet data are also available for rhinoceros auklets breeding on Año Nuevo Island off central California. The proportion of anchovy in the diet of rhinoceros auklets in 2022 continued a string of above-average years, while the proportion of juvenile rockfish was again slightly below average (Fig. M.4). The proportion of market squid was slightly above average, while the proportion of Pacific saury was again close to zero.
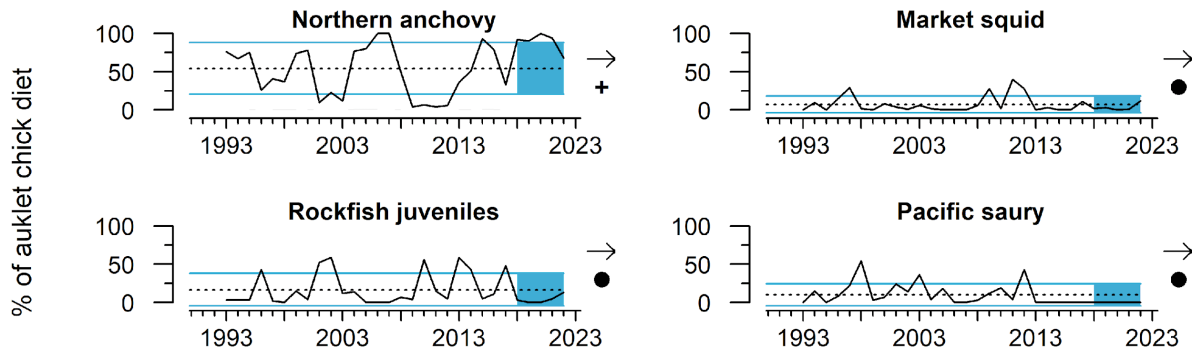
Figure M.4: Percentages of key prey items delivered to rhinoceros auklet chicks at Año Nuevo Island, 1993-2022. Data provided by Oikonos Ecosystem Knowledge and Point Blue Conservation Science (danielle@oikonos.org). Lines, colors, and symbols are as in Fig. 2.1.

The length of anchovy provided to rhinoceros auklet chicks at Año Nuevo in 2022 was 1 s.d. below the long-term average, and contributed to a significant downward trend over the past five years (Fig. M.5). In recent years, researchers have expressed concern that anchovy, while abundant, may have been too large to be ingested by rhinoceros auklet and other colonial seabird chicks. Fledgling production for piscivorous seabirds in the region was generally average to above average in 2022, which may indicate that smaller prey is more conducive to chick success.
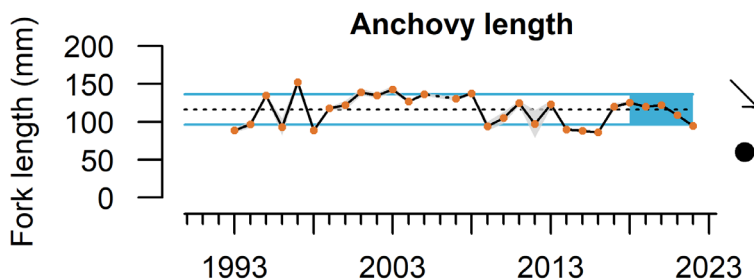
Figure M.5: Fork length of anchovy brought to rhinoceros auklet chicks at Año Nuevo from 1993-2022. Gray envelope is ±1 s.d. Data provided by Oikonos Ecosystem Knowledge and Point Blue Conservation Science (ryan@oikonos.org). Lines, colors, and symbols are as in Fig. 2.1.

M.3   SEABIRD AT-SEA DENSITIES

Seabird densities on the water during the breeding season can track marine environmental conditions and may reflect regional production and availability of forage. Data from this indicator type can establish habitat use and may be used to detect and track seabird population movements or increases/declines as they relate to ecosystem change. We monitor and report on at-sea densities of three focal seabird species in the Northern, Central, and Southern CCE. Sooty shearwaters migrate to the CCE from the southern hemisphere in spring and summer to forage near the shelf break on a variety of small fish, squid and zooplankton. Common murres and Cassin's auklets are resident species that feed primarily over the continental shelf; Cassin's auklets prey mainly on zooplankton and small fish, while common murres target a variety of pelagic fish.

At-sea density patterns varied among CCE regions and focal species in 2022. In the Northern CCE, sooty shearwater and common murre at-sea densities were below average in 2022 (Fig. M.6, top row). The 2022 anomaly for sooty shearwater was the lowest of the time series for this region, and the recent sooty shearwater density trend is negative, although no data were collected in 2020 or 2021 due to COVID-19 restrictions, so that trend should be interpreted with care. Cassin's auklet at-sea density in the Northern CCE was above average in 2022 and their density has trended upward in recent years. In the Central CCE, sooty shearwater and common murre at-sea densities were well above average, and both species' densities have trended upward in recent years (Fig. M.6, middle row). Cassin's auklet at-sea density in the Central CCE was near average in 2022. In the Southern CCE, sooty shearwater, Cassin's auklet and common murre at-sea densities were near average in 2022 (Fig. M.6, bottom row). Both sooty shearwater and common murre densities have negative short-term trends, but data were not collected in the Southern CCE in 2020 and 2021, so again, these trends should be interpreted with care.
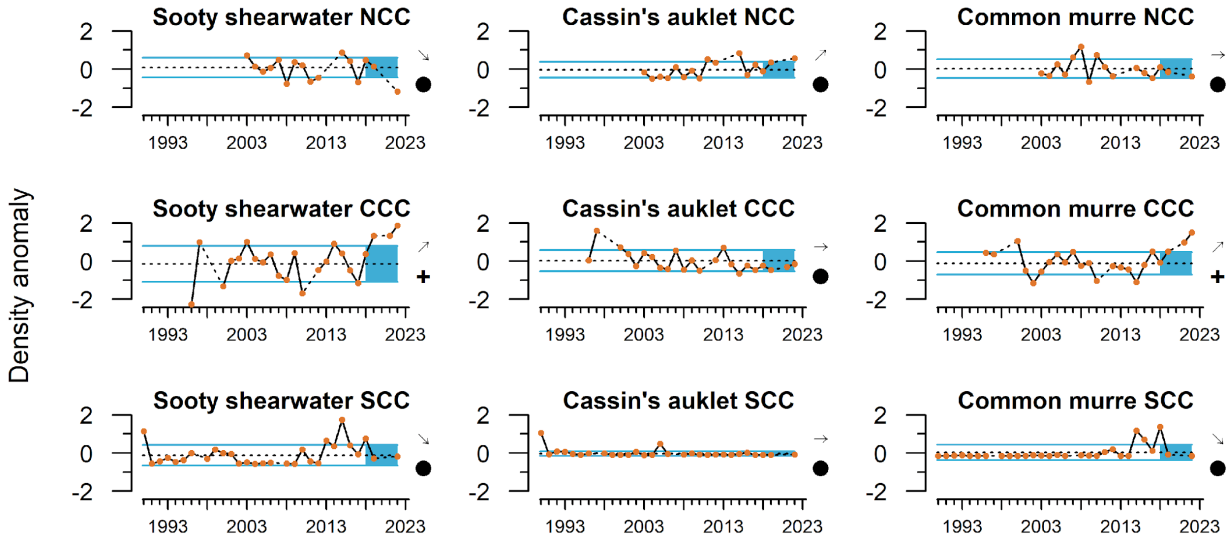
Figure M.6: Anomalies in summer at-sea densities of sooty shearwaters, Cassin's auklets and common murres in the Northern, Central, and Southern CCE. Data are shipboard counts, transformed as ln(bird density/km^2 +1) and expressed as an anomaly relative to the long-term mean. Seabird abundance data from the Northern CCE were collected and provided by J. Zamon, NMFS/NWFSC. Seabird abundance data from the Central and Southern CCE are collected on SWFSC RREAS and CalCOFI surveys, respectively, and are provided by B. Sydeman, Farallon Institute. Lines, colors, and symbols are as in Fig. 2.1.

M.4 SEABIRD MORTALITY

Monitoring of dead beached birds provides information on the health of seabird populations, ecosystem health, and unusual mortality events. CCIEA reports from the anomalously warm and unproductive years of 2014–2016 noted major seabird mortality events in each year. In 2022, no unusual seabird mortality events were reported by two beach monitoring programs (see below). However, there was a dramatic die-off of brown pelicans in southern California in May and June of 2022 due to starvation. The root cause has not been determined yet. Food supply was not thought to be the cause, as the pelican's main food source, northern anchovy, were abundant, provided that they were at an accessible depth. Nor was there evidence of avian influenza or domoic acid poisoning.

The University of Washington-led Coastal Observation And Seabird Survey Team (COASST) documented average encounter rates of dead beachcast Cassin's auklets, common murres, and sooty shearwaters in the Northern CCE (Fig. M.7). COASST documented an above-average encounter rate for northern fulmars, though not at the level of an unusual mortality event; the northern fulmar encounter rate has trended upward in recent years.
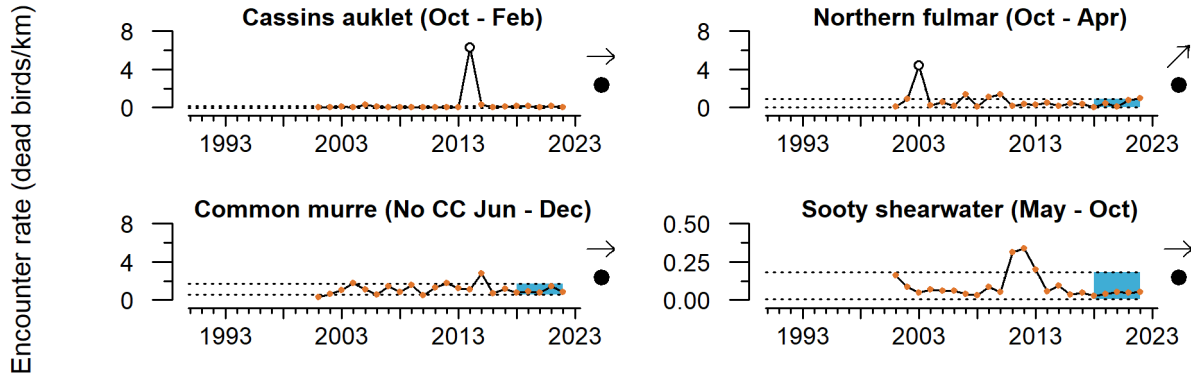
Figure M.7: Encounter rates of dead beachcast birds in Washington, Oregon and northern California. The mean and trend of the last five years (blue shaded area) are evaluated relative to the full time series with outliers (open circles) removed. Dotted lines indicate ±1 s.d. of the full time series with outliers removed. Data provided by the Coastal Observation and Seabird Survey Team (https://depts.washington.edu/coasst/). Symbols at right are as in Fig. 2.1.

In the Central CCE (Point Arena to Point Año Nuevo, California), the Beach Watch program documented variable encounter rates for indicator species, but no unusual mortality events in 2022 (Fig. M.8).
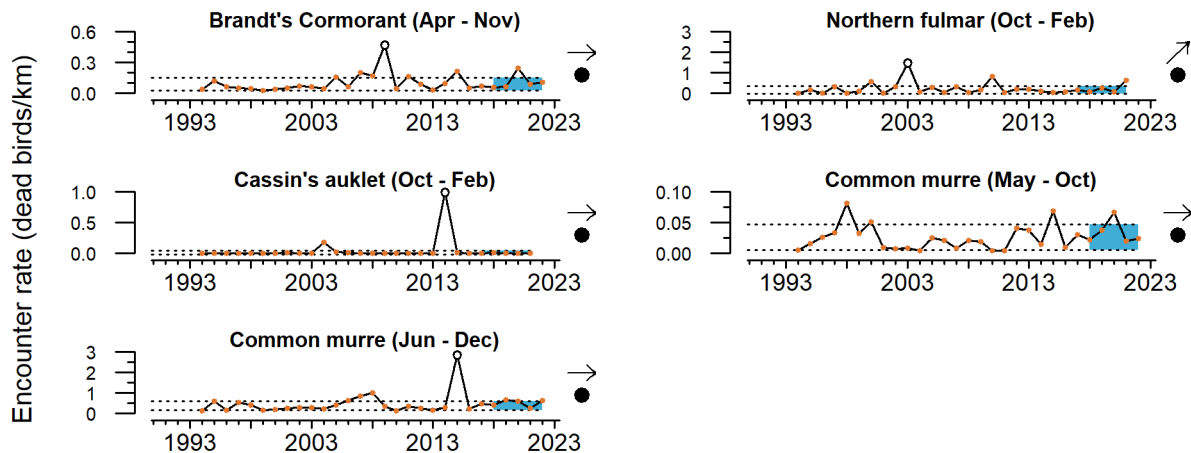
Figure M.8: Encounter rate of dead beachcast birds in north-central California. The mean and trend of the last five years (blue shaded area) are evaluated relative to the full time series with outliers (open circles) removed. Dotted lines indicate ±1 s.d. of the full time series with outliers removed. Data are from Beach Watch (https://farallones.noaa.gov/science/beachwatch.html). Symbols at right are as in Fig. 2.1.

The BeachCOMBERS program conducts surveys of beached seabirds on central and southern California beaches from Point Año Nuevo to Malibu. The time series had not been updated at the time of this writing, but will be added to future reports.

Appendix N: HARMFUL ALGAL BLOOMS

Harmful algal blooms (HABs) of diatoms in the genus *Pseudo-nitzschia* have been a recurring concern along the West Coast. Certain species of *Pseudo-nitzschia* produce the toxin domoic

acid, which can accumulate in filter feeders and extend through food webs to cause harmful or lethal effects on people, marine mammals, and seabirds (Lefebvre et al. 2002; McCabe et al. 2016). Because domoic acid can cause amnesic shellfish poisoning in humans, fisheries that target shellfish (including razor clam, Dungeness crab, rock crab, and spiny lobster) are delayed, closed, or operate under a health advisory in the recreational sector when domoic acid concentrations exceed regulatory thresholds for human consumption. Fishery closures can cost tens of millions of dollars in lost revenue, plus cause a range of sociocultural impacts in fishing communities (Dyson and Huppert 2010; Ritzman et al. 2018; Holland and Leonard 2020; Moore et al. 2020), and can also cause "spillover" of fishing effort into other fisheries.

Ocean conditions associated with El Niño events or positive PDO regimes may further exacerbate domoic acid toxicity and fishery impacts, and domoic acid toxicity also tracks anomalies of southern copepod biomass (Fig. 3.1) (McCabe et al. 2016; McKibben et al. 2017). The largest and most toxic HAB of *Pseudo-nitzschia* on the West Coast occurred in 2015, coincident with the 2013-2016 marine heatwave, and caused the longest-lasting and most widespread HAB-related fisheries closures on record (McCabe et al. 2016; Moore et al. 2019; Trainer et al. 2020) and resulted in the appropriation of >$25M in federal disaster relief funds (McCabe et al. 2016).

According to thresholds set by the U.S. Food and Drug Administration (FDA 2011), domoic acid levels ≥20 parts per million (ppm) trigger actions for all seafood and tissues except Dungeness crab viscera, for which the level is >30 ppm (California applies this to rock crab viscera as well). Under evisceration orders, Dungeness crab can be landed when the viscera exceeds the threshold but the meat does not, provided that the crab are eviscerated by a licensed processor. Oregon was the first West Coast state to pass legislation allowing evisceration, in November 2017, followed by California in October 2021. Washington adopted an emergency evisceration rule in February 2021, and is considering legislation to grant long-term authority for issuing evisceration orders.

HAB conditions on the Washington coast in 2022 were similar to 2020, with low levels of *Pseudo-nitzschia* present throughout the spring and early summer followed by a relatively short but highly toxic bloom in the fall. Low levels of domoic acid remained present in Washington razor clams during the spring and early summer of 2022, but were below the regulatory limit for human consumption (Fig. N.1), and did not interfere with state and tribal razor clam harvests during this time. Intermittent upwelling-downwelling conditions helped lead to the rapid development of a toxic bloom in late July that disrupted the state and tribal razor clam fisheries. Domoic acid levels exceeded the action level in razor clams and ended harvests from Quinault beaches on September 5, 2022, and the opening of Mocrocks and Point Grenville was canceled due to exceedances of domoic acid in razor clam tissue on September 14, 2022. This was followed by a second pulse of very toxic *Pseudo-nitzschia* in late October that further elevated levels of domoic acid in clams, ending all razor clam harvest in Washington on November 2, 2022. No domoic acid was detected in the viscera of Dungeness crab during the fall and winter of 2022 (Fig. N.1). However, Washington had delayed the opening of the 2022/23 fishery into 2023 per the Tri-State protocols due to low meat yields.
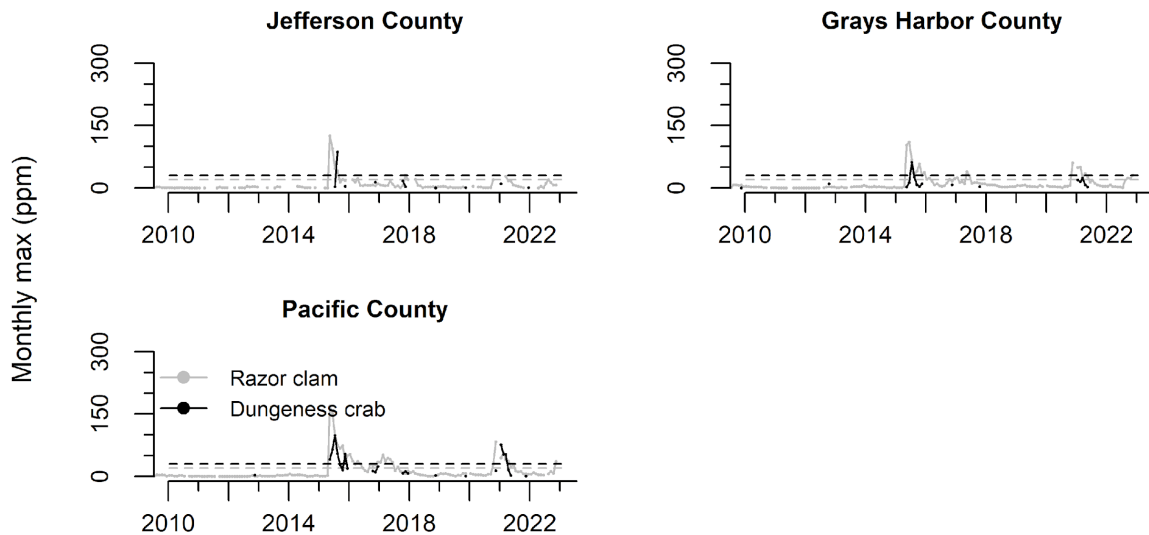
Figure N.1: Monthly maximum domoic acid concentration in razor clams and Dungeness crab viscera through December 2022 by coastal counties in Washington (north to south). Horizontal dashed lines are the management thresholds of 20 ppm (clams, gray) and 30 ppm (crab viscera, black). Data compiled by the Washington Department of Health, from samples collected and analyzed by a variety of local, tribal, and state partners.

Domoic acid exceedances resulted in multiple closures of Oregon shellfish fisheries in 2022, with the entire Oregon coast closed to harvesting of some species in response to a particularly toxic bloom of *Pseudo-nitzschia* in the fall. Lengthy exceedances of domoic acid in shellfish were again observed in southern Oregon, the result of persistent toxic blooms of *Pseudo-nitzschia* associated with a northern California "hot spot" that emerged in 2015 (Trainer et al., 2020). At the start of 2022, the razor clam fishery was open in northern and central Oregon, but had been closed since November 24, 2021 from Cape Blanco to the Oregon/California border. Beginning July 1, 2022, the entire Oregon coast was open to razor clam harvesting. Abundances of toxic *Pseudo-nitzschia* in nearshore waters increased in late August on the northern Oregon coast, and by the beginning of September domoic acid accumulation was seen in shellfish. By the end of September and the beginning of October, an extremely toxic bloom of *Pseudo-nitzschia* developed on the central and southern coast, significantly more toxic than the north coast bloom, and domoic acid in razor clams increased to levels that shut down the fishery along the entire Oregon coast (Fig. N.2). The closures were implemented in two stages: northern Oregon (OR/WA border to Cascade Head) was closed on September 23, and the rest of the Oregon coast (Cascade Head to the OR/CA border) was closed on September 30. On October 14, mussels exceeded the regulatory threshold, resulting in a closure from Yachats River to the OR/CA border. This closure lasted until November 4. On November 18, recreational crabbing was closed from Tahkenitch Creek to the Oregon/California border. The 2022/23 Oregon commercial Dungeness crab fishery was delayed into 2023 per the Tri-State protocols due to a combination of low meat yields in some areas and elevated levels of domoic acid in crab viscera in other areas of the Oregon coast (Fig. N.2).
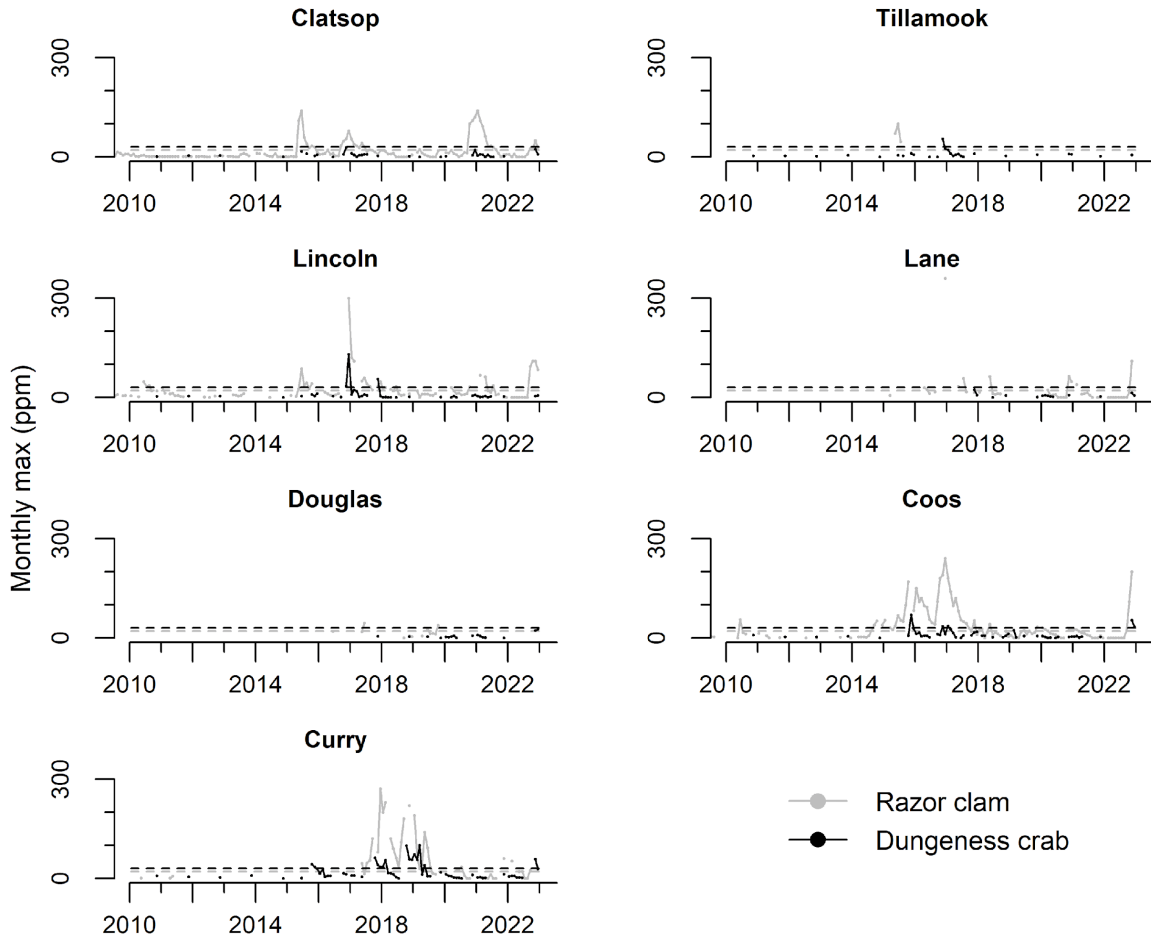
Figure N.2: Monthly maximum domoic acid concentration in razor clams and Dungeness crab viscera through December 2022 by coastal counties in Oregon (north to south). Horizontal dashed lines are the management thresholds of 20 ppm (clams, gray) and 30 ppm (crab viscera, black). Razor clam tissue sampling is conducted twice monthly from multiple sites across the Oregon coast. Data compiled and reported by Oregon Department of Fish and Wildlife from analyses conducted by the Oregon Department of Agriculture.

Domoic acid continued to be problematic for the razor clam fishery in northern California (Fig. N.3), consistent with this region being a domoic acid "hot spot," but had little impact on other California shellfish fisheries. At the beginning of 2022, the razor clam fishery in Del Norte County had been closed since December 16, 2021. It re-opened on June 27, 2022, but closed again on November 3, 2022, due to elevated levels of domoic acid, likely indicating persistent, if low-level, production of domoic acid in this region. Domoic acid exceedances in mussels in Humboldt County occurred in October, but the statewide annual quarantine on mussels for paralytic shellfish poisoning, another HAB toxin, was already in place at that time. There were no domoic acid-related closures of spiny lobster or Dungeness crab fisheries in 2022, but the northern rock crab fishery remained closed in two areas due to domoic acid concerns, as they have been since November 2015 (data not shown; see https://wildlife.ca.gov/Fishing/Ocean/Health-Advisories). Even though no domoic acid was detected in the viscera of Dungeness crab during the fall and winter of 2022 (Fig. N.3), the 2022/23 commercial Dungeness crab fishery was delayed in California for the fourth year in

a row until December 31, 2022 due to low meat yields in northern California and the potential for humpback whale entanglement south of the Sonoma/ Mendocino county line. Additionally, a *Pseudo-nitzschia* bloom offshore of the Santa Barbara Channel in August and September produced high subsurface levels of domoic acid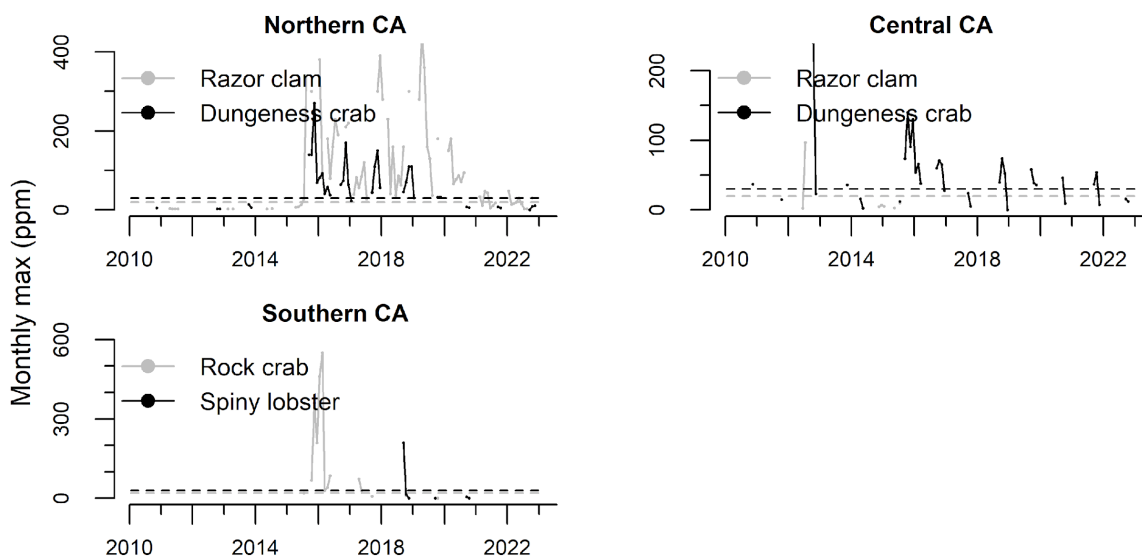 that caused significant stranding of California sea lions (https://sccoos.org/california-hab-bulletin/september-2022/).

Figure N.3: Monthly maximum domoic acid concentration in razor clams, Dungeness crab, rock crab, and spiny lobster through December 2022 in California (Northern CA: Del Norte to Mendocino counties; Central CA: Sonoma to San Luis Obispo counties; Southern CA: Santa Barbara to San Diego counties). Horizontal dashed lines are the management thresholds of 20 ppm (clams and lobsters, gray) and 30 ppm (crab viscera, black). Data compiled by the California Department of Public Health from samples collected by a variety of local, tribal, and state partners.

Appendix O: ECOSYSTEM STATE INDEX

In response to interest from the Council and several advisory bodies, the CCIEA team has engaged in research to take information from a large number of physical and ecological indicators of the CCE and reduce them down to a smaller number of indexes that can summarize overall changes in ecosystem state and potentially provide early warnings of pending changes in ecosystem structure and function. This research was reviewed by the SSC-ES in September 2017, and was introduced in our 2018 ESR (Harvey et al. 2018) and updated in last year's report (Appendix E of Harvey et al. 2022). Here, we extend the ecosystem state indicator analysis through 2022, following methods described by Hunsicker et al. (2022). Hunsicker et al. (2022) applied an approach called dynamic factor analysis (DFA) to attempt to identify shared trends within indicator time series from the central and southern CCE, including many time series presented in this report. The analysis focuses on species and life stages that respond quickly to climate variability, and avoids species and life stages that respond with lag effects, so that changes in the trends can be more specifically correlated with changes in climate and ocean drivers. The DFA yielded a single shared trend among ecological variables for time series spanning from the 1950s through 2018; this

"ecosystem state index" included a clear ecological response to the marine heatwave of 2014-2016, although not of a magnitude or persistence that would suggest thorough reorganization of the food web (Hunsicker et al. 2022).

In Figure O.1, we show the ecosystem state index with central and southern CCE ecological data updated through 2022. The index captures the strong response of the ecosystem to two strong El Niño events (1982–1983 and 1997–1998) and to unusually low productivity conditions (2005). It also reflects the ecosystem's response to two marine heatwaves (2014-2016 and 2019). Since 2020, subsequent to the two marine heatwave events, the ecosystem state index has been close to its central tendency (Fig. O.1). The value in 2022 was similar to 2021, implying that the shared trend within the ecological indicators in the central and southern portions of the CCE did not change dramatically in 2022 surveys.
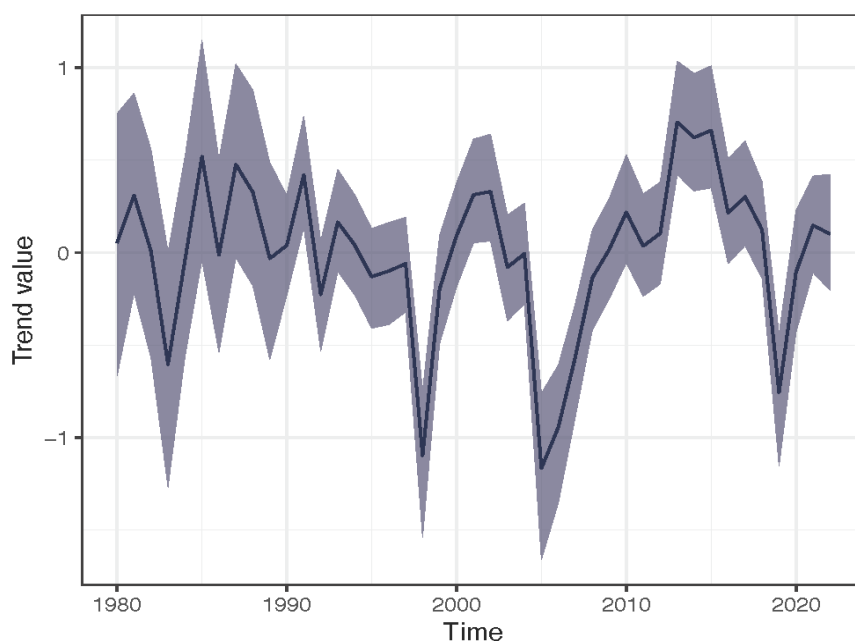

Figure O.1: Ecosystem state index (black line) with 95% credible intervals (gray envelope) in the southern and central CCE, 1980-2022. Large negative values in the index are associated with major El Niño events (1982-1983, 1997-1998), the anomalously unproductive conditions in 2005, and a major marine heatwave in 2019. The 2014-2016 heatwave known as the "Blob" is associated with the strong, extended positive values. Courtesy of M. Hunsicker, NMFS/NWFSC.

Appendix P: STATE-BY-STATE FISHERY LANDINGS AND REVENUE

The Council and EWG have requested information on state-by-state fisheries landings and revenues; these values are presented here. Commercial landings and revenue data are best summarized by the Pacific Fisheries Information Network (PacFIN; pacfin.psmfc.org), and recreational landings are best summarized by the Recreational Fisheries Information Network (RecFIN; www.recfin.org). Data from 1981 to 2022 were downloaded from PacFIN and RecFIN on January 10, 2023. Landings provide the best long-term indicator of fisheries

removals. Revenues are calculated based on consumer price indices in 2022 dollars. Status and trends are estimated relative to a frame of reference of 1991-2020.

P.1 STATE-BY-STATE LANDINGS

Total fisheries landings in Washington decreased from 2018 to 2022, with the lowest total landings in the time series observed in 2022 (Fig. P.1). These patterns were driven primarily by a steep decrease in Pacific whiting landings over the last five years, including a 39% decrease in 2022 from 2021. Commercial shrimp was the only fishery in Washington with a significantly increasing 5-year trend. Commercial salmon landings remained >1 s.d. below the long-term average. All other major commercial fisheries showed no trends and were within 1 s.d. of the long-term average from 2018 to 2022.

Total landings of recreational catch data (excluding salmon and halibut) in Washington were complete through October 2022 and showed a decrease of >1 s.d. of long-term averages from 2018 to 2022 (Fig. P.1). The only exception to this decreasing trend was in 2019 when albacore landings were at their greatest value of the entire time series. Recreational landings of Chinook and coho salmon were within 1 s.d. of the long-term average from 2017 to 2021 (2022 data were not available at time of report).
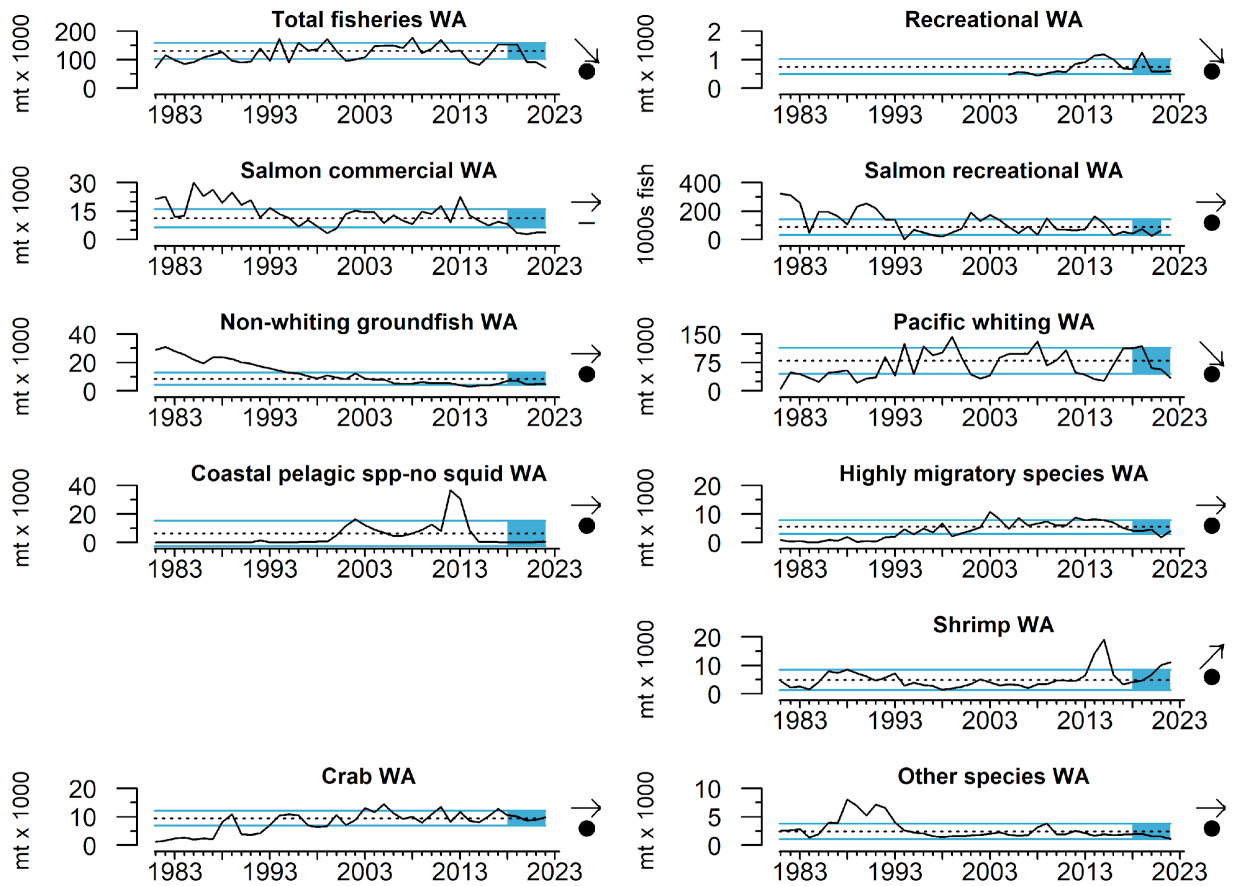

Figure P.1: Annual Washington landings from West Coast commercial (data from PacFIN) and recreational (data from RecFin) fisheries, including total landings across all fisheries from 1981 - 2022. Lines, colors, and symbols are as in Fig. 2.1.

Total fisheries landings in Oregon were consistently >1 s.d. above the long-term average from 2018 to 2022 (Fig. P.2). Similar to Washington, these patterns were driven primarily by landings of Pacific whiting, which were also consistently >1 s.d. above the long-term average for the most recent five years. Commercial landings of crab decreased by >1 s.d. of the long-term average from 2018 to 2022. Although lower in 2022 than in 2021, landings of market squid in Oregon ports over the last five years remained >1 s.d. above the long-term state average. Commercial landings of all other commercial fisheries showed no significant recent trends and had short-term averages within 1 s.d. of long-term averages.

Recreational fisheries landings data (excluding salmon and Pacific halibut) in Oregon were complete through September 2022 appear close to the long-term average (Fig. P.2). Similar to Washington, albacore landings in 2019 were at their greatest of the entire time series and were responsible for the large positive outlier in total recreational landings. Recreational landings of Chinook and coho salmon showed no significant recent trend, and have been within 1 s.d. of the long-term average since 2018 (2022 data were not available at time of report).
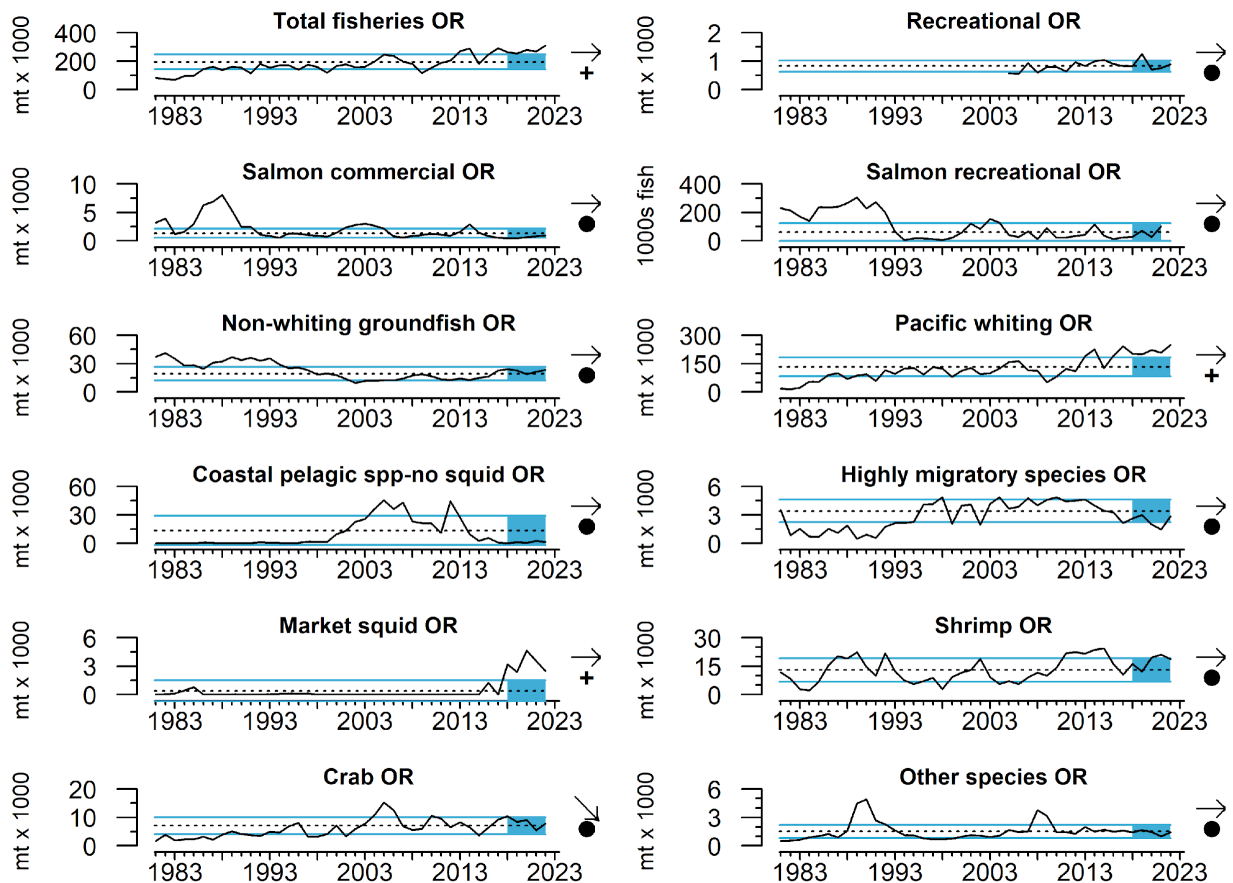

Figure P.2: Annual Oregon landings from West Coast commercial (data from PacFIN) and recreational (data from RecFin) fisheries, including total landings across all fisheries from 1981 - 2022. Lines, colors, and symbols are as in Fig. 2.1.

Total fisheries landings in California increased slightly in 2022, but remained >1 s.d. below the long-term average, primarily due to below-average CPS finfish landings and significant

decreasing trends in shrimp and crab landings (Fig. P.3). Market squid were the only California fishery that had significant increases in landings from 2018 to 2022, and returned to the long-term average in 2022. All other major fisheries showed no significant trends and were within 1 s.d. of long-term averages, with the exception of Other species, which remained consistently >1 s.d below the long-term average over the last five years.

Recreational landings data (excluding salmon, Pacific halibut and HMS) in California were complete through October 2022. Recreational landings had both a decreasing trend and below-average status (>1 s.d. below the long-term average) over the past five years (Fig. P.3). The decreasing trend was largely due to decreased landings of lingcod and vermilion rockfish over the last five years. Also in 2022, eight of the top ten landed recreationally species in California decreased from 2021, and many of these species had relatively small 2022 landings compared to various years over the previous 5-10 years (this excludes HMS, whose recreational catch data were incomplete at the time of this writing). Recreational salmon landings in California were within 1 s.d. of the long-term average over the last 5 years, but were near the lower edge of that range in 2020 and 2021.
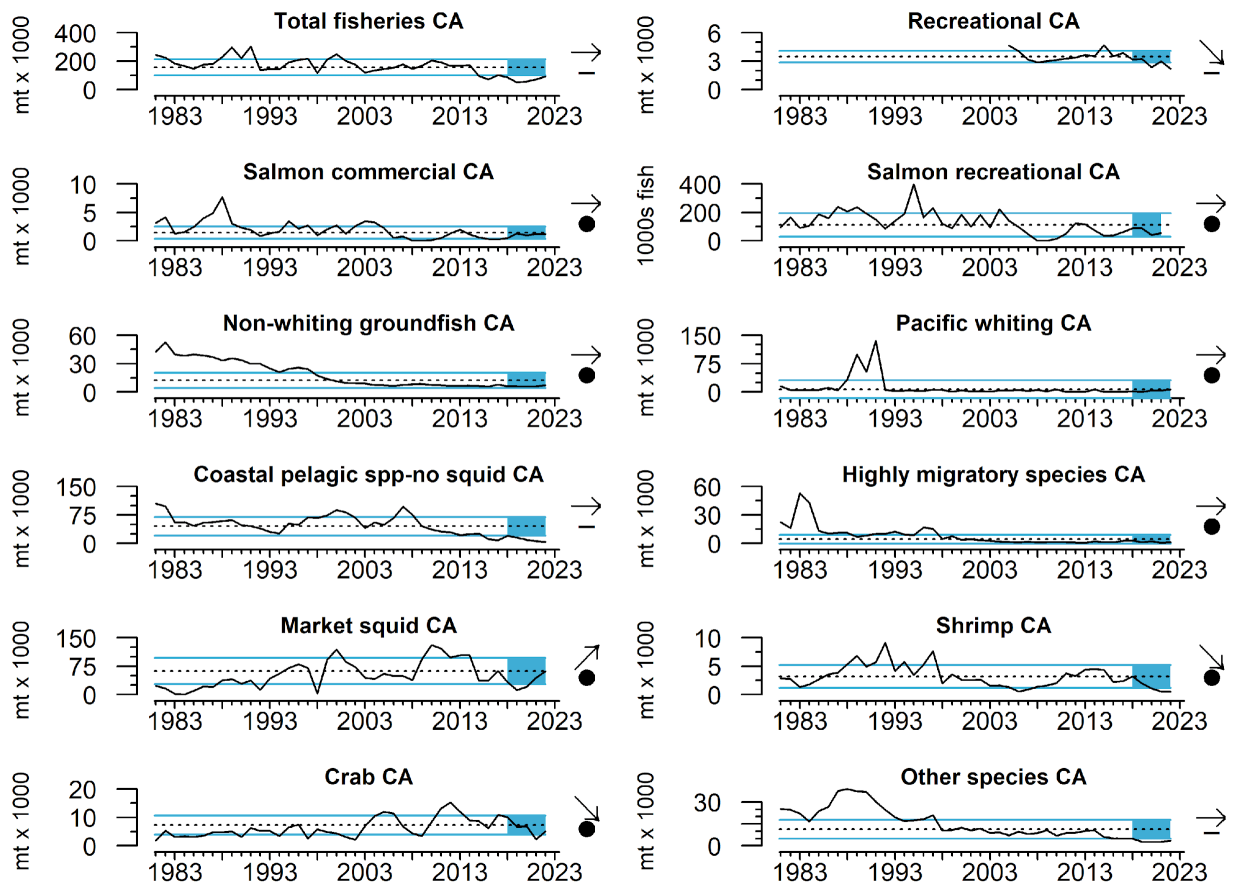

Figure P.3: Annual California landings from West Coast commercial (data from PacFIN) and recreational (data from RecFin) fisheries, including total landings across all fisheries from 1981-2022. Lines, colors, and symbols are as in Fig. 2.1.

P.2   COMMERCIAL FISHERY REVENUES

Total revenue across West Coast commercial fisheries in 2022 increased by 10% from 2021, based on data currently available (Fig. P.4). Over the most recent five years, total revenue was highly variable, but remained within 1 s.d. of the long-term average. Recent revenue patterns have been driven by an increase in market squid revenues over the last five years and smaller increases in crab, non-whiting groundfish, Pacific whiting and HMS revenues since 2020. Revenue for 6 of 9 commercial fisheries increased from 2021 to 2022: HMS (101%), market squid (28%), crab (27%), non-whiting groundfish (19%), Other species (18%) and Pacific whiting (7%). In contrast, CPS finfish (-68%), shrimp (-20%) and salmon (-13%) fisheries generated less revenue in 2022 than 2021. Revenue from crab landings was >1 s.d. above the long-term average, while revenues from non-whiting groundfish, CPS finfish and HMS were >1 s.d. below long-term averages over the last five years. All other fisheries' revenues showed no trends and were within 1 s.d. of long-term averages. Comparing landings (Fig. 4.1 in the main report) and revenue among fisheries reveals two contrasting relationships that highlight the importance of variation in price-per-pound within and across commercial fisheries: crab landings decreased over the past five years even as revenue averaged >1 s.d. above long-term mean, and shrimp landings increased while revenue remained relatively unchanged over the last five years.
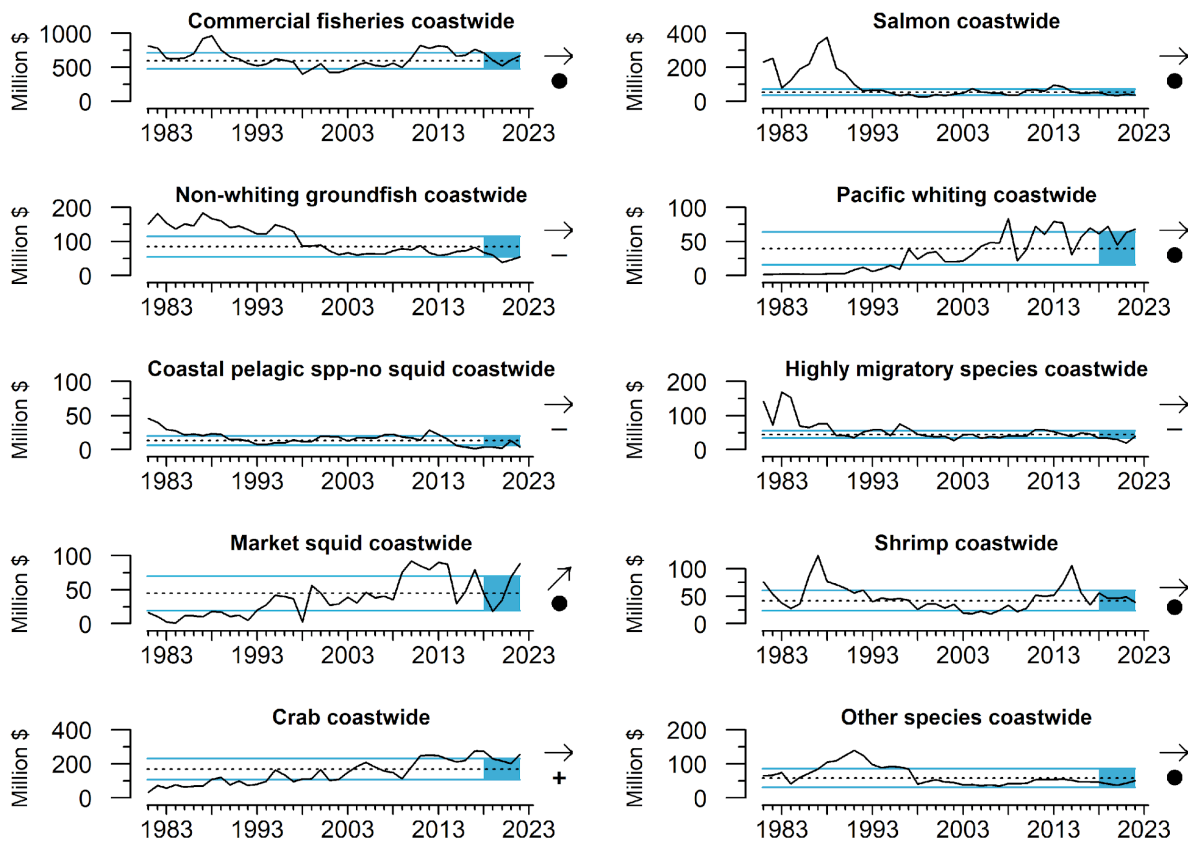

Figure P.4: Annual coastwide revenue (ex-vessel value in 2022 dollars) from West Coast commercial fisheries (data from PacFin) from 1981-2022. Whiting revenue includes shoreside and at-sea values from PacFIN, NORPAC (North Pacific Groundfish Observer Program) and NMFS Office of Science & Technology. Lines, colors, and symbols are as in Fig. 2.1.

Total revenue across commercial fisheries in Washington decreased from 2018 to 2022, with a 14% decrease in 2022 from 2021 levels (Fig. P.5). These patterns are largely driven by a decreasing trend in revenue from Pacific whiting fisheries and the variability in revenue from crab landings over the last five years. Overall, 3 of 8 major fisheries increased in revenue in 2022 from 2021 levels: HMS (131%), CPS finfish (9%) and non-whiting groundfish (2%). In contrast, revenue from Pacific whiting (-36%), Other species (-30%), salmon (-23%), shrimp (-17%) and crab (-4%) fisheries was lower in 2022 compared to 2021. Crab fisheries' revenue was >1 s.d. above long-term averages and non-whiting groundfish revenue was >1 s.d. below long-term averages, while all other fisheries were within long-term averages over the last five years. Revenue from salmon and Pacific whiting fisheries declined from 2018 to 2022, while all other fisheries showed no significant revenue trends over the last five years in Washington.
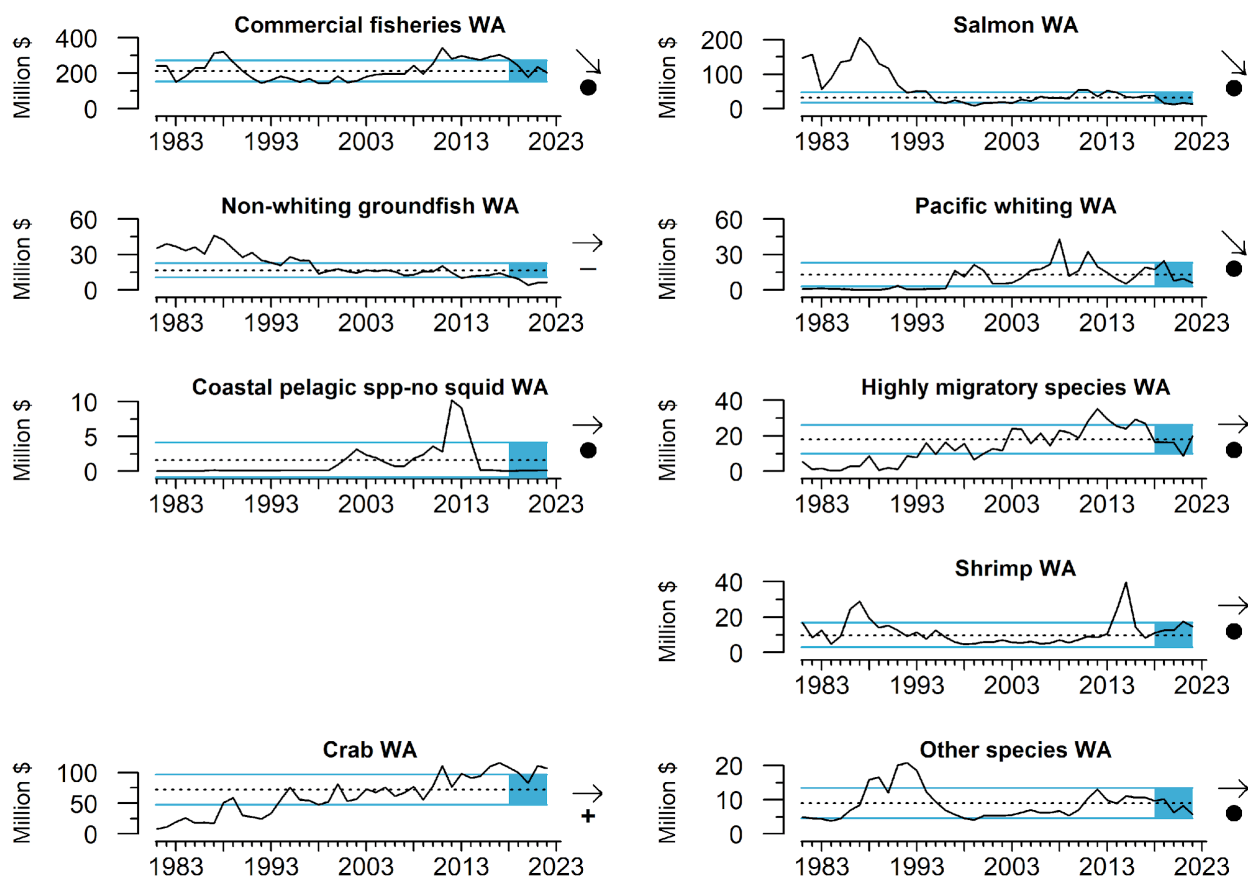

Figure P.5: Annual Washington revenue (ex-vessel value in 2022 dollars) from West Coast commercial fisheries (data from PacFin) from 1981-2022. Whiting revenue includes shoreside and at-sea values from PacFIN, NORPAC (North Pacific Groundfish Observer Program) and NMFS Office of Science & Technology. Lines, colors, and symbols are as in Fig. 2.1.

Total revenue across commercial fisheries in Oregon was >1 s.d. above the long-term average from 2018 to 2022, with a 22% increase in 2022 from 2021 levels (Fig. P.6). These patterns are largely driven by changes in revenue from crab, Pacific whiting and non-whiting groundfish fisheries over the last five years. Overall, 6 of 9 major fisheries in Oregon increased in revenue in 2022 from 2021 levels: CPS finfish (244%), HMS (102%), crab

(41%), non-whiting groundfish (25%), Pacific whiting (14%) and salmon (9%). In contrast, revenue from market squid (-31%), shrimp (-25%), and Other species (-6%) was lower in 2022 compared to 2021. Even though there was a relatively large increase in revenue observed in the CPS finfish fishery, its revenue levels are still very low in Oregon. Pacific whiting, market squid and crab fisheries' revenue were all >1 s.d. above long-term averages, while all other fisheries were within ±1 s.d. of long-term averages over the last five years. There were no significant trends observed for any fishery from 2018 to 2022 in Oregon.
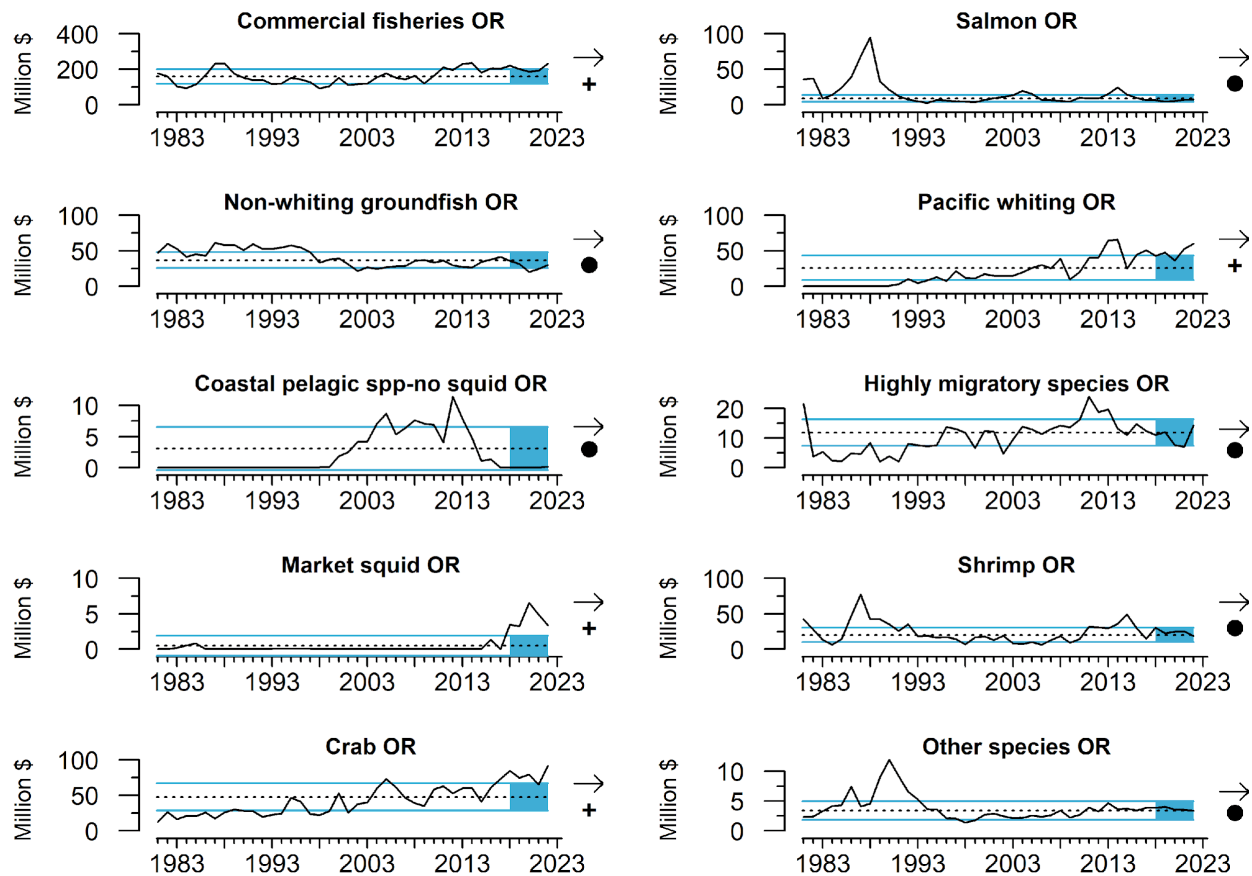

Figure P.6: Annual Oregon revenue (ex-vessel value in 2022 dollars) from West Coast commercial fisheries (data from PacFin) from 1981-2022. Whiting revenue includes shoreside and at-sea values from PacFIN, NORPAC (North Pacific Groundfish Observer Program) and NMFS Office of Science & Technology. Lines, colors, and symbols are as in Fig. 2.1.

Total revenue across commercial fisheries in California was nearly 1 s.d. below the long-term average for much of the last five years, but a 30% increase in 2022 from 2021 has total revenue near its long-term average (Fig. P.7). These patterns are largely driven by variation in revenue from market squid, crab and Other species fisheries from 2018 to 2022. Overall, 6 of 9 major fisheries increased in revenue in 2022 from 2021 levels: crab (127%), Pacific whiting (83%), market squid (33%), Other species (33%), HMS (32%) and non-whiting groundfish (16%). In contrast, revenue from CPS finfish (-70%), salmon (-13%) and shrimp (-10%) fisheries was lower in 2022 compared to 2021. Even though there was a relatively large increase in revenue observed in the Pacific whiting fishery, its revenue levels are still very low, and this revenue comes from fishing events that occur in California waters but are

processed at sea and landed outside of California. Revenue from market squid and Pacific whiting fisheries increased from 2018 to 2022, while revenue from crab and shrimp fisheries decreased; all others showed no short-term revenue trends . Revenue in all fisheries were within ±1 s.d. of their respective long-term averages over the last five years in California.
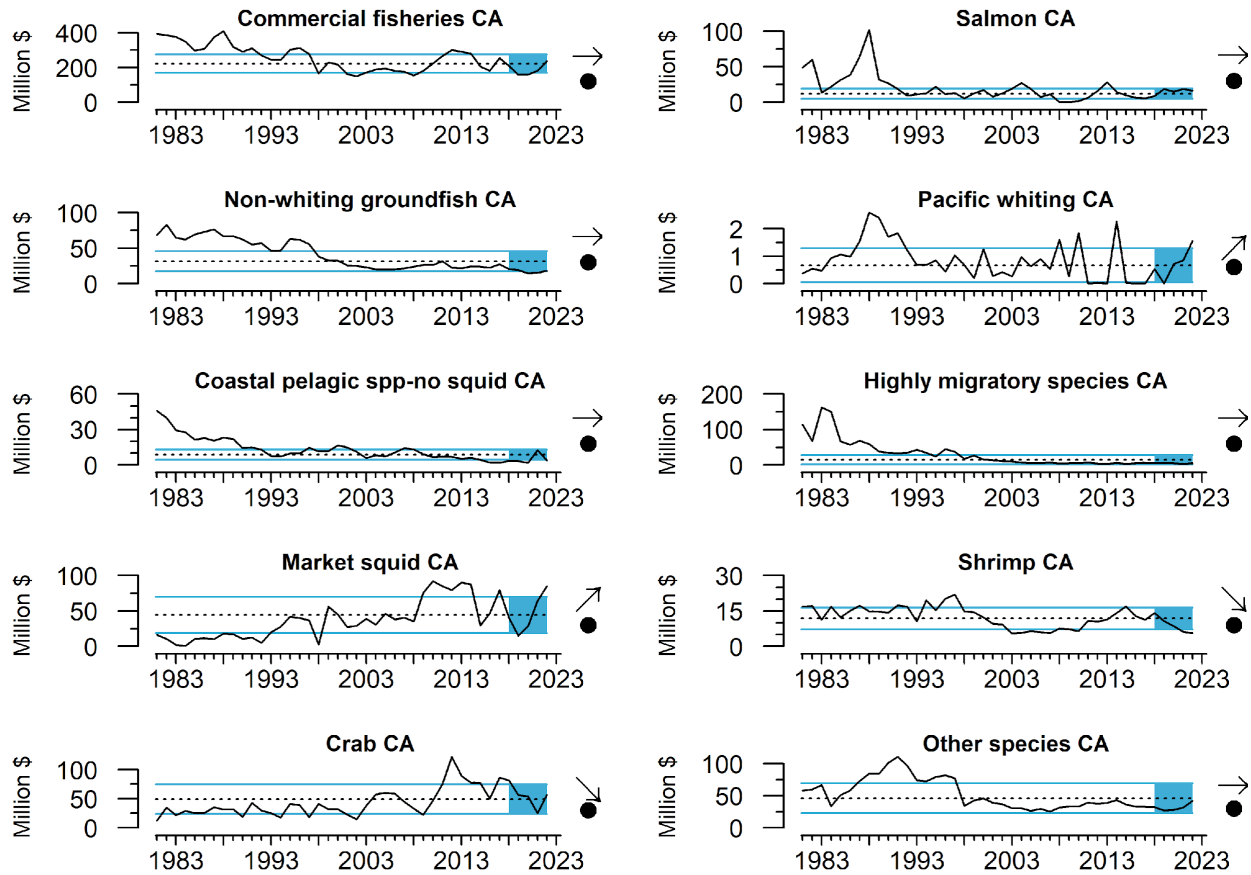

Figure P.7: Annual California revenue (ex-vessel value in 2022 dollars) from West Coast commercial fisheries (data from PacFin) from 1981-2022. Whiting revenue includes shoreside and at-sea values from PacFIN, NORPAC (North Pacific Groundfish Observer Program) and NMFS Office of Science & Technology. Lines, colors, and symbols are as in Fig. 2.1.

Appendix Q: POTENTIAL FOR SPATIAL INTERACTIONS AMONG OCEAN-USE SECTORS

New ocean-use sectors of the economy (e.g., renewable energy and aquaculture) are becoming a reality off the West Coast, particularly with the Bureau of Ocean Energy Management's (BOEM) recent offshore wind energy (OWE) Call Area and Wind Energy Area (WEA) designations and leases. Understanding how oceanic and atmospheric processes, protected and managed species and their habitats, fisheries, fishing communities, and NMFS scientific surveys will be affected by new ocean-use sectors is needed to ensure effective marine spatial planning and adaptive management, and to minimize conflicts across the West Coast into the future.

In last year's ESR (Harvey et al. 2022), we mapped indicators of spatial and temporal variation in fishing effort for the groundfish bottom trawl fishery in areas within and surrounding newly-established WEAs off California[8] and planning areas off Oregon. This year, we expand on this effort by presenting time series of fishing effort (main body, Section 4.2) and revenue and maps of potential conflicts between nine commercial and recreational fisheries and six NMFS scientific surveys that operate within the boundaries of two OWE Call Areas approximately 15 nm off the coast of Oregon[9]. For each analysis described below and in Section 4.2, we used logbook and at-sea observer recorded set and retrieval coordinates, duration fished or amount of gear used, and matched PacFIN fish ticket information from each fishery to estimate annual and cumulative fishing effort (hours or gear-hours) and revenue (ex-vessel adjusted for inflation (AFI) re. 2020 USD), summarized (i) across both Call Areas and (ii) on a 2x2-km grid (except for the two albacore fisheries, which are at a resolution of 10 arcmin and were downscaled to the 2x2-km grid using an areal-weighted mean approach).

Q.1 TEMPORAL VARIATION IN THE OVERLAP BETWEEN OREGON CALL AREAS AND FISHERY REVENUES

In the main body of the ESR (Section 4.2), we presented time series of fishing effort within the two Call Areas off the coast of Oregon for eight commercial fisheries across varying years of available data. Fishing effort data in the Dungeness crab fishery were included for years in which 100% of the effort data had been entered; other years have typically had ~30% of the effort data entered and were not used.

Here, we present time series of fishing revenue derived from landings within the two Call Areas from 2011 to 2020 (Fig. Q.1). Revenue from commercial landings captured within the two Call Areas varied widely, but revenue from the at-sea whiting fishery has been consistently highest over the last decade (Fig. Q.1; note vertical axis scales). Annual effort and revenue values were highly correlated (mean r = 0.9) in four of the six fisheries with data for both metrics from 2011-2020 (albacore troll, groundfish longline, groundfish pot,

---

and shrimp trawl), while at-sea whiting (r = 0.3) and shoreside-processed whiting (r = 0.5) fisheries showed much less correlation between these two indicators of the fishery.
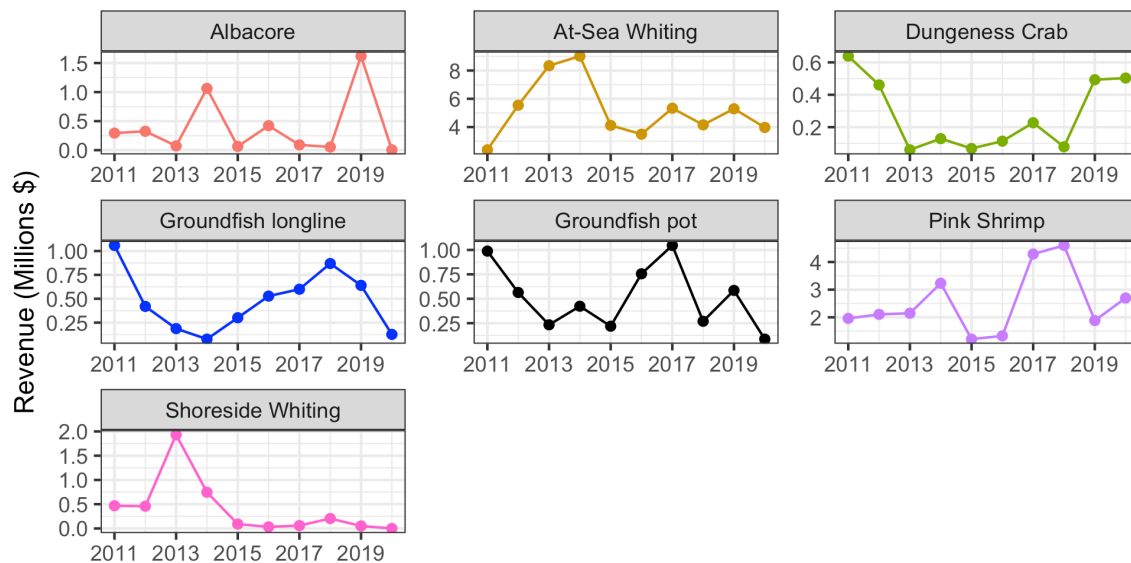

Figure Q.1: Annual fishing revenue from 2011-2020 for commercial fishing events that occurred within the two offshore wind energy Call Areas off the coast of Oregon. Revenue is ex-vessel adjusted for inflation (AFI) re. 2020 dollars. (Groundfish bottom trawl revenue analysis was incomplete at the time of this report.)

Q.2 SPATIAL VARIATION IN THE OVERLAP BETWEEN OREGON CALL AREAS AND FISHERIES EFFORT AND REVENUES

We evaluated the overall suitability of space within the two Oregon Call Areas for OWE development relative to the spatial overlap with nine fisheries that operate in the region.[10] The nine fisheries included: at-sea and shoreside whiting; groundfish bottom trawl, fixed-gear pot and fixed-gear longline; pink shrimp trawl; Dungeness crab; and commercial and charter albacore tuna. Other fisheries were considered but not included due to time constraints or the lack of spatial data at the required resolution.

We used the cumulative fishing effort and revenue values described above to calculate a multivariate "Ranked Importance" metric for each 2x2-km grid cell within the two Call Areas. This metric combines the most important spatial characteristics of the effort and revenue metrics into a single value, which should be useful for marine spatial planning analyses being performed by BOEM. Ranked Importance was calculated in three steps. First, for both effort and revenue layers, we ranked each grid cell in descending order according to the value of either effort or revenue. Second, we normalized the ranked effort and ranked revenue data between values of 0 and 1 by subtracting the minimum value of the dataset from each value and dividing by the difference between the minimum and maximum values of the dataset.

---

[10] https://www.pcouncil.org/documents/2023/02/nmfs-odfw-fisheries-data-recommendations-or-boem-call-area.pdf/

Third, for each grid cell, we selected the highest normalized value between the effort and revenue normalized values.

Maps for each of the three metrics characterizing each fishery (effort, revenue and ranked importance) are in Figures Q.2-Q.10. While all of the maps included in this report have been screened for confidentiality (individual grid cells containing information from less than three vessels were not disclosed), the final overall relative suitability map incorporated confidential and non-confidential grid cells. Overall, these maps show a wide range of importance across these fisheries. The eastern regions of both Call Areas, particularly at depths less than ~600 m, showed relatively high importance for at-sea whiting (Fig. Q.2), shoreside whiting (Fig. Q.3) and groundfish fixed-gear longline (Fig. Q.6), whereas pink shrimp (Fig. Q.7) and Dungeness crab (Fig. Q.8) fisheries were operating mostly at depths shallower than ~200 m. Depths between ~400 to ~800 m in both Call Areas were particularly important to groundfish bottom trawl fisheries (Fig. Q.4), while the western boundary was most important to the commercial albacore troll (Fig. Q.9) and recreational albacore charter fisheries (Fig. Q.10).
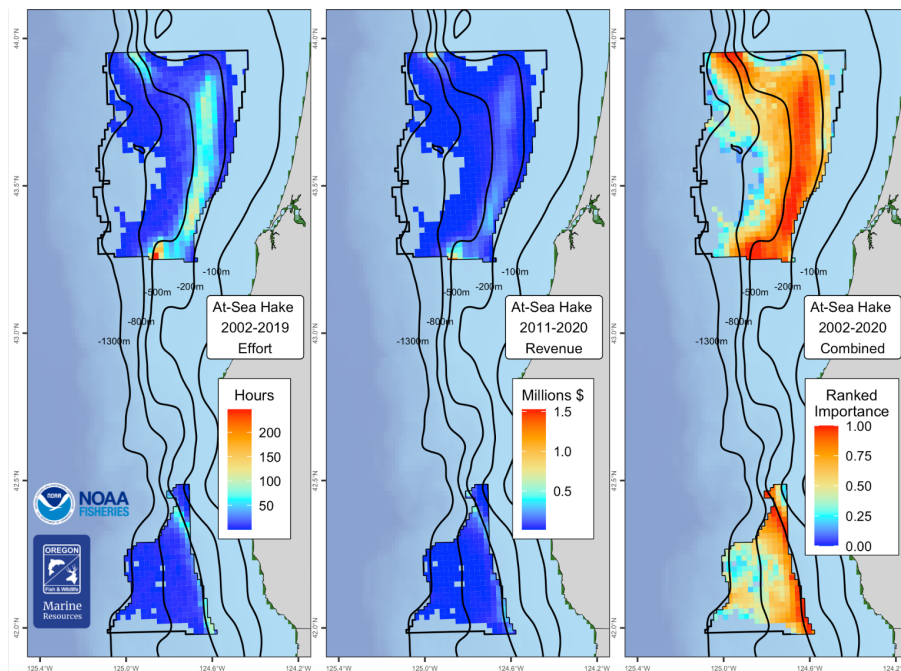

Figure Q.2: Cumulative sum of fishing effort (left), revenue (middle; AFI re. 2020 dollars) and ranked importance (right) within the offshore wind energy Call Areas off Oregon for the at-sea hake (whiting) fishery. Years of data used to calculate each metric shown in legend.
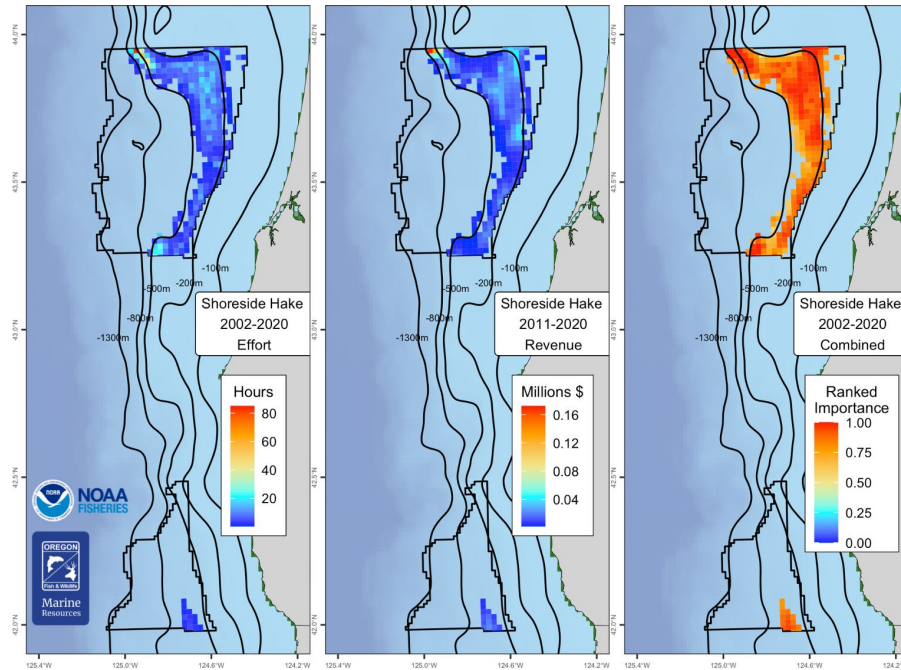
Figure Q.3: Cumulative sum of fishing effort (left), revenue (middle; AFI re. 2020 dollars) and ranked importance (right) within the offshore wind energy Call Areas off Oregon for the shoreside hake (whiting) fishery. Years of data used to calculate each metric shown in legend.
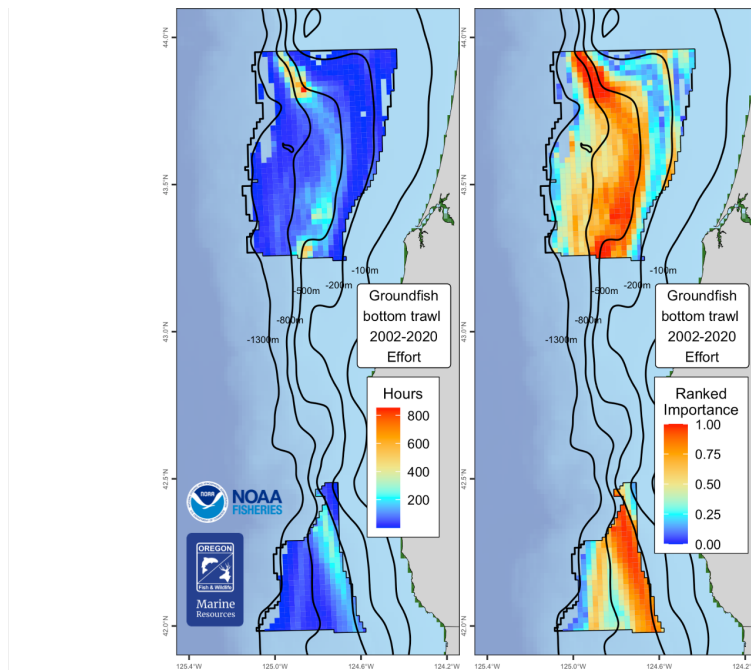

Figure Q.4: Cumulative sum of fishing effort (left) and ranked importance (right) within the offshore wind energy Call Areas off Oregon for the groundfish bottom trawl fishery. Years of data used to calculate each metric shown in legend. (Revenue analysis for this fishery was incomplete at the time of this report.)
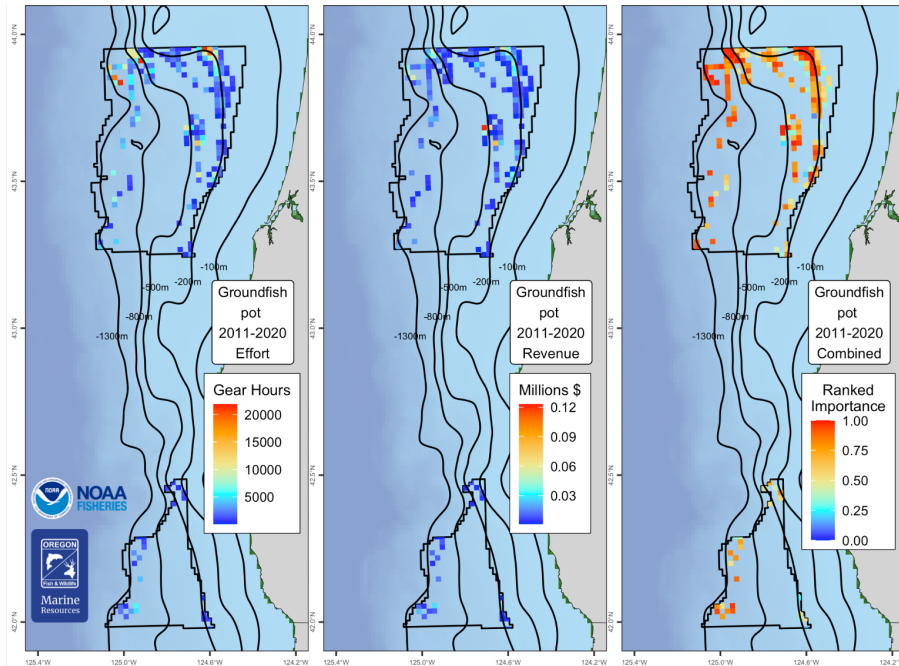
S-83

Figure Q.5: Cumulative sum of fishing effort (left), revenue (middle; AFI re. 2020 dollars) and ranked importance (right) within the offshore wind energy Call Areas off Oregon for the groundfish fixed-gear pot fishery. Years of data used to calculate each metric shown in legend.
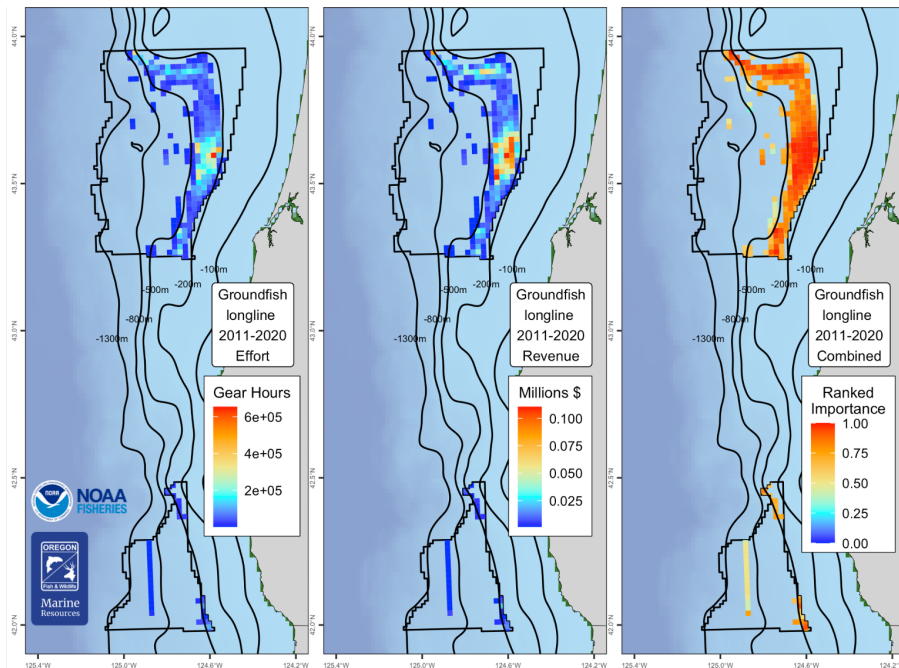

Figure Q.6: Cumulative sum of fishing effort (left), revenue (middle; AFI re. 2020 dollars) and ranked importance (right) within the offshore wind energy Call Areas off Oregon for the groundfish fixed-gear longline fishery. Years of data used to calculate each metric shown in legend.
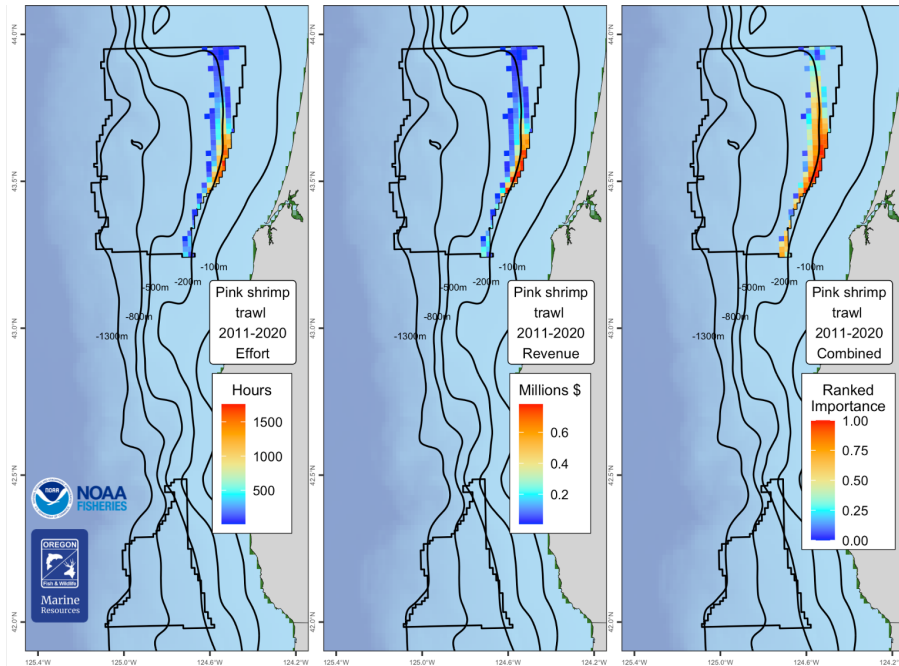
Figure Q.7: Cumulative sum of fishing effort (left), revenue (middle; AFI re. 2020 dollars) and ranked importance (right) within the offshore wind energy Call Areas off Oregon for the pink shrimp trawl fishery. Years of data used to calculate each metric shown in legend.

Figure Q.8: Cumulative sum of fishing effort (left), revenue (middle; AFI re. 2020 dollars) and ranked importance (right) within the offshore wind energy Call Areas off Oregon for the Dungeness crab fishery. Years of data used to calculate each metric shown in legend.
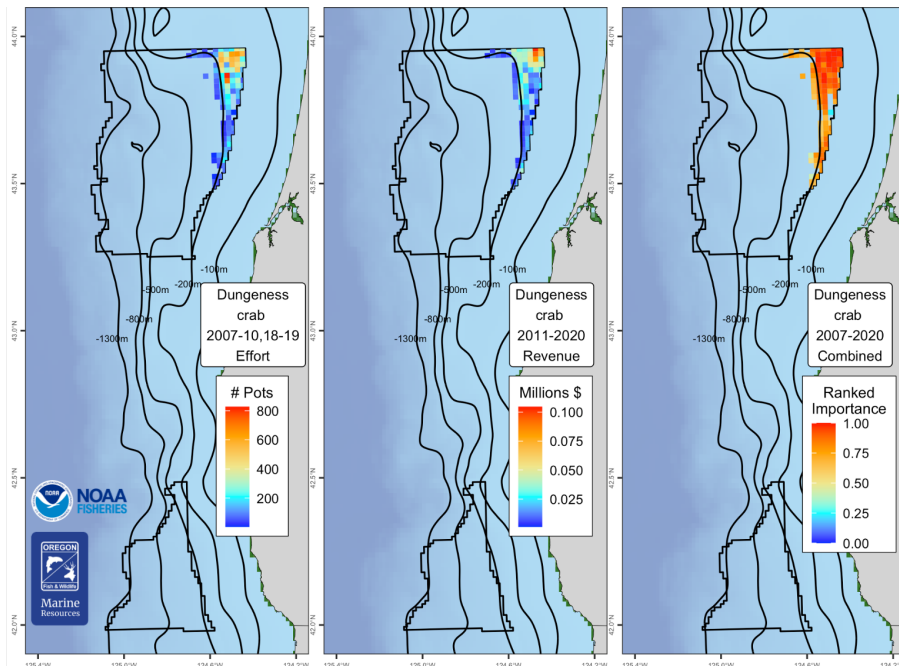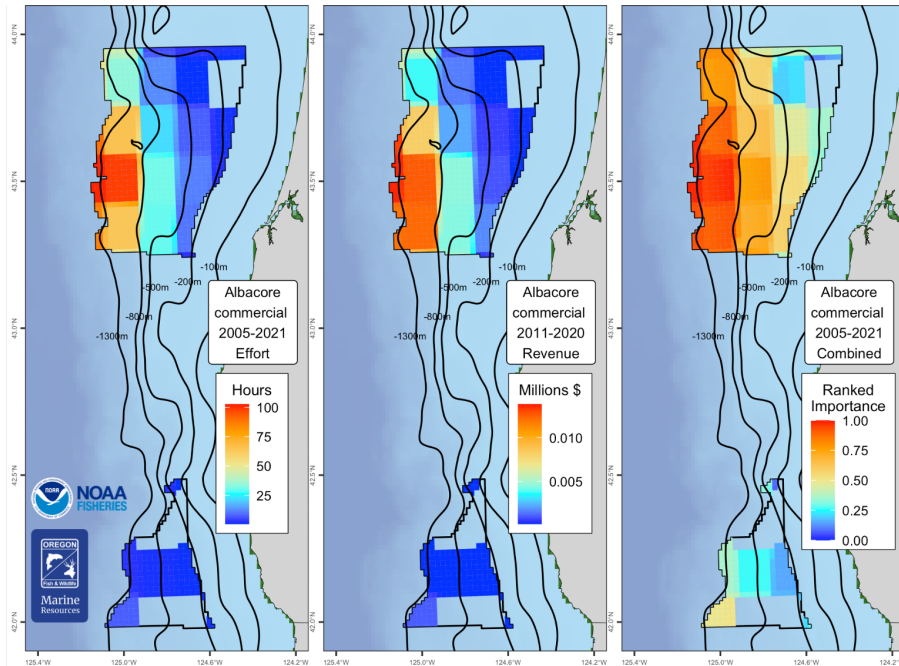
Figure Q.9: Cumulative sum of fishing effort (left), revenue (middle; AFI re. 2020 dollars) and ranked importance (right) within the offshore wind energy Call Areas off Oregon for the albacore troll fishery. Years of data used to calculate each metric shown in legend.
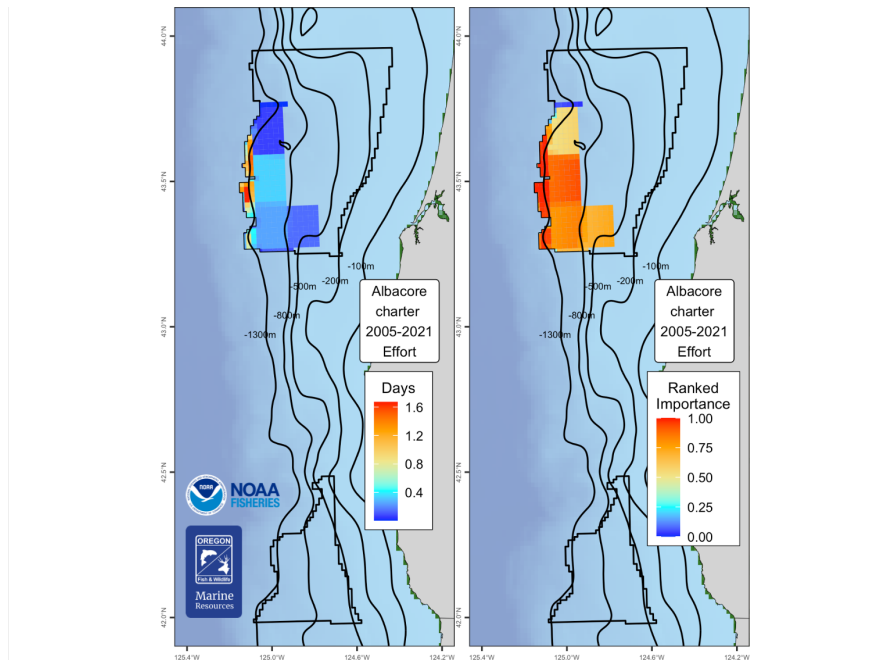
Figure Q.10: Cumulative sum of fishing effort (left) and ranked importance (right) within the offshore wind energy Call Areas off Oregon for the recreational albacore charter fishery. Years of data used to calculate each metric shown in legend.

Finally, we used the Ranked Importance data for each fishery to calculate an overall suitability score across all fisheries for each grid cell (Fig. Q.11), using methods described in NOAA's Aquaculture Opportunity Area Atlas (Riley et al. 2021). Specifically, the Ranked

Importance data for each fishery were transformed using a z-membership function and then the geometric mean of those transformed values was calculated across all fisheries for each grid cell. This geometric mean represents the suitability score of a grid cell for OWE development relative to the importance of these areas to the nine fisheries included; thus, a relative suitability score of 1.00 is most suitable for OWE, while relative suitability scores closer to 0 are least suitable. Large areas of the two Call Areas, particularly at depths between ~200 & ~500 m, are heavily used by fisheries, while the western half of the southern Call Area has relatively less overlap with fisheries.

(Figure Q.11 also appears in the main body as Figure 4.4, but is included again here for convenience and emphasis as a key take-away for this analysis.)

Figure Q.11: Overall relative suitability scores of 2x2-km grid cells within the Oregon Call Areas. Scores near 1.00 (blue cells) are most suitable for offshore wind energy development relative to the eight commercial fisheries mapped above, while scores near zero (orange cells) are less suitable due to fishery conflicts.
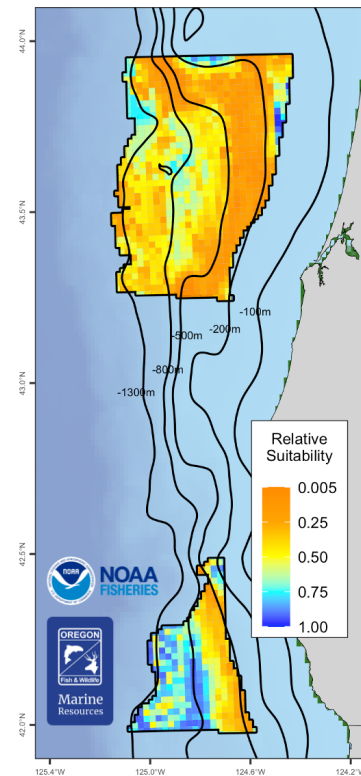
Q.2   OVERLAP BETWEEN OREGON CALL AREAS AND RESEARCH SURVEYS

In addition to conflict with commercial and recreational fisheries, there are several long-standing NMFS scientific surveys that would be affected by OWE development in these two Call Areas. These surveys are conducted on an annual or biennial basis across numerous platforms that are likely to be limited in areas of OWE development. These surveys are used to monitor and assess populations of managed fish and marine mammal stocks, threatened and endangered species and the habitats they all rely upon.[11]

There are six surveys that NMFS conducts within the two Call Areas: the West Coast Groundfish Bottom Trawl Survey, Integrated Ecosystem and Pacific Hake Survey, West Coast Pelagic Fish Survey, northern limb of the Rockfish Recruitment and Ecosystem Assessment Survey (this limb was formerly known as the "Pre-Recruit Survey"), Northern California Current Ecosystem Survey, and West Coast Marine Mammal Survey. Data collected on these surveys are used routinely in analyses included in this ESR, and also form the backbone of stock assessments for the Council. Figures Q.12 and Q.13 show the spatial overlap between the two Call Areas and these surveys (except for the Marine Mammal Survey which has overlapped a very small portion of the southeastern edge of the southern Call Area in the past). Similarly, overlap between these and other NMFS surveys in Wind Energy Areas off

---

[11] https://www.regulations.gov/comment/BOEM-2022-0009-0178

California will impact monitoring and analyses in the future (see NOAA's letter[12] to BOEM for the California proposed sale notice for more information). NMFS and BOEM recently developed a Federal Survey Mitigation Strategy specific to the U.S. Northeast region (Hare et al. 2022), and will develop a similar strategy for the West Coast.
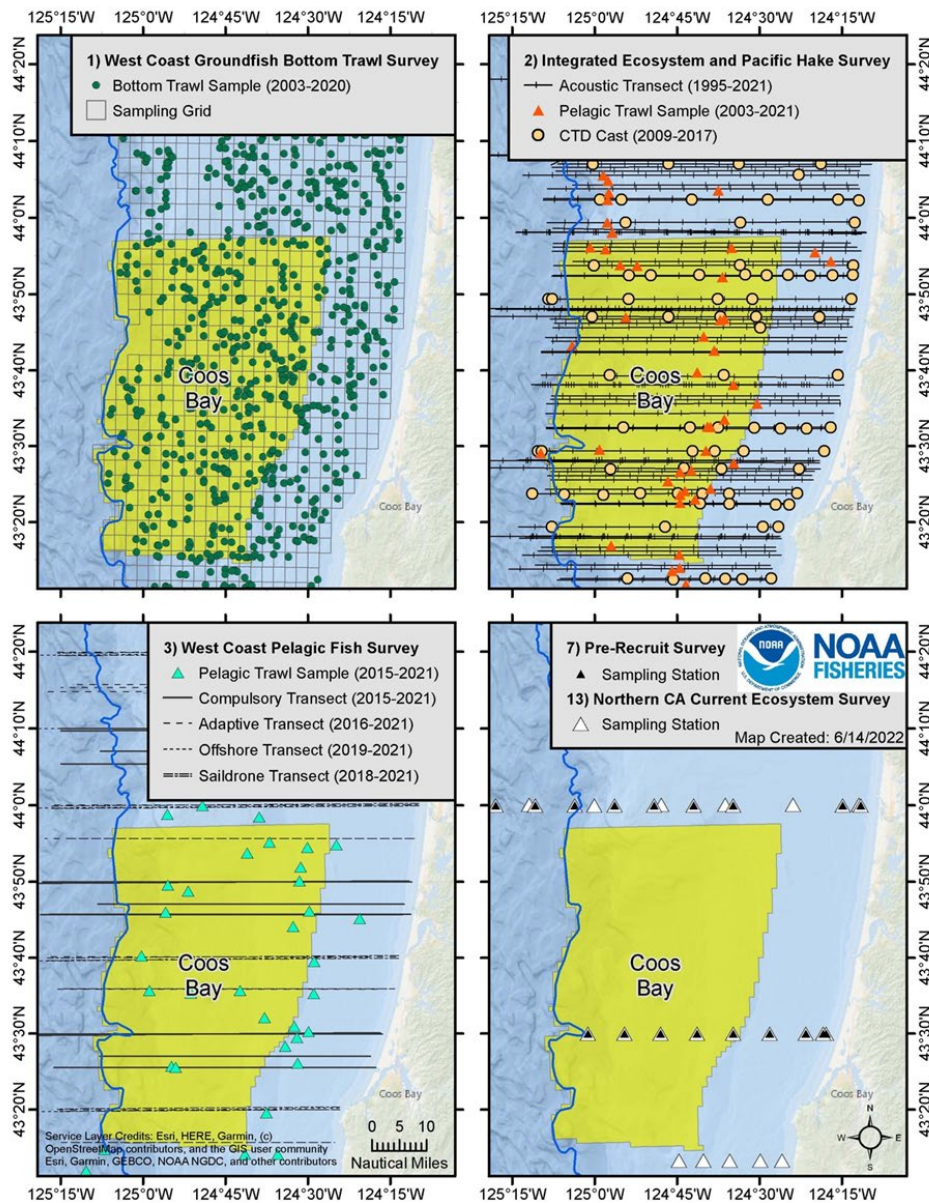
Figure Q.12: NOAA Fisheries scientific surveys conducted within the Coos Bay Call Area and vicinity (individual views). Although a total of six NOAA Fisheries surveys overlap the call areas, the West Coast Marine Mammal Survey is not shown in this figure.

---

[12] https://www.regulations.gov/comment/BOEM-2022-0017-0040
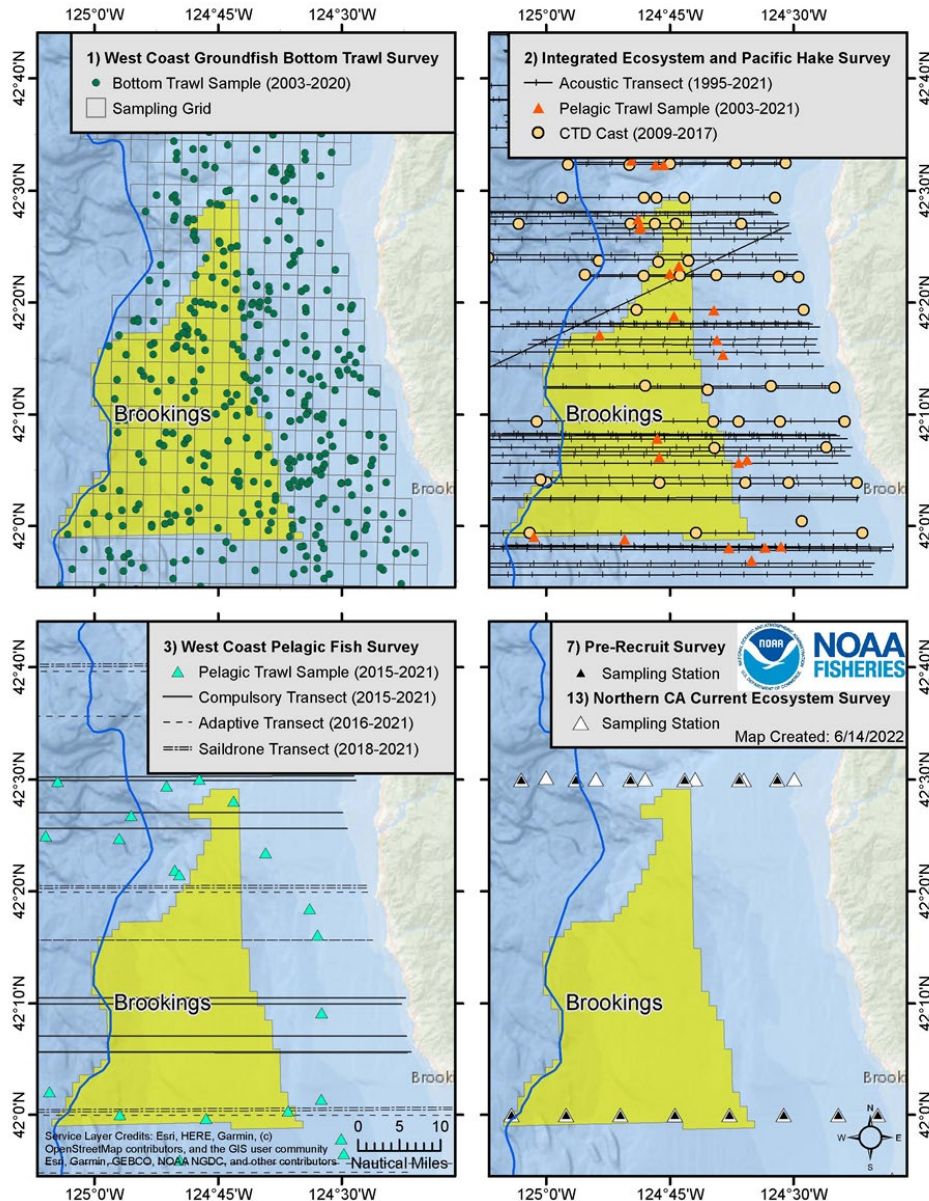
Figure Q.13: NOAA Fisheries scientific surveys conducted within the Brookings Call Area and vicinity (individual views). Although a total of six NOAA Fisheries surveys overlap the call areas, the West Coast Marine Mammal Survey is not shown in this figure.

Appendix R: SOCIAL VULNERABILITY OF FISHING-DEPENDENT COMMUNITIES

In Section 5.1 of the main report, we present information on the Community Social Vulnerability Index (CSVI) as an indicator of social vulnerability in coastal communities that are dependent upon commercial fishing. Fishery dependence can be expressed in terms of engagement, reliance, or by a composite of both. Engagement refers to the total extent of fishing activity in a community; it can be expressed in terms of commercial activity (e.g.,

landings, revenues, permits, processing, etc.) or recreational activity (e.g., number of boat launches, number of charter boat and fishing guide license holders, number of charter boat trips, number of bait and tackle shops, etc.). Reliance is the per capita engagement of a community; thus, in two communities with equal engagement, the community with the smaller population would have a higher reliance on fisheries.

In the main body of the report, Figure 5.1 plots CSVI in 2020 against commercial reliance for the five most reliant communities in 2020 from each of five regions of the CCE. Here, we present a similar plot of CSVI relative to commercial fishing engagement scores from 2020 (Fig. R.1). Communities above and to the right of the dashed lines are at least 1 s.d. above the averages of both indices, as averaged across all commercial fishing communities. Of particular note are communities like Westport, Crescent City, Fort Bragg, and Port Orford that have relatively high commercial fishing engagement results in addition to a high CSVI composite result. Communities in this region of the plot are both highly engaged and have relatively high social vulnerabilities, and thus may be highly vulnerable to commercial fishing downturns. Shocks due to ecosystem changes or management actions may produce especially high individual and community-level social stress in these communities. As discussed in past meetings, these data are difficult to groundtruth and require further study.
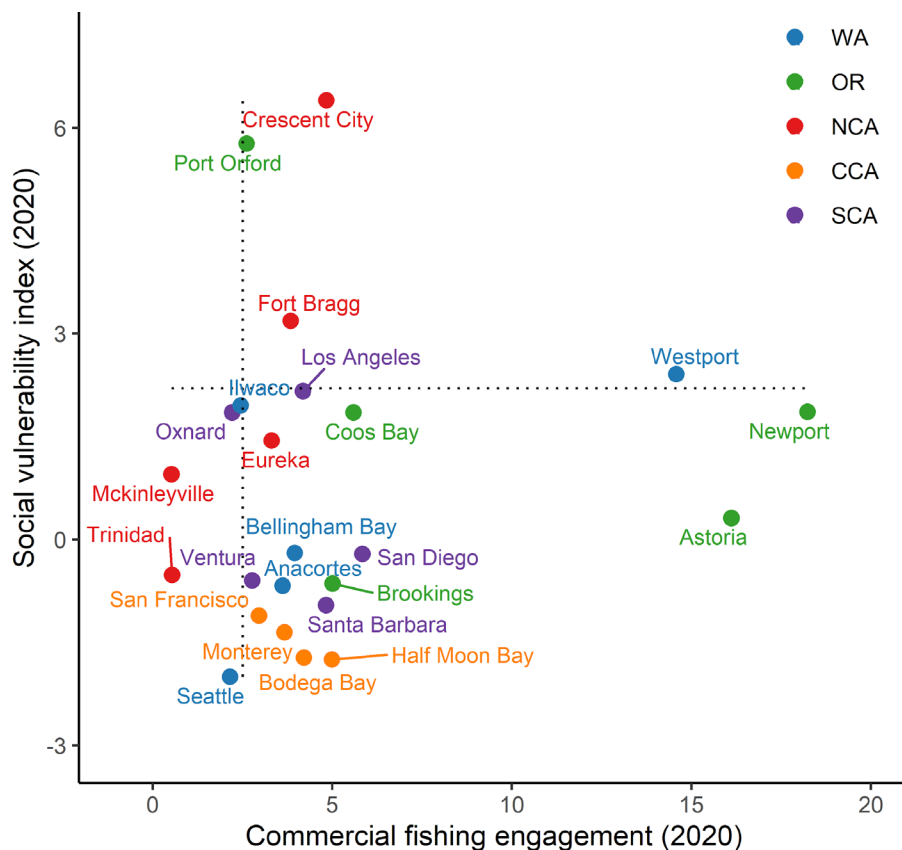

Figure R.1: Commercial fishing engagement and social vulnerability scores in 2020 for communities in Washington, Oregon, and northern, central and southern California. The five highest-scoring communities for fishing engagement are shown for each region. Dotted lines indicate 1 s.d. above the means for all communities.

Information on community-level recreational fishing engagement (number of boat launches, number of charter boat and fishing guide license holders, total charter boat trips, bait shops, etc.) has not been updated beyond 2016. Thus we do not have updated comparisons of CSVI with recreational fishing reliance or engagement. Efforts are ongoing to develop new data sources to support recreational fishing analyses, and exclude inland recreational fisheries activities outside of Council purview.

Appendix S: FISHERY DIVERSIFICATION INDICATORS

Catches and prices from many fisheries exhibit high interannual variability, leading to high variability in fisher's revenue, but variability can be reduced by diversifying activities across multiple fisheries or regions (Kasperski and Holland 2013). Individuals may have good reasons to specialize, including reduced costs or greater efficiency; thus while diversification may reduce income variation, it does not necessarily promote higher average profitability. We use the Effective Shannon Index (ESI) to examine diversification of fishing revenue for more than 28,000 vessels fishing off the West Coast and Alaska over the last 40 years. In the main body of the report (Fig. 5.2), ESI increases as revenues are spread across more fisheries, and as revenues are spread more evenly across fisheries; ESI = 1 when a vessel's revenues are from a single species group and region; ESI = 2 if revenues are spread evenly across 2 fisheries; ESI = 3 if revenues are spread evenly across 3 fisheries; and so on. If revenue is not evenly distributed across fisheries, then the ESI value is lower than the number of fisheries a vessel enters.

Coastwide, average diversification by species group has been trending down for decades across virtually all vessel classifications (main report, Fig. 5.2). Changes in diversification are due both to entry and exit of vessels and changes for individual vessels. Although vessels remaining in the fishery have become less diverse on average, less-diversified vessels have been more likely to exit, and newer entrants generally have been more diversified than those who left (Abbott et al. 2022). Within the average trends are wide ranges of diversification levels and strategies, and some vessels remain highly diversified.

As with individual vessels, the variability of landed value at the port level is reduced with greater diversification of landings. Revenue diversification scores are highly variable year-to-year for some ports, making it difficult to discern trends, but some ports have seen declines since the early 1990s. In 2021, most major ports other than Bellingham and Seattle saw a decline in diversification relative to 2020 (data not shown). These indices do not include income for recreational charter fleets, which may be an important component of revenue diversification for some ports.

Diversification can take other forms. Spreading effort and catch over the year, or simply fishing more weeks of the year, can both increase revenue and decrease interannual variation of revenue just as species diversification does. In fact, Abbott et al. (2022) showed that reductions in revenue variation associated with species diversification can be explained mainly by increased temporal diversification, which can be achieved by fishing in multiple fisheries but also by fishing for more weeks of the year in a single fishery.

Below, Figure S.1 shows temporal diversification for the same vessel groups and classes shown in the main body (Fig. 5.2). Here again we use an ESI metric, now calculated based on the number of weeks fished in a given year, and on how evenly revenue is distributed across those weeks. Like the species diversification metric, this index increases the more weeks of the year a vessel has revenue and the more evenly that revenue is distributed across weeks. For example, if fishing occurred in 15 weeks and revenue was evenly distributed across those 15 weeks, the temporal ESI = 15. If revenue were more concentrated in some of those weeks, ESI < 15.

Unlike species diversification, which has been trending down since the early 1990s for most vessel groups (main report, Fig. 5.2), temporal diversification generally trended up though the early 2000s and oscillated without a clear trend through 2014 (Fig. S.1). However, since 2014, temporal diversification has declined for most vessel groups other than West Coast vessels with average revenue under $25K (Fig. S.1c). This mainly reflects individual vessels fishing fewer weeks of the year on average. Much of the decline since 2014 can be attributed to reduced effort and compression of fishing seasons for salmon and Dungeness crab, as well as impacts of COVID-19 in 2020 and 2021.
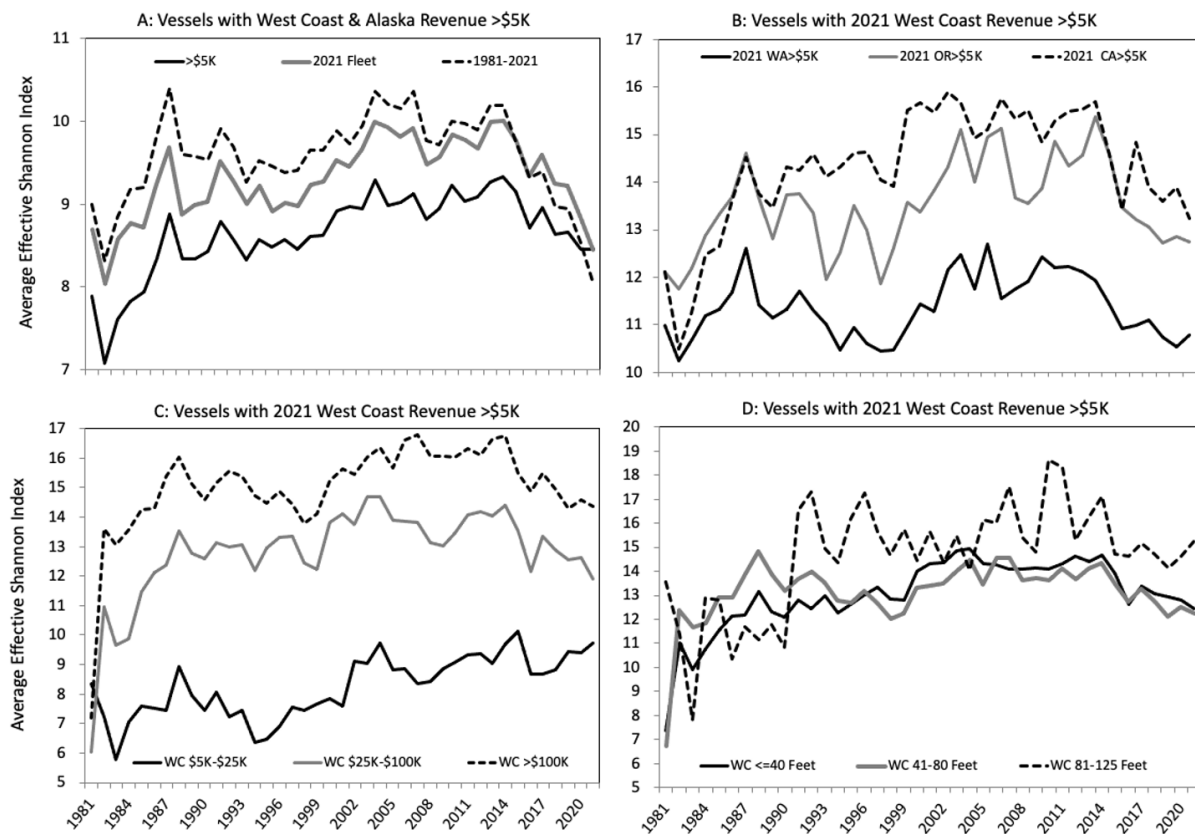

Figure S.1: Trends in temporal diversification for West Coast and Alaskan fishing vessels (top left) and for vessels in the 2021 West Coast Fleet, grouped by state (top right), average gross revenue class (lower left) and length class (lower right). Data from D. Holland (NMFS/NWFSC).

Appendix T: FISHERY REVENUE CONCENTRATION

In the past three ESRs, we worked with the SSC-ES to develop an index of concentration or consolidation of ex-vessel fishery revenue in West Coast port groups, as one possible way of indicating if fishery access opportunities are changing within and across ports and/or FMPs, possibly in relation to meeting requirements of NS-8. We use the Theil Index (Theil 1967) as an annual measure of geographic concentration of fishery revenue. Though it typically measures economic inequality, the Theil Index may be developed and applied in varying contexts. Here, we use the Theil Index as an annual estimate of how observed revenue is concentrated within ports, relative to what revenues would be if they were distributed across those ports with perfect equality. An increase in the Theil Index for a particular fishery or group of fisheries indicates that revenue is becoming more concentrated in a smaller number of ports.

In the Section 5.3 of the main body, we show how total commercial fisheries revenue has not exhibited high levels or extended trends of geographic concentration, but that different fishery management groups demonstrated clearer trends or patterns of variability at the IO-PAC port scale over the study period, but that different fishery management groups demonstrated clearer trends or patterns of variability (Fig. 5.3). In last year's ESR, we provided additional detail on Theil Indexes for groundfish and HMS revenues (see Appendix S of Harvey et al. 2022). Here, we highlight annual changes in the Theil Index for CPS in more depth.

As shown in Figure 5.3 and here in Figure T.1, Theil Index values for CPS revenues on the West Coast have decreased over the last 40 years, indicating a reduction in geographic concentration of CPS revenues. This finding differs from what we have previously reported. In past reports (e.g., Harvey et al. 2022), when we calculated the CPS Theil index, the underlying data included landings of Humboldt squid, Pacific bonito, Pacific herring and round herring, because those species had been classified as CPS in the PacFIN database, but that issue was identified by the CPSMT and corrected in 2022. Prior to this correction, the Theil Index for CPS had appeared to be variable but not to have clearly persistent trends across the last 40 years (Harvey et al. 2022). Without the influence of Pacific herring landings in northern ports on revenue concentration, the long-term declining trend in CPS Theil index has become clear, and the main driver has been a shift of revenue out of southern port groups from the earlier decades to more recent decades (Fig. T.1, bottom). One potential explanation is that market squid revenue has become less consolidated in southern ports over time, and sardine revenue in northern ports in the 2000s and early 2010s may have contributed further to the declining trend.

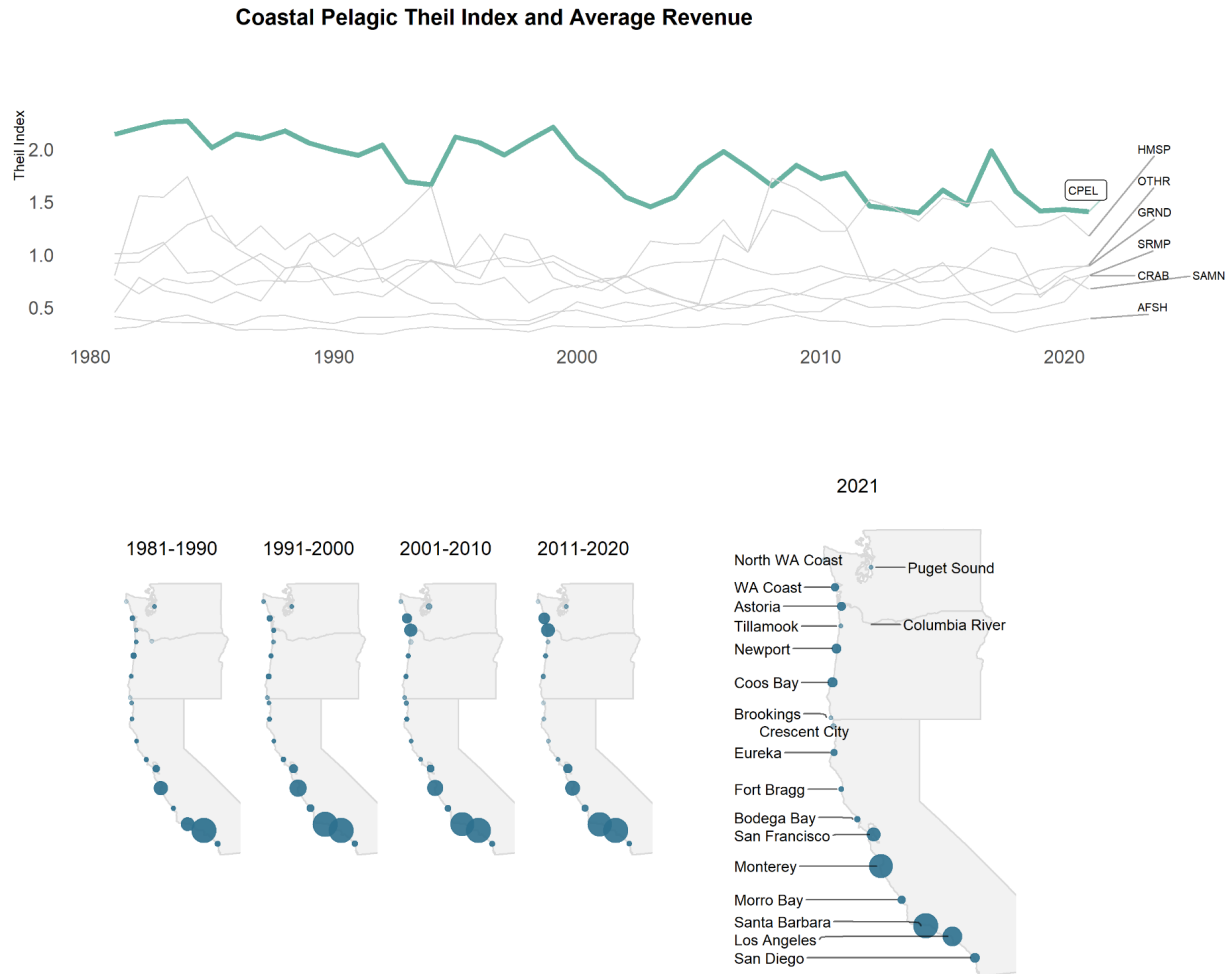**Coastal Pelagic Theil Index and Average Revenue**

Figure T.1: Theil Index of geographic concentration of commercial CPS fishery revenue in West Coast IO-PAC port groups, 1981-2021. Top: time series of Theil Index values for major fishery groups, including all fisheries combined (AFSH); CPS are highlighted in heavy green. Increasing Theil value indicates greater geographic concentration of revenue. Bottom: maps of CPS revenues in IO-PAC port groups through time, where bubble size for a port group is proportional to average annual CPS revenue for that increment.

We have made no effort yet to attribute changes in Theil Indexes to management actions, environmental drivers, food web changes, or changes within coastal communities. It is therefore premature to conclude that this is an effective indicator in the context of NS-8, or what changes in the index mean for Council considerations. We also note that pooling coastal communities into IO-PAC port groups is a coarser scale than intended for NS-8 considerations, which are attuned to communities rather than port groups. Community-scale estimation of the Theil Index is possible, and we would expect different qualitative and quantitative outcomes than those presented here if the scale is refined to the community level. Community-scale estimation would increase the complexity of data analysis, presentation and visualization, which is an important consideration as we continue to develop this metric.

Appendix U: REFERENCES

Abell R, Thieme ML, Revenga C, Bryer M, et al (2008) Freshwater ecoregions of the world: A new map of biogeographic units for freshwater biodiversity conservation. BioScience 58:403–414

Abbott JE, Sakai Y, Holland DS (2022) Species, space, and time: a quarter-century of fishers' diversification strategies on the US West Coast. Fish and Fisheries. doi: 10.1111/faf.12712

Addicott ET, Kroetz K, Reimer MN, Sanchirico JN, et al (2019) Identifying the potential for cross-fishery spillovers: A network analysis of Alaskan permitting patterns. Canadian Journal of Fisheries and Aquatic Sciences 76:56–68

Anderson SC, Ward EJ, English PA, Barnett LA (2022) sdmTMB: An R package for fast, flexible, and user-friendly generalized linear mixed effects models with spatial and spatiotemporal random fields. bioRxiv2022.03.24.485545; doi: doi.org/10.1101/2022.03.24.485545

Anderson SC, Ward EJ, Shelton AO, Adkison MD, et al (2017) Benefits and risks of diversification for individual fishers. Proceedings of the National Academy of Sciences USA 114:10797–10802

Beaudreau AH, Ward EJ, Brenner RE, Shelton AO, et al (2019) Thirty years of change and the future of Alaskan fisheries: Shifts in fishing participation and diversification in response to environmental, regulatory and economic pressures. Fish and Fisheries 20:601–619

Brodie S, Smith JA, Muhling BA, Barnett LA, et al (2022) Recommendations for quantifying and reducing uncertainty in climate projections of species distributions. Global Change Biology. 28(22):6586-601.

Brodie S, Pozo Buil M, Welch H, Bograd SJ, et al (in prep), Skillful ecological forecasts for marine resource management

Burke BJ, Peterson WT, Beckman BR, Morgan C, et al (2013) Multivariate models of adult Pacific salmon returns. PloS One. 11;8(1):e54134.

Chan F, Barth JA, Lubchenco J, Kirincich A, et al (2008) Emergence of anoxia in the California Current large marine ecosystem. Science 319(5865):920.

Cushing D (1990) Plankton production and year-class strength in fish populations: An update of the match/mismatch hypothesis. In: Advances in Marine Biology. Elsevier, pp 249–293

Demer DA, Zwolinski JP, Byers KA, Cutter GR, Renfree JS, Sessions TS, Macewicz BJ (2012) Prediction and confirmation of seasonal migration of Pacific sardine (*Sardinops sagax*) in the California Current Ecosystem. Fishery Bulletin, 110(1): 52-71.

Devincenzi G, Micarelli P, Viola S, Buffa G, et al (2021) Biological sound vs. anthropogenic noise: Assessment of behavioural changes in *Scyliorhinus canicula* exposed to boats noise. Animals 11(1):174.

Dyson K, Huppert DD (2010) Regional economic impacts of razor clam beach closures due to harmful algal blooms (HABs) on the Pacific coast of Washington. Harmful Algae 9:264–271

FDA (2011) Fish and Fishery Products Hazards and Controls Guidance (fourth ed.) Appendix 5: FDA and EPA Safety Levels in Regulations and Guidance. Department of Health and Human Services, Food and Drug Administration. pp 439-442. https://www.fda.gov/media/80637/download

Feely RA, Sabine CL, Hernandez-Ayon JM, Ianson D, Hales B (2008) Evidence for upwelling of corrosive" acidified" water onto the continental shelf. Science 320:1490–1492

Fisher JL, Peterson WT, Rykaczewski RR (2015) The impact of El Niño events on the pelagic food chain in the northern California Current. Global Change Biology 21:4401–4414

Fisher MC, Moore SK, Jardine SL, Watson JR, Samhouri JF (2021) Climate shock effects and mediation in fisheries. Proceedings of the National Academy of Sciences. 12;118(2):e2014379117.

FitzGerald AM, John SN, Apgar TM, Mantua NJ, Martin BT (2021) Quantifying thermal exposure for migratory riverine species: Phenology of Chinook salmon populations predicts thermal stress. Global Change Biology 27:536-549.

Flanders Marine Institute (2019). Maritime Boundaries Geodatabase: Maritime Boundaries and Exclusive Economic Zones (200 NM), version 11. Available online at https://www.marineregions.org/. https://doi.org/10.14284/386

Frawley TH, Muhling BA, Brodie S, Fisher MC, et al (2021) Changes to the structure and function of an albacore fishery reveal shifting social-ecological realities for Pacific Northwest fishermen. Fish and Fisheries 22(2):280-97

Friedman WR, Martin BT, Wells BK, Warzybok P, et al (2019) Modeling composite effects of marine and freshwater processes on migratory species. Ecosphere 10(7), e02743.

Fuller EC, Samhouri JF, Stoll JS, Levin SA, Watson JR (2017) Characterizing fisheries connectivity in marine social–ecological systems. ICES Journal of Marine Science 74(8):2087-96.

Hall JE, Greene CM, Stefankiv O, Anderson JH, et al (2018) Large river habitat complexity and productivity of Puget Sound Chinook salmon. PLoS ONE 13(11):e0205127.

Haltuch MA, Johnson KF, Tolimieri N, Kapur MS, Castillo-Jordán CA (2019) Status of the sablefish stock in U.S. waters in 2019. Pacific Fisheries Management Council, 7700 Ambassador Place NE, Suite 200, Portland, OR. 398 p.

Hare JA, Blyth BJ, Ford KH, Hooker BR, et al (2022) NOAA Fisheries and BOEM Federal Survey Mitigation Implementation Strategy–Northeast U.S. Region. NOAA Technical Memorandum 292. Woods Hole, MA. 33 pp

Harvey C, Garfield T, Williams G, Tolimieri N, Hazen E (2018). California Current Integrated Ecosystem Assessment (CCIEA) California Current Ecosystem Status Report, 2018. Report to the Pacific Fishery Management Council. March 2018, Agenda item F.1.a.

Harvey C, Garfield T, Williams G, Tolimieri N (2021) California Current Integrated Ecosystem Assessment (CCIEA) California Current Ecosystem Status Report, 2021. Report to the Pacific Fishery Management Council. March 2021, Agenda item I.1.a.

Harvey C, Garfield T, Williams G, Tolimieri N (2022) 2021-2022 California Current Ecosystem Status Report. Report to the Pacific Fishery Management Council. March 2022, Agenda item H.2.a.

Hobday AJ, Alexander LV, Perkins SE, Smale DA, et al (2016) A hierarchical approach to defining marine heatwaves. Progress in Oceanography 141:227-38.

Holland DS, Leonard J (2020) Is a delay a disaster? Economic impacts of the delay of the California Dungeness crab fishery due to a harmful algal bloom. Harmful Algae 98:101904

ISC (2022) Stock assessment of Pacific bluefin tuna in the Pacific Ocean in 2022. ISC/22/ANNEX/13. International Scientific Committee for Tuna and Tuna-Like Species in the North Pacific Ocean.

Jacox MG, Edwards CA, Hazen EL, Bograd SJ (2018). Coastal upwelling revisited: Ekman, Bakun, and improved upwelling indices for the U.S. West Coast. Journal of Geophysical Research: Oceans, 123. https://doi.org/10.1029/ 2018JC014187

Jager HI, Cardwell HE, Sale MJ, Bevelhimer MS, Coutant CC, Van Winkle W (1997) Modelling the linkages between flow management and salmon recruitment in rivers. Ecological Modelling 103:171-191.

Jepson M, Colburn LL (2013) Development of social indicators of fishing community vulnerability and resilience in the U.S. Southeast and Northeast regions. National Marine Fisheries Service. NOAA tech. memo. NMFS-F/SPO 129. https://repository.library.noaa.gov/view/noaa/4438

Joh H, Di Lorenzo E (2017) Increasing coupling between NPGO and PDO leads to prolonged marine heatwaves in the Northeast Pacific. *Geophysical Research Letters*, *44*(22), 11-663.

Jordan MS (2012) Hydraulic predictors and seasonal distribution of *Manayunkia speciosa* density in the Klamath River, CA, with implications for ceratomyxosis, a disease of salmon and trout. MS Thesis, Departments of Water Resources Science and Microbiology, Oregon State University, Corvallis Oregon.

Kapur MS., Lee Q, Correa GM, Haltuch M, et al (2021) DRAFT Status of Sablefish (*Anoplopoma fimbria*) along the US West Coast in 2021. Pacific Fishery Management Council, Portland, OR. 136 p.

Karp MA, Brodie S, Smith JA, Richerson K, et al (2023) Projecting species distributions using fishery-dependent data. Fish and Fisheries, 24, 71– 92. https://doi.org/10.1111/faf.12711

Kasperski S, Holland DS (2013) Income diversification and risk for fishermen. Proceedings of the National Academy of Sciences 110:2076–2081

Keister JE, Di Lorenzo E, Morgan CA, Combes V, Peterson WT (2011) Zooplankton species composition is linked to ocean transport in the northern California current. Global Change Biology 17:2498–2511

Keller AA, Wallace JR, Methot RD (2017) The Northwest Fisheries Science Center's West Coast groundfish bottom trawl survey: History, design, and description. U.S. Department of Commerce, NOAA Technical Memorandum NMFS-NWFSC-136. DOI: 10.7289/V5/TM-NWFSC-136.

Kroetz K, Reimer MN, Sanchirico JN, et al (2019) Defining the economic scope for ecosystem-based fishery management. Proceedings of the National Academy of Sciences 116:4188–4193

Lefebvre KA, Bargu S, Kieckhefer T, Silver MW (2002) From sanddabs to blue whales: The pervasiveness of domoic acid. Toxicon 40:971–977

Leising AW (in revision for submission to Frontiers in Mar. Sci.) Phenology of Northeast Pacific Large Marine Heatwaves impacting the California Current System

Leonard JL, Watson PS (2011) Description of the input-output model for Pacific Coast fisheries. NWFSC/NOAA. NOAA technical memorandum NMFS-NWFSC ; 111. https://repository.library.noaa.gov/view/noaa/8718

Limm MP, Marchetti MP (2009) Juvenile chinook salmon (*Oncorhynchus tshawytscha*) growth in off-channel and main-channel habitats on the Sacramento River, CA using otolith increment widths. Environmental Biology of Fishes 85:141–151

Lindgren F, Rue H (2015) Bayesian spatial modelling with r-INLA. Journal of Statistical Software 63:1–25

Litzow MA, Hunsicker ME, Bond NA, Burke BJ, et al (2020) The changing physical and ecological meanings of North Pacific Ocean climate indices. Proceedings of the National Academy of Sciences USA 117(14):7665-7671.

Litzow MA, Ciannelli L, Puerta P, Wettstein JJ, et al (2018) Non-stationary climate–salmon relationships in the Gulf of Alaska. Proceedings of the Royal Society B, 285(1890), p.20181855

Mais KF (1974) Pelagic fish surveys in the California Current. State of California, Resources Agency, Dept. of Fish and Game, Sacramento, CA: 79 pp.

Mais KF (1977) Acoustic surveys of Northern anchovies in the California Current System, 1966-1972. Journal du Conseil International pour l'exploration de la Mer 170:287–295

Mantua N, Johnson R, Field J, Lindley S, et al (2021) Mechanisms, impacts, and mitigation for thiamine deficiency and early life stage mortality in California's Central Valley Chinook Salmon. North Pacific Anadromous Fish Commission, Technical Report 17:92-93

Martin B, Pike A, John SN, Hamda N, et al (2017) Phenomenological vs. biophysical models of thermal stress in aquatic eggs. Ecology Letters 20:50–59.

Marshall KN, Kaplan IC, Hodgson EE, Hermann A, et al (2017) Risks of ocean acidification in the California Current food web and fisheries: ecosystem model projections. Global Change Biology 23(4):1525-39

Mastrandrea MD, Field CB, Stocker TF, Edenhofer O, et al (2017) Guidance note for lead authors of the IPCC 5th Assessment Report on consistent treatment of uncertainties. https://www.ipcc.ch/site/assets/uploads/2017/08/AR5_Uncertainty_Guidance_Note.pdf

Maunder M, Xu H, Minte-Vera C, Valero JL, et al (2022) Skipjack tuna in the Eastern Pacific Ocean, 2021: interim assessment. Document SAC-13-07. Inter-American Tropical Tuna Commission, Science Advisory Committee, 13th Meeting.

McCabe RM, Hickey BM, Kudela RM, Lefebvre KA, et al (2016) An unprecedented coastwide toxic algal bloom linked to anomalous ocean conditions. Geophysical Research Letters 43(19):10-366.

McClure M, et al. (in press). Vulnerability to climate change of managed stocks in the California Current large marine ecosystem. Frontiers in Marine Science.

McKibben SM, Peterson W, Wood AM, Trainer VL, et al (2017) Climatic regulation of the neurotoxin domoic acid. Proceedings of the National Academy of Sciences 114:239–244

Melin SR, Orr AJ, Harris JD, Laake JL, DeLong RL (2012) California sea lions: an indicator for integrated ecosystem assessment of the California Current System. California Cooperative Oceanic Fisheries Investigations Reports 53:140-52.

Michel CJ (2019) Decoupling outmigration from marine survival indicates outsized influence of streamflow on cohort success for California's Chinook salmon populations. Canadian Journal of Fisheries and Aquatic Sciences 76:1398–1410

Moore SK, Cline MR, Blair K, Klinger T, et al (2019) An index of fisheries closures due to harmful algal blooms and a framework for identifying vulnerable fishing communities on the US West Coast. Marine Policy 110:103543.

Moore SK, Dreyer SJ, Ekstrom JA, Moore K, et al (2020) Harmful algal blooms and coastal communities: Socioeconomic impacts and actions taken to cope with the 2015 US West Coast domoic acid event. Harmful algae 96:101799.

Morgan CA, Beckman BR, Weitkamp LA, Fresh KL (2019) Recent ecosystem disturbance in the northern California Current. Fisheries 44:465–474

Munsch SH, Greene CM, Johnson RC, Satterthwaite WH, et al (2019) Warm, dry winters truncate timing and size distribution of seaward-migrating salmon across a large, regulated watershed. Ecological Applications 29(4):e01880.

Munsch SH, Greene CM, Johnson RC, Satterthwaite WH, et al (2020) Science for integrative management of a diadromous fish stock: interdependencies of fisheries, flow, and habitat restoration. Canadian Journal of Fisheries and Aquatic Sciences 77(9):1487-504.

NMFS (2022) NOAA NMFS-NCCOS-IOOS comments_OR Call_Letter to BOEM_6-28-22_FINALsigned. Accessed: https://www.regulations.gov/comment/BOEM-2022-0009-0178, January 24, 2023.

Neveu E, Moore AM, Edwards CA, Fiechter J, et al (2016) An historical analysis of the California Current circulation using ROMS 4D-Var: System configuration and diagnostics. Ocean Modelling 99:133-51.

Nomura K, Samhouri JF, Johnson AF, Giron-Nava A, Watson JR (2020) Fisheries connectivity measures of adaptive capacity in small-scale fisheries. ICES Journal of Marine Science 79:519-31.

PFMC (2022a) Pacific Coast fishery ecosystem plan for the U.S. portion of the California Current large marine ecosystem. Pacific Fishery Management Council, Portland, OR.

PFMC (2022b) Preseason report I. Stock abundance analysis and environmental assessment Part 1 for 2022 ocean salmon fishery regulations. Pacific Fishery Management Council, Portland, OR.

PFMC (2022c) Scientific and Statistical Committee report on methodology review– preliminary fishery impact model topics and final assessment methodologies. September 2022, Agenda Item G.4.a, Supplemental SSC Report 1. Pacific Fishery Management Council, Portland, OR.

PFMC (2022d) Pacific Coast salmon fishery management plan. Pacific Fishery Management Council, Portland, OR.

PFMC (2022e) Scientific and Statistical Committee report on final methodology review. November 2022, Agenda Item D.2.a, Supplemental SSC Report 1. Pacific Fishery Management Council, Portland, OR.

PFMC (2022f) Salmon Technical Team report on methodology review. November 2022, Agenda Item D.2.a, Supplemental STT Report 1. Pacific Fishery Management Council, Portland, OR.

Perry RW, Brandes PL, Burau JR, Klimley AP, et al (2013) Sensitivity of survival to migration routes used by juvenile Chinook salmon to negotiate the Sacramento-San Joaquin River Delta. Environmental Biology of Fishes 96:381-92.

Peterson WT, Fisher JL, Peterson JO, Morgan CA, et al (2014) Applied fisheries oceanography: Ecosystem indicators of ocean conditions inform fisheries management in the California Current. Oceanography 27(4):80-9.

Reis GJ, Howard JK, Rosenfield JA (2019) Clarifying effects of environmental protections on freshwater flows to—and water exports from—the San Francisco Bay estuary. San Francisco Estuary and Watershed Science 17(1)

Riley KL, Wickliffe LC, Jossart JA, MacKay JK, et al (2021) An Aquaculture Opportunity Area Atlas for the U.S. Gulf of Mexico. NOAA Technical Memorandum NOS NCCOS 299. Beaufort, NC. 545 pp. https://doi.org/10.25923/8cb3-3r66

Ritzman J, Brodbeck A, Brostrom S, McGrew S, et al (2018) Economic and sociocultural impacts of fisheries closures in two fishing-dependent communities following the massive 2015 US West Coast harmful algal bloom. Harmful Algae 80:35-45.

Robertson RR, Bjorkstedt EP (2020) Climate-driven variability in *Euphausia pacifica* size distributions off northern California. Progress in Oceanography 188:102412.

Santora JA, Mantua NJ, Schroeder ID, Field JC, et al (2020) Habitat compression and ecosystem shifts as potential links between marine heatwave and record whale entanglements. Nature Communications 11(1):536.

Santora JA, Rogers TL, Cimino MA, Sakuma KM, et al (2021) Diverse integrated ecosystem approach overcomes pandemic-related fisheries monitoring challenges. Nature Communications 12(1):6492.

Satterthwaite, W. 2022. Literature review for Sacramento River fall Chinook conservation objective and associated S_{MSY} reference point. Pages 49-75 of PFMC, 2022. 2022 Salmon methodology review materials. November 2022, Agenda Item D.2, Attachment 1 (Electronic only). Pacific Fishery Management Council, Portland, OR.

Satterthwaite WH, Carlson SM, Allen-Moran SD, Vincenzi S, et al (2014) Match-mismatch dynamics and the relationship between ocean-entry timing and relative ocean recoveries of Central Valley fall run Chinook salmon. Marine Ecology Progress Series 511:237-48.

Smith, JA, Muhling B, Sweeney J, Tommasi D, et al (2021) The potential impact of a shifting Pacific sardine distribution on US West Coast landings. Fisheries Oceanography, 30(4), 437-454.

Stierhoff KL, Zwolinski JP, Demer DA (2019) Distribution, biomass, and demography of coastal pelagic fishes in the California Current Ecosystem during summer 2018 based on acoustic-trawl sampling. U.S. Dep. Commer., NOAA Tech. Memo., NMFS-SWFSC-613: 83 pp.

Stierhoff KL, Zwolinski JP, Demer DA (2020) Distribution, biomass, and demography of coastal pelagic fishes off central and southern California during spring 2019 based on acoustic-trawl sampling. U.S. Dep. Commer., NOAA Tech. Memo., NMFS-NWFSC-626. 80 pp.

Stierhoff KL, Renfree JS, Rojas-González RI, Vallarta-Zárate JRF, et al (2023) Distribution, biomass, and demographics of coastal pelagic fishes in the California Current Ecosystem during summer 2021 based on acoustic-trawl sampling. U.S. Dep. Commer., NOAA Tech. Memo., NMFS-SWFSC-676: 86 pp.

Stierhoff KL, Renfree JS, Zwolinski JP, Demer DA (In prep) Distribution, biomass, and demographics of coastal pelagic fishes in the California Current Ecosystem during summer 2022 based on acoustic-trawl sampling. U.S. Dep. Commer., NOAA Tech. Memo.

Strange JS (2012) Migration strategies of adult Chinook salmon runs in response to diverse environmental conditions in the Klamath River basin. Transactions of the American Fisheries Society 141:1622-1636.

Sturrock AM, Satterthwaite WH, Cervantes-Yoshida KM, Huber ER, et al (2019) Eight decades of hatchery salmon releases in the California Central Valley: Factors influencing straying and resilience. Fisheries 44:433-444.

Sykes GE, Johnson CJ, Shrimpton JM (2009) Temperature and flow effects on migration timing of Chinook salmon smolts. Transactions of the American Fisheries Society 138:1252-1265.

Szoboszlai AI, Thayer JA, Wood SA, Sydeman WJ, Koehn LE (2015) Forage species in predator diets: synthesis of data from the California Current. Ecological Informatics 29:45-56.

Szuwalski CS, Hollowed AB (2016) Climate change and non-stationary population processes in fisheries management. ICES Journal of Marine Science, 73:1297-1305.

TNC & WWF (2008) Freshwater Ecoregions of the World. The Nature Conservancy and World Wildlife Fund, Inc., Washington, DC USA. URL https://www.feow.org/files/downloads/GIS_hs_snapped.zip Accessed: 10 Jan 2023.

Theil H (1967) Economics and Information Theory. Amsterdam Chicago: North-Holland Pub. Co.; Rand McNally. 488 pp.

Thiault L, Gelcich S, Marshall N, Marshall P, et al (2020) Operationalizing vulnerability for social–ecological integration in conservation and natural resource management. Conservation Letters 13:e12677.

Thompson AR, Harvey CJ, Sydeman WJ, Barceló C, et al (2019a) Indicators of pelagic forage community shifts in the California Current Large Marine Ecosystem, 1998–2016. Ecological Indicators 105:215-228.

Thompson AR, Schroeder ID, Bograd SJ, Hazen EL, et al (2019b) State of the California Current 2018–19: a novel anchovy regime and a new marine heatwave? California Cooperative Oceanic Fisheries Investigations Reports 60:1-65.

Thorson JT (2019) Guidance for decisions using the vector autoregressive spatio-temporal (VAST) package in stock, ecosystem, habitat and climate assessments. Fisheries Research 210:143–161

Tolimieri N, Wallace J, Haltuch M (2020) Spatio-temporal patterns in juvenile habitat for 13 groundfishes in the California Current ecosystem. PloS One 15:e0237996

Tolimieri N, Haltuch M (2023) Sea-level index of recruitment variability improves assessment model performance for sablefish *Anoplopoma fimbria*. Canadian Journal of Fisheries and Aquatic Sciences, in press. doi.org/10.1139/cjfas-2022-0238

Trainer VL, Moore SK, Hallegraeff G, Kudela RM, et al (2020) Pelagic harmful algal blooms and climate change: Lessons from nature's experiments with extremes. Harmful Algae 91:101591.

USFWS (1995) Sacramento-San Joaquin Delta Native Fishes Recovery Plan. U.S. Fish and Wildlife Service, Portland, Oregon.

Wells, BK, Grimes CB, Sneva JG, McPherson S, Waldvogel JB (2008) Relationships between oceanic conditions and growth of Chinook salmon (*Oncorhynchus tshawytscha*) from California, Washington, and Alaska, USA. Fisheries Oceanography 17:101-125.

Wells BK, Santora JA, Henderson MJ, Warzybok P, et al (2017) Environmental conditions and prey-switching by a seabird predator impact juvenile salmon survival. Journal of Marine Systems 174:54-63

Zwolinski JP, Demer DA, Cutter Jr GR, Stierhoff K, Macewicz BJ (2014) Building on fisheries acoustics for marine ecosystem surveys. Oceanography 27(4):68-79.